Molecular Structures and Physicochemical Properties of Native and Modified Barley Starches with Various Amylose Content

BY

SangGuan You

A Thesis

Submitted to the Faculty of Graduate Studies

In Partial Fulfillment of the Requirements

for the Degree of

DOCTOR OF PHILOSOPHY

Food and Nutritional Sciences

University of Manitoba

Winnipeg, Manitoba

THE UNIVERSITY OF MANITOBA

FACULTY OF GRADUATE STUDIES

*****

COPYRIGHT PERMISSION

Molecular Structures and Physicochemical Properties of

Native and Modified Barley Starches with Various Amylose Content

BY

SangGuan You

A Thesis/Practicum submitted to the Faculty of Graduate Studies of The University of

Manitoba in partial fulfillment of the requirement of the degree

Doctor Of Philosophy

I hereby declare that I am the sole author of this thesis

I authorize the University of Manitoba to lend this thesis to other institutions or individuals for the purpose of scholarly research

SangGuan You

I further authorize the University of Manitoba to reproduce this thesis by photocopying or by other means, in total or in part, at the request of other institutions or individuals for the purpose of scholarly research

SangGuan You

The University of Manitoba requires the signatures of all persons using or photocopying this thesis. Please sign below and give address and date.

ACKNOWLEDGEMENTS

There are many people I wish to thank for making this thesis possible. First of all, I would like to thank my advisor, Dr. M.S. Izydorczyk, whose determination, motivation, management, and ingenuity helped me getting through my PhD. Especially, her editorial corrections and suggestions have made this thesis far better than it would otherwise have been. In addition, her encouragement and support have significantly influenced my personal and professional life to continuously move ahead.

I am also grateful to the members of my PhD committee, Dr. M. Eskin, Dr. A.W. MacGregor, and my external examiner Dr. S. Cui for their insight, encouragement, and comments.

I would like to thank my MSc. advisor, Dr. S-T. Lim, and professors, Dr. Y.-J. Park, Dr. I.H. Jung and Dr. S.M. Kim for their encouragement and sincere concerns about my career. Special thanks to Dr. S. Stevenson, and Dr. K.R. Preston for their arrangement and support of my life in Grain Research Laboratory.

I would like to also express my sincere gratitude to my lab members, S. Bazin, T. Chornick, S. Nam, and L. Dushinicky. My sincerest thanks extend to the staff and graduate students of the department of Food Science for their support and friendship.

The financial assistance provided by the Natural Sciences and Engineering Research Council of Canada is gratefully acknowledged.

Finally, special thanks go to my family, my wife, my sons, my sisters, my parents and my parent's in-laws for their endless support and love.

ABSTRACT

Traditionally, barley has been used primarily in malting and animal feeds, and to a lesser extent in human foods. In order to increase the utilization of barley in terms of human consumption, it is necessary to understand the physicochemical properties of its constituents. Starch is a major component of barley grain, and its functionality predominately affects the textural properties of barley containing foods. The following study examined the granular and molecular characteristics as well as functional properties of native and modified barley starches varying in amylose content from 0 to 42%.

Normal and waxy types of starch granules exhibited bimodal size distributions, with large (10-25μm) and small (<10μm) granules having different relative proportions. High amylose starch granules were distributed unimodally with the highest proportion of granules measuring 3μm. The weight average molecular weight (M_w) of amylopectin and amylose, obtained from high performance size exclusion chromatography (HPSEC) coupled to a multiangle light scattering (MALS) and a refractive index (RI) detection system, ranged from 136×10^6 to 305×10^6 (g/mol) and from 2.73×10^6 to 5.67×10^6 (g/mol), respectively. Amylopectin from waxy types of starches had the highest M_w, whereas amylopectin from high amylose starch had the lowest. Amylose and amylopectin polymers from normal barley starch were completely separated using flow-field flow fractionation (flow-FFF) with the application of two cross-flows, 0.35mL/min followed by 0.1mL/min. Choosing an appropriate rate for the second cross-flow allowed for better insights into the molecular weight distribution of amylopectin polymers, and revealed that it had a more compact molecular conformation than that of amylose polymers.

Substantial starch solubilization was observed during α-amylolysis of starch

granules, with waxy starch solubilized 36-56%, normal starch 24-39%, and high amylose starch 13-20%. On the other hand, relatively little solubilization (<9%) was found during the acid/alcohol treatment. Despite the severe granular deformation, especially in the enzyme-treated zero amylose starch, starch polymers retained their macromolecular structures, indicating that both crystalline and amorphous regions were degraded by α-amylase. On the other hand, acid appeared to preferentially hydrolyze the amorphous regions, causing significant degradation of starch polymers. These results were further supported by X-ray diffractometry, DSC, and solid-state CP/MAS ^{13}C NMR spectroscopy. The enzyme (50U/g, 24h) and acid (2%HCl/MeOH, 10h) treated high amylose barley starches showed increased potential for gelation.

Starch and β-glucan blends (5% w/w total carbohydrate concentration; ratio of starch:β-glucan - 100:0, 85:15, 70:30, 55:45) exhibited increases in the apparent viscosity and viscoelastic properties compared to solutions of individual polymers at the corresponding concentrations, indicating some interactions and co-entanglements between starch and β-glucan polymers. In the high concentration systems (15% w/w total carbohydrate concentration; ratio of starch:β-glucan - 100:0, 95:5, 90:10), the addition of β-glucan had relatively little effect on the viscoelastic properties of the blends, indicating that the blend networks at higher concentrations were governed mostly by strong junction zones formed by the starch polymers. However, some interactions between starch and β-glucan polymers were also detected in the modified high amylose starch and β-glucan blend systems (95:5 blends). The starch digestibility of the blend was inversely proportional to the elastic properties of the networks.

TABLE OF CONTENTS

PAGE

ACKNOWLEDGEMENTS iv

ABSTRACT vi

TABLE OF CONTENTS viii

LIST OF TABLES xii

LIST OF FIGURES xiv

CHAPTER 1 INTRODUCTION 1

CHAPTER 2 LITERATURE REVIEW 5
- Morphological Properties 5
- Starch Polymers 8
- Crystalline Properties 12
- Molecular Weight of Starch Polymers 16
- Physical Properties 18
  - Gelatinization 18
  - Gelation and Retrogradation 21
- Starch Modifications 24
  - α-Amylolysis 24
  - Acid/Alcohol Hydrolysis 27
  - Starch/Hydrocolloid Blends 30

CHPATER 3 MOLECULAR CHARACTERISTICS OF BARLEY STARCHES WITH VARIOUS AMYLOSE CONTENT 32
- Abstract 32
- Introduction 33
- Materials and Methods 35
  - Materials 35
  - Chemical Analyses 35
  - Isolation of Starch 35
  - Size Distribution of Starch Granules 36

Determination of M_w of Starch Polymers..... 36
Results and Discussion..... 39
Amylose Content and Granular Size Distribution..... 39
M_w and R_g of Starch Polymers..... 42
Molecular Characteristics of Debranched Starches..... 50
Conclusions..... 57

CHAPTER 4 SEPARATION AND CHARACTERIZATION OF BARLEY STARCH POLYMERS BY A FLOW-FIELD FLOW FRACTIONATION TECHNIQUE IN COMBINATION WITH MULTIANGLE LIGHT SCATTERING AND DIFFERENTIAL REFRACTIVE INDEX DETECTION..... 58
Abstract..... 58
Introduction..... 60
Materials and Methods..... 64
Materials..... 64
Sample Preparation..... 64
Apparatus and Procedures..... 65
Results and Discussion..... 69
Separation of Starch Components..... 71
Conclusions..... 88

CHAPTER 5 PHYSICOCHEMICAL PROPERTIES AND MOLECULAR STRUCTURE OF MODIFIED BARLEY STARCH GRANULES WITH VARIOUS AMYLOSE CONTENT. PART I: α-AMYLASE HYDROLYSIS..... 89
Abstract..... 89
Introduction..... 91
Materials and Methods..... 95
Materials..... 95
α-Amylase Modification of Starch Granules..... 95
Morphological Properties of Starch Granules..... 96
X-Ray Diffraction Patterns of Starch Granules..... 96
CP/MAS ^{13}C NMR Spectra of Starch Granules..... 96
Molecular Characteristics of Starch Polymers..... 97
Thermal Properties of Starches..... 98
Digestibility of α-Amylase Treated Starches..... 99

Rheological Properties of Starches..... 99
Results and Discussion..... 101
Starch Solubilization during α-Amylolysis..... 101
X-Ray Diffractometry and CP/MAS ^{13}C NMR of Hydrolyzed Starches..... 108
Molecular Weight and Structure of Hydrolyzed Starch Polymers..... 112
Thermal Properties..... 124
Digestibility of Hydrolyzed Starches..... 129
Rheological Properties of Starches..... 131
Conclusions..... 136

CHAPTER 6 PHYSICOCHEMICAL PROPERTIES AND MOLECULAR STRUCTURE OF MODIFIED BARLEY STARCH GRANULES WITH VARIOUS AMYLOSE CONTENT. PART II: ACID/ ALCOHOL HYDROLYSIS..... 137
Abstract..... 137
Introduction..... 139
Materials and Methods..... 142
Materials..... 142
Acid-Alcohol Modification of Starch Granules..... 142
Starch Solubilization..... 142
M_w Analysis of Starch Polymers..... 143
Debranching of Acid Treated Starches..... 143
Other Physical and Rheological Measurements of Starches..... 144
Results and Discussion..... 145
Solubilization and Morphology of Acid-Treated Barley Starches..... 145
Molecular Weight of partially Hydrolyzed Starches..... 149
Debranching of Partially Hydrolyzed Starches..... 157
Internal Structures of Partially Hydrolyzed Starches..... 164
Thermal Properties..... 166
α-Amylase Digestibility of Acid/Alcohol Treated Starches..... 175
Dynamic Viscoelasticity..... 177
Conclusions..... 182

CHAPTER 7 FLOW AND VISCOELASTIC PROPERTIES OF HIGH AMYLOSE HULLESS BARLEY STARCH AND β-GLUCAN BLENDS..... 183

Abstract 183
Introduction 185
Materials and Methods 188
Materials 188
Preparation of Mixed Systems 188
Rheological Measurements 190
α-Amylase Digestibility of Mixed Systems 190
Results and Discussion 191
Low Concentration System (5% w/w) 191
High Concentration System (15% w/w) 210
Digestibility of Starch/β-Glucan Blends 217
Conclusions 224

CHAPTER 8 GENERAL DISCUSSION 225
Granular and Molecular Characteristics of Barley Starches 225
Modifications of Barley Starches 229
Summary and conclusions 237
Future studies 238
CHAPTER 9 LITERATURE CITED 240

LIST OF TABLES

TABLE		PAGE
Table 3.1	Starch and amylose content in various genotypes of barley	40
Table 3.2	Weight average molecular weights (M_w), radii of gyration (R_g), and polydispersity values (M_w/M_n) of barley starches	45
Table 3.3	Weight average molecular weights (M_w), radii of gyration (R_g), and polydispersity values (M_w/M_n) of amylose after debranching of starch samples with isoamylase	53
Table 3.4	Molecular characteristics of amylopectin linear branches obtained after debranching of starch samples with isoamylase	55
Table 4.1	Weight average molecular weights (M_w) and radii of gyration (R_g) of normal and zero amylose starches after application of various cross-flows	76
Table 4.2	Weight average molecular weights (M_w), radii of gyration (R_g), and sample recoveries of separated amylose and amylopectin from normal and zero amylose starches by two cross-flows	81
Table 5.1	Effect of α-amylolysis on solubilization, M_w, and R_g of various barley starches	116
Table 5.2	Weight average molecular weights (M_w) of amylose after debranching of native and enzyme-treated barley starches	119

Table 5.3	DSC gelatinization temperatures and enthalpies of native and α-amylase-treated starches.....	128
Table 6.1	The yield of 2% HCl/1-butanol modified starch residues after 96h treatment.....	147
Table 6.2	Weight average molecular weights (M_w) of native and acid/alcohol-treated starches.....	154
Table 6.3	Weight average molecular weights (M_w) and relative content of debranched amylose fractions in native and acid/alcohol-treated normal and high amylose starches....	160
Table 6.4	DSC transition characteristics of native and acid/alcohol-treated starches.....	172
Table 7.1	Concentrations and compositions of starch and β-glucan blends.....	189
Table 7.2	Rheological properties of blends, and HA starch and HMW-BG solutions alone after 2 hours of storage.....	207
Table 7.3	Rheological properties of blends, and HA starch and LMW-BG solutions alone after 2 hours of storage.....	209
Table 7.4	Rheological properties of blends, and modified HA starch and HMW-BG solutions alone after 2 hours of storage....	212
Table 7.5	Rheological properties of blends, and HA starch gels after 2 hours of storage.....	215
Table 7.6	Rheological properties of blends, and modified HA starch gels after 2 hours of storage.....	216
Table 7.7	The amount of reducing sugars liberated during α-amylase (10 U/g) hydrolysis of HA starch and blends of HA starch with BG (mg glucose/g starch).....	223

LIST OF FIGURES

FIGURE		PAGE
Figure 2.1	Small and large granules of barley starches in barley endosperm	6
Figure 2.2	Schematic diagram of α-D-glucose and linear chain structure of amylose	9
Figure 2.3	Schematic diagram of amylopectin with a branch point at the 1→6 position	10
Figure 2.4	A schematic view of starch granule structure	11
Figure 2.5	Crystalline structure of B-starch	13
Figure 2.6	Crystalline structure of A-starch	14
Figure 2.7	Schematic illustration of amylose-lipid complex	15
Figure 2.8	Different combinations of starch, water, and temperatures that influence starch behaviour	20
Figure 2.9	Storage modulus (G') vs. time for 5% (w/w) amylose gel at various temperatures	23
Figure 2.10	Storage modulus (G') development of 20% (w/w) waxy maize amylopectin gel at 1°C	24
Figure 2.11	Hydrolysis patterns of hulless barley starches of waxy (CDC Alamo), normal (CDC Dawn), and high amylose (SB 94893) types by α-amylases from porcine pancreas (A) and from *Bacillus species* (B)	26
Figure 2.12	Acid hydrolysis patterns of small and large hulless barley starch granules from SB 89528 (waxy), Condor (normal), and Glacier (high amylose)	29

Figure 3.1	Size distribution of granules in barley starches with variable amylose content.....	41
Figure 3.2	HPSEC profiles of normal (Falcon), high amylose (92-55-06-48), waxy (CDC Candle), and zero amylose (CDC Alamo) barley starches.....	43
Figure 3.3	Relative molecular weight vs. elution volume for high (a) and low (b) molecular weight fractions in normal (Falcon), high amylose (92-55-06-48), waxy (CDC Candle), and zero amylose (CDC Alamo) barley starches.....	46
Figure 3.4	Molar mass distribution in normal (Falcon), high amylose (92-55-06-48), waxy (CDC Candle), and zero amylose (CDC Alamo) barley starches.....	47
Figure 3.5	HPSEC profiles of normal (Falcon), high amylose (92-55-06-48), waxy (CDC Candle), and zero amylose (CDC Alamo) barley starches after debranching with isoamylase.....	51
Figure 4.1	Flow FFF-MALS-RI system and diagram of flow FFF channel (insert).....	66
Figure 4.2	Effects of various cross-flows on elution profiles of pullulan standard (P-1600) (a); channel and frit flows 0.2 and 1.4mL/min, respectively. Effects of various frit flows on elution profiles of pullulan standard (P-1600) (b); channel and cross flows 0.2 and 0.6mL/min, respectively..	70
Figure 4.3	Elution profiles of different pullulan standards (P-200, P-800, and P-1600) with channel, frit, and cross-flows of 0.2, 1.4, and 1.0mL/min, respectively.....	72
Figure 4.4	Elution profiles of a mixture of pullulan standards (P-200 and P-1600) with channel, frit, and cross-flows of	

	0.2, 1.4, and 0.6mL/min, respectively.....	73
Figure 4.5	Effects of various cross-flows on elution profiles of normal barley starch with channel and frit flows of 0.1 and 1.0mL/min, respectively.....	75
Figure 4.6	Effects of various cross-flows on elution profiles of zero amylose starch; channel and frit flows of 0.1 and 1.0mL/min, respectively. Cumulative molar mass distribution of zero amylose starch is shown in the insert.....	78
Figure 4.7	Refractive index (RI) (a) and light scattering (LS) (b) fractograms of normal barley starch. Separation of amylose and amylopectin on application of two cross-flows: 0.35mL/min (12min) followed by 0.1mL/min.....	80
Figure 4.8	Elution profiles of normal barley starch with constant initial cross-flow (0.35mL/min) followed by various second cross-flows (0.08-0.2mL/min).....	83
Figure 4.9	Refractive index (RI) (a) and light scattering (LS) (b) fractograms of zero amylose starch: initial cross-flow 0.35mL/min (12min) followed by 0.1mL/min.....	85
Figure 4.10	Distribution of R_g and M_w for amylose and amylopectin polymers.....	87
Figure 5.1	The extent of solubilizations of barley starches with various amylose content during α-amylolysis at two different enzyme levels (50 U and 500 U of α-amylase /g of starch).....	102
Figure 5.2	Effect of amylose content on the solubilization rate at the initial (0-8h) and second (8-48h) stages of α-amylase hydrolysis.....	103

Figure 5.3 Scanning electron photomicrographs of native and enzyme-treated (50U α-amylase /g of starch, 48h) zero amylose (A,B), normal (C,D), and high amylose (E,F) barley starch granules, respectively..... 104

Figure 5.4 Scanning electron photomicrographs of mechanically cracked enzyme-treated zero amylose waxy (A,B), normal (C,D), and high amylose (E,F) barley starch granules (50U α-amylase/g of starch, 24h)..... 105

Figure 5.5 X-ray diffraction patterns of native and enzyme-treated barley starches (500 U of α-amylase /g of starch, 48h)..... 109

Figure 5.6 CP/MAS ^{13}C NMR spectra of native and enzyme-treated barley starches (500 U of α-amylase /g of starch, 48h).... 111

Figure 5.7 HPSEC elution profiles of native and α-amylase-treated normal (a), high amylose (b), zero amylose (c) barley starches. Weight average molecular weight (M_w) distributions of native and enzyme-treated barley starches (insert)..... 113

Figure 5.8 HPSEC elution profiles and weight average molecular weights (M_w) of debranched native and enzyme-treated normal (a), and high amylose (b) barley starch polymers... 117

Figure 5.9 HPAEC profiles of debranched linear chains of native and enzyme-hydrolyzed normal (a), high amylose (b), and zero amylose (c) barley starches..... 120

Figure 5.10 DSC thermograms of native and enzyme-treated normal (a), high amylose (b), and zero amylose (c) barley starches (40% w/w)..... 125

Figure 5.11 The extent of solubilizations of native and enzyme-hydrolyzed barley starches after 24h of α-amylolysis (N24% and N39%; Normal barley starches solubilized

24% and 39%, H13% and H20%; high amylose barley starches solubilized 13% and 20%, Z36% and Z56%; zero amylose barley starches solubilized 36% and 56%, respectively)..... 130

Figure 5.12 The temperature dependence of initial network formations (G' and G") of native and enzyme-treated barley starch solutions (40% w/w) upon cooling from 50°C to 5 °C (5 °C/min)..... 132

Figure 5.13 Gel network development of native and enzyme-treated barley starch pastes (40% w/w) during storage for 20h at 5 °C..... 133

Figure 6.1 Starch solubilization during acid/alcohol hydrolysis in the two different acid concentrations (0.36% and 2% HCl/MeOH and EtOH)..... 146

Figure 6.2 Scanning electron photomicrographs of native and acid/alcohol-treated (2% HCl/BuOH, 96h) normal (A,B), high amylose (C,D), waxy (E,F), and zero amylose (G,H) barley starches..... 148

Figure 6.3 HPSEC profiles and weight average molecular weight (M_w) distributions of native and acid/alcohol-treated barley starches (0.36% and 2% HCl/MeOH, EtOH and BuOH, 10h and 96h)..... 150

Figure 6.4 HPSEC debranched chain length profiles of native and acid/alcohol-treated normal (a) and high amylose (b) starches. Insert; HPSEC debranched amylose chain length profiles and weight average molecular weights (M_w) in peaks..... 158

Figure 6.5 HPSEC debranched chain length profiles of native and acid/alcohol-treated zero amylose starch (2% HCl/MeOH, EtOH and BuOH, 96h)..... 162

Figure 6.6	HPAEC debranched chain length profiles of native and acid/alcohol-treated barley starches (2% HCl/MeOH, EtOH and BuOH, 96h).....	163
Figure 6.7	X-ray diffraction patterns of native and acid/alcohol-treated barley starches (2% HCl/BuOH, 96h).....	165
Figure 6.8	Solid-state CP/MAS ^{13}C NMR spectra of native and acid/alcohol-treated barley starches (2% HCl/BuOH, 96h)...	167
Figure 6.9	DSC endothermic profiles of native and acid/alcohol-treated starches (0.36% and 2% HCl/MeOH, EtOH, BuOH, 10h and 96h).....	168
Figure 6.10	The α-amylase digestibility of native and acid/alcohol-treated barley starches (2% HCl/BuOH, 96h).....	176
Figure 6.11	The temperature dependence of initial network formations (G' and G") of native and acid/alcohol-treated barley starches (40% w/w) upon cooling from 50°C to 5 °C (cooling rate of 5 °C/min).....	178
Figure 6.12	The time dependence of network developments of native and acid/alcohol-treated barley starches (40% w/w) during storage for 20h at 5 °C.....	179
Figure 7.1	Steady shear viscosity profiles of freshly prepared HA starch (a) and enzyme-modified HA starch (b, 50U/g, 24h) at concentrations ranging from 2.75% to 5% (w/w).....	192
Figure 7.2	Steady shear viscosity profiles of freshly prepared HMW-BG and LMW-BG solutions at concentrations ranging from 0.75% to 2.25% (w/w).....	193
Figure 7.3	Steady shear viscosity profiles of HA starch and	

	HMW-BG blends at a total polymer concentration of 5% (w/w).....	193
Figure 7.4	Steady shear viscosity profiles of HA starch and LMW-BG blends at a total polymer concentration of 5% (w/w).....	195
Figure 7.5	Steady shear viscosity profiles of modified HA starch and HMW-BG blends at a total polymer concentration of 5% (w/w).....	195
Figure 7.6	Steady shear viscosity profiles of modified HA starch and LMW-BG blends at a total polymer concentration of 5% (w/w).....	196
Figure 7.7	The mechanical spectra of G' and G" against frequency of freshly prepared HA starch at 5%, 4.25%, 3.5%, and 2.75% (w/w).....	198
Figure 7.8	The mechanical spectrum of G' and G" against frequency of freshly prepared modified HA starch at 5% (w/w).....	199
Figure 7.9	The development of G' and G" during storage for 2h at 20°C for HA starch samples at 5%, 4.25%, 3.5%, and 2.75% (w/w).....	200
Figure 7.10	The development of G' and G" during storage for 2h at 20°C for modified HA starch at 5% and 3.5% (w/w)...	201
Figure 7.11	The mechanical spectra of G' and G" against frequency (a), and the development of G' and G" during storage for 2h at 20°C (b) for HMW-BG solutions at 2.25% and 0.75% (w/w).....	203
Figure 7.12	The mechanical spectra of G' (a), and tan δ (b) against frequency of freshly prepared HA starch and HMW-BG blends at a total concentration of 5%.....	204

Figure 7.13	The development of G' (a), and tan δ (b) during storage for 2h at 20°C for HA starch and HMW-BG blends at a total concentration of 5%.....	205
Figure 7.14	The mechanical spectra of G' (a), and tan δ (b) against frequency of freshly prepared HA starch and LMW-BG blends at a total concentration of 5%.....	208
Figure 7.15	The mechanical spectra of G' (a), and tan δ (b) against frequency of freshly prepared HA starch and LMW-BG blends at a total concentration of 5%.....	211
Figure 7.16	The mechanical spectra of G' (a), and tan δ (b) against frequency of freshly prepared HA starch at 15%, 14.25%, and 13.5% (w/w).....	213
Figure 7.17	The mechanical spectra of G' (a), and tan δ (b) against frequency of freshly prepared modified HA starch at 15%, 14.25%, and 13.5% (w/w).....	214
Figure 7.18	The mechanical spectra of G' (a), and tan δ (b) against frequency of freshly prepared HA starch and HMW-BG blends at a total concentration of 15% (w/w).....	218
Figure 7.19	The mechanical spectra of G' (a), and tan δ (b) against frequency of freshly prepared modified HA starch and HMW-BG blends at a total concentration of 15% (w/w)...	219
Figure 7.20	The mechanical spectra of G' (a), and tan δ (b) against frequency of freshly prepared HA starch and LMW-BG blends at a total concentration of 15% (w/w).....	220
Figure 7.21	The mechanical spectra of G' (a), and tan δ (b) against frequency of freshly prepared modified HA starch and LMW-BG blends at a total concentration of 15% (w/w)...	221

CHAPTER 1

Introduction

Barley is one of the most widely cultivated cereal crops that can provide valuable nutrients required by humans and domestic animals. Its high adaptability to various climates and growing conditions has led to worldwide production averaging 145.9 million tonnes per year over the last decade. Barley is the fourth largest cereal grain crop produced worldwide after wheat, rice, and corn. In Canada, barley production ranks second after wheat. From 1993 to 2003, the average barley production in Canada was 12.4 million tonnes. Barley has had three distinct end-uses - alcoholic beverages, animal feed, and human food - but patterns of its utilization have changed throughout history. In the ancient world, barley was grown mostly to provide food staples for human nutrition. Drastic changes in consumption patterns in the Western World took place at the beginning of the 20th century, when grains such as rice, wheat, and maize, gained greater preference. The consumption of barley for food dropped drastically, except for barley used in the production of alcoholic beverages, especially beer. The world's use of malting barley for beer production significantly increased after the Second World War, but this trend has reversed itself at the end of the 20th century, especially in the West. The use of malting barley in Asia, however, continues to increase. Cultivation of barley for feed is a more recent development, but it has significantly exceeded other uses, and the majority of barley produced today is used for feeding animals.

Although relatively little effort has so far been made to increase and diversify barley utilization outside the malting and feed industry, recent studies which have elucidated the role of grains in prevention and treatment of many human diseases might

revive interest in barley for food purposes. The food industry is continuously searching for natural ingredients with unique and functional properties, and facing the challenge and opportunity to develop novel, palatable, attractive and healthy grain-based products, which will gain acceptance among consumers.

Barley grain consists mainly of carbohydrates (78-83%), proteins (8-15%), and lipids (2-3%) (MacGregor and Fincher 1993). Carbohydrates are major components, with starch being the principal constituent (60-65%). Barley is high in total dietary fibre (~ 10-20%), and mixed linkage β-glucan, which have been shown to lower plasma cholesterol, reduce glycemic index and reduce risk of colon cancer (Bhatty 1993). Minor barley components, including tocols, phenolic compounds, phytin, vitamin E, proanthocyanidins, and catechins, have also received some attention due to their antioxidant properties (Slavin et al. 2000). Barley is an excellent source of B-complex vitamins, especially thiamine, pyridoxine, pantotheic acid, niacin, biotin, and folacin as well as minerals such as phosphorus, potassium, and calcium (Jadhav et al. 1998).

Starch is the major component of barley grain and the dominant constituent of barley flour, controlling the major characteristics of barley products. In the mature barley grain, starch exists in granular form, with two distinct populations of large (A-type) and small (B-type) granules. The small granules account for 90% of the total number of granules, but only 10% of their total weight (MacGregor and Fincher 1993). Starch is composed of two polysaccharides, amylose (AM) and amylopectin (AP), with AP constituting approximately 75% of the starch in normal barley. Two single gene mutations can alter the AM and AP ratio. When the generic trait of waxy starch is present, starch contains 95-100% amylopectin. The other mutation increases the amylose content up to 40%. Several barley varieties have recently been developed with amylose content ranging from 0 to 40%. Variability in amylose/amylopectin ratio

can significantly affect barley starch swelling as well as gelatinization and pasting properties, thus providing useful material for targeted products within the food industry (Vasanthan and Bhatty 1996). It has been reported that replacement of 20% of wheat flour in yeast-leavened bread with waxy and non-waxy barley flour did not substantially affect loaf volume and produced bread with a slightly softer texture (Klamczynski and Czuchajowska 1999). On the other hand, the incorporation of high amylose barley flour into Asian noodles increased their firmness and chewiness (Hatcher et al. 2004). More studies are needed to clearly understand the relationships between barley starch characteristics and textural properties of starch-containing food products.

Despite the existence of strong barley breeding programs in Canada and the availability of barley starch, relatively little research has been done on molecular characteristics and functional properties of barley starches, especially when compared to the extensively studied wheat and corn starches. Even though, theoretically, Canada is capable of producing several million tonnes of barley starches annually, the majority of Canadian industries using starch in food and industrial applications are importing native and modified corn and potato starches from abroad. More comprehensive knowledge of the molecular and genetic basis of barley starch functionality will provide new opportunities for barley starch and barley grain utilization and production.

In light of the above considerations, the main objective of this thesis has been to gain a better understanding of the fine structural characteristics and physicochemical properties of barley starches with variable amylose and amylopectin content. Detailed studies in terms of size and distribution of starch granules, molecular weight of amylose and amylopectin polymers, length and distribution of linear chains in amylopectin, and the thermal and rheological properties of starches were conducted. The inherent difficulties in accurate determinations of molecular weight of

starch polymers necessitated a new approach to our studies; in addition to the traditional size exclusion chromatography, the flow-field flow fractionation technique coupled with multiangle light scattering detection system was used to investigate the molecular characteristics of barley starch polymers. The chemical and enzymatic modifications of barley starches were conducted: (1) to determine the effect of amylose content on the degree and rate of the enzyme and acidic hydrolyses; (2) to examine the physical and molecular characteristics of the starch material remaining after α-amylolysis and acid hydrolysis; and (3) to better understand how the susceptibility of various hulless barley starches to enzymic and acid hydrolysis relates to their molecular structure and organization inside the granules. Finally, the aim of blending high amylose barley starches (native and enzyme-modified) with barley β-glucans was to obtain binary polysaccharide systems with unique textural characteristics. The effects of different polymer ratios, molecular weights of β-glucans as well as different total carbohydrate concentrations in the blends on the flow and viscoelastic properties of the mixed systems were investigated.

CHAPTER 2

Literature Review

Morphological properties

Starch is the major storage carbohydrate in all higher plants and occurs as discrete granules in the leaf, stem (pith), root (tuber), seed, fruit and pollen (Lineback 1984). The shape and size of the starch granules depend on their botanical origin (Badenhuizen 1965). Maize and oat starches exhibit polyhedral or round granular morphology, while wheat, barley and sorghum starch granules are disc-like or spherical (Banks and Greenwood 1975; French 1984; Trubell 1944). The potato starch granules have an oval shape and range in size from 15 to 100μm in diameter, while rice starch granules have a polyhedral, spherical compound shape, and range in size from 1 to 3μm in diameter (Thomas and Atwell 1999). Some cereals, including oat, wheat and barley, have both large (A-type) and small (B-type) granules (Fig. 2.1). It has been suggested that the biosynthesis of large and small granules occurs at two different stages of development (May and Buttrose 1959; MacGregor et al. 1971; Buleon et al. 1998).

Small granules (2-4μm) of normal barley starch have been reported to constitute 80-90% of the total number of granules but only 10-15% of the total starch weight (MacGregor and Fincher 1993). Large barley starch granules (10-30μm) make up a small proportion (10-20%) of the total number of granules but a high proportion (85-90%) of the total weight of starch (MacGregor and Fincher 1993). In a recent report (Tang et al. 2001), a trimodal size distribution of normal barley starch granules was observed. The authors reported that the size distribution of large, medium and small

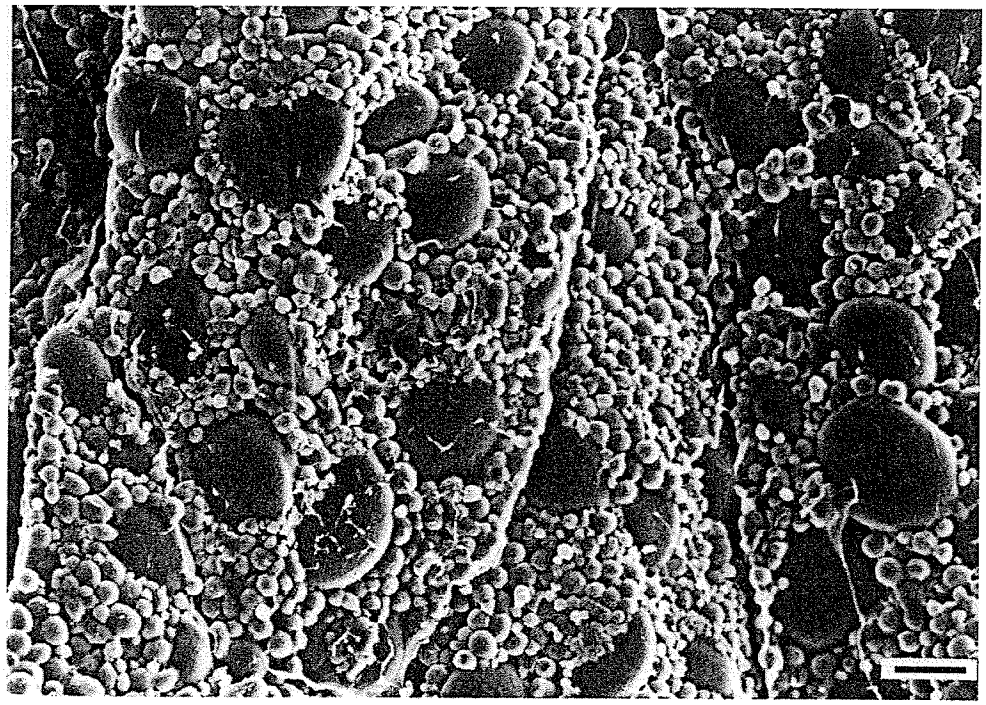

Figure. 2.1. Small and large granules of barley starches in barley endosperm. Bar=10μm (MacGregor and Fincher 1993).

normal barley starch granules was 7.7-44.9, 5.1-26.1 and 0.9-5.1μm with a relative proportion of 62.5-69.2%, 20.6-23.0% and 10.2-14.5% (weight %), respectively (Tang et al. 2001).

In high amylose barley starch, small granules (B-type, average diameter 4μm) are larger and the large granules (A-type, average diameter 10.8μm) are smaller than the corresponding granule types in normal barley starch (Banks et al. 1973; Morrison et al. 1986). Furthermore, B-type granules of high amylose barley starch constitute a relatively higher proportion than the corresponding granule type in normal barley starch, thereby, showing a more uniform size distribution (Morrison et al. 1986; Song and Jane 2000).

Waxy barley starch granules usually show a bimodal size distribution similar to that observed for normal starch (Morrison et al. 1986; Zheng et al. 1998). However, a trimodal size distribution of waxy barley starch granules has also been reported,

with the size distribution and proportion (weight %) of the three granular populations (large, medium and small) being 7.0-39.2μm and 82.0%, 3.5-7.0μm and 7.6%, and 1.2-3.5μm and 10.4%, respectively (Tang et al. 2001).

Barley starch granules were isolated by steeping barley kernels in acetate buffer (0.02M, pH 6.5), grinding the soften kernels, and then by sieving (150μm and 75μm mesh) (MacGregor 1979). In order to remove the protenacious materials, the isolated barley starches were further purified by a process of resuspension, partial sedimentation and centrifugation, followed by a multiple extraction of starch slurries with toluene. Starch granules were also isolated from the lightly cracked cereal grains (wheat, oat, barley, and sorghum) by steeping and sieving procedures, in which, to further purify the starches, protein fractions were removed using protease (Morrison et al. 1984) or 80% CsCl with centrifugation (Sulaiman and Morrison 1990). Barley starch granules have also been isolated from barley flour by an alkaline steeping method using 0.1% NaOH (Tang et al. 2000).

Starch granules normally exhibit smooth surfaces under scanning electron microscopy (Banks and Greenwood 1975; French 1984; MacGregor and Fincher 1993; Song and Jane 2000). However, it has been proposed that the surface of the starch granule is actually more like a 'hairy billiard ball' (Lineback 1986). A recent study, using two complementary techniques, low voltage scanning electron microscopy (LVSEM) and atomic force microscopy (AFM), showed evidence that starch polymer chains protrude through the granule's surface (Baldwin et al. 1998). It was reported that starches from various botanical sources possess significant differences in their surface topology. For example, a rougher surface was observed in potato than in wheat starch. It was

suggested that the 10 to 300nm diameter of 'raised nodule' structures, revealed by the AFM at the surface of potato and wheat starch granules, are the ends of the starch polymers of the crystalline amylopectin clusters (Baldwin et al. 1998).

The existence of pores on the surface of granules is another important characteristic of starch granules. Fannon and co-workers (1992) proposed that the surface pores act as sites of the initial enzyme attack, allowing enzyme molecules direct access to the granule interior. In addition to the pores on the surface of starch granules, interior channels were also observed in sorghum and corn starch granules by transmission electron microscopy and fluorescence microscopy (Fannon et al. 1992; 1993; Huber and BeMiller 1997).

Starch polymers

The starch granule is composed of two primary components, amylose and amylopectin. Amylose is essentially a linear polymer (Fig. 2.2) composed of α-D-glucopyranose residues linked through 1→4 linkages, and contains relatively few branches linked via α-D-(1→6) linkages (~ 9 to 20 branch points per molecule) (Hizukuri 1996). The average degree of polymerization (DP) of amylose may vary from 324 to 4920 depending on the plant origin (Hizukuri et al. 1981; Morrison and Karkalas 1990; Takeda et al. 1987; Wang and White 1994; Yoshimoto et al. 2000). In aqueous solutions, amylose assumes a random coil conformation with a variable amount of short single helical structures (Banks and Greenwood 1975). The helices are constantly undergoing transitions between helical structures and random coil structures (Banks and Greenwood 1975). When amylose undergoes retrogradation, the polymer chains have a tendency to associate together to form double helices (Gidley 1992). Amylose is also able to assume a stable single helical conformation by forming an inclusion complex

with iodine, organic alcohols, and fatty acids (Hoseney 1994).

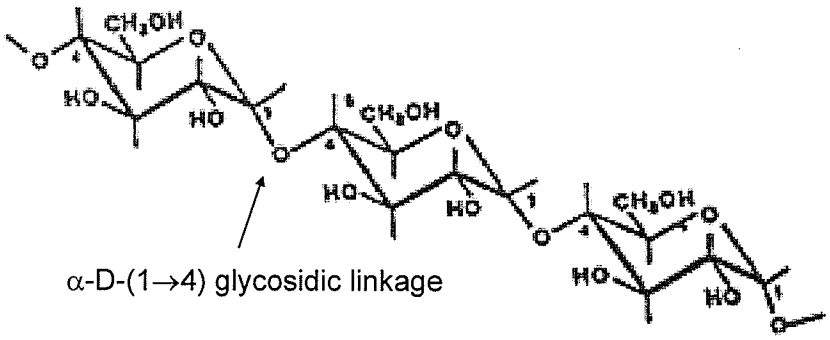

Figure. 2.2. Schematic diagram of α-D-glucose and linear chain structure of amylose

It has been reported that monoacyl lipids induce the formation of amylose-lipid complexes during gelatinization, and thus influence such physicochemical properties of starch as granule swelling, amylose leaching, pasting viscosity, and gelation (Biliaderis 1992; 1998; Eliasson and Gudmundsson 1996).

Amylopectin, on the other hand, is a heavily branched polymer with side chains attached to the linear α-D-(1→4) polymer by α-D-(1→6) linkages (Fig. 2.3a). The branch point linkages (α-D-(1→6)) constitute 4-5% of total linkages in the polymer chain (Hizukuri 1996). Amylopectin is a much larger molecule than amylose, with a degree of polymerization ranging from 9600 to 15,900 (Takeda et al. 2003). For analysis and characterization of amylopectin structure, Peat and co-workers (1952; 1956) classified the chains of amylopectin into types A, B, and C. The A chains are linear and linked to C-6 of the other chains via their reducing ends. The B chains carry the A or other B chain at their C-6, and the C chain is a single chain having one reducing end (Fig 2.3b).

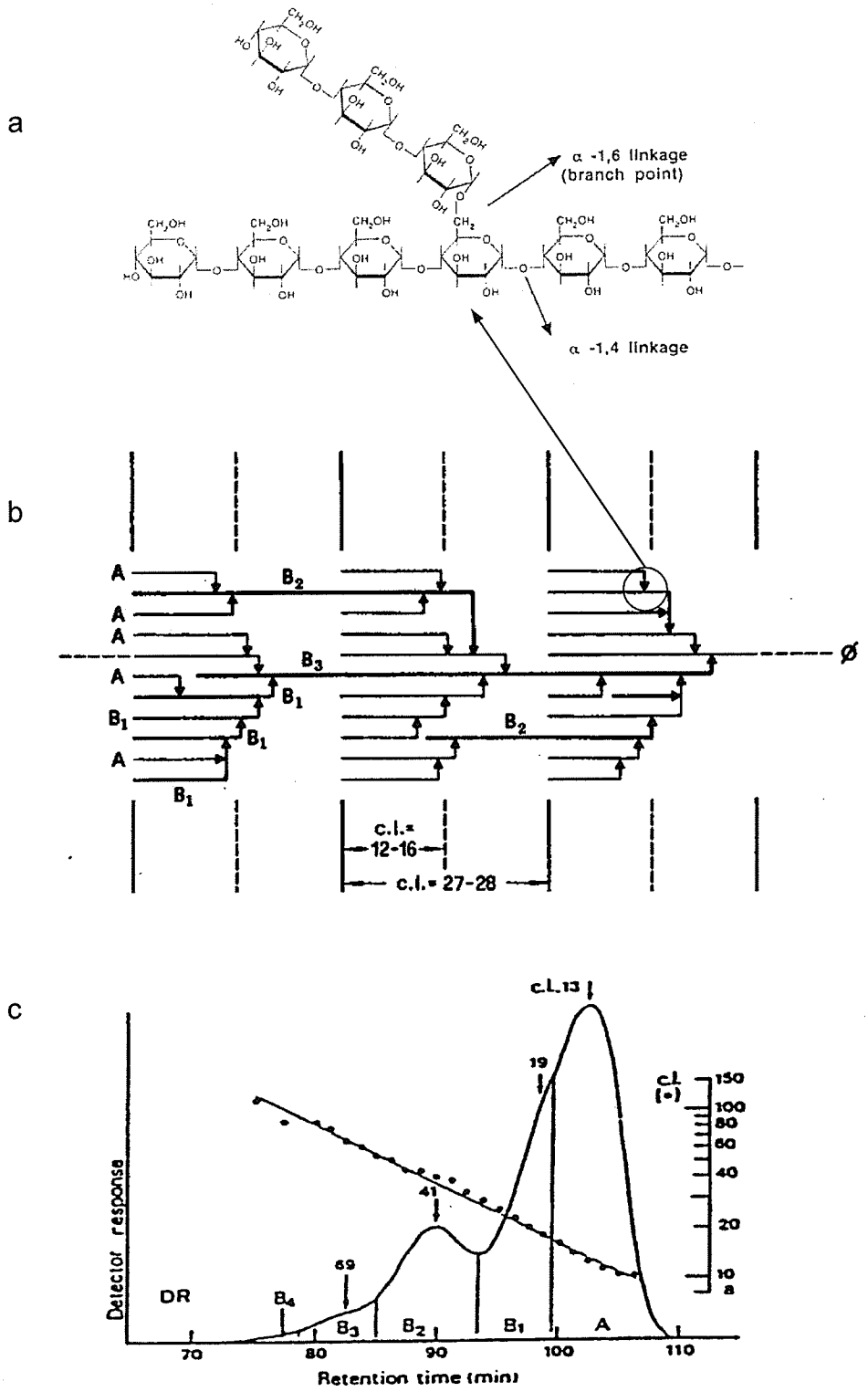

Figure 2.3. Schematic diagram of amylopectin with a branch point at the 1→6 position (a); A generalized diagram demonstrating the cluster model structure for amylopectin (b) (Hizukuri 1986); Molecular distribution profile for waxy rice amylopectin by gel-permeation HPLC (c) (Hizukuri 1986).

B chains are referred to as B1-B4, depending on the chain length (CL) and the number of clusters connected by the chains. The average chain lengths of A and B1-B4 chains for different starches range from 12 to 16, 20 to 24, 42 to 48, 69 to 75, and 101 to 119, respectively (Bello-Perez et al. 1996; Hizukuri 1986; Mua and Jackson 1997; Wang and White 1994). Debranched amylopectin chains from various starches, as assessed by gel filtration chromatography, exhibit polymodal size distribution, which supports the cluster model structure for amylopectin (Fig. 2.3c, Hizukuri 1986; MacGregor and Morgan 1984; Yoshimoto et al. 2000; 2001). Starch granules are semicrystalline, comprised of crystalline and amorphous domains (Fig. 2.4a,b). The crystalline domains are believed to be built up mainly by A chains and outer B chains that are in the form of double helices (Fig. 2.4c, Sarko and Wu 1978). The thickness of crystalline domains is about 6 nm (14-18 glucose units) (Fig. 2.4d, Ball et al. 1996; Donald et al. 1997; French 1972; Robin et al. 1974).

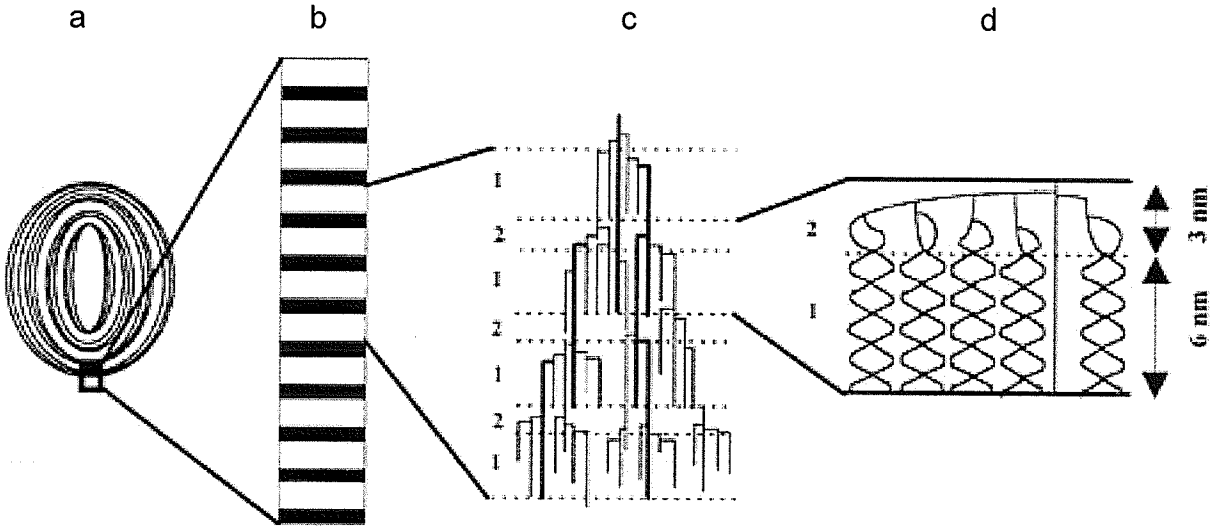

Figure 2.4. A schematic view of starch granule structure. A single granule, comprising concentric rings of alternating amorphous and crystalline regions (a); The semi-crystalline growth ring contains stacks of amorphous and crystalline lamellae (b); The currently accepted cluster structure for amylopectin with the semi-crystalline growth ring (c). A single cluster displaying the double helical structures (d) (Ball et al. 1996).

Crystalline properties

Starch granules, being partially crystalline, give distinctive X-ray diffraction patterns. X-ray scattering diffractograms of starches generally show four crystalline polymorphs: pattern A, characteristic of cereal grain starches (Cheetham and Tao 1998; Zobel 1988); pattern B, characteristic of tuber, fruit, and stem starches, such as potato, sago, and banana (Lineback 1984); pattern C, an intermediate between A and B-type patterns, characteristic of legume starches, such as pea and bean (Gernat et al. 1990; Zobel 1988); and pattern V, characteristic of crystalline amylose helical inclusion compounds (Eliasson and Gudmundsson 1996). A unit cell of B-type starch consists of two left-handed, parallel-stranded double helices that are arrayed in parallel, and contain 12 glucose residues and 36 water molecules (Fig. 2.5). The repeating unit consists of three D-glucopyranosyl units in the double helix with six residues per turn of each chain and a repeat distance of 2.1 nm (Imberty et al. 1988 a,b). The unit cell for A shows a monoclinic array containing 12 residues located in two left-handed chains (Fig. 2.6), but there are only four water molecules between the helices (Imberty et al. 1988 a,b). In the single helical (V) conformation, amylose has 6 glucosyl residues per turn, stabilized by hydrogen bonds between the hydroxyl groups of adjacent glucosyl residues. The complexing ligands, fatty acids or lipids, reside within the helix (Fig. 2.7, Zobel 1988).

The formation of crystallites is influenced by several factors. Shorter average chain length in amylopectin, high temperature during the formation of crystallites, high concentration of polymers, as well as the presence of salts with a high number in the lyothropic series, water soluble alcohols, and/or organic acids favour the formation of A- rather than B-crystals (Gidley and Bulpin 1989). Hizukuri and co-workers (1981; 1983) also suggested that the average CL of amylopectin is a major determinant of the

crystalline polymorphism observed among native starches. It was reported that amylopectins of the B-type starches have longer chain lengths than those of the A-type. Transitions between A and B through a C-state have been observed with the A-structure being the most stable:

Melt → B-Structure → C-Structure → A-Structure

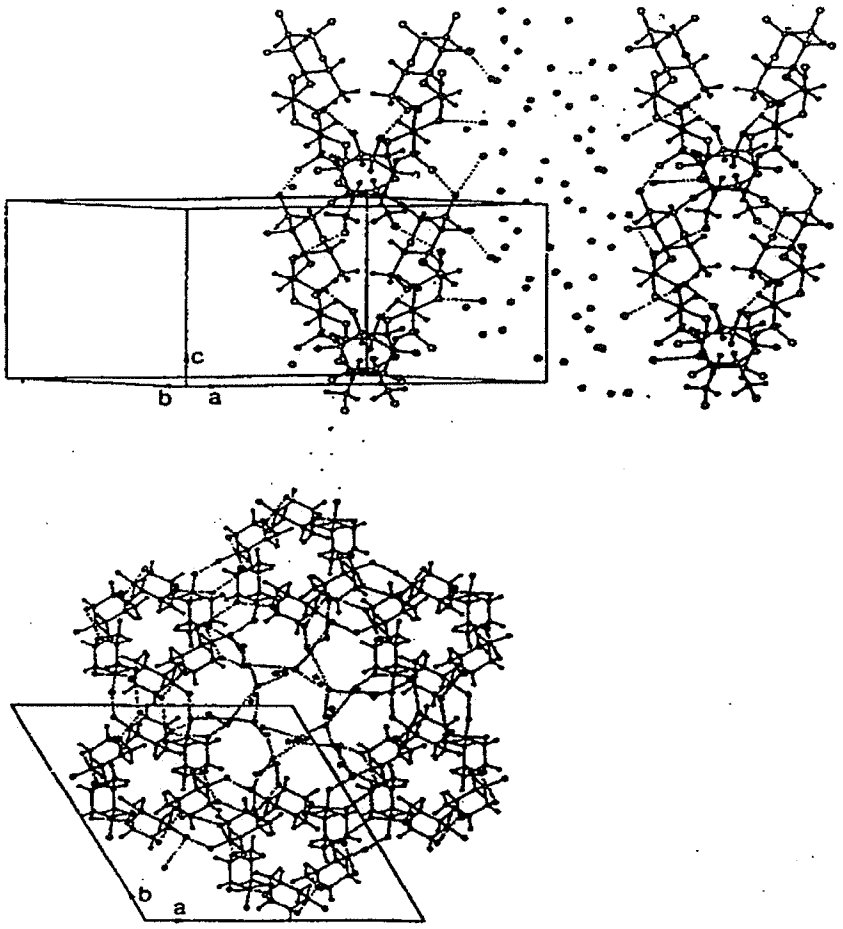

Figure. 2.5. Crystalline structure of B-starch. Top: Two strands of double helices represented in three dimensions along their fiber axis. Bottom: Projection of the structure onto the (a,b) plane showing the unit cell and nearby double helices (Zobel 1992).

- Water molecules: closed circles.
- Hydrogen bond: broken lines.

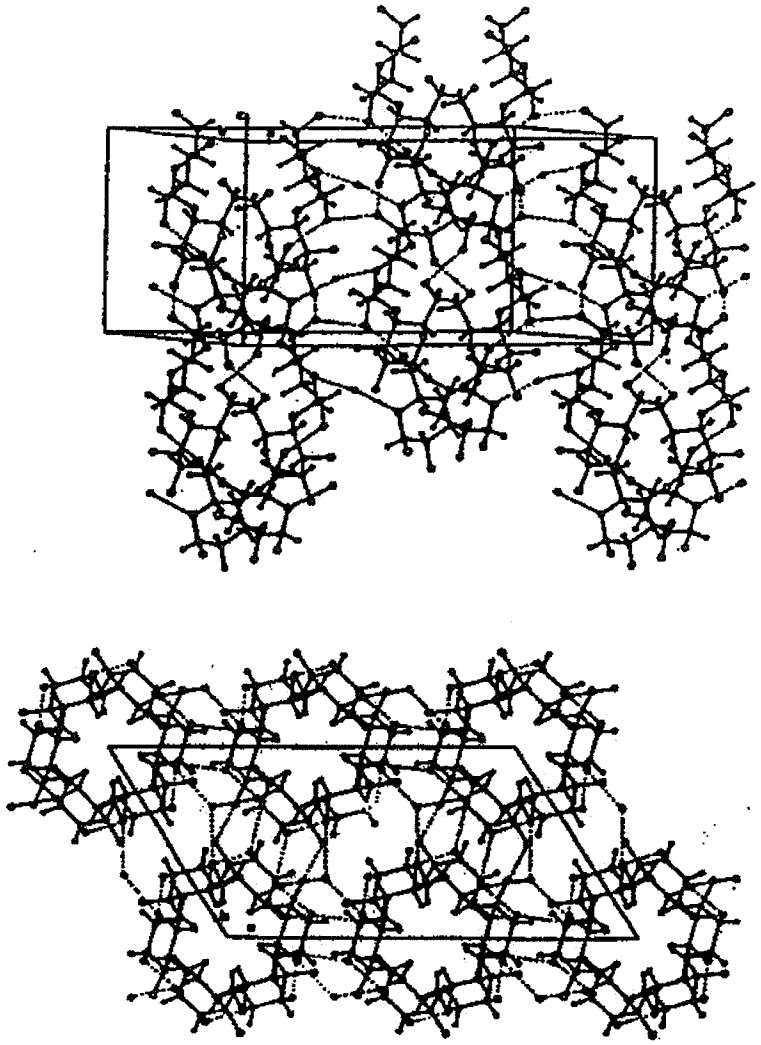

Figure. 2.6. Crystalline structure of A-starch. Top: Double helices in three dimensions along their fiber axis. Bottom: Projection of the structure onto the (a,b) plane showing the unit cell and nearby double helices (Zobel 1992).

- Water molecules: closed circles.
- Hydrogen bond: broken lines.

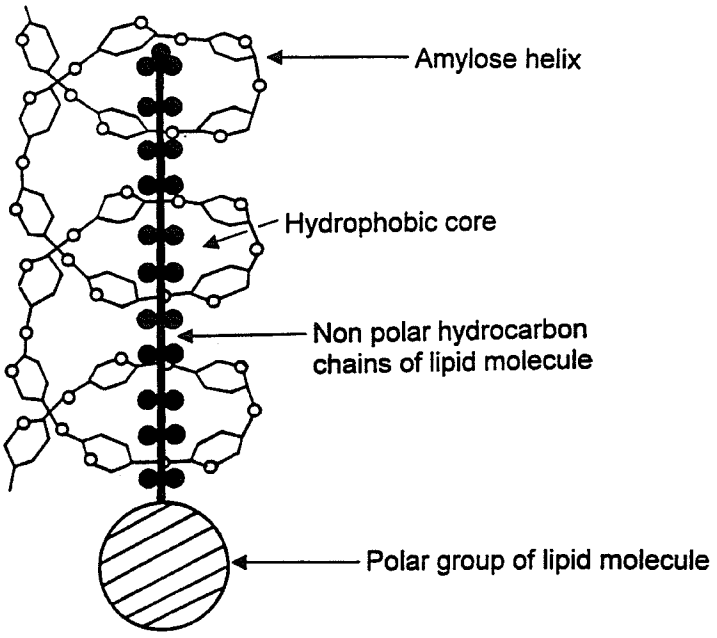

Figure. 2.7. Schematic illustration of amylose-lipid complex (Carlson et al. 1979)

Despite substantial differences in their amylose content (0-40%), all barley starches show the same A-type X-ray pattern, pointing to the lack of differences in the amylopectin structure among different barley types (Song and Jane 2000; Tang et al. 2001; 2002; Yoshimoto et al. 2000; Yoshimoto et al. 2001; Yoshimoto et al. 2002). Only Salomonsson and Sundberg (1994) reported that the average amylopectin chain length of high amylose barley starch was five glucose units longer than that of normal and waxy barley starches.

Molecular weight of starch polymers

The determination of molecular weight (M_w) and size of starch polymers has proven to be a challenging task mainly because of the difficulties associated with complete dissolution of starch polymers without their degradation and/or aggregation (Bello-Perez et al. 1998; Hanselmann et al. 1995; Jackson 1991; Millard et al. 1997; You and Lim 2000). It has been reported that although starch granules are ruptured with mechanical and thermal treatments in solvents such as DMSO or aqueous alkali solutions, the starch polymers often are not completely dispersed (Aberle et al. 1994; Banks et al. 1972). Successful applications of autoclave and microwave heating for dissolution of starch polymers have been reported (Aberle et al. 1994; Bello-Perez et al. 1998; Fishman et al. 1996; Hanselmann et al. 1995; You and Lim 2000). You and Lim (2000) showed the effect of various dissolution methods on the M_w of corn starch polymers. It was clearly shown that after dispersion of starch polymers in aqueous alkali (1M-NaOH), an additional physical treatment was necessary to provide a better solubilization of starch polymers for the improved high-performance size exclusion chromatography (HPSEC) elution of large molecules (You and Lim 2000).

Amylose and amylopectin can theoretically be separated using size exclusion chromatography (SEC) (Bello-Perez et al. 1998; Fishman et al. 1996; You and Lim 2000). However, none of the SEC columns have been able to provide a molecular weight distribution of amylopectin polymers because amylopectin elutes in the exclusion volume of the SEC columns (Hanselmann et al. 1995; Sullivan et al. 1992). This has negated the use of calibration standards for the estimation of amylopectin's molecular weight and has led to the use of a multi-angle light scattering (MALS) and a refractive index (RI) detector (Bello-Perez et al. 1998; Fishman et al. 1996; Yokoyama et al. 1998; You and Lim 2000). The absolute molecular weight of both starch polymers,

amylose and amylopectin, has been successfully measured by the HPSEC-MALS-RI system (Aberle et al. 1994; Bello-Perez et al. 1998; Fishman et al. 1996; Yokoyama et al. 1998; You and Lim 2000). The M_w values of amylose and amylopectin vary depending on the source of starch, the dissolution method, and the configuration of the HPSEC system (Aberle et al. 1994; Bello-Perez er al. 1998; Fishman et al. 1996; Klavons et al. 1997; Yokoyama et al. 1998; You and Lim 2000).

Although continuous efforts have been made to increase the resolving power of SEC columns, new techniques may offer greater improvements in separation of starch polymers. During separation in SEC columns, shear degradation or alteration of starch polymers may occur due to internal friction between starch polymers and the packing material (Yokoyama et al. 1998). Recently, the flow field-flow fractionation (flow FFF) technique has been developed as an alternative to SEC and has proven especially applicable to the separation of very high molecular weight polymers (Giddings et al. 1992; Giddings 1995). In contrast to the tubular shaped and packed size exclusion columns, flow-FFF consists of a thin, rectangular shaped channel with no packing material. Fractionation takes place in a completely liquid medium, therefore, there is less shearing of large molecules and no interaction with packing material in the FFF channel (Jiang et al. 2000). The actual separation of macromolecules is a function of their differential diffusion coefficient against the cross flow and the parabolic profile of the channel flow (Giddings and Caldwell 1989). A liquid flow having a parabolic velocity profile is pumped through the flow-FFF channel during separation and transports the sample components through the channel and to the detectors. An external field, perpendicular to the channel flow, called the cross flow, is also applied. The cross flow forces the sample components towards the accumulation wall, where they form a characteristic concentration distribution. Small sample components with high diffusion coefficients travel a greater distance from the accumulation wall and are transported through the flow-FFF channel more rapidly due to the parabolic velocity profile of

channel flow. High MW species, on the other hand, remain closer to the accumulation wall where the flow is sluggish and are retained in the channel longer. Generally, sample components are eluted in the order of increasing size: small molecules first, followed by large molecules (Giddings and Caldwell 1989).

The coupling of flow FFF and the MALS detector made possible the separation and characterization of large macromolecules such as polivinyl pyrrolidone (Jiang et al. 2000), dextran, and pullulan (Wittgren and Wahlund 1997). Most recently, it has been demonstrated that fractionation of starch polysaccharides using the flow FFF-MALS-RI system was a promising alternative to the SEC-MALS-RI system (Roger et al. 2001). However, no M_w data could be obtained for amylose polymers due to the weak MALS signals, and the repeatability of the results was not confirmed (Roger et al. 2001). Therefore, further modifications of the flow FFF-MALS-RI method are still required for the proper determination of the molecular weights of amylose and amylopectin polymers.

Physical properties

Gelatinization. The term "gelatinization" is used to describe the swelling and hydration of granular starches, as well as the melting of starch crystallites which occurs when starch is heated in the presence of water (Biliaderis 1990; Cooke and Gidley 1992; Donovan 1979; Eliasson and Gudmundsson 1996; French 1984). Native starch granules are insoluble in water below their gelatinization temperature due to the semicrystalline structure of the starch granule and the hydrogen bonds formed between hydroxyl groups in the starch polymers (Eliasson and Gudmundsson 1996). When dry starch granules are placed in water, a small amount of water is absorbed. It has been reported that starch granules swell slightly in cold water (10-20%), due to the diffusion and absorption of

water into the amorphous regions; however, this swelling is reversible upon drying (Biliaderis 1989). When starch granules are heated in water to higher temperatures, a point is reached at which granule swelling becomes irreversible and structural order disappears (Biliaderis 1990; Cooke and Gidley 1992; Donovan 1979; Eliasson and Gudmundsson 1996; French 1984;). The gelatinization occurs over a certain range of temperatures (Fig. 2.8). For a single starch granule in an excess amount of water this temperature range may be 1-2 °C, whereas for a whole population of granules it spreads over 10 to 15 °C (Evans and Haisman 1982; Liu and Lelievre 1993).

During the gelatinization of starch granules, a number of structural changes occur. With the onset of gelatinization (T_o), the birefringence begins to disappear. This loss of birefringence, measured by an optical microscope with crossed polarizers and a heating stage, indicates the loss of order in the granules (Burt and Russell 1983; Eliasson 1983). As the starch suspension is continuously heated, the crystallites start to melt, causing the X-ray diffraction pattern to disappear (Zobel 1988). Since gelatinization is an endothermic process, thermal analysis methods and differential scanning calorimetry (DSC) in particular, have been used to follow the changes in starch granules during gelatinization (Biliaderis 1990; Cooke and Gidley 1992; Donovan 1979; French 1984). Several factors affect the gelatinization temperature of starch granules, including the amount of water, chain length of linear branches in amylopectin, the extent of crystalline perfection, double helical and crystalline orders, and amylose content (Jane et al. 1999; Sasaki et al. 2000).

Among various types of corn starches, the high amylose maize V and VII starches display much higher onset (T_o) and melting temperatures (T_p) (by 6-7 °C) than normal and waxy corn starches (Jane et al. 1999). These differences are attributed to much

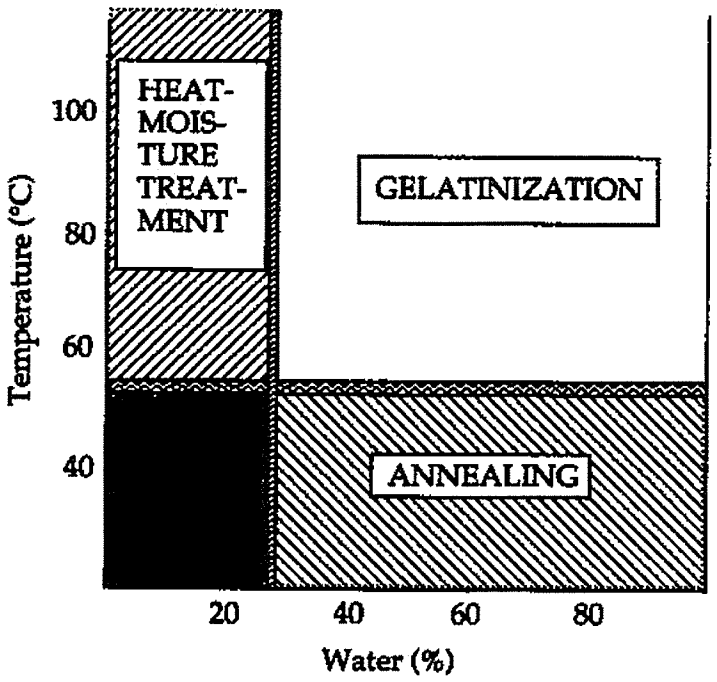

Figure. 2.8. Different combinations of starch, water, and temperatures that influence starch behaviour (Eliasson and Gudmundsson 1996)

longer branch chain lengths in high amylose than in waxy and normal maize starches (Jane et al. 1999). Studying a variety of barley starches, Vasanthan and Bhatty (1996) reported the highest T_p for high amylose barley starch (65.7 - 68.4 °C), followed by waxy (62.6 - 64.0 °C), and normal starch (58.0 - 61.0 °C). However, very small differences in T_p between high amylose (62.8 - 63.2 °C) and normal barley starch (59.0 - 60.3 °C) were reported by Song and Jane (2000). These authors also reported that amylopectins in all barley starches had relatively short branched chain lengths and a low proportion of longer chains (DP 18-21), suggesting a defective crystalline structure responsible for the very low T_p in barley starches.

Gelation and Retrogradation. Depending on the concentration, a gelatinized starch dispersion takes on the consistency of either a loose paste or gel upon cooling. At concentrations above the critical concentration (usually > 6%), a gelatinized starch dispersion will develop a three-dimensional network forming a viscoelastic gel, in which the swollen granules are embedded into a continuous matrix of entangled amylose molecules (Ring 1985). The associations of starch polymers in a gel are attained mainly by non-covalent hydrogen bonds between the chains.

The rheological behaviour of starch gels is influenced predominantly by the amount and characteristics of both dispersed (amylopectin-enriched swollen granules) and continuous (amylose network) phases as well as by the interactions of starch components with water (Launay and Lisch 1983). Starch gelation is an important quality determinant in many processed food systems, including baked and extruded products, soups, and dressings.

Amylose, due to its linear nature, is considered to be primarily responsible for the gelation of starch. Amylose gels generally exhibit a rapid rise in storage modulus (G'), followed by a phase of much slower increase in G' at longer times (Fig. 2.9, Biliaderis and Zawistowski 1990; Clark et al. 1989; Gidley 1989). The first step of amylose gelation is a network formation, in which the left-handed double helical chain segments are formed. This is followed by aggregation of helices and formation of the B-type structures (Clark et al. 1989; Gidley 1989). At concentrations above 1.5%, a gel is formed, while for concentrations below 1.5% (w/w), a precipitate is formed (Ellis and Ring 1985). After the initial network is established, the strength of the amylose gel improves with time due to subsequent chain aggregation (Miles et al. 1985b). Amylose gels are thermally stable and do not melt even after being heated to 120 °C (Ellis and Ring 1985).

In contrast to amylose, amylopectin gelation requires much higher polysaccharide concentrations (usually above 10%) (Ring et al. 1987). The rate of gel formation is very slow and a constant value of G' cannot be obtained even after 30-40 days (Fig. 2.10, Ring et al. 1987). The elasticity and rigidity of amylopectin gels originate from the formation of partially crystalline structures by the outer linear chains of amylopectin (Biliaderis 1998; Clark et al. 1989; Gidley 1989). The rate of gelation varies with the origin of amylopectin; for example, it can be very high for pea and very low for maize starches (Kalichevsky et al. 1990). Amylopectin gels are thermo-reversible, and they melt when heated to 40-60 °C (Ring et al. 1987).

Since starch gels are metastable, non-equilibrium systems, they undergo structural transformations as a result of further chain aggregation and recrystallization during storage which leads to the formation of more ordered structures and eventually crystallites (Kulp and Ponte 1981; Ring 1985; Swinkels 1985). These molecular interactions are collectively termed "retrogradation". According to the definition of Miles et al. (1985a), retrogradation consists of two separate processes: gelation of amylose molecules exuded from the granules during gelatinization and recrystallization of amylopectin (Miles et al. 1985a,b). The initial development in firmness is attributed to a rapid establishment of a cross-linked network of amylose chains at concentrations above the coil overlap concentration (~1.5%). Subsequent increases in rigidity of starch gels are linked to recrystallization of amylopectin short chains (Ring et al. 1987). This process exerts a major and usually unacceptable influence on the texture of foods rich in starch, by squeezing water out of gels and pastes (Biliaderis 1998; Hoseney 1994). Retrogradation has been considered the main factor responsible for staling of bread and other baked products (Eliasson and Gudmundsson 1996; Kulp and Ponte 1981).

Retrogradation is a complex process and depends on many factors, such as starch

origin, amylose/amylopectin ratio, fine molecular structure of both polymers, concentration, cooking and cooling regimes, pH, and additives (lipids, salts, and sugars) (Swinkels 1985). Waxy barley starch was reported to have a lower degree of retrogradation than waxy maize and waxy rice starches (Shi and Seib 1992). It was postulated that starch retrogradation appeared to be directly proportional to the mole fraction of unit chains with DP 14-24 and inversely proportional to the mole fraction of DP 6-9. Repeated freeze-thaw cycles were reported to drastically accelerate the retrogradation and syneresis processes (Radley 1976). Mestres and co-workers (1988) reported that after extrusion cooking, amylose and amylopectin polymers appear to co-crystallize, whereas after drum drying, amylose and amylopectin polymers crystallize separately.

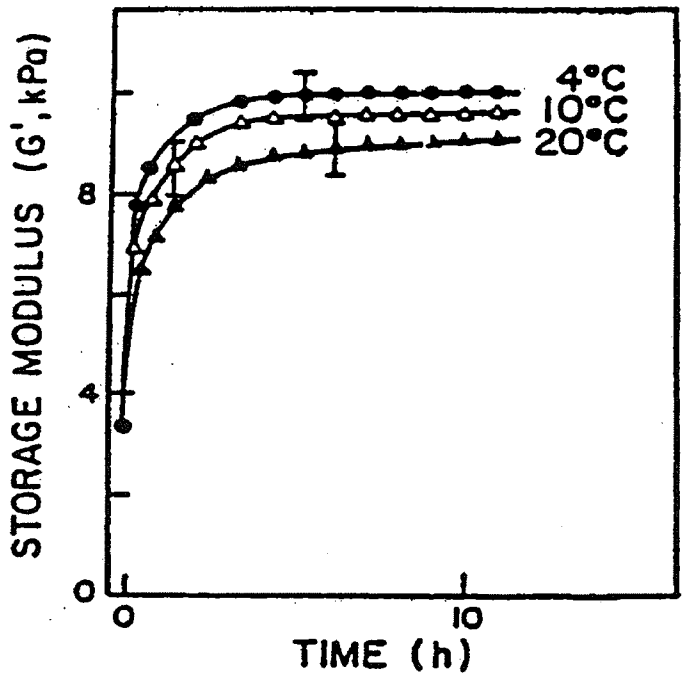

Figure. 2.9. Storage modulus (G') vs. time for 5% (w/w) amylose gel at various temperatures (Biliaderis and Zawistowski 1990).

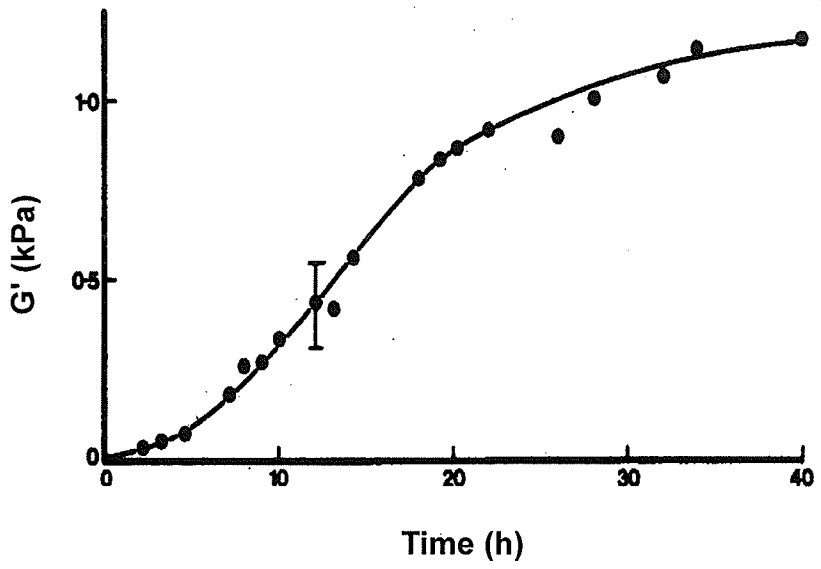

Figure. 2.10. Storage modulus (G') development of 20% (w/w) waxy maize amylopectin gel at 1°C (Ring et al. 1987).

Starch Modifications

α-Amylolysis. α-Amylolysis is a degradation process catalyzed by enzymes (α-amylases) that cleave the inner α-(1-4)-glycosidic linkages of starch polymers, and produce a complex mixture of linear and branched α-dextrins (Myrback and Neumuller 1950). α-Amylolysis is used in the production of sweeteners, maltodextrins and low dextrose equivalency (DE) syrups, and chemicals. α-Amylolysis is also used as a probe for studying the ultrastructure of starch (French 1984; Gallant et al. 1997; Nigam and Singh 1995).

α-Amylolysis of barley starches exhibits a two-stage hydrolysis pattern; a relatively fast rate of hydrolysis initially, followed by a slow rate thereafter (Fig. 2.11, Li et al. 2004; MacGregor and Ballance 1980; Vasanthan and Bhatty 1996). The rapid rate of α-amylolysis at the initial stage was attributed to the preferential hydrolysis of the amorphous regions in starch granules (Li et al. 2004; Vasanthan and Bhatty 1996).

At the later stage, α-amylolysis was suggested to be confined mainly to the crystalline regions of the starch granules. The rate of α-amylolysis at the second stage is thus dependent on starch crystallinity (Vasanthan and Bhatty 1996). Recently, however, Lauro et al. (1999) suggested that α-amylase was able to simultaneously solubilize the amorphous and crystalline regions.

Among the different types of barley starches, waxy starch is the most readily hydrolyzed during the initial stage of α-amylolysis, whereas high amylose starch is the least (Vasanthan and Bhatty 1996). The authors suggested that the highly compact amorphous regions of high amylose starches resist the penetration of the enzyme, thereby suppressing the hydrolysis rate. In addition, the higher lipid content in high amylose starches, compared to that in waxy and normal starches, was suggested to impart some degree of resistance to α-amylolysis (Vasanthan and Bhatty 1996). Li et al. (2004), however, reported that high amylose barley starch showed a higher rate of hydrolysis than normal starch during the initial stage of α-amylolysis (0-20h) (Fig. 2.11). The authors suggested that the increased susceptibility of high amylose starches to amylases compared to that of normal starches is perhaps due to the higher proportion of small granules in high amylose barley starch. Small granules showed a higher degree of hydrolysis than large granules, which was attributed to the higher surface area per unit weight of the former (Li et al. 2004; MacGregor and Ballance 1980; MacGregor and Morgan 1986; Vasanthan and Bhatty 1996).

The pattern of enzyme attack on starch granules was reported to vary for small and large granules and for types of barley starches (Vasanthan and Bhatty 1996). While the small granules from waxy starch showed erosions only on the granule surface, the large granules exhibited both surface erosion and pinholes.

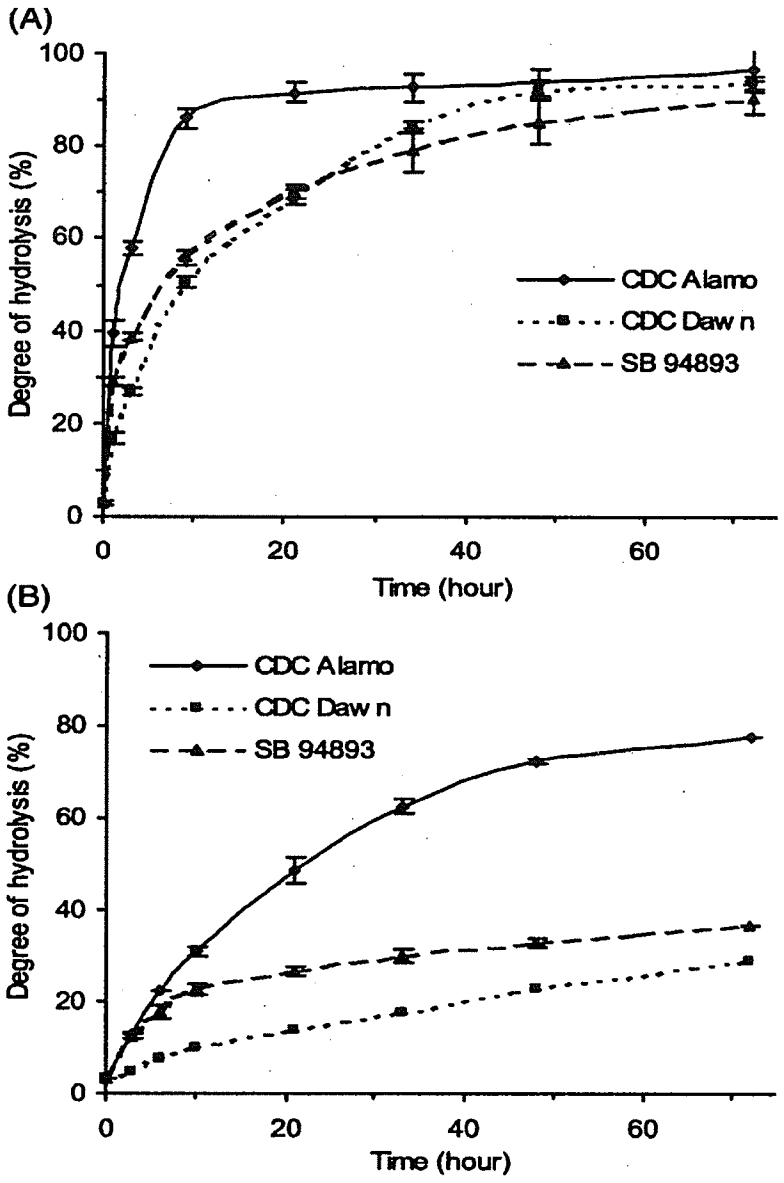

Figure. 2.11. Hydrolysis patterns of hulless barley starches of waxy (CDC Alamo), normal (CDC Dawn), and high amylose (SB 94893) types by α-amylases from porcine pancreas (A) and from *Bacillus species* (B) (Li et al. 2004).

Normal starch showed pinholes and appeared to be hydrolyzed from inside out, whereas high amylose starch granules only had surface erosion. Lauro et al. (1999) also suggested that α-amylolysis of large barley starch granules (normal type) proceeds through pinholes from the inside out.

Lauro et al. (1999) reported a substantial decrease of the molecular weight of starch polymers after partial α-amylolysis (46% solubilized). However, Colonna et al. (1988) reported that even after 91% hydrolysis, the molecular size of wheat starch residues was similar to that of the native starch, with the exception of a small peak at a lower molecular weight area. Leach and Schoch (1961) also reported that after 50% hydrolysis of corn and sorghum starches the intrinsic viscosities of the starch residues were very similar to those of the parent starches.

Acid/alcohol hydrolysis. Acid hydrolysis is a traditional method to modify native starches and to alter their solubility, viscosity, and/or gelation properties (Kerr 1952; Leach et al. 1959). During acid hydrolysis, the hydroxonium ion (H_3O^+) carries out an electrophilic attack on the oxygen atoms of the α-(1-4)-glycosidic linkages, cleaving the linkages and reducing the chain length of the starch polymers (Wolrom et al. 1963).

A two-stage hydrolysis process was observed, when various types of barley starches were hydrolyzed with 2.2 N HCl at 35 °C (Fig. 2.12, Li et al. 2001; Vasanthan and Bhatty 1996). It has been suggested that the relatively fast hydrolysis of starch polymers that occurs mainly in the amorphous regions of starch granules was followed by a slower hydrolysis of the densely packed crystalline regions (Vasanthan and Bhatty 1996). Among the different types of barley starches, high amylose starches were reported to be the least susceptible to acid hydrolysis, whereas waxy starches were the most (Li

et al. 2001; Vasanthan and Bhatty1996). At the initial stage of hydrolysis, the lower susceptibility of high amylose starch was attributed to the highly compact amorphous regions, which seemed to resist the penetration of acid into the granules (Vasanthan and Bhatty 1996). At the later stage of hydrolysis, differences in hydrolysis became significantly larger among different types of barley starches, implying that the starches differ with respect to the organization of the double helical chains within their crystalline domains (Li et al. 2001).

Ma and Robyt (1987) hydrolyzed potato and waxy maize starches with 0.36% HCl in various alcohols (methanol, ethanol, 2-propanol and 1-butanol), and reported that the rate of hydrolysis was strongly dependent on the type of alcohol used to carry out the hydrolysis. It was observed that the DP values of the dextrins produced during hydrolysis were dependent on the combination of acid and alcohol used for the modifications. It was suggested that by varying the concentration of acid and the type of alcohol, starch hydrolyzates with desirable DP values could be obtained. Compared to the Lintner procedure (Lintner 1886), the time required to produce soluble starch by the acid/alcohol treatment was substantially reduced (from 1 week to 1 hour).

The DP values of the modified starches were dependent on the source of starch as well as on the type and ratio of alcohols used to carry out the hydrolysis. It was suggested that the various alcohols produce different modifications of native starch granules because of different concentration of acid inside the granule. In addition, however, there was also differential susceptibility to hydrolysis of the various glycosidic bonds in the granule, depending on the alcohol used and the concentration of the acid.

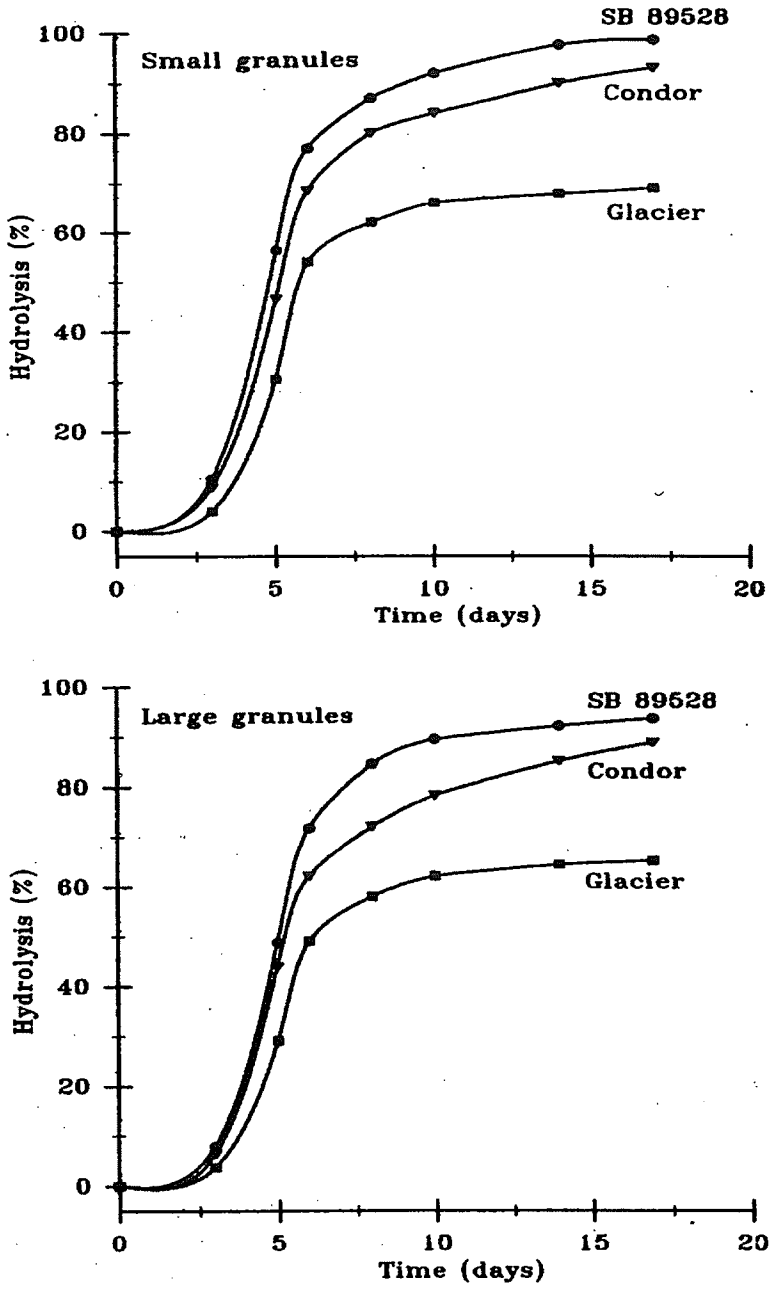

Figure. 2.12. Acid hydrolysis patterns of small and large hulless barley starch granules from SB 89528 (waxy), Condor (normal), and Glacier (high amylose) (Vasanthan and Bhatty 1996).

Starch/hydrocolloid blends. The rheological properties of starch and hydrocolloid blends have been investigated in several studies (Alloncle et al. 1989; Alloncle and Doublier 1991; Christianson et al. 1981; Eidam et al. 1995; Freitas et al. 2003; Kulicke et al. 1996; Liu et al. 2003; Sajjan and Rao 1987; Tye 1988; Yoshimura et al. 1996; 1998; 1999). Alloncle et al. (1989) studied the rheological properties of corn starch-galactomannan mixtures, and found that the blends exhibited higher viscosity than individual polymers. The authors suggested that in starch blends, described as suspensions of swollen particles dispersed in a continuous macromolecular medium, the galactomannan polymers are located in the continuous phase. Therefore, the dramatic increase in viscosity of the mixed systems was attributed to a relative increase in galactomannan concentration induced by the swelling of the starch granules during gelatinization and by the incompatibility between amylose and galactomannans (Alloncle et al. 1989; Eidam et al. 1995; Kulicke et al. 1996).

Eidam et al. (1995) investigated the viscoelastic behaviour of blends of maize starch and various hydrocolloids. The authors found that the kinetics of gel formation and the viscoelasticity of the blends were strongly dependent on the kind of hydrocolloid. The presence of hydrocolloids in starch paste increased the viscous property but generally decreased the elastic property of the mixture systems (Eidam et al. 1995; Kulicke et al. 1996; Yoshimura et al. 1998; 1999). It was suggested that hydrocolloids did not physically interact with the starch polymers to form network structures. In general, the presence of a hydrocolloid prevented the formation of permanent cross-links among starch polymers and reduced the elasticity of the systems (Eidam et al. 1995). Kulicke et al. (1996) proposed that by increasing the amount of galactomannan in the mixture, the number of permanent network points (junction zones) formed by starch polymers decreased, while the number of temporary network points, attributed to

galactomannan entanglements increased. ι-Karrageenan, on the other hand, initially retarded the gelation of the blend, but eventually increased its elastic property (Eidam et al. 1995). It was suggested that specific intermolecular interactions which occurred between ι-karrageenan and amylose polymers increased the rigidity of the blends. Liu et al. (2003) also reported that the addition of yellow mustard mucilage (YMM) to wheat and rice starches increased hardness, adhesiveness, chewiness, and springiness of their gel textures, indicating some interactions between YMM and starch polymers.

CHAPTER 3

Molecular Characteristics of Barley Starches with Various Amylose Content[1]

Abstract

The granular and molecular characteristics of four types of hulless barley starches (normal, high amylose, waxy and zero amylose) were investigated by particle size analysis and size exclusion chromatography (SEC) with light scattering detection. Although bimodal size distribution of granules was observed for normal, waxy and zero amylose starches, the proportion of large to small granules for each type of starch differed substantially. The granular size distribution of high amylose starches was unimodal, showing the highest proportion of small granule (3 μm). For the intact starch molecules, weight average molecular weights (M_w) of high (amylopectin) and low (amylose) molecular weight fractions were in the range from $136x10^6$ to $305x10^6$ and from $2.73x10^6$ to $5.67x10^6$, respectively. The lowest M_w values were observed for amylopectin in high amylose starches. A good correlation ($r^2 = 0.96$) between M_w and radius of gyration (R_g) of all amylopectins was found. After debranching of starch samples, significantly lower M_w values were observed for amylose, indicating the existence of branches in amylose molecules. Debranched amylopectins exhibited trimodal distributions of long B, intermediate B and short B+A chains. The longest amylopectin branches were found in high amylose barley starches.

[1]Published in Carbohydrate Polymers (2002) 49:33-42 by S. You and M.S. Izydorczyk

Introduction

The ever growing interest in barley as a component of food systems has stemmed largely from the potential health benefits of β-glucans, a group of minor non-starch polysaccharides, present in barley grain. The other abundant group of barley polysaccharides, starch polymers, has also attracted scientific attention, although not as extensive as, for instance, corn, potato or wheat starches. Some of the recently developed hulless barley genotypes contain starches with a broad range of amylose content, varying between 0 and 40% (Izydorczyk et al. 2000). Since the amylose content is known to affect various functional properties, such as gelatinization, pasting, and swelling, variability in amylose level predisposes barley starches for a wide range of applications in food production. Barley starches contain both small and large granules, and a bimodal distribution of starch granules was reported by Jane et al. (1994), MacGregor and Fincher (1993), and Morrison et al. (1986). The small and large starch granules can be fractionated by decantation (Takeda et al. 1988), and by pin-milling and air-classification (Vasanthan and Bhatty 1995) techniques. Recent studies have shown, however, that there are no significant differences in the molecular structure of starch polymers from small and large granules (Tang et al. 1999; Vasanthan and Bhatty 1996).

The length and distribution of linear branch chains in barley amylopectin can be typically determined by enzymic hydrolysis of the branching points (α-(1→6) linkages), followed by either gel permeation chromatography (GPC) or high performance anion-exchange chromatography (HPAEC) combined with an enzyme reactor and a pulse amperometric detector (ENZ-PAD). Tester et al. (1991) reported no variations in chain lengths of debranched amylopectins from normal, waxy and high amylose starches, as measured by GPC on Sepharose CL 6B. Song and Jane (2000), using HPAEC-ENZ-PAD,

also observed no difference in the trimodal chain profiles and chain lengths of debranched amylopectins from normal, waxy and high amylose barley starches, but showed differences in the presence of chains with the highest detectable degree of polymerization (DP) values. They found that the highest detectable DP values of normal, waxy and two types of high amylose debranched amylopectins were 82, 67, 79 and 78, respectively. Salomonsson et al. (1994), on the other hand, reported bimodal distributions of debranched amylopectins and found that the average chain length of high amylose debranched amylopectin chains was five glucose units longer than those of normal and waxy amylopectin chains. The M_w of barley starch polymers, amylopectin and amylose, has not yet been accurately measured.

Because of their availability and unique characteristics, barley starches may have a potential for providing useful materials for targeted food products. More thorough and systematic studies, however, are needed to fully elucidate the molecular structure of barley starches and explain the origin of their physical and functional properties. In this study, barley starches were carefully extracted from several barley genotypes with a wide range of amylose content, and the molecular structure of amylose and amylopectin polymers was examined.

Materials and Method

Materials

Four genotypes of hulless barley starches - normal, high amylose, waxy and zero amylose - isolated from eight varieties of barleys, were assessed. One variety, Falcon, obtained from James Farms Ltd. (Winnipeg, MB), was grown in 1998 in Manitoba, Canada. The others, SB90354, 92-55-06-54, 92-55-06-48, CDC Candle, SR 93139, SB94792 and CDC-Alamo, were grown in 1997 in Saskatchewan, Canada, at the Crop Development Centre, University of Saskatchewan, Saskatoon, Canada.

Chemical analyses

The starch content in barley samples was measured enzymatically using the total starch assay kit (Megazyme, Ireland). The results are reported on a dry weight basis. Amylose content in de-fatted barley starches was determined by the potentiometric titration method (Schoch 1967). Barley samples were de-fatted by extraction in the Soxhlet apparatus with 3:1 (v/v) n-propanol : water for 12 h prior to the amylose determination.

Isolation of starch

The starch isolation procedure used in this study was based on the methods of Morrison et al. (1984), South and Morrison (1990) and Sulaiman and Morrison (1990). Two additional enzymes, lichenase and β-xylanase were applied to disrupt the cell walls and release starch granules, thereby enhancing the quantity of isolated starch. Coarsely grounded barley kernels (10g) were steeped in 0.02N HCl (100mL) solution and swirled gently overnight at 4°C. After neutralization with 0.2N NaOH and centrifuging at 4000*g*,

the precipitate was scraped into a mortar with 30mL of 0.1M Tris-HCl buffer containing 0.5% $NaHSO_3$ (pH 7.0), followed by enzyme treatments, proteinase K (15 U/g barley, Roche Diagnostics Ltd. Canada), lichenase (2 U/g barley, Megazyme) and β-xylanase (8 U/g barley, Megazyme). The samples were digested overnight in a Neslab EX-700 shaking water bath (shaking speed=1) at 25°C. After incubation, the contents were sieved on a 75μm (#200) sieve, followed by centrifuging (28,000*g*, 10 min) the slurries. The precipitate was re-suspended with 4mL of water and then layered over 100mL of 80% CsCl solution, followed by centrifuging at 28,000g for 30 min. After centrifuging, the starch pellet was washed with water and filtered on a 0.45μm membrane (HVLP). Approx. 10mL of acetone was filtered through the starch to remove remaining water. The starch was allowed to air-dry overnight.

Size distribution of starch granules

Granule size distribution was determined using a computer assisted Olympus Image Analyzer System and CUE 2 software. The purified starch (20mg) was dispersed thoroughly in 500μL of 20 times diluted iodine solution, followed by centrifuging shortly at 5,000rpm. The residue was spread on a slide glass with two drops of water containing 0.1% Tween, and then measured by an Olympus microscope through a CCD video camera. At least five random microscope fields were measured per sample.

Determination of M_w of starch polymers

Solubilization of starch. Granular starch was gelatinized and then purified with 90% DMSO and alcohol precipitation, as stipulated by the method of Jane and Chen (1992). The purified starch (7mg) was steeped in ethyl-alcohol (0.1mL), redissolved in 1N NaOH (1mL), diluted with water (8mL) and neutralized with 1N HCl. The starch

solution was autoclaved for 20 min (121°C), filtered through a 3.0μm cellulose acetate membrane, and then injected into the high-performance size exclusion chromatography (HPSEC) coupled with multi-angle light scattering (MALS) and refractive index (RI) detection system.

Preparation of debranched starch. The starch solution (3mL), dissolved as above, was incubated with isoamylase (500 units) in 1mL of acetate buffer (0.1M, pH 3.5) for 24 hrs at 40°C (Ramesh et al. 1999). After incubation with the enzyme, the digested starch solution was neutralized with 1N NaOH, heated in a boiling water bath for 5 min to stop enzyme activity, filtered through a 0.45μm membrane, and finally injected into the HPSEC-MALS-RI system. The profiles of debranched zero amylose waxy starch were used to evaluate the completeness of debranching with isoamylase. After 24 hrs of incubation with the enzyme, a complete hydrolysis of amylopectin (zero amylose starch) was verified, as indicated by the lack of any high molecular weight material in the elution profile.

HPSEC-MALS-RI system. The calibration constants of the RI and MALS detectors were determined by the method of You et al. (1999). Normalization of the photo diodes located around the scattering cell was done using BSA. The HPSEC system consisted of a pump (Waters 510), an injection valve (Model 7010, Rheodyne) with a 200μL sample loop, a guard column (TSK PWH, Tosoh Corp.), SEC columns, MALS (Dawn DSP, Wyatt Technology) and RI (Waters 410). For intact starch molecules, only TSK G5000 PW column (7.8×600mm, TSK PW, Tosoh Corp.) was used to determine the profiles of amylopectin and amylose; however, TSK G2500 PWXL (7.8×300mm, TSK PWXL, Tosoh Corp.), TSK G3000 PWXL (7.8×300 mm, TSK

PWXL, Tosoh Corp.) and TSK G5000 PW columns were employed to get the profiles of debranched amylopectin and amylose molecules. The columns were kept at room temperature. The flow rate of mobile phase (0.15M $NaNO_3$ containing 0.02% NaN_3), which was filtered through 0.2μm and then 0.1μm of cellulose acetate membranes, was 0.4mL/min. Calculations of M_w and R_g were performed by the Astra 4.72 software (Wyatt Technology) using the Berry extrapolation method. Pullulan standards with known M_w values (P-50, M_w 47,300; P-400, M_w 404,000; P-800, M_w 788,000) were used to determine the proper experimental setup and calculations.

Results and Discussion

Amylose content and granular size distribution

Eight starch preparations were isolated from barley varieties with varying content and composition of starch polymers (Table 3.1). The highest amount of starch was found in the two normal barley varieties, whereas the genotypes with atypical amylose content contained substantially less starch. This is in agreement with previous reports, which also observed that some barley genotypes with an altered ratio of amylose to amylopectin contained lower amounts of starch (Bhatty and Rossnagel 1998; Oscarsson et al. 1996). It appears that the presence of waxy or high amylose genes in barley may substantially affect the carbohydrate metabolism in the grain. High amylose and waxy barleys were reported to contain significantly higher β-glucan content than their normal counterparts (Bhatty 1999; Izydorczyk et al. 2000). Xue et al. (1997) reported higher content of free sugars as well as β-glucans in six waxy barley isotypes.

The yield of isolated starches corresponded well with the starch content of the barley samples used, indicating that no losses, especially of small granules, occurred during the isolation process. The purity of the starch preparations was greater than 99% in all cases as revealed by the starch content of the samples (results not shown).

Barley starches are known to consist of a mixture of large, lenticular granules (10-25μm) and smaller, irregularly shaped granules (<10μm) (MacGregor and Fincher 1993) distributed in a bimodal fashion. Our study confirmed those results: the granule diameter ranged from 2 to 26μm (Fig. 3.1). The relative frequency of small and large granules differed, however, among the different types of starches, and the distribution did not follow the bimodal pattern in all cases. The greatest amount of large granules

Table 3.1. Starch and amylose content in various genotypes of barley.

Barley	Starch content[a] (%, w/w)	Starch yield[b] (%)	Amylose content[c] (%)
Normal			
Falcon	62.0±0.4	62.8	23.7
SB90354	58.7±0.5	58.1	24.3
High amylose			
92-55-06-54	53.0±0.5	55.8	41.5
92-55-06-48	53.7±0.4	54.4	41.9
Waxy			
CDC Candle	56.0±0.6	58.2	4.2
SR93139	55.5±0.4	56.0	5.8
Zero amylose			
SB94792	53.5±0.4	56.1	0
CDC Alamo	52.7±0.5	55.5	0

[a] Results reported on a dry weight basis n=2 ± SD.

[b] Yield of starch obtained after isolation from whole barley.

[c] Determined by potentiometric titration with iodine.

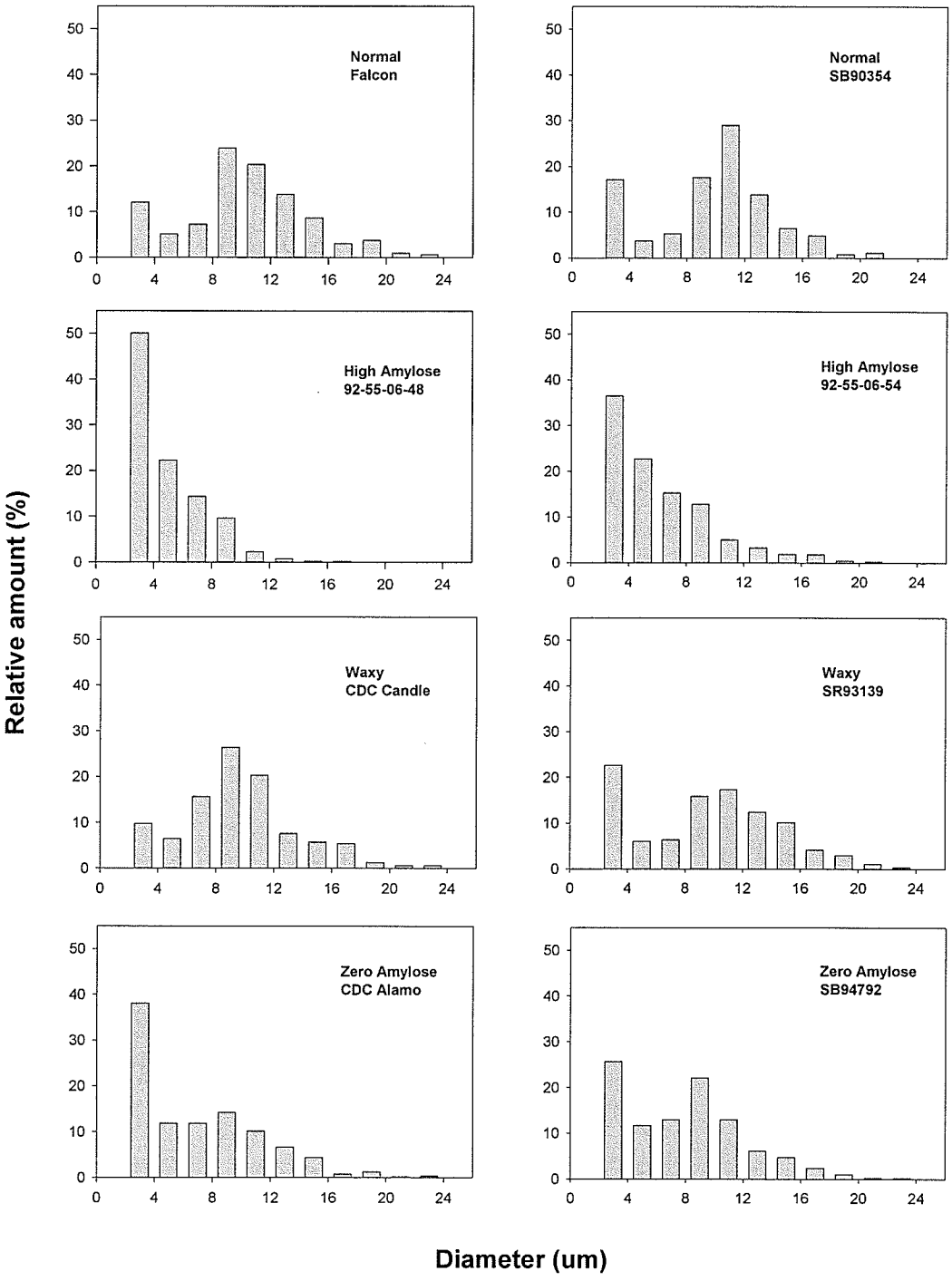

Figure 3.1. Size distribution of granules in barley starches with variable amylose content

($\geq$ 8μm in diameter) was found in normal starches (74.7%), whereas the smallest in high amylose starches (19.4%). The waxy and zero amylose waxy starches contained 66.4% and 43.9% of the large granules, respectively. Even though the proportion of large to small granules in normal and waxy starches differed substantially, their bimodal distribution was still observed. High amylose starch granules, on the other hand, were distributed unimodally, with the highest proportion of 3μm granules and sharply decreasing amounts of larger granules. Some differences in the granule size distribution were observed not only among the different types of barleys but also between samples within the same starch type.

M_w and R_g of starch polymers

The elution profiles of various barley starches from the SEC column are presented in Fig. 3.2. The chromatograms indicate a good separation of the large and small molecular weight starch components. The first, high molecular weight peak in the chromatograms, with concentration maxima at the elution volume (V_e) of approximately 12.0mL, constitutes the majority of amylopectin fraction in each starch sample, whereas the second, low molecular weight peak, at V_e maximum about 16.0mL, corresponds largely to amylose. The relative proportion of the two peaks gives some indication of the concentrations of amylose and amylopectin in each type of starch. However, determination of amylose content in the samples on the basis of chromatographic data (i.e. integration of peaks) would likely lead to an overestimation of amylose content because some amylopectins also elute in the lower molecular weight region, traditionally assigned to amylose.

The weight average molecular weights of high and low molecular weight

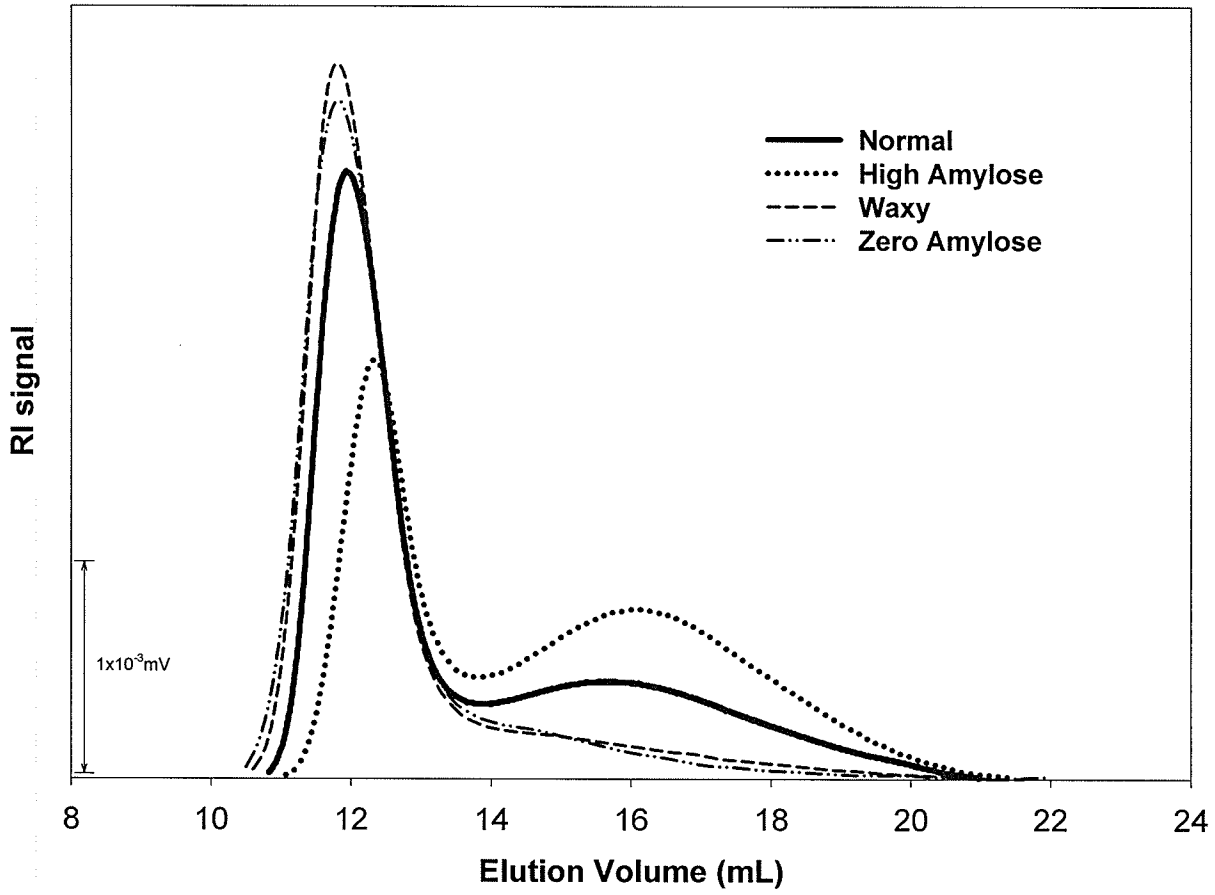

Figure 3.2. HPSEC profiles of normal (Falcon), high amylose (92-55-06-48), waxy (CDC Candle), and zero amylose (CDC Alamo) barley starches.

components in each starch sample are compiled in Table 3.2. There were significant differences in the molecular weights and radii of gyration among the high M_w polymers (amylopectins). Amylopectins from waxy and zero amylose starches had the highest average molecular weight, whereas those from high amylose starches the lowest. Interestingly, there was a good correlation ($r^2 = 0.96$) between the molecular weights of all amylopectins and their dimensions, as estimated from the R_g. Figure 3.3a shows the relationship between the molecular weights and the elution volume. Some differences in the slopes of M_w dependence on V_e among amylopectins from different barley types were observed only for the higher V_e values. This could indicate some branching differences between amylopectins from waxy vs. normal or high amylose starches. But, it is also conceivable that some of the linear polymers (i.e. amylose-like) start to elute in this region and that they contribute to the change of slope of the M_w vs. V_e relationship. In general, our results revealed significant differences in the M_w and R_g but rather small differences in the conformation of amylopectins from different types of barley starches.

Polydispersity values (M_w/M_n) of amylopectins from waxy and zero amylose starches were lower than those from normal and high amylose starches. The broad distribution of molecular masses for amylopectins in normal and high amylose starches can be clearly seen in Figure 3.4, where differential weight fraction is plotted as a function of molecular mass. Amylopectins from normal and high amylose starches exhibited a broad range of polymer populations with both higher and lower molar masses than amylopectins from waxy barley starches.

The molar masses and dimensions of barley amylopectin found in this study fall in the range reported for amylopectin of other botanical origin. Bello-Perez et al. (1998) reported molecular mass of $2.2 \pm 0.2 \times 10^8$ (g/mol) for waxy maize amylopectin,

Table 3.2. Weight average molecular weights (M_w), radii of gyration (R_g), and polydispersity values (M_w/M_n) of barley starches.

Starch Type	High M_w Fraction			Low M_w Fraction			Recovery
	$M_w \times 10^{-6}$(g/mol)	R_g(nm)	M_w/M_n	$M_w \times 10^{-6}$(g/mol)	R_g(nm)	M_w/M_n	(%)
Normal							
Falcon	226 ± 9.9 b	223 ± 4 d	1.90	5.67 ± 0.90	107 ± 4	1.12	86.1
SB90354	284 ± 4.2 a	240 ± 1 c	1.93	4.42 ± 0.01	98 ± 2	1.23	87.8
High Amylose							
92-55-06-54	141 ± 4.9 c	172 ± 1 e	1.93	2.70 ± 0.10	64 ± 1	2.61	85.6
92-55-06-48	136 ± 6.7 c	164 ± 5 e	1.85	2.73 ± 0.10	65 ± 2	2.21	81.2
Waxy							
CDC Candle	297 ± 2.8 a	249 ± 1 b	1.58	31.9 ± 7.5	141 ± 13	nd	71.6
SR93139	303 ± 11.0 a	250 ± 1 b	1.57	39.8 ± 3.3	149 ± 9		69.9
Zero Amylose							
SB94792	299 ± 0.7 a	262 ± 3 a	1.59	30.5 ± 0.1	141 ± 6	nd	64.7
CDC Alamo	305 ± 0.7 a	266 ± 1 a	1.60	40.7 ± 13.0	148 ± 17		71.5

[a] Mass recovery after HPSEC corresponds to the proportion (%) of injected material, recovered in the column effluent.

Values followed by the same letter (column) are not significantly different ($p \leq 0.05$).

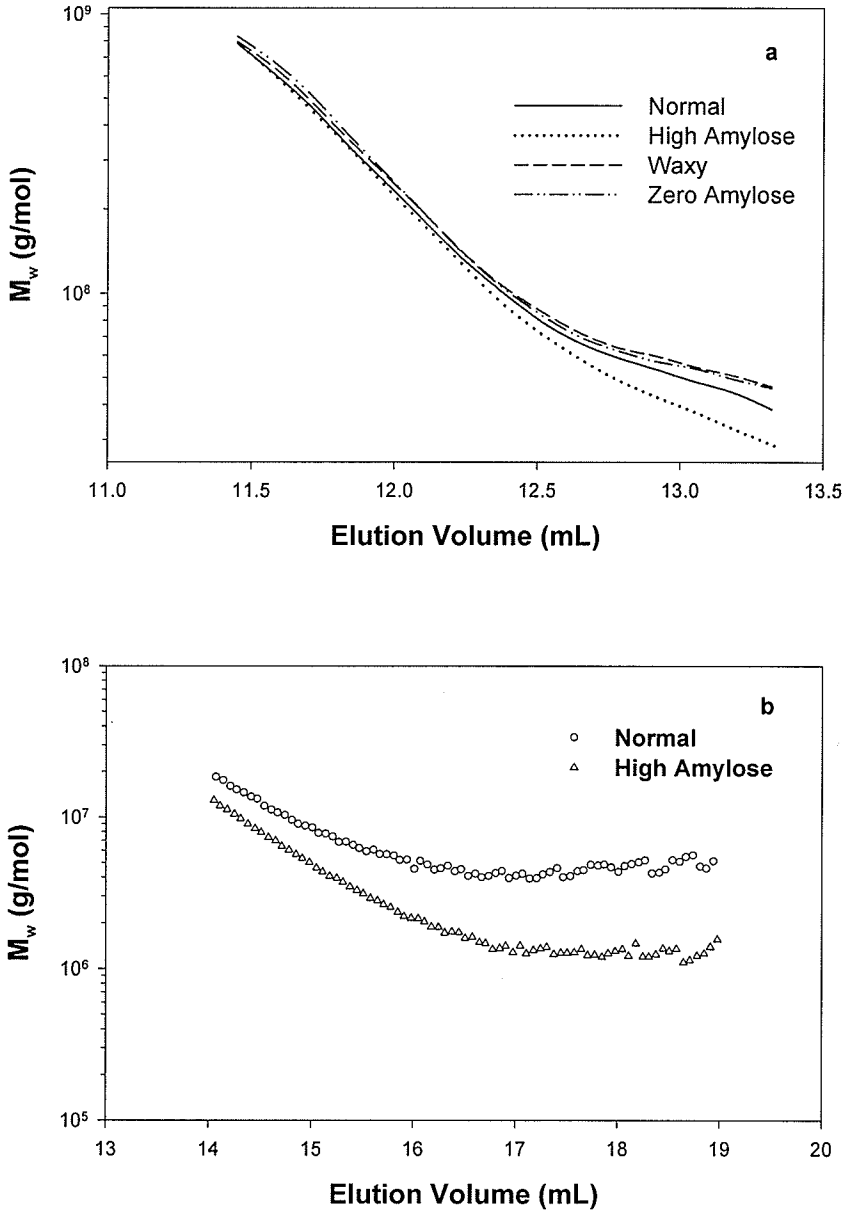

Figure 3.3. Relative molecular weight vs elution volume for high (a) and low (b) molecular weight fractions in normal (Falcon), high amylose (92-55-06-48), waxy (CDC Candle), and zero amylose (CDC Alamo) barley starches.

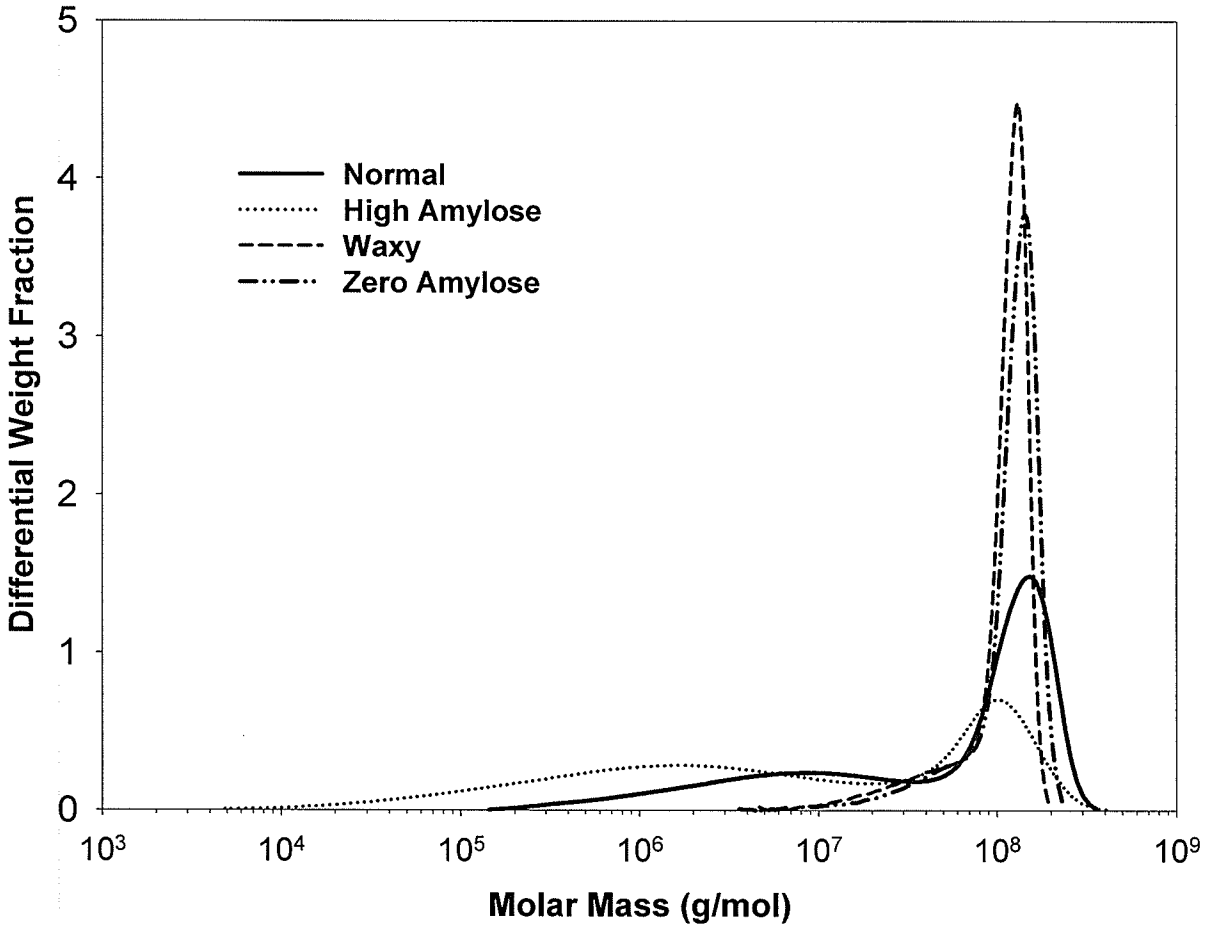

Figure 3.4. Molar mass distribution in normal (Falcon), high amylose (92-55-06-48), Waxy (CDC Candle), and zero amylose (CDC Alamo) barley starches

$1.9 \pm 0.3 \times 10^8$ (g/mol) for normal maize, and $3.5 \pm 0.2 \times 10^7$ (g/mol) for high amylose maize. Much lower values were communicated, however, by Fishman and Hoagland (1994) for waxy ($2.0 \pm 0.2 \times 10^7$ g/mol), normal ($1.3 \pm 0.2 \times 10^7$ g/mol), and Amy V ($8.0 \pm 0.4 \times 10^6$ g/mol) maize starches. These discrepancies might be due to different solubilization methods used in various studies. It is well known that in order to determine properly the molecular weight of starches, complete solubilization of starch polymers, amylose and amylopectin, in an appropriate solvent must be ensured. Concurrently, the degradation of starch polymers must be avoided. Degradation or incomplete solubilization of starch polymers may lead to underestimation of true molecular weight of starch polymers. On the other hand, incomplete disaggregation would lead to overestimation of the molecular weights. Due to the unique molecular structure and not yet sufficiently understood physico-chemical behaviour of starches in solution, complete solubilization of starch possesses a problem. Various approaches to achieve starch dissolution have been attempted ranging from mild to more severe treatments. Fishman and co-workers (1994, 1996) dissolved starch in water by microwave heating (80 seconds) in a high pressure vessel. Recently Bello-Perez et al. (1998) reported that the optimum conditions for starch solubilization involved pre-treatment of samples with dimethyl sulphoxide and dissolution by microwave heating for 35 seconds in a high pressure vessel (maximum temperature 143°C). Many workers have attempted to solubilize starch by autoclaving under various conditions. Aberle et al. (1994) reported that optimum autoclave temperature for molecular dissolution without degradation varied from 135-155°C depending on the origin of starch. Hanselmann and co-workers (1995; 1996) observed a decrease in molecular weight of waxy corn starch when the samples were autoclaved at 175°C for longer than 20 minutes. However, the

authors also postulated that the higher molecular weight obtained after shorter autoclaving period might be due to the fact that a heating period of 20 min was not sufficiently long to dissolve starch completely and, therefore, the high molecular weight corresponds to large aggregates of starch polymers. You and Lim (2000) reported that autoclaving (121°C, 20 min) or microwave heating (35 sec) provided better HPSEC recovery and higher M_w for starch molecules than simple dissolution in hot water. Our studies concurred with the previously published data; lower M_w and lower recoveries were obtained when the barley starches were not autoclaved (data not shown).

Although the elution volumes of the low molecular weight peaks assigned to amylose in normal and high amylose starches showed no prominent differences (Fig. 3.2), the calculated molecular weights were significantly different, with the average M_w of amyloses in the two normal starches almost twice as high as those of the two high amylose starches (Table 3.2). The differences in the relationship between M_w vs. V_e are also shown in Figure 3.3b; at the same elution volume, amylose from normal starch displayed greater M_w than high amylose samples. Normally, different slopes of log M_w vs. V_e might indicate variations in the conformation of polymers. In this case, however, the observed differences in the molecular weight and conformation of the low M_w material might arise from the fact that some of branched material (i.e. amylopectin) eluted in this region traditionally assigned to amylose. This was apparent from the elution profiles of waxy and zero amylose starches, which showed a small but definite population of polymers eluting in the volumes assigned normally to amylose, despite very small content or even absence of amylose fraction in these particular samples. The molecular weights and radii of gyration of these materials in waxy samples remained, however, very high (Table 3.2). Accurate determination of

molecular characteristics of amylose may, therefore, be rendered problematic by the presence of branched material eluting in the same volumes.

Substantial differences in polydispersity among the low molecular weight fractions were observed (Table 3.2). Polydispersity of high amylose starches was much greater than normal and waxy starches (Table 3.2 and Fig. 3.3). Of the four types of barley starches, high amylose starches contained polymers with the broadest range of molecular masses (Fig. 3.3).

The overall mass recovery after HPSEC ranged from approximately 65% to 87% and appeared to be dependent on the amylose/amylopectin ratio in the samples (Table 3.2). In general, normal and high amylose starches showed higher HPSEC recovery than waxy and zero amylose starches. The higher recovery of samples containing a higher proportion of amylose has been reported previously (Bello-Perez et al. 1998; Yokoyama et al. 1998). Difficulties associated with total solubilization of starch polymers and non-quantitative elution of amylopectin, in particular, have been blamed for low mass recovery after SEC of starches.

Molecular characteristics of debranched starches

Debranched amylose. The elution profiles of the starch samples treated with the debranching enzyme are shown in Figure 3.5. In addition to the low molecular weight material (V_e: 31-37mL) originating from debranched amylopectin, the high amylose, normal, and waxy starches also showed a high molecular weight peak (V_e: 20-31mL) presumed to be the amylose fraction. The presence of at least two populations of linear polymers in high amylose and normal starches can be inferred

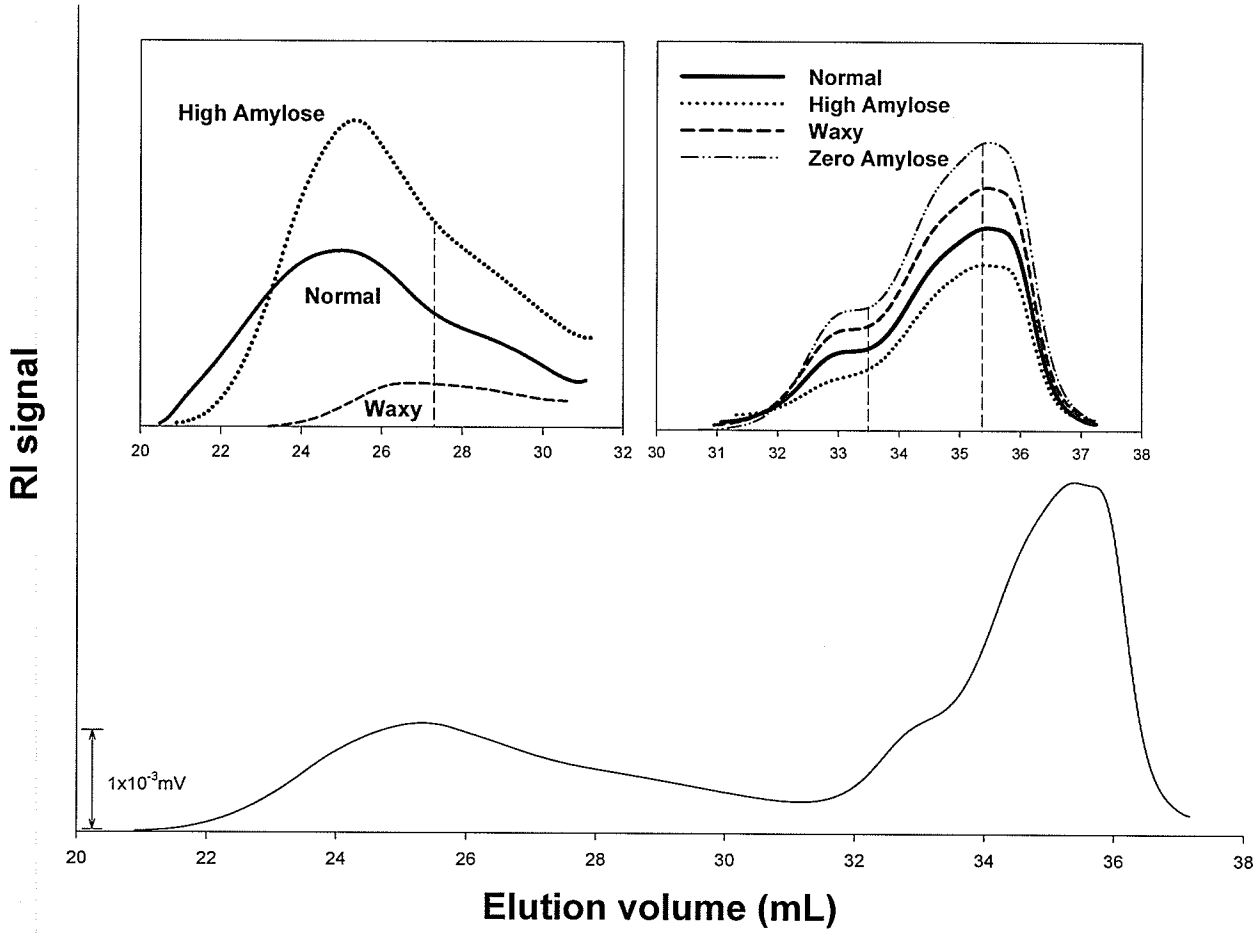

Figure 3.5. HPSEC profiles of normal (Falcon), high amylose (92-55-06-48), waxy (CDC Candle), and zero amylose (CDC Alamo) barley starches after debranching with isoamylase.

from the shapes of the eluting peaks. The average molecular weights of the two populations, referred to as Fraction I and II, are compiled in Table 3.3. The molecular weights of the debranched amylose fractions were significantly lower than those determined from the elution of intact starches (Table 3.2). Non symmetrical shapes of the peaks as well as rather low molecular weights of amylose fractions obtained after enzymic treatments of starch samples suggest a certain degree of branching in amylose fractions of barley starches. Interestingly, there were some differences between M_w and R_g of debranched amylose fractions (Table 3.3) in normal and high amylose starches but not of the same magnitudes as in intact materials (Table 3.2). These results confirmed our earlier supposition that the differences in molecular characteristics of amyloses inferred from the SEC of intact starches may have been intensified by the presence of amylopectin in the low M_w peak traditionally assigned to amylose. The content of amylose fraction determined from the integration of high (amylose) and low (debranched amylopectin) M_w peaks is also presented in Table 3.3. It has been suggested the long B chains of amylopectin molecules might also bind some iodine and, therefore, lead to an overestimation of the true amylose content in starches (Ramesh et al. 1999; Song and Jane 2000; Takeda and Hizukuri 1987). In this study, however, the calculated amylose contents obtained from the integration of chromatograms are in good agreement with the total amylose content measured by the iodine potentiometric method (Table 3.1). These results indicate a possible alternative for the amylose content measurement by HPSEC technique. In order to obtain valid results, however, the quantitative elution of the polymeric material as well as good resolution of the chromatographic column must be guaranteed.

Table 3.3. Weight average molecular weights (M_w), radii of gyration (R_g), and polydispersity values (M_w/M_n) of amylose after debranching of starch samples with isoamylase.

Sample	Fraction I			Fraction II			Amylose Content (%)[a]
	$M_w \times 10^{-3}$(g/mol)	R_g(nm)	M_w/M_n	$M_w \times 10^{-3}$(g/mol)	R_g(nm)	M_w/M_n	
Normal							
Falcon	796 ± 42.4 ab	45.8 ± 3.9 ab	1.79	100 ± 7.0 a	32.1 ± 1.6 a	1.05	24.4
SB90354	861 ± 36.0 a	46.8 ± 1.0 ab	1.7	101 ± 5.0 a	26.1 ± 1.8 a	1.15	24.3
High amylose							
92-55-06-54	782 ± 59.0 ab	43.1 ± 1.8 ab	1.5	97.9 ± 2.6 a	21.1 ± 0.6 a	1.2	38.1
92-55-06-48	695 ± 68.6 bc	41.6 ± 3.0 ab	1.59	88.3 ± 1.5 a	26.7 ± 5.8 a	1.16	38.5
Waxy							
CDC Candle	821 ± 29.0 ab	50.5 ± 1.2 a	1.95	nd[b]	nd		5.1
SR93139	591 ± 3.5 c	37.5 ± 4.5 b	1.9				5.3

[a] Determined from chromatography data.

[b] nd, not detected.

Values followed by the same letter (column) are not significantly different ($p \leq 0.05$).

Debranched amylopectin. The debranched amylopectin molecules from four types of barley starches exhibited similar profiles, all showing trimodal distributions of long B (V_e: 31-33.5mL), intermediate B (V_e: 33.5-35.4mL), and short B or A chains (V_e; 35.4-37.2mL) (Fig. 3.5, Table 3.4). The M_w of long B chains from the debranched amylopectins varied from 9.5×10^3 to 21.6×10^3 g/mol, which corresponds to the DP values from 59 to 133. The highest M_w and DP values for the long B chain were observed for high amylose starch, followed by normal, waxy, and zero amylose starches. The relative amounts of the long chains in high amylose samples were, however, the lowest. These results do not confirm the results of the recent studies by Song and Jane (2000), where the distribution of linear chains was studied with HPAEC combined with PAD. They reported that normal starch contained the longest linear chains with the DP values of 82. These discrepancies may be due to the differences in the varietal origin of starches as well as to differences in the methods employed for the detection of the debranched chains.

The M_w values of the intermediate B chains ranged from 3.8×10^3 to 6.3×10^3 g/mol, which corresponds to the DP of 23 to 39. The intermediate B chains of high amylose starch had relatively higher DP values than those of other starches. The lowest DP values of intermediate B chains were found in waxy and zero amylose starches. Song and Jane (2000) reported no significant differences in the average length of intermediate chains from four varieties of barley starches. The M_w of short B or A chains from the debranched amylopectins were in the range of 1.1×10^3 to 1.9×10^3g/mol (DP 6.8 - 12).

Interestingly, the molecular size of the linear chains of amylopectins was not

Table 3.4. Molecular characteristics of amylopectin linear branches obtained after debranching of starch with isoamylase.

Sample	B chains (long)		B chains (intermediate)		B(short) + A chains	
	$M_w \times 10^{-3}$ (g/mol)	Relative amount[a] (%)	$M_w \times 10^{-3}$ (g/mol)	Relative amount (%)	$M_w \times 10^{-3}$ (g/mol)	Relative amount (%)
Normal						
Falcon	17.7±1.2 ab	18.9	5.5±0.3 b	50.1	1.5±0.5 a	30.9
SB90354	16.1±0.8 b	18.5	5.3±0.1 b	50.2	1.5±0.2 a	31.2
High amylose						
92-55-06-54	21.6±0.7 a	16.3	5.7±0.1 ab	53.1	1.2±0.0 a	30.6
92-55-06-48	21.3±3.2 a	16.1	6.3±0.5 a	53.2	1.9±0.4 a	30.7
Waxy						
CDC Candle	13.6±0.1 bc	18.0	4.1±0.1 c	51.8	1.4±0.0 a	30.1
SR93139	11.2±1.1 c	17.7	4.4±0.1 c	52.0	1.1±0.1 a	30.2
Zero amylose						
SB94792	9.5±0.4 c	18.0	3.8±0.1 c	51.7	1.2±0.1 a	30.3
CDC Alamo	11.1±0.8 c	18.2	4.3±0.0 c	51.8	1.6±0.1 a	30.6

[a] % of the sum of B chains (long)+B chains (intermediate)+B(short)+A chains

Values followed by the same letter (column) are not significantly different ($p \leq 0.05$).

in good agreement with their molecular weights, indicating that R_g of the short B or A chains was greater than R_g of long and intermediate B chains. A similar observation was recently made by You et al. (1999). It is possible that the short glucan chains (DP 6-12) remain fully stretched during the chromatographic analysis, whereas the longer chains (DP > 20) are capable of assuming more folded or even coiled conformation supported by numerous secondary forces. It has been well documented that polymeric chains of α-glucans have a high tendency to adopt random coil structures with helical segments in alkaline and neutral aqueous solutions (Rao et al. 1998).

Conclusions

Significant differences in the granule size distribution and molecular characteristics of amylose and amylopectin were found in barley starches with variable amylose content. The bimodal distribution of starch granules was observed for normal and waxy barley starches but the proportion of large and small granules in these samples differed substantially. High amylose starch granules exhibited a rather unimodal granule distribution characterized by the highest proportion of 3μm granules. The M_w and R_g of amylopectins from waxy barleys were significantly higher than those from normal and high amylose starches. The length of some linear chains in amylopectin from high amylose samples was found to be significantly larger than in normal and waxy starches. The amylose polymers in normal and high amylose barley starches exhibited a certain degree of branching. The M_w of amylose in high amylose barley starch appeared to be lower than in normal barley starch. The substantial differences in molecular characteristics of barley starches may have significant influence on their physicochemical and functional performance. The exact nature of that influence will now have to be fully investigated.

CHAPTER 4

Separation and Characterization of Barley Starch Polymers by a Flow-Field Flow Fractionation Technique in Combination with Multiangle Light Scattering and Differential Refractive Index Detection[2]

Abstract

Flow-field flow fractionation (flow-FFF) with frit inlet and frit outlet mode (FIFO) was coupled on-line to multiangle light scattering (MALS) and refractive index (RI) detectors to investigate the molecular characteristics of normal and zero amylose barley starch polymers. Application of two different cross-flows, 0.35mL/min followed by 0.1mL/min, and constant channel and frit flows of 0.1 and 1.0mL/min, respectively, permitted a complete separation of amylose and amylopectin. The improved signals from the detectors due to application of the FIFO mode enabled the proper characterization of the small molecular weight species, as well as significantly enhanced the reproducibility of the measurements. The weight average molecular weight (M_w) and radii of gyration (R_g) values for amylose and amylopectin in the normal starch samples were 2.3×10^6 and 280×10^6, and 107nm and 260nm, respectively. The M_w and R_g of amylopectin in the zero amylose starch samples were 360×10^6 and 267nm, respectively. The slopes (α) obtained by plotting log M_w vs. log R_g for amylose and amylopectin were 0.6 and 0.3, respectively. These results are in good agreement with the theoretical prediction of the molecular conformation of amylose and amylopectin.

[2]Published Cereal Chemistry (2002) 79(5):624-630. By S. You, S.G. Stevenson, M.S. Izydorczyk, and K.R. Preston

Introduction

Starch is composed of two primary components, amylose and amylopectin. Although both polymers are built up of the same sugar unit, they differ significantly in solubility, molecular structure, molecular weight, and conformation (Hizukuri 1996). Amylose is a mostly linear polymer, composed of α-D-glucopyranose residues linked through 1→4 linkages. Amylopectin is a large branched molecule with side chains attached to the linear α-(1→4) polymer by α-(1→6) linkages. The average molecular weight (M_w) of amylose may range from 1×10^5 to 1×10^6 g/mol, whereas that of amylopectin ranges from 10×10^6 to 500×10^6 g/mol (Banks et al. 1972). Amylopectin and amylose have been successfully separated using size exclusion chromatography (SEC), however, amylopectin due to its extremely high molecular weight elutes in the exclusion volumes of the SEC columns (Sullivan et al. 1992). This makes the use of calibration standards for the estimation of its molecular weight not feasible. The absolute molecular weight of both starch polymers has been successfully determined by combining a multi-angle light scattering (MALS) detector with SEC columns (Aberle et al. 1994; Bello-Perez et al. 1998; Fishman et al. 1996; You et al. 1999; You and Lim 2000). This technique is thought to be able to provide accurate determination of the molecular weight of the starch components provided that adequate starch solubilization and separation of amylose and amylopectin have been achieved, and that complete recovery of starch after the chromatographic elution can be ensured. Despite continuous efforts to enhance the resolving power of SEC columns, improvements in separation of starch polymers are still possible and remain desirable. Also, the SEC technique fails to provide information about the distribution of molecular weight in amylopectin since this polymer elutes as a relatively narrow peak in the void volume of

all SEC columns. Even when pore diameters of the SEC support particles are relatively large compared to the particle diameter and even when the largest molecules might theoretically show differing migration due to a combination of hydrodynamic chromatography and size exclusion chromatography effects (Stegeman et al. 1991), to the best of our knowledge a good separation of amylopectin polymers has not yet been achieved. Possible shear degradation/alteration of large molecules, such as amylopectin, inside the SEC column is another consideration that encourages the search for a more appropriate separation method for the starch polymers.

Recently, another separation technique, flow-field flow fractionation (flow-FFF), has been developed as an alternative to SEC and has proven especially applicable to separation of very high molecular weight polymers (Giddings et al. 1992; Giddings 1995). In contrast to the tubular-shaped and packed SEC column, FFF consists of a thin, open, rectangular-shaped channel with no packing material. Fractionation takes place in a completely liquid medium. Less shearing of large molecules and no interactions between the eluting species and the packing material occur in the FFF channel. The technique is, therefore, more suitable for characterization of very large macromolecules. One wall of the channel, called the accumulation wall, is permeable to liquids. A liquid flow having a parabolic velocity profile is pumped through the channel during separation. An external field, perpendicular to the channel flow, called the cross-flow, is also applied during separation. The actual separation of macromolecules is a function of their differential diffusion coefficient against the cross flow and the parabolic profile of the channel flow.

The coupling of flow-FFF and the MALS detector makes possible the determination of absolute molecular weight and size of the fractionated molecules from flow-FFF. The flow-FFF-MALS system is reported to be a powerful tool for

separation and characterization of large macromolecules such as polivinyl pyrrolidone (Jiang et al. 2000), dextran and pullulan (Wittgren and Wahlund 1997).

Recently flow-FFF has been successfully applied to separate and characterize such water soluble polymers as gum arabic (Picton et al. 2000), dextrans and pullulans (Viebke and Williams 2000a), κ-carrageenan (Wittgren et al. 1998), and xanthan (Viebke and Williams 2000b). To our knowledge however, only a few studies have utilized the FFF technique to separate and characterize starch polymers. Lou et al. (1994) obtained only a partial separation of amylose and amylopectin using thermal FFF and dimethyl sulphoxide as a solvent. Sedimentation FFF was shown to fractionate only very large macromolecules (50-500nm) and, therefore, be applicable to amylopectin only (Hanselmann et al. 1995). Most recently, Roger et al. (2001) have indicated that fractionation of starch polysaccharides using flow-FFF coupled to MALS and RI detectors was a promising alternative to the SEC/MALS/RI system. The FFF/MALS/RI system was used to separate corn starch polymers with varying amylose/amylopectin ratios. The authors initially used high cross-flow to elute amylose then reduced cross-flow to elute amylopectin. A frit outlet was used to remove 50% of the channel flow between the end of the channel and detector to increase detector signal. This allowed measurement of the average molecular weight and radius of gyration for amylopectin but no data could be obtained for amylose due to the low signal that was generated by the amylose. Also, the repeatability of the results was not confirmed in their study. In our lab we have developed an automated frit inlet/frit outlet (FIFO) flow-FFF procedure for the fractionation of wheat proteins (Stevenson et al. 1999). Using recycled frit and cross-flow, this procedure eliminates the need for stopped-flow relaxation, gives superior sensitivity and reproducibility (higher detector signal to noise ratio) and provides much higher potential throughput relative to

conventional flow-FFF techniques. In this paper we describe the application of this procedure to the fractionation and characterization of barley starch amylose and amylopectin.

Materials and Methods

Materials

Normal and zero amylose (waxy) barley starches were isolated from hulless barley, cvs. Falcon and CDC Alamo, respectively, according to the procedure in Chapter 3. Bovine serum albumin (BSA; Sigma Chemical Co., St. Louis, MO, USA) was used to normalize the photo diodes located around the scattering cell in MALS and to obtain the delay volume between MALS and RI. Three pullulan standards, P-200 (M_w 212,000), P-800 (M_w 788,000), and P-1600 (M_w 1.66×10^6) (Shodex Standards P-82, Showa Denko, Tokyo, Japan), were used to examine the flow-FFF-MALS-RI system. All water was purified through a Milli-Q water purification system (Millipore, Mississauga, ON, Canada) prior to use.

Sample preparation

Pullulans were dissolved in distilled water (2 mg/ml), filtered through a 0.45μm membrane (Pall Gelman Laboratory, Ann Arbor, MI, USA), and injected into a flow-FFF-MALS-RI system.

Granular normal and zero amylose barley starches were gelatinized in 90% DMSO and precipitated with ethanol (Jane and Chen 1992). Various methods for starch solubilization were considered, namely microwave heating (140-150°C, Bello-Perez et al. 1998) and autoclaving (121°C, You and Lim 2000). Because of previous positive experience with dissolution of starch by autoclaving (Chapter 3), the purified starches (4mg) were redissolved in boiling water (8mL) for 5 min, autoclaved (121°C) for 20 min, and then centrifuged for 5 min at 8,000*g*. This treatment resulted in 75-80% solubilization as determined by measuring the total carbohydrate content (Dubois et al.

1956) in the supernatant.

Apparatus and procedures

Flow-FFF was performed using a model 1000-FIFO universal fractionator (PostNova Analytics USA, Salt Lake City, UT) as described previously (Stevenson et al. 1999). The frit inlet (FI) was used for hydrodynamic relaxation to replace stopped-flow relaxation and the frit outlet (FO) was used to remove eluent at the channel outlet to concentrate sample going to the detector (Fig. 4.1). Eluent removed through the frit outlet was re-circulated through a pump back to the frit inlet while cross-flow through the membrane was recycled through a pump back into the cross-flow to maintain pressure stability. The channel dimensions were as follows: length 27.7cm, breadth 2.0cm and thickness 0.0254cm. A YM-10 cellulose membrane (Amicon, M_W cutoff : 10,000 Daltons) was placed on top of the accumulation wall inside the flow-FFF channel. Sample solutions were injected via an injection valve (Model 7725, Rheodyne) with a 20μL sample loop. The fractionated macromolecules from flow FFF were monitored by MALS (Dawn DSP, Wyatt Technology, Santa Barbara, CA, USA) and RI (Waters 410, Waters, Mississauga, ON, Canada) detectors, which were calibrated using toluene and five different concentrations of NaCl solution, respectively. Calculations of the M_w and R_g were performed using the Astra 4.72 software (Wyatt Technology, Santa Barbara, CA, USA). The Berry extrapolation (1^{st} order) was used to calculate M_w and R_g. The dn/dc values of 0.148 and 0.146 mL/g were used for pullulan standards and starches, respectively. Water containing 0.002% FL-70 and 0.005% sodium azide was used as a mobile phase.

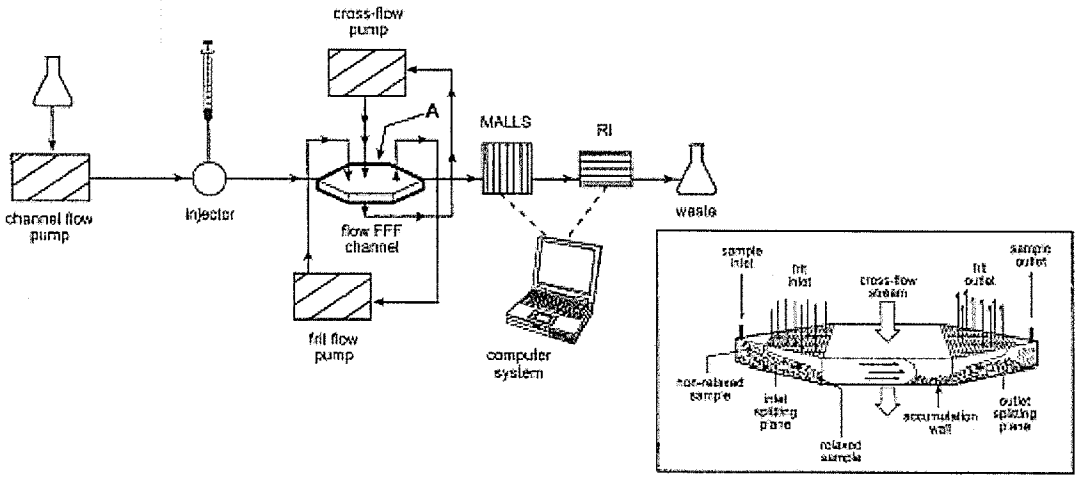

Figure 4.1. Flow-FFF-MALS-RI system and diagram of flow-FFF channel (inset)

It was filtered through 0.2μm and then 0.1μm nylon membranes (Osmonics Inc., MN, USA), and degassed with stirring under vacuum for at least 2 hrs. Three Shimadzu LC-10AD dual piston pumps (Man-Tech Sci., Guelph, ON) were used to provide channel, cross and frit flows for the flow-FFF-MALS-RI system.

The effect of various cross-flows (0.5 - 1.0mL/min) and frit flows (1.4 - 2.7mL/min) at a fixed channel flow of 0.2mL/min on the sample profile was examined using pullulan P-1600. The following flow conditions were applied to investigate the separation of various pullulan standards; channel flow: 0.2mL/min, cross-flow: 1.0mL/min and frit flow: 1.4mL/min. A mixture (1:1) of pullulans (P-200 and P-1600) was also injected into flow-FFF-MALS-RI system with the flow conditions of channel flow of 0.2mL/min, cross-flow of 0.6mL/min and frit flow of 1.4mL/min.

The effect of various cross-flows (0.1 - 0.4mL/min) on the eluting profiles of normal and zero amylose starches with a channel flow of 0.1mL/min and frit flow of 1.0mL/min was examined. In order to separate amylose and amylopectin molecules in a solution of normal barley starch, two different cross-flows were applied during the measurement. The initial cross-flow was 0.35mL/min, and then, after the elution of amylose molecules (12 min), the cross-flow was reduced abruptly to 0.1mL/min to allow amylopectin molecules to elute. This procedure was also applied to zero amylose starch. The amylopectin fractions of normal and zero amylose starches were examined with various cross-flows from 0.08 - 0.2mL/min after the initial cross-flow of 0.35mL/min for 12 min.

Sample recoveries were calculated from the ratio of the mass eluted from the channel as determined by the RI detector and the mass injected as determined by

measuring the total carbohydrates (Dubois et al. 1956). All treatments were carried out a minimum of two times on different days.

Results and Discussion

Pullulan standards with average molecular weights of 0.2×10^6, 0.78×10^6 and 1.6×10^6 were initially used as model carbohydrates to assess the efficiency of the FIFO flow-FFF/MALS/RI system and to aid in designing conditions for separating starch polymers. Preliminary studies showed that a channel flow of 0.2mL/min and a frit flow of 1.4mL/min provided the best resolution without overly long running times (data not shown). A value of 7 for the ratio of frit to channel flows gave efficient hydrodynamic relaxation at the entrance to the channel and concentrated the pullulans in the channel outlet by removing most of the eluent through the frit outlet. This increase in component concentration greatly increased signal to noise ratios of the RI and MALS detectors allowing straightforward determination of concentration and molecular size parameters.

The effects of various cross-flows on the elution profiles of the largest pullulan standard (P-1600) are shown in Fig. 4.2a. As the cross-flow increased from 0.5 to 1.0mL/min with constant channel (0.2mL/min) and frit (1.4mL/min) flows, the elution of pullulan molecules was delayed. In agreement with theory (Giddings and Caldwell 1989), the magnitude of the applied cross-flow determines the relative position of the molecules in the FFF channel, and consequently their elution time. Symmetrical peaks with normal (Gaussian) distribution were obtained with higher rates of cross-flow; however, the elution time was longer. Lower cross-flows significantly reduced the elution time and caused the appearance of a small shoulder peak at the lowest retention time. This shoulder peak may be an overloading phenomenon where some of the components are displaced into faster moving regions where elution occurs earlier than

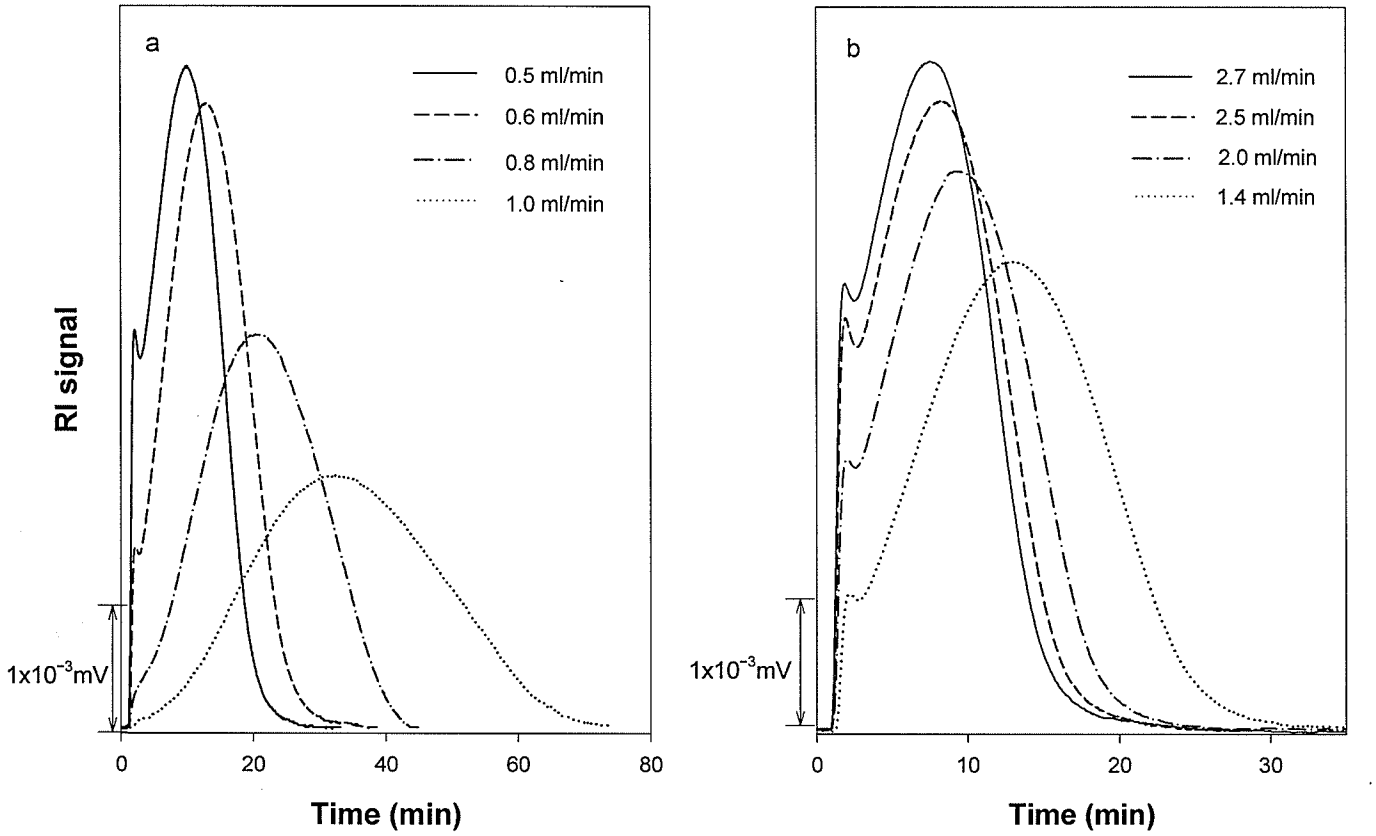

Figure 4.2. Effects of various cross-flows on elution profiles of pullulan standard (P-1600) (a); channel and frit flows 0.2 and 1.4mL/min, respectively. Effects of various frit flows on elution profiles of pullulan standard (P-1600) (b); channel and cross-flows 0.2 and 0.6mL/min, respectively.

expected (Benincasa 2000). Different rates of the cross-flow also affected the accuracy of the calculated average molecular weights. With the cross-flows of 1.0 and 0.8mL/min, the calculated M_w were in good agreement with the expected value while with lower cross-flows less accurate values were obtained, probably because of the presence of the void peak. The effects of various frit flows with fixed channel (0.2mL/min) and cross flows (0.6mL/min) on the elution profiles of P-1600 are shown in Fig. 4.2b. The higher frit flow facilitated faster elution of pullulan molecules, but it was accompanied by the appearance of the void peak. Again, higher rates of the frit flow lowered the accuracy of M_w determination.

Fig. 4.3 shows the elution pattern of three different pullulan standards, run separately, using a cross-flow of 1.0mL/min with a channel flow of 0.2mL/min and a frit flow of 1.4mL/min. P-200 eluted first with a retention time (t_r) of 9.3 min, followed by P-800 with t_r of 23 min and P-1600 with t_r of 34 min. Calculated molecular weights of 224,000, 868,000 and 1.6×10^6 g/mol for P-200, P-800 and P-1600 pullulan standards, respectively, were in good agreement with the values provided by the manufacturer. Sample recoveries were above 97%.

The fractogram of a pullulan mixture containing P-200 and P-1600 is presented in Fig. 4.4. Although it appears that only partial separation of the two pullulans was obtained under the conditions described above, calculated average molecular weights of the species eluting at t_r 2-8 min (206,000 g/mol) and t_r 8-25 min (1.2×10^6 g/mol) corresponded relatively well with the expected values.

Separation of starch components

Because of the large differences in the molecular weight between pullulan and

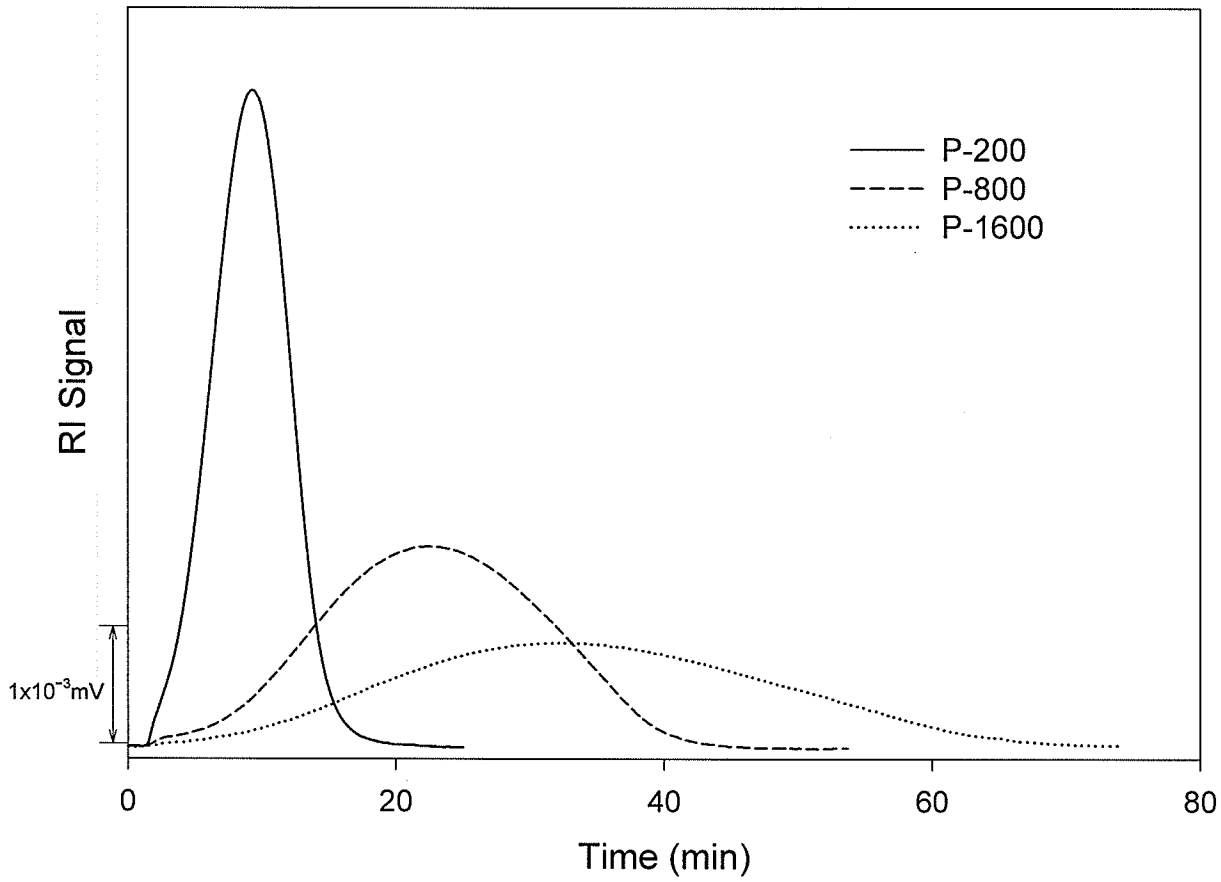

Figure 4.3. Elution profiles of different pullulan standards (P-200, P-800, and P-1600) with channel, frit, and cross-flows of 0.2, 1.4, and 1.0mL/min, respectively.

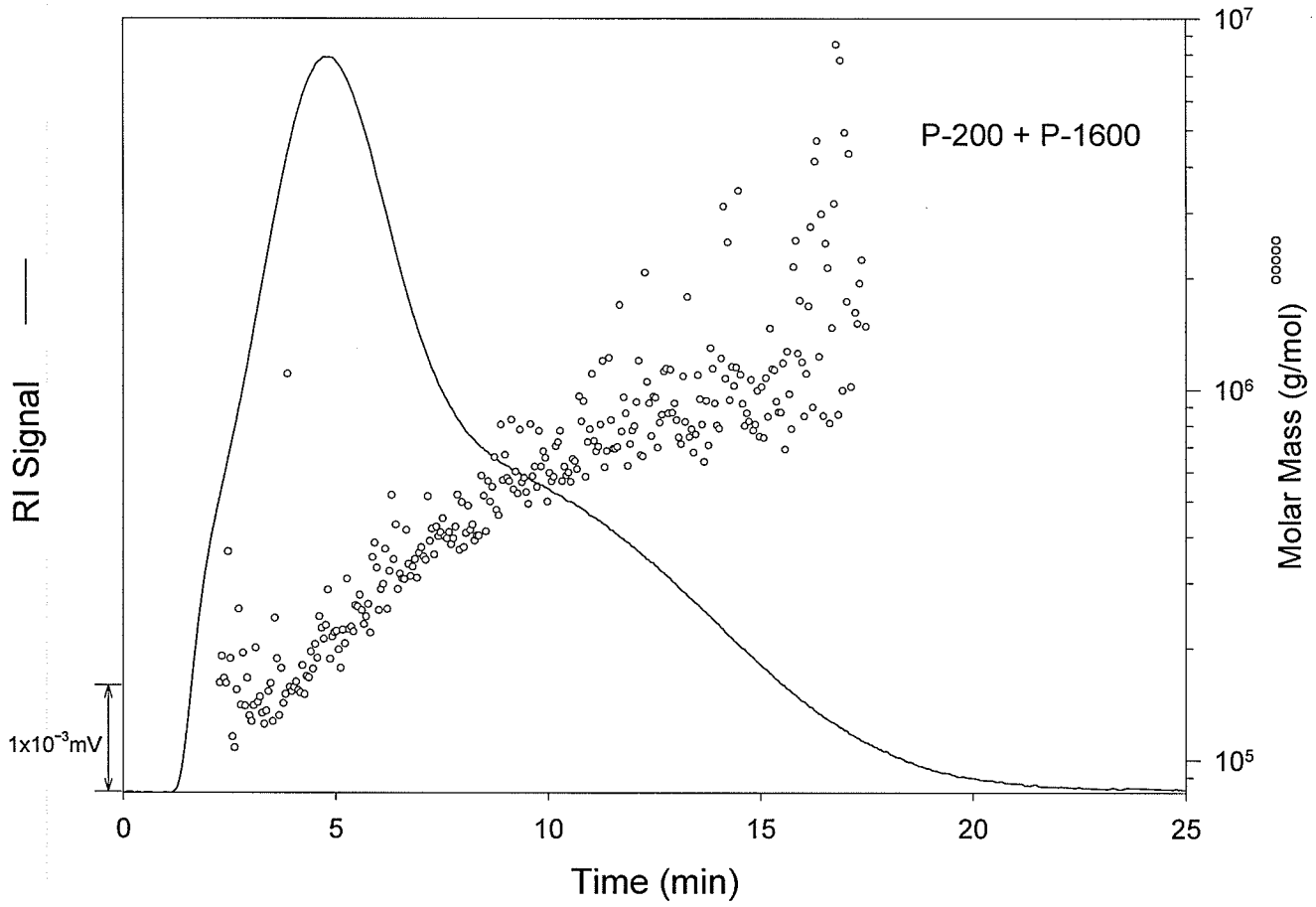

Figure 4.4. Elution profile of a mixture of pullulan standards (P-200 and P-1600) with channel, frit, and cross-flows of 0.2, 1.4, and 0.6mL/min, respectively.

starch polymers, it was necessary to change the elution conditions for the latter. Upon application of a cross-flow 0.5mL/min, quantitative elution of starch molecules was not achievable within acceptable analysis time, as indicated by continuous but low signal from the RI detector (results not shown). It was necessary, therefore, to apply a lower cross-flow. Recently, Jiang et al. (2000) also reported that lower cross-flows were more suitable for elution and measurement of high molecular weight water-soluble polyvinyl pyrrolidone (M_w up to 10^7). In order to maintain good resolution, the authors also implemented lower channel flow to compensate for the lower cross-flow. In our studies, the ratio of frit to channel flows was kept within the range of 7 to 10, as recommended by the FFF manufacturer (Post Nova Analytics USA, Salt Lake City), and frit and channel flows of 1.0 and 0.1mL/min, respectively, were applied. Figure 4.5 shows the effects of various cross-flows (0.1-0.4mL/min) on the RI profile of the eluting polymers in normal starch under these conditions. No separation of amylose and amylopectin was achieved with 0.1mL/min cross-flow as indicated by the appearance of one fairly symmetrical peak with an elution time between 2 and 10 min. Average values of M_w of 133×10^6 g/mol and R_g of 183nm (Table 4.1) for this material have no real meaning since no separation of amylose and amylopectin was accomplished. A significant decrease in the size of this peak (to about 35% of the original size) and the appearance of peak tailing were observed with increasing cross-flows from 0.1 to 0.3mL/min. A further increase of the cross-flow to 0.4mL/min caused only a small shift of the major peak's retention time. Generally the retention time (t_r) of the major peak slightly increased with increasing rate of cross-flow (Table 4.1).

It appears that higher cross-flows delayed the elution of the high molecular weight starch polymers. This was demonstrated by the substantial decrease in the average M_w

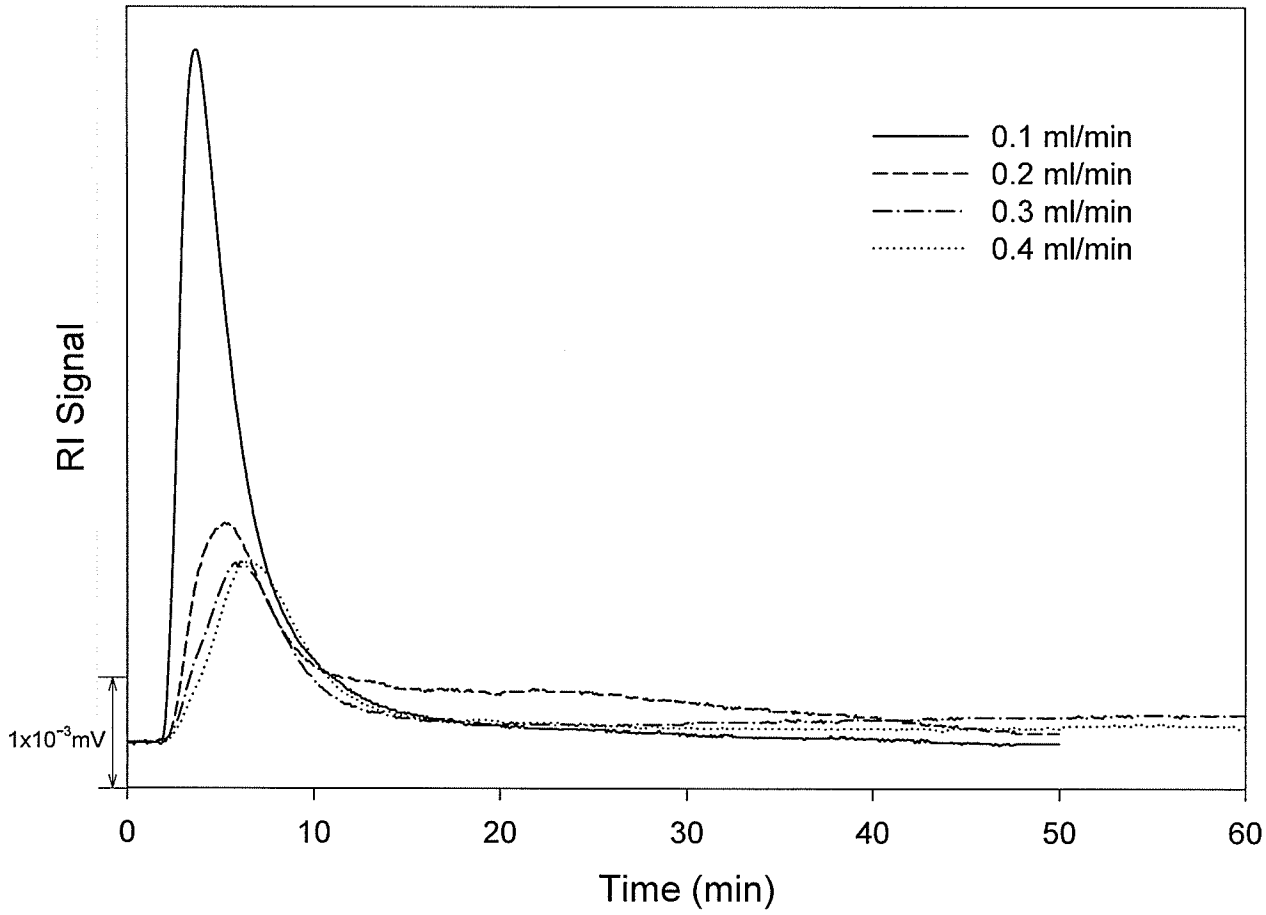

Figure 4.5. Effects of various cross-flows on elution profiles of normal barley starch with channel and frit flows of 0.1 and 1.0mL/min, respectively.

Table 4.1. Weight average molecular weights (M_w) and radii of gyration (R_g) of normal and zero amylose starches after the application of various cross flows

	Normal Starch			Zero Amylose Waxy Starch	
Cross-flow (mL/min)	t_r (min)	$M_w \times 10^{-6}$ (g/mol)	R_g (nm)	$M_w \times 10^{-6}$ (g/mol)	R_g (nm)
0.1	6	133 ± 7.1	183 ± 9.9	187 ± 8.5	197 ± 5.4
0.15	6.8	58 ± 9.9	192 ± 7.1	156 ± 36	205 ± 1.4
0.2	7.5	30 ± 3.5	178 ± 15	191 ± 27	234 ± 0.7
0.25	8	11 ± 2.3	189 ± 13	164 ± 25	240 ± 5.7
0.3	8.3	2.9 ± 0.5	163 ± 7.1	216 ± 43	270 ± 22
0.35	8.5	2.1 ± 0.3	117 ± 27		
0.4	8.9	1.9 ± 0.1	123 ± 18		

and R_g of molecules eluting at t_r 2-10 min with increasing cross-flows from 0.1 to 0.35mL/min (Table 4.1). Only a slight decrease in M_w was observed with the increase in the cross-flow to 0.4mL/min. The molecular weight and R_g of the species eluting between t_r 2-10 min upon application of the cross-flow ≥ 0.35mL/min (Table 4.1) correspond to the molecular dimensions of amylose polymers (You and Lim 2000). It is likely, therefore, that application of the cross-flow 0.35mL/min causes an initial retention of most of the amylopectin molecules inside the FFF channel while allowing the complete elution of amylose molecules. Eventually, slow elution of amylopectin occurs, but the process is very long, as indicated by elevated RI baselines (Fig. 4.5). Application of substantially lower cross-flow (0.1mL/min), on the other hand, causes co-elution of both small and large molecules.

Various cross-flows were also applied to elute the waxy barley starch containing no amylose (Fig. 4.6). With a very low cross-flow (0.1mL/min), the elution of amylopectin was achieved within 24 minutes. The peak, however, was rather asymmetrical with a portion of the material being eluted at a later stage. With increased cross-flow (0.2mL/min), the elution of amylopectin was obtained within 50 minutes. The elution profile showed a broader distribution of molecular weights (Fig. 4.6, insert) at increased cross-flow rates. At higher cross-flow rates the elution of the entire population of amylopectin molecules was not achieved within a reasonable time. These results indicate, therefore, that upon application of appropriate cross-flow, it is feasible to obtain information about the molecular weight distribution in amylopectin. This has not been possible with size exclusion chromatography since with the majority of SEC packing materials amylopectin elutes as a narrow peak in the void volume. These results also support the contention that upon application of a cross-flow ≥ 0.3mL/min the species

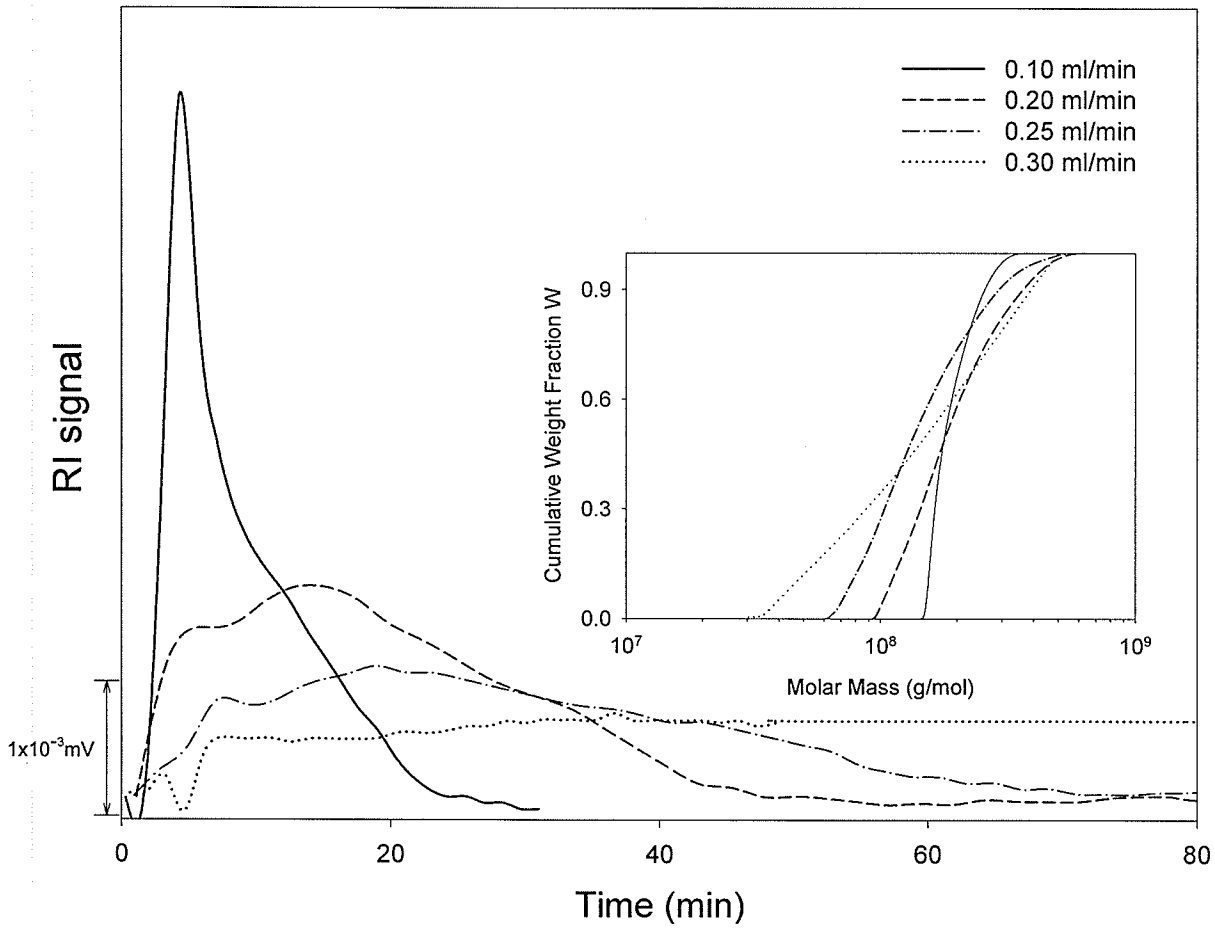

Figure 4.6. Effects of various cross-flows on elution profiles of zero amylose starch; channel and frit flows of 0.1 and 1.0mL/min, respectively. Cumulative molar mass distribution of zero amylose starch is shown in the inset

eluting between t_r 2-10 min contain mainly amylose.

The results presented above make it evident that efficient separation of amylose and amylopectin cannot be achieved with the application of any single rate of the cross-flow. The experimental conditions were, therefore, altered to allow application of an initial cross-flow of 0.35mL/min for the first 12 minutes followed by substantial reduction of the cross-flow to 0.1mL/min. A clear separation of polymers was obtained when a sample of normal starch was subjected to these elution conditions, as indicated by the appearance of two well resolved peaks, one at t_r 3-12 min and the other eluting only a few minutes after the change of the cross-flow at t_r 15-35 min. (Fig. 4.7a). Strong signals were obtained from both the RI and MALS detectors (Fig. 4.7a and b). The average M_w and R_g of the polymers eluting in the first peak were 2.3×10^6 g/mol and 107nm, respectively. These values clearly imply the presence of amylose polymers in the first peak. The average M_w and R_g of amylopectin polymers eluting in the second peak were 274×10^6 g/mol and 260nm, respectively (Table 4.2). Previous studies in Chapter 3, which employed the SEC-MALS-RI system for the separation of amylose and amylopectin in barley starches, estimated the M_w of the fractions corresponding to amylose and amylopectin at 5.67×10^6 g/mol and 226×10^6 g/mol, respectively. Considerable difference in the M_w of the amylose fraction in particular, as estimated on the basis of the SEC and the flow-FFF, may reflect substantial differences in the efficiency of separation of starch polymers achieved by these two techniques. In the SEC-MALLS-RI system, the estimation of M_w of amylose may be affected by amylopectin polymers eluting in the same region as the amylose fractions. Similar discrepancies in the M_w of gum arabic polysaccharides estimated with SEC-MALS-RI and flow-FFF-MALS-RI systems were recently reported by Picton et al. (2000).

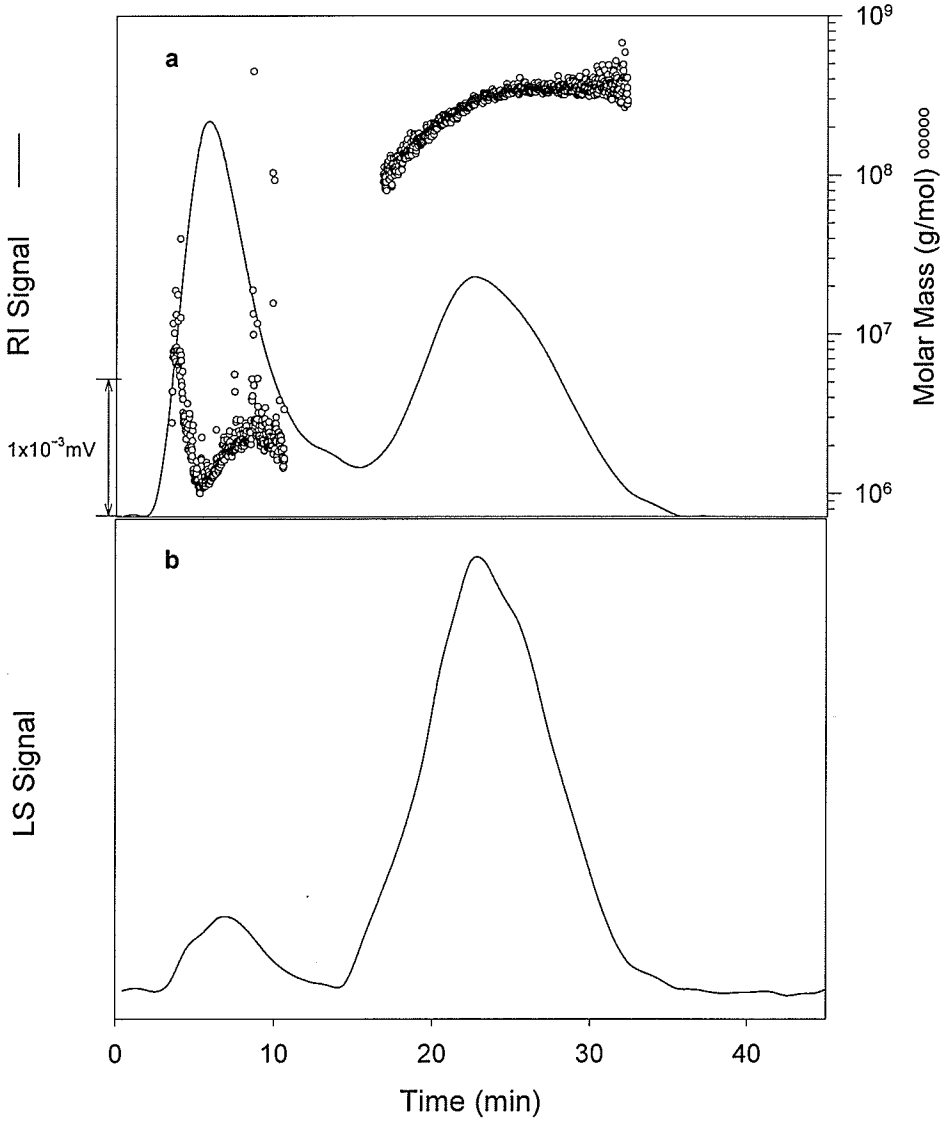

Figure 4.7. Refractive index (RI) (a) and light scattering (LS) (b) fractograms of normal barley starch. Separation of amylose and amylopectin on application of two cross-flows: 0.35mL/min (12 min) followed by 0.1mL/min.

Table 4.2. Weight average molecular weights (M_w), radii of gyration (R_g) and sample recoveries of the separated amylose and amylopectin from normal and zero amylose starches by two cross- flows.

	Normal Starch		Zero Amylose Waxy Starch	
	Amylose	Amylopectin	Amylose	Amylopectin
$M_w \times 10^{-6}$ (g/mol)	2.3 ± 0.1	280 ± 7.8		360 ± 9.9
R_g (nm)	107 ± 5.6	260 ± 14		267 ± 2.8
Recovery (%)	70.8 ± 2.0			50.0 ± 4.0

Recently, Roger et al. (2001) have also used two different rates of the cross-flow, 0.6mL/min followed by a stepwise decrease to 0.1mL/min, to achieve separation of amylose and amylopectin by flow FFF. Elution of polymers was obtained faster (11 min) than in our experiments (35 min). However, the elution of amylose was obscured by the presence of a void peak; also the signal from the light scattering detector was too low to afford characterization of this polymer.

Comparison of the areas under the two peaks indicated that the low molecular weight species eluting in the first peak constituted 46.8% of the entire population eluted under the above conditions. These values are not in good agreement with the total amylose content (26%) in the normal barley starch as measured previously by potentiometric iodine titration (Chapter 3). Since only 70.3% of the total sample was recovered, it is possible that a portion of the amylopectin was retained in the FFF channel and was not eluted under the experimental conditions. It is also possible that due to problems with incomplete solubilization of starch, the material applied to the FFF channel contained a different proportion of amylose and amylopectin compared to that in the native starch samples.

To optimize the elution of amylopectin, different rates of the second cross-flow (in the range of 0.08 to 0.20mL/min) were tested using a sample of normal barley starch (Fig. 4.8). A decrease of the second cross-flow to 0.08mL/min slightly improved the amylopectin recovery and shortened the elution time. On the other hand, increasing the rates of the second cross-flow progressively extended the elution of amylopectin over a broader range of volume and afforded a better insight into the distribution of molecular weights in amylopectin. Recovery of amylopectin was, however, progressively reduced.

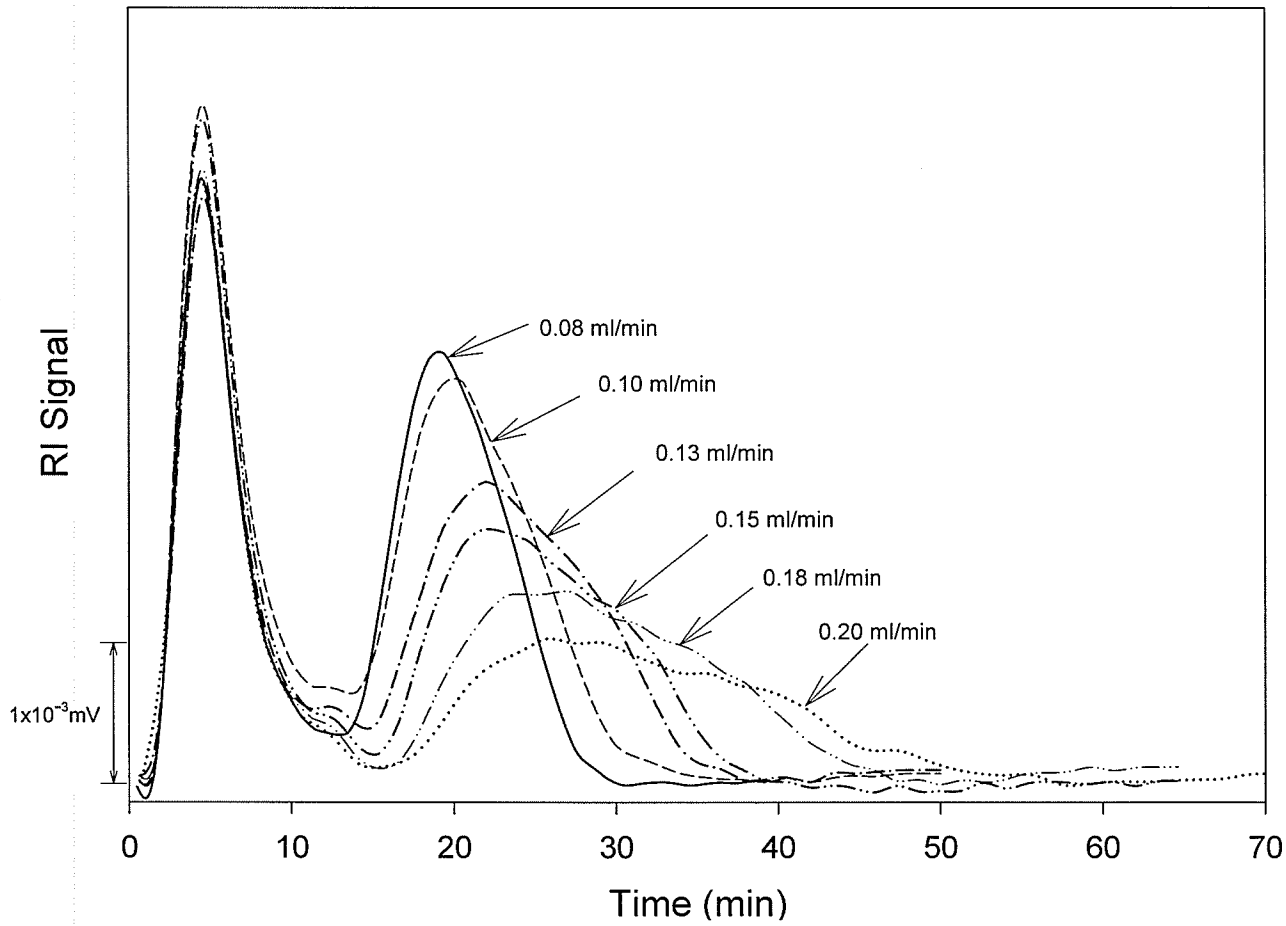

Figure 4.8. Elution profiles of normal barley starch with constant initial cross-flow (0.35 mL/min) followed by various second cross-flows (0.08-0.2 mL/min).

Another barley starch sample containing no amylose was also eluted under the two different cross-flow conditions used for the separation of amylose and amylopectin. As shown in Fig. 4.9 (a and b), only one peak corresponding to the high molecular weight amylopectin fraction was observed. The M_w and R_g were 360×10^6 g/mol and 267nm, respectively (Table 4.2). The sample recovery, however, was only 50%. Slightly lower values of M_w (299×10^6 g/mol) and of R_g (262 nm) for the same sample were obtained using the SEC/MALS system (sample recovery was 71%) (Chapter 3). The low sample recovery obtained with the FFF technique is not fully understood although we have shown before that the high rate of cross flow has a particularly negative effect on the recovery of amylopectin (Figure 4.7). Such low sample recovery raises a question whether the M_w obtained from this experiment was representative of the whole population of amylopectin chains injected into the channel. Because the M_w of amylopectin obtained with the FFF technique was higher than that obtained for the same sample with SEC (which had substantially higher recovery), it is rather unlikely that the high molecular weight amylopectin chains were specifically retained in the channel and, therefore, not eluted and measured by the detectors. These results show, however, that the recovery problems in the FFF technique are mostly associated with amylopectin. Similar observations have been made in SEC studies (Yokoyama et al. 1998; Bello-Perez et al. 1998). It appears that the low recovery of amylopectin in the SEC column or FFF channel is associated with difficulties in solubilizing and maintaining this polymer in solution. The behaviour of amylopectin in solution and its tendency for aggregation, especially under conditions of shear stress as generated by the combining effects of channel, frit, and cross flows, is not sufficiently understood. More research is needed to optimize the FFF conditions (especially finding the optimum ratio of the channel to frit

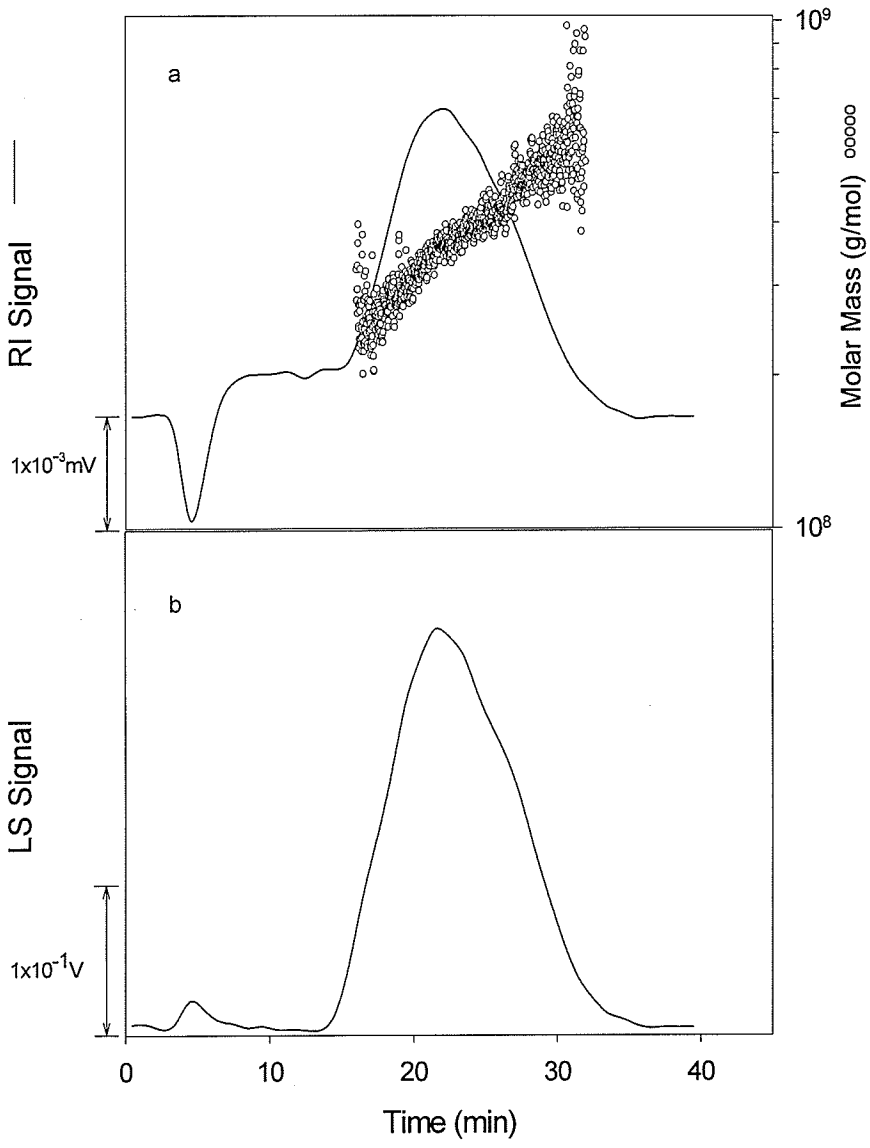

Figure 4.9. Refractive index (RI) (a) and light scattering (LS) (b) fractograms of zero amylose starch. initial cross-flow 0.35 mL/min (12 min) followed by 0.1 mL/min.

to cross flows) to obtain better sample recovery without loss of resolution. Repeated gelatinization of amylopectin in DMSO followed by precipitation with ethanol might improve solubilization and dispersity of amylopectin in solution.

Molecular conformations of amylose and amylopectin polymers from normal starch were examined by plotting log R_g vs. log M_w (Fig. 4.10). The slope of the line corresponds to the exponent α in the equation $R_g^{1/2} = KM_w^{\alpha}$, and is related to the conformation of polymers in solution (Astra for Windows User's Guide). Theoretically, the following values of α are assigned to sphere, random coils, and rigid rods: 0.33, 0.50, and 1.0, respectively (Astra for Windows User's Guide). For amylose rather scattered data points were obtained when log R_g vs. log M_w was plotted but the calculated α value of 0.6 for the slope suggested a very different conformation than that obtained for amylopectin (α = 0.3). The above results are in a good agreement with theoretical predictions because amylopectin, due to its branching characteristics, assumes a more compact conformation in solution than amylose.

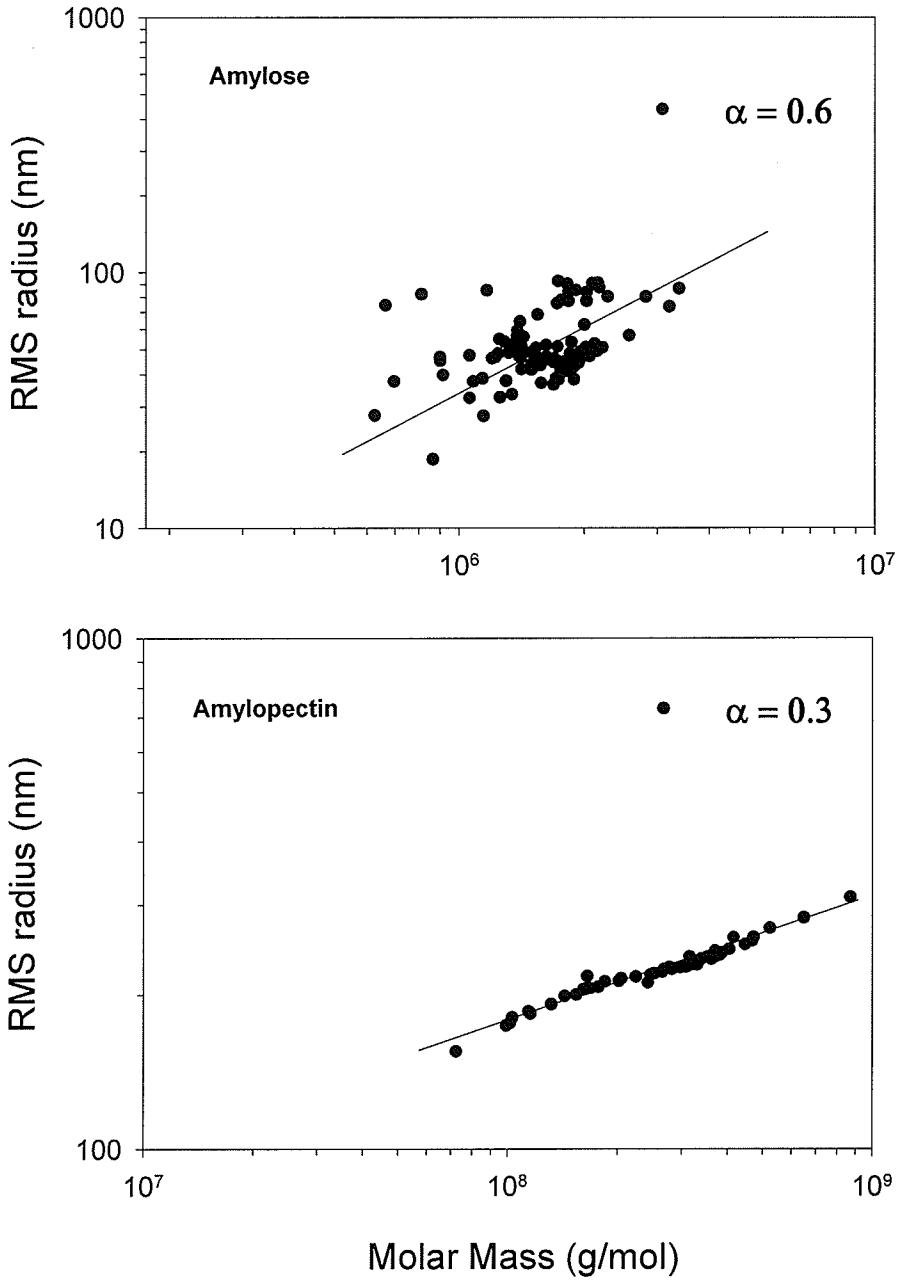

Figure 4.10. Distribution of R_g and M_w for amylose and amylopectin polymers

Conclusions

The results of the present study indicate that flow-FFF-MALS offers the means for separation and size characterization of starch polymers. The key factor determining good polymer resolution is using two appropriate rates of the cross-flow; the initial higher rate of the cross-flow allows elution of only amylose, and the subsequent lower cross-flow affords elution of amylopectin. Appropriate rate of the second cross-flow allows better insights into the distribution of molecular weights in amylopectin. The use of the FIFO mode eliminated the requirements for stop-flow relaxation and pressure balancing and resulted in a more stable baseline, enhanced resolution and better reproducibility of the molecular weight measurements. The enhanced signals obtained due to the application of the FIFO mode enabled the proper characterization of amylose. In addition, recycling the eluent via the FIFO mode creates the potential for automation of the system. However, further optimization is still needed to improve the recovery of the amylopectin molecules in particular. Also, development of appropriate strategies ensuring complete solubilization of starch in water is required to obtain valid characterization of both polymers, amylose and amylopectin, using the flow FFF/MALS/RI system.

CHAPTER 5

Physicochemical Properties and Molecular Structure of Partially Hydrolyzed Barley Starches with Various Amylose Contents. Part I: α-Amylase Hydrolysis

Abstract

Isolated hulless barley starches with varying amylose contents (0-40%) were subjected to α-amylase (*Bacillus licheniformis*) hydrolysis (for up to 48h) at two enzyme levels (50U/g and 500U/g). Waxy starch exhibited the greatest solubilization (36-56%), followed by normal (24-39%) and high amylose starch (13-20%). The X-ray diffraction patterns of enzyme-treated normal (39% solubilization) and high amylose starches (20% solubilization) were similar to those of native starches, implying that both amorphous and crystalline regions inside the starch granules were hydrolyzed concurrently. A small increase in the crystallinity was observed for waxy starch (56% solubilization). α-Amylolysis slightly increased the enthalpy (ΔH) values of amylopectin, but no changes in the gelatinization temperature (T_p) were observed in enzyme-treated normal and high amylose starches. The ΔH and T_p of amylose-lipid complexes increased in enzyme-treated starches. Enzyme-treated waxy starches exhibited increases in ΔH and T_p values of amylopectin. Relatively small decreases in the average molecular weights (M_w) of starch components were observed after α-amylolysis; even after extensive hydrolysis of the zero amylose starch (56% solubilization) only about a three-fold decrease in the M_w of amylopectin was observed. Partially hydrolyzed normal and high amylose barley

starches were less susceptible to further hydrolysis and formed stronger gels than their native counterparts. Enzyme-treated waxy barley starches, on the other hand, exhibited similar degree of enzyme susceptibility as native starches to further α-amylolysis. In addition, the enzyme treated waxy barley starch solution showed no evidence of network development during storage for 20h.

Introduction

α-Amylase (1,4-α-D-glucan glucanohydrolase, E.C. 3.2.1.1) belongs to the endo-hydrolase class of enzymes that are capable of cleaving the inner α-(1→4)-glycosidic linkages of starch polymers. The hydrolysis of soluble amylose and amylopectin by α-amylase produces a complex mixture of linear and branched α-dextrins. This process causes a rapid breakdown of macromolecules, large decrease in viscosity, loss in iodine staining power, and a gradual increase in the reducing values (Hizukuri 1996).

α-Amylolysis of amylose polymers proceeds essentially in two stages: an initial rapid and random breakdown is followed by a slow and non-random hydrolysis in the second phase (Myrback and Neumuller 1950). The exact mechanism of bond scissions may vary depending on the enzyme source. For example, it has been postulated that during the first phase of hydrolysis, cereal α-amylases split one bond per encounter with a substrate molecule (Hill and MacGregor 1988). α-Amylases from other sources utilize the multiple-attack mechanism, according to which a number of bonds are catalyzed before the enzyme dissociates and forms an active complex with another substrate molecule (Robyt 1984). It is postulated that the active site of the enzyme has at least nine subsites, each capable of binding to a glucose residue of the α-glucan chain. The catalytic center of cereal amylases is located between subsites 6 and 7, whereas that of α-amylase from *Bacillus* sp. between subsites 3 and 4 (Hill and MacGregor 1988; Robyt and French 1963). During the second phase of hydrolysis, as the substrate becomes smaller, the possibility that it will form an active complex with the enzyme decreases and the rate of hydrolysis becomes slower.

α-Amylolysis rate of amylopectin polymers is much slower than that of amylose

polymers, which is attributed to the presence of short branches joined by α-(1→6) linkages to the core of the molecule (Manners 1985). The initial products from amylopectin hydrolysis are large branched dextrins, but after prolonged hydrolysis by α-amylases, a mixture of small and large branched and linear dextrins is obtained.

An important property of α-amylases is their ability to hydrolyze intact starch granules. The rate and extent of hydrolysis of granular starches and soluble starch polymers, however, are different due to the unique molecular organization of amylose and amylopectin within granules. Also one is a soluble substrate and the other is insoluble. Generally, the botanical origins of starch, the physical and molecular characteristics of starch polymers as well as the sources of α-amylases influence the hydrolysis kinetics of starch granules by α-amylases (Banks and Greenwood 1975; Leach and Schoch 1961).

According to the current hairy billiard ball model of starch granules, the ends of amylose chains and amylopectin clusters protrude from the surface of starch granules and, therefore, they could form enzyme-starch complexes (Lineback 1986). The surface pores and inside channels in starch granules appear to be characteristic features of some starches, and they are suggested to be the initial site of the enzyme attack. They are also thought to facilitate access of hydrolytic enzymes into the interior of starch granules (Fannon et al. 1992; Huber and BeMiller 1997). According to Planchot et al. (2000), the hydrolysis of the native granules must start by pitting and exo-corrosion.

The size of starch granules appears to play a role in their susceptibility to enzymolysis. Isolated and purified small barley starch granules were found to have a greater susceptibility to cereal α-amylases than large ones (Bertoft and Kulp 1986; MacGregor and Balance 1980; MacGregor and Morgan 1986). This was attributed to the

larger surface area of small granules when compared to large ones on an equal weight basis (MacGregor and Morgan 1986). An increased enzymic susceptibility of purified small starch granules from wheat has also been reported (Kruger and Marchylo 1985; Manelius et al. 1997).

It has been generally accepted that waxy starches or starches containing a low amount of amylose are more susceptible to enzyme attack than high amylose starches (Cone and Wolters 1990; Leach and Schoch 1961; MacGregor and Ballance 1980). The starch crystallinity type also appears to affect significantly the efficiency of granular solubilization by α-amylase, and it has been reported that the B-type crystals are less susceptible to enzyme attacks than the A-type (Planchot et al. 1997). The differences in the locations of branch points (α-(1→6)-glycosidic linkages) in amylopectin of A and B-type starch granules were suggested to influence the degree of hydrolysis by α-amylase (Jane et al. 1997). A-type starches, containing higher amounts of short chains (DP 6 - 12) than B-type starches, have the branch points localized within the crystallites. This presumably creates weak points in the starch crystallites and increases their susceptibility to α-amylolysis. Gerard et al. (2001) studied the amylolysis of the maize mutant starches with various amylose contents and various types and levels of crystallinity. The authors concluded that the extent of hydrolysis was correlated more with the amount of B-type crystallinity than with the amylose content or crystallinity levels.

Despite several published studies on hydrolysis of barley starch granules by α-amylase (Bertoft and Kulp 1986; Bertoft and Avall 1992; Bertoft et al. 2000; Lauro et al. 1999; MacGregor and Ballance 1980; MacGregor and Morgan 1986; Maeda et al. 1978), relatively little is known about the molecular structure and physicochemical properties

of polymers remaining in the enzyme-modified granules. In the present work, granular hulless barley starches with various amylose contents were hydrolyzed by α-amylase. The objectives of this work were to determine the effect of amylose content on the degree and rate of the enzyme hydrolysis, to examine the physical and molecular characteristics of the starch material remaining after α-amylolysis, and to better understand how the enzymic susceptibility of various hulless barley starches relates to their molecular structure and organization inside the granules.

Materials and Methods

Materials

Three types of starches: normal, high amylose, and zero amylose, were isolated from three hulless barley genotypes: Falcon, CDC 92-55-06-48, and CDC Alamo, respectively, according to the previously reported procedure (Chapter 3).

α-Amylase modification of starch granules

α-Amylase (*Bacillus licheniformis*, 3000 U/mL, Megazyme, Bray, Ireland) was added to the starch suspension (0.5g starch/10mL of 0.1 M ammonium acetate, pH 6.0) to provide enzyme concentrations of 50 U or 500 U per gram of starch (50U/g and 500U/g). The starch-enzyme suspensions were gently shaken (Labquake shaker, Labindustries, Berkeley, CA, USA) at 20°C. After predetermined hydrolysis times (4, 8, 16, 24, and 48h), the starch-enzyme suspensions were centrifuged (6,725*g*, 10min). The supernatants were saved for further analysis, whereas the residual starch granules were resuspended in a buffer (2mL, 0.2M Na_2HPO_4-0.1M citric acid, pH 2.5) for 1h to inactivate α-amylase. Subsequently, the residual starch suspensions were centrifuged (6,725*g*, 10min), resuspended in a buffer (3mL, 0.2M Na_2HPO_4-0.1M citric acid, pH 6.5), centrifuged (6,725*g*, 10min), and washed with water and acetone. The residual starch samples were then dried overnight at room temperature. The amount of solubilized carbohydrates during α-amylolysis was determined by further digestion of the supernatant with thermostable α-amylase (*Bacillus licheniformis*, #FAA, Ankom Tech. Corp., Fairport, NY, USA) and amyloglucosidase (*Aspergillus niger*, Boehringer Mannheim, Laval, Quebec, Canada). The resulting glucose contents in the supernatant

were measured with a Gluco-quant assay kit (Boehringer Mannheim, Laval, Quebec, Canada), according to the procedure of Salomonsson et al. (1984). The rate of solubilization (%/h) was obtained from the amount of solubilized carbohydrate (%) divided by hydrolysis time (h).

Morphological properties of starch granules

Native and enzyme-treated starch samples were coated in a Hummer VII (Anatech, Ltd. Springfield, VA, USA) sputter coater on a 45° holder with 40nm of gold (coat with 20nm, rotate the stubs 180°, and coat with another 20nm of gold). Gold-coated starch samples were examined with a JEOL JSM-6400 scanning electron microscope (SEM) at 10KV and photographed on Kodak TMAX 100 Black and White Professional film.

X-ray diffraction patterns of starch granules

The X-ray patterns of starch granules were obtained using a diffractometer (Model PW1729, Philips, Almeic, Netherlands) after equilibrating starch granules in a 90% relative humidity chamber for 2 days at room temperature. The diffractometer was operated at 30mA and 40kV. The scanning region of the diffraction angle (2θ) was from 3° to 30° at 0.02° step size with a count time of 2 second.

CP/MAS ^{13}C NMR spectra of starch granules

The solid-state CP/MAS ^{13}C NMR spectra of starch granules were recorded at 500 MHz using a Bruker AMX 500 NMR spectrometer (Bruker Spectrospin Ltd., Conventry, UK) operating at room temperature. Starch samples hydrated to 33% moisture content were packed into 7mm magic-angle spinning sample rotor. The magic angle spinning

rate and decoupling field were 2.5 kHz and 60 kHz, respectively. The 90° pulse width was 4 μs with a repetition time of 3 s. A contact time of 1 ms was used for starch samples. The accumulation of at least 1000 scans was done for each spectrum. The analysis of spectra was carried out by SpinWorks (V. 2.2) software.

Molecular characteristics of starch polymers

Starch dissolution. The granular native and enzyme-treated starches were gelatinized in 90% DMSO, precipitated with ethanol, and then dried by the method of Jane and Chen (1992). The gelatinized starch samples (3mg) were wetted in ethyl alcohol (0.1mL), redissolved in 1N NaOH (1mL) at 60°C for 5 min, diluted with water (8mL) and neutralized with 1N HCl. The starch solution was autoclaved for 20min (121°C), filtered through a 3.0μm cellulose acetate membrane, and then injected into the high-performance size exclusion chromatography (HPSEC) coupled with multi-angle light scattering (MALS) and refractive index (RI) detection system.

Preparation of debranched starch. The DMSO gelatinized starches (25mg) were redissolved in 5mL of 1N-NaOH at 60°C for 5 min, distilled water and 1N-HCl (1:3:1, respectively). The 3mL of starch solution was incubated with isoamylase (*Pseudomonas amyloderamosa*, 59,000U/mL, Hayashibara Biochemical Laboratories Inc., Okayama, Japan) at the enzyme concentration of 500 U/g by adding 1mL of acetate buffer (0.1M, pH 3.5) for 24h at 40°C. After incubation, the starch-enzyme solution was neutralized with 1 N NaOH, heated in a boiling water bath for 5min to inactivate isoamylase, filtered through a 0.45μm membrane, and then injected into the HPSEC-MALS-RI system.

HPSEC-MALS-RI analysis. The components of the HPSEC-MALS-RI system were the same as previously reported (Chapter 3), and the calibration and normalization of MALS (Dawn DSP, Wyatt Technology) were performed by the previously reported method (You et al. 1999). A TSK G5000PW column (7.8×600 mm, TSK PW, TosoBiosep, Montgomeryville, PA, USA) was used to determine the elution profiles of native and α-amylase-treated starches, whereas TSK G5000 PW, G3000 PWXL (7.8×300mm), and G2500PWXL (7.8×300mm) columns were employed to obtain the elution profiles of debranched starch samples. The calculated weight average molecular weight (M_w) and radius of gyration (R_g) were obtained from ASTRA 4.72 software (Wyatt Technology, Santa Barbara, CA, USA).

Debranched chain length analysis. The debranched chain length profiles of native and enzyme-treated starches were determined by high performance anion exchange chromatography (HPAEC, Dionex Carbopac PAI column, Dionex Corp. Sunnyvale, CA, USA) with a pulsed amperometric detector (PAD, Dionex, PAD II, gold electrode, 10k nA output, Dionex Corp. Sunnyvale, CA, USA), as previously reported by MacGregor et al. (1999).

Thermal properties of starches

The differential scanning calorimetry (DSC) analyses of native and enzyme-treated starches were carried with a DSC 2920 (TA Instruments, New Castle, DE, USA). Starch samples (3.8-4.0mg) were suspended in water (40% w/w) and hermetically sealed in DSC pans (TA Instruments, New Castle, DE, USA). The starch suspensions were heated

from 25°C to 130°C with a heating rate of 10°C/min. The empty pan was used as a reference. The gelatinization onset (T_o), peak (T_p), and complete (T_c) temperatures were measured, and enthalpy change (ΔH) was calculated from TA analysis software (TA Instruments).

Digestibility of α-amylase treated starches

The partially α-amylase-hydrolyzed barley starches: normal starch, 24% solubilized (N24%) and 39% solubilized (N39%); high amylose starch, 13% solubilized (H13%) and 20% solubilized (H20%); and zero amylose starch, 36% solubilized (Z36%) and 56% solubilized (Z56%) were treated with α-amylase (*Bacillus licheniformis*, 3000 U/mL, Megazyme, Bray, Ireland) at the enzyme concentration of 50 U per gram of starch up to 24h according to the previously mentioned procedure. The amount of solubilized carbohydrates from the supernatant was determined in order to investigate the extent of solubilization of partially hydrolyzed starch samples.

Rheological properties of starches

The development of viscoelastic properties of native and enzyme-hydrolyzed starches was monitored by the small deformation mechanical measurements using the stress controlled rheometer (Rheometrics SR 500, Rheometrics Scientific Inc., Piscataway, NJ, USA) and a parallel plate geometry. Starch samples (40% w/w) were solubilized in sealed containers by heating in boiling water for 20min and cooling to 50°C. Hot pastes were placed between the plates and covered with mineral oil to prevent any moisture losses. All measurements were conducted at a frequency of 0.5Hz and a constant 0.5% strain by applying the autostress adjustment mode, while the starch

solutions were cooled from 50°C to 5°C (5°C/min) and stored at 5°C for 20h. All analyses were conducted in triplicate. The coefficient of variation of G' and G" values was less than 5% in all cases.

Results and Discussion

Starch solubilization during α-amylolysis

Differences in the amount of solubilized carbohydrates during α-amylolysis of various barley starches are shown in Fig. 5.1. During the initial eight hours of hydrolysis, at both enzyme levels, all barley starches exhibited relatively high solubilization rates, followed by much slower rates thereafter. Among the three different types of barley starches, the highest hydrolysis rate and the greatest amount of solubilized carbohydrate were found for zero amylose waxy barley and the lowest for high amylose barley (Fig. 5.1 and 5.2). The SEM confirmed these observations (Fig. 5.3). α-Amylase treatments significantly affected the appearance of zero amylose starch granules, creating sponge-like structures with large pores. Relatively uniform erosion was observed at 24h of hydrolysis even at the lowest enzyme concentration. The hydrolysis of normal starch granules was less uniform. The SEM micrographs obtained after 48h of hydrolysis (50 U/g) showed the majority of granules having no visible signs of enzyme attack and a few having numerous pores (Fig. 5.3). The high amylose starch granules showed almost no evidence of enzyme erosion (Fig. 5.3). Enzyme hydrolyzed granules were gently cracked in an attempt to study the effect of α-amylolysis on the inside of the granules. It appears that waxy and normal starch granules exhibited both radial and tangential hydrolysis patterns, and also that the endoerosion was confined only to certain areas of the granules as shown by the channels penetrating right through the granules (Fig. 5.4 A-D). The hydrolysis pattern in high amylose granules appeared to be quite different (Fig. 5.4 E-F), however relatively few high amylose granules were hydrolyzed, compared with normal or waxy starch.

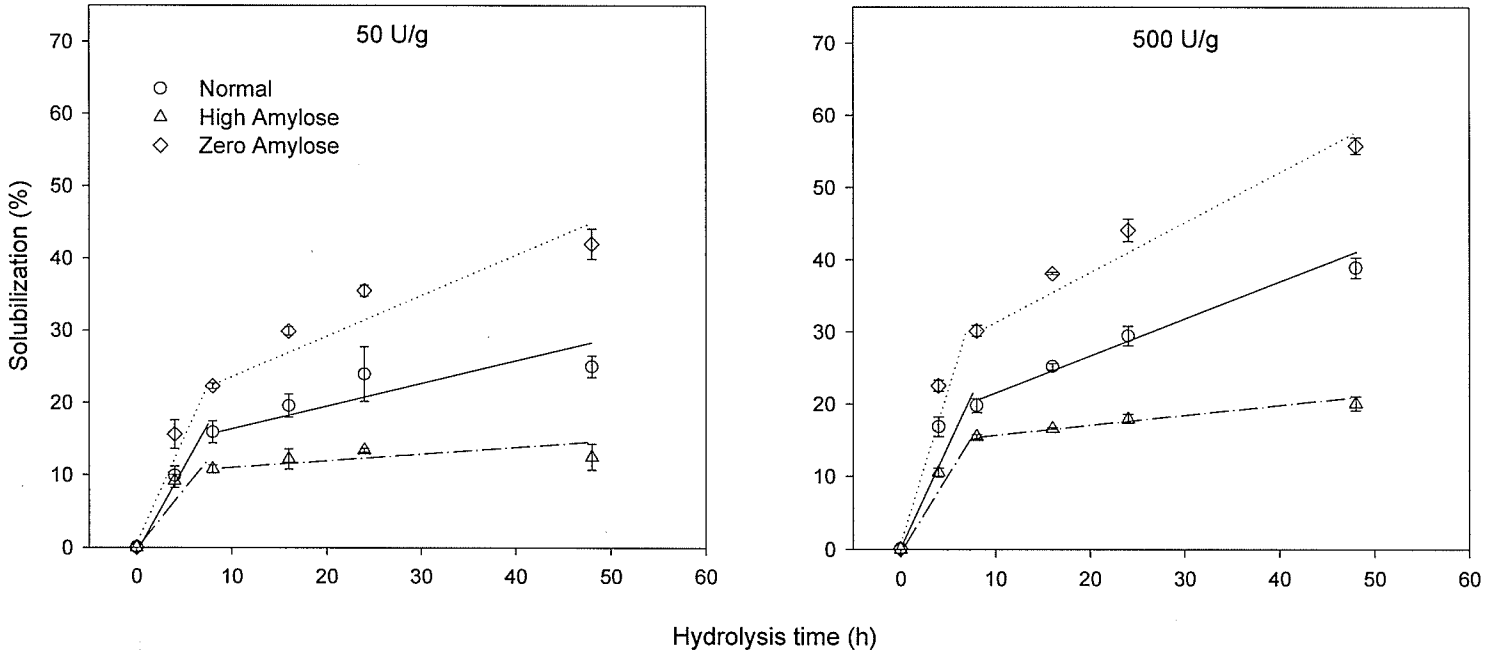

Figure. 5.1. The extent of solubilizations of barley starches with various amylose content during α-amylolysis at two different enzyme levels (50 U and 500 U of α-amylase /g of starch).

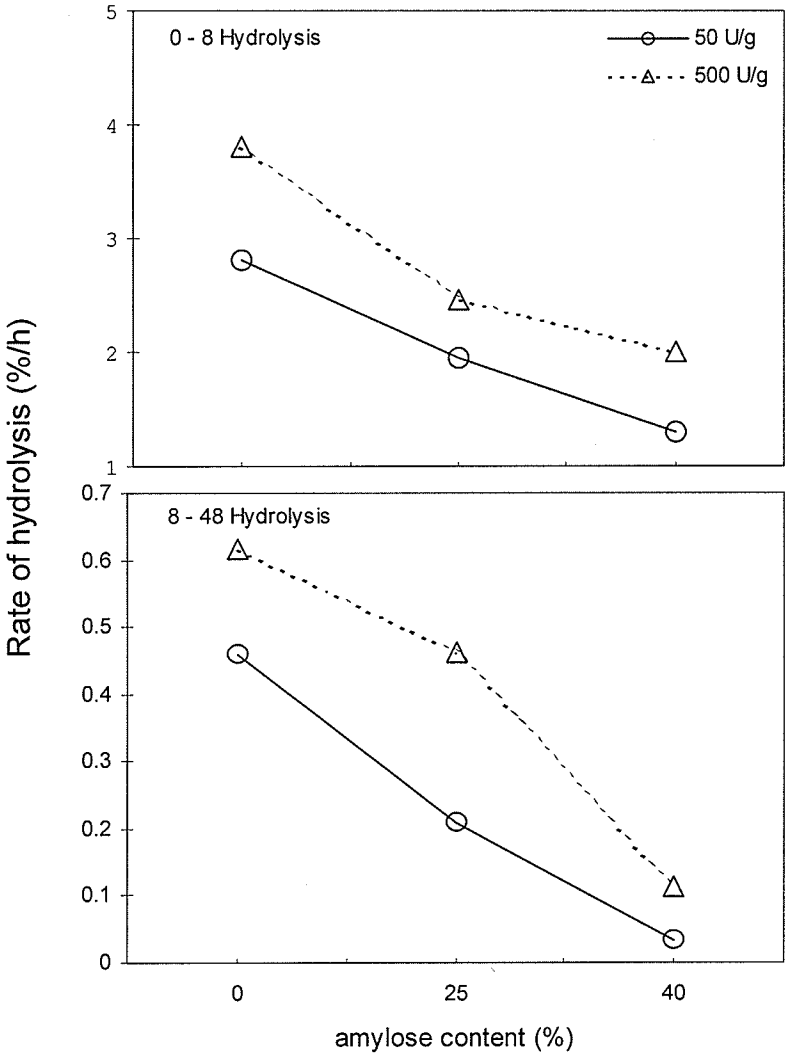

Figure. 5.2. Effect of amylose content on the solubilization rate at the initial (0-8h) and second (8-48h) stages of α-amylase hydrolysis.

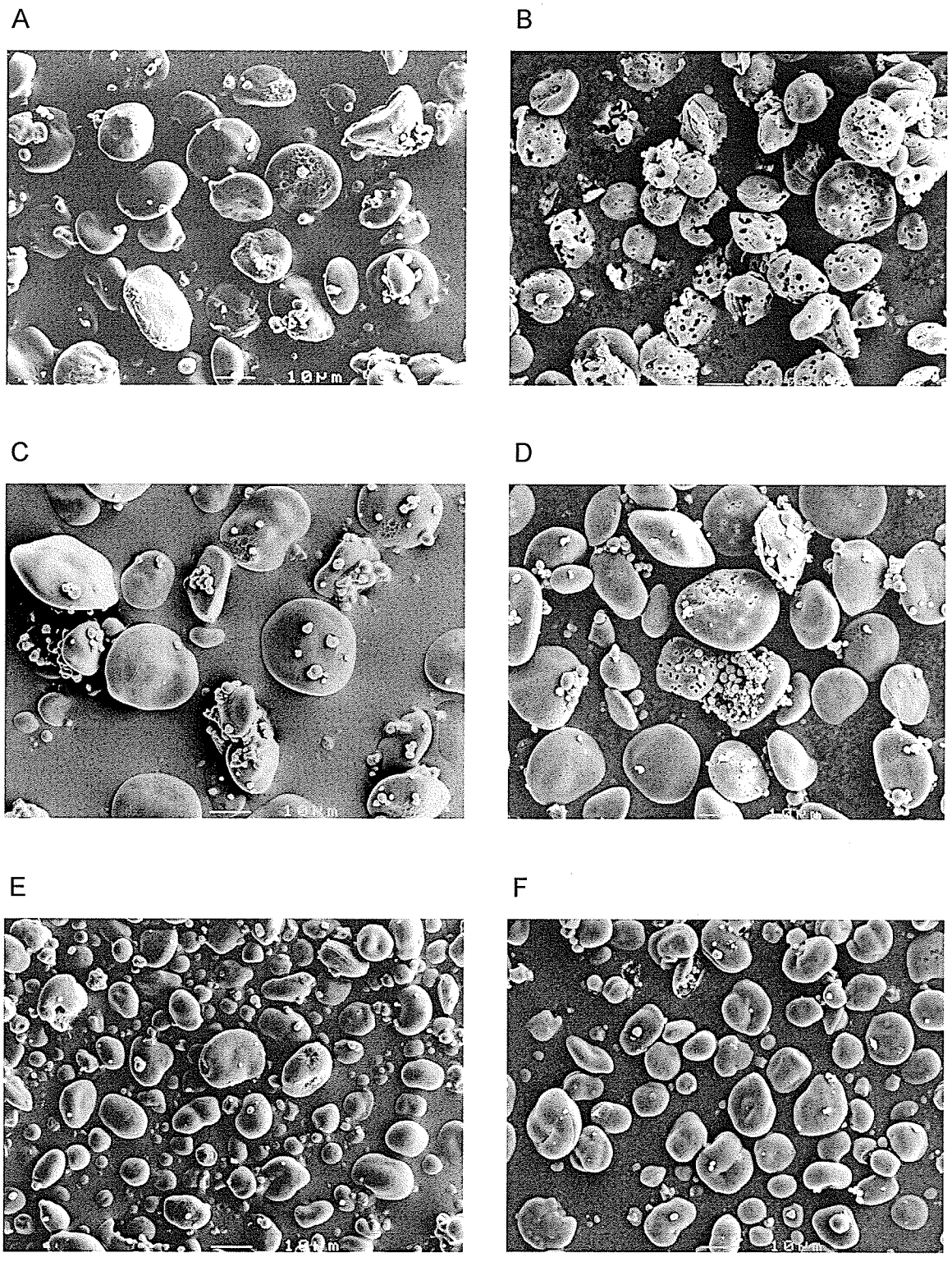

Figure. 5.3. Scanning electron photomicrographs of native and enzyme-treated (50U α-amylase /g of starch, 48h) zero amylose (A,B), normal (C,D), and high amylose (E,F) barley starch granules, respectively.

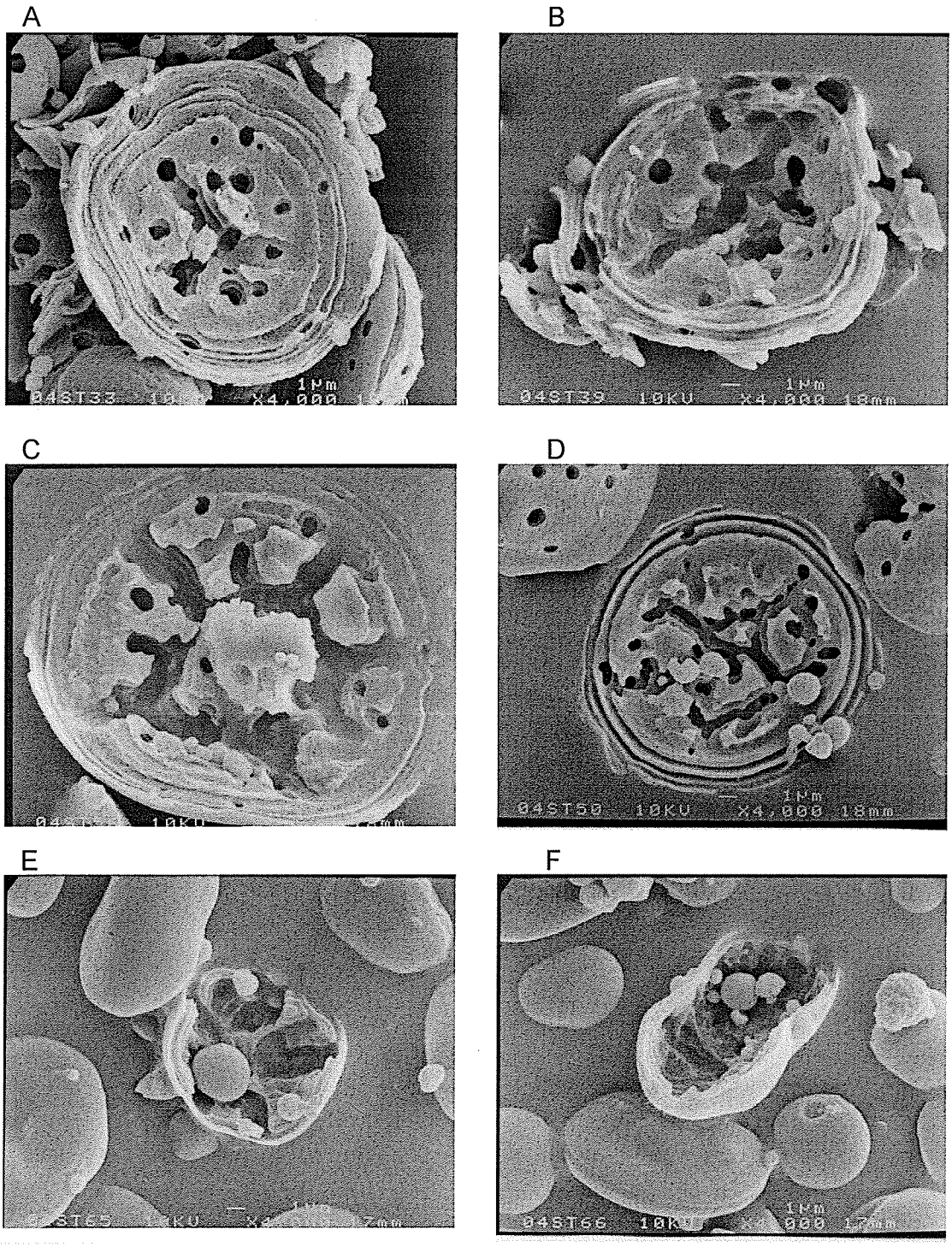

Figure. 5.4. Scanning electron photomicrographs of mechanically cracked enzyme-treated zero amylose (A,B), normal (C,D), and high amylose (E,F) barley starch granules (50U α-amylase/g of starch, 24h).

The rate of solubilization of starch granules during the initial stage of α-amylolysis (0-8h) somewhat decreased with the increasing amylose content of the granules (Fig. 5.2). The rate of solubilization (at 500 U α-amylase/g starch) of zero amylose waxy starch granules was 1.9 and 1.5 times higher than that of high amylose and normal starch granules, respectively. The difference in the hydrolysis rate during the initial stage may be associated with the differences in the surface area and structure as well as with the differences in the porosity of granules from different starches. The presence of some pinholes in the native zero amylose waxy starches (Fig. 5.3) might have facilitated adsorption and binding of α-amylase to the granules and, therefore, a faster initial solubilization rate. No visible pores were observed in the native granules of normal and high amylose starches. The origin of the pores on the surface of zero amylose waxy starches is not clearly understood. It has been suggested that the surface pores might be formed due to α-amylolysis in situ, during drying processes in the cereal kernel, or they may be artifacts generated during the isolation of starch granules. The pores may also be integral features of some starch granules (Fannon et al. 1992). Apparently, some micropores on the starch granules surfaces are not visible by SEM but can be visualized by fluorescence microscopy (Huber and BeMiller 1997).

Several workers have reported that isolated small granules of barley starches were more susceptible to cereal α-amylase hydrolysis than large granules (Bertoft and Kulp 1986; MacGregor and Balance 1980; MacGregor and Morgan 1986). This was attributed to the larger surface area of small granules than that of an equal weight of large granules. The results of this study do not clearly indicate that bacterial α-amylase preferentially attacks the small barley granules when they are present in mixtures with large granules. No evidence of preferential hydrolysis of small granules was provided by the SEM

evaluation (Fig. 5.3). The small granules, especially in normal starch, appeared to be somewhat less corroded than large ones (Fig. 5.3). However, small and large granule counts were not carried out after hydrolysis to confirm these observations. Colonna et al. (1988) reported that during the α-amylolysis of wheat starch granules, the majority of large granules disappeared, indicating their preferential hydrolysis. Planchot and co-workers (1995) also reported that high amylose corn starches, with higher amounts of small granules than normal or waxy corn starches, were more resistant to α-amylolysis.

The rates of solubilization during the second stage of hydrolysis (8 - 48h) were much lower, but substantially more affected by the amount of amylose in the granules than the initial rates (Fig. 5.2). The rate of solubilization of zero amylose waxy starch granules was 5.6 and 1.3 times greater than that of high amylose and normal granules, respectively. These differences are probably associated with the differences in the physical organization of amylose and amylopectin inside the granule. The granular architecture determines how easily the enzyme can penetrate into the granules and how fast and effectively the enzyme-substrate complexes can be formed. It appears that very little penetration of α-amylase inside the high amylose starch granules occurred up to 48h of hydrolysis. This is in contrast to the results observed for zero amylose and normal barley starches (Fig. 5.1 and 5.2). The limited penetration of α-amylase into the granule may be caused by higher density of the granules, restricted swelling capacity, and/or higher amount of amylose-lipid complexes in the high amylose starch granules. Recently, Li et al. (2003) proposed that waxy barley starches have wider intercrystalline amorphous growth rings and more open crystalline lamella than normal and high amylose granules.

X-Ray diffractometry and CP/MAS ^{13}C NMR of hydrolyzed starches

The X-ray diffractograms of native and enzyme-treated (E500 U/g, 48h) barley granules are shown in Fig. 5.5. No significant differences were observed in the X-ray diffraction patterns between native and enzyme-treated normal (39% solubilized) and high amylose (20% solubilized) starches, although a slight increase was detected in the intensity of the peak at 20° (2θ) assigned to amylose-lipid complex (Song and Jane 2000; Zobel 1988). These observations may imply that both amorphous and crystalline regions inside the granules were hydrolyzed concurrently. The SEM micrographs (Fig. 5.4) of mechanically cracked enzyme-treated starches also indicate concurrent hydrolysis of amorphous and crystalline regions. Similar results were reported for α-amylase-treated corn and wheat starches (Colonna et al. 1988; Gerard et al. 2001). The increase in the intensity of amylose-lipid complexes after partial hydrolysis may be attributed to their greater resistance to α-amylolysis and/or formation during enzymatic degradation. Although it is generally agreed that *de novo* synthesized amylose-lipid complexes are resistant to enzymic hydrolysis (Gernat et al. 1990, Seneviratne and Biliaderis 1991), Gerard and co-workers (2001) have recently pointed out that the ultrastructure of the crystalline amylose-lipid complex inside the granule is not known and, therefore, its resistance to α-amylolysis may vary for different starches.

An increase in the crystallinity level was observed for enzyme-treated zero amylose barley starch (56% solubilized), as indicated by the higher diffraction intensities. This may be associated either with the preferential hydrolysis of weakly organized regions inside starch granules (thus leaving the more ordered structures intact) or with the reorganization of local crystallites towards more highly ordered structures.

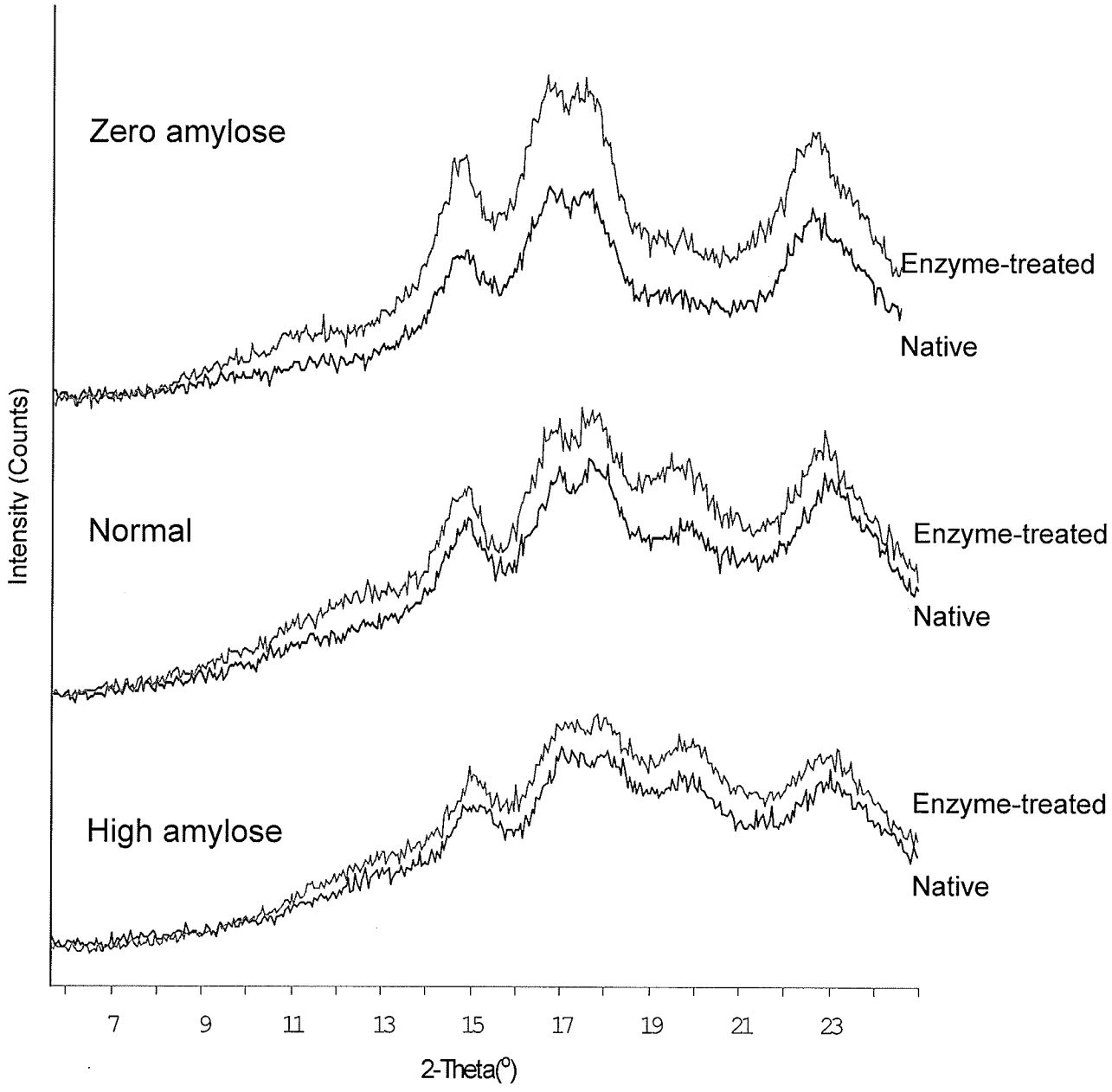

Figure. 5.5. X-ray diffraction patterns of native and enzyme-treated barley starches (500 U of α-amylase /g of starch, 48h); upper line: enzyme-treated starch, lower line: native starch.

Fig. 5.6 shows the solid-state CP/MAS ^{13}C NMR spectra of native and enzyme-treated starches. Assignments of resonances were based on the literature data (Gidley and Bociek 1985; Morgan et al. 1995). Resonances at 99-104 ppm and 81-84 ppm are assigned to C-1 and C-4, respectively. The large signal at 70-73 ppm is associated with C-2, C-3 and C-5, whereas the resonance at 59-62 ppm is associated with C-6 of the glucose residue (Cheetham and Tao 1998; Singh et al. 1993). The CP/MAS ^{13}C NMR provided further evidence for the presence of amylose-lipid complexes in the enzyme-treated normal and high amylose starches. The spectra of these starches exhibited a more pronounced resonance at 81 ppm, which has been assigned to C-4 of amylose-lipid complexes (Gidley and Bociek 1988; Morgan et al. 1995). Additionally, all enzyme-treated starches showed some increases in the intensity of signals at ~ 61 ppm. This resonance is assigned to C-6 of the glucose residues. In amylose, almost all C-6 carry the primary hydroxyl groups, whereas in amylopectin, some C-6 are involved in the glycosidic linkage and carry the α-(1→4)-linked chains. Despite these differences, only small changes in the chemical shift of C-6 are observed for amylose (61.11 ppm) and amylopectin (60.72 ppm) (Cheetham and Tao 1998). It is possible, however, that the observed increase in intensity of the peak at ~ 61 ppm is due to changes in the relative amount of branching points (at C-6) between native and enzyme-treated samples. The NMR spectra also showed narrowing of the linewidth of C-1 peaks in the enzyme-treated starches, especially in the zero amylose starch (Fig. 5.6). This may indicate more ordered and uniform conformation and even a higher crystalline order in the granules after amylolysis.

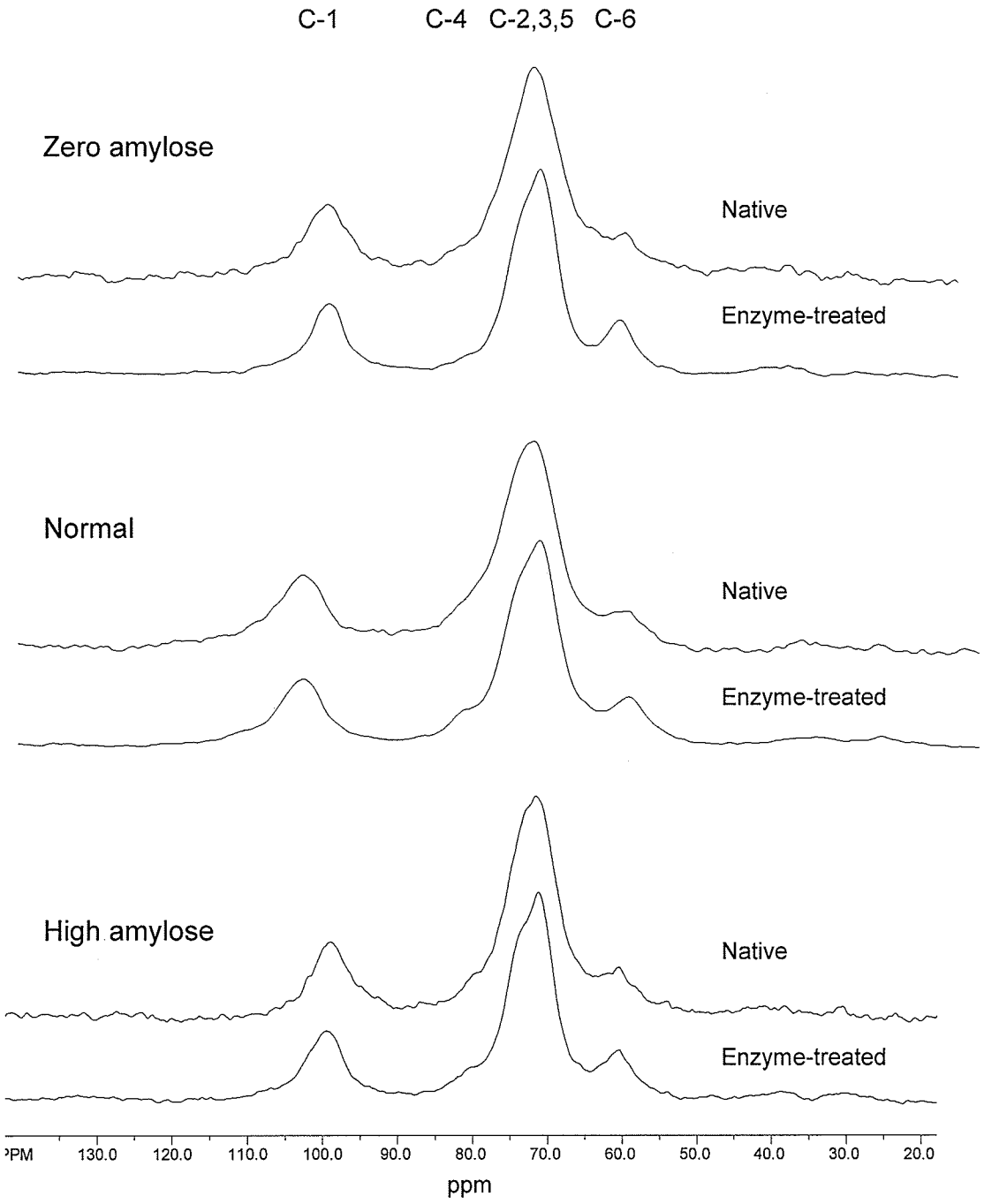

Figure. 5.6. CP/MAS ^{13}C NMR spectra of native and enzyme-treated barley starches (500 U of α-amylase /g of starch, 48h)

Molecular weight and structure of hydrolyzed starch polymers

The molecular weight distribution of starch polymers remaining after partial enzymic hydrolysis of the granules is shown in Fig. 5.7a-c. The first peak, eluted between 10 and 12mL, represents the high molecular weight amylopectin, whereas the second peak, at higher elution volumes, corresponds mainly to amylose (Chapter 3). It has been shown, however, that a portion of amylopectin may also elute in the latter region and, therefore, the accurate determination of the M_w of amylose may be compromised (Chapter 3). For all three types of barley starches, some changes in the M_w distribution were observed after α-amylolysis; however, both starch polymers remained in their macromolecular forms (Table 5.1, Fig. 5.7a-c). The M_w of amylopectin decreased more in zero amylose waxy than in normal and high amylose starches with the increasing hydrolysis time and the amount of enzymes used for hydrolysis. After 56% solubilization, about a three-fold decrease in the M_w of amylopectin was observed in the zero amylose waxy sample.

The M_w of amylopectin in normal starch also decreased after α-amylolysis; however, the changes were less drastic than for the zero amylose starch. The higher amount of species eluting between 12 and 20mL in the partially hydrolyzed normal starch (Fig. 5.7a) may indicate some hydrolysis products eluting in this region. Therefore, the decrease in the M_w of species eluting in this region does not necessarily indicate that the M_w of amylose decreased substantially during α-amylolysis (Table 5.1). The M_w of high amylose starch components was the least affected by α-amylolysis; only very small changes in the M_w of amylose and amylopectin were observed (Fig. 5.7b and Table 5.1).

The elution profiles of debranched amylose in normal and high amylose starches are shown in Fig. 5.8a-b. As previously reported (Chapter 3), amylose in barley starches

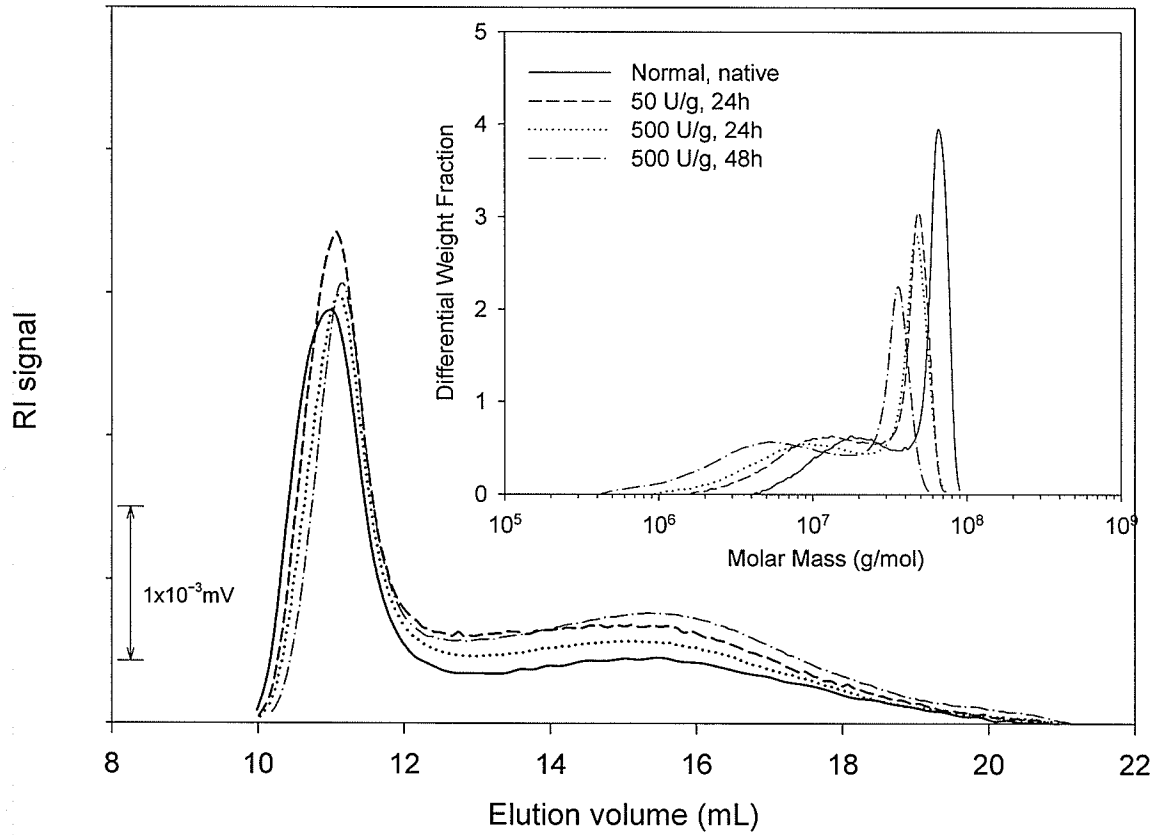

Figure. 5.7a. HPSEC elution profiles of native and α-amylase-treated normal barley starches. Weight average molecular weight (M_w) distributions of native and enzyme-treated barley starches (inserts).

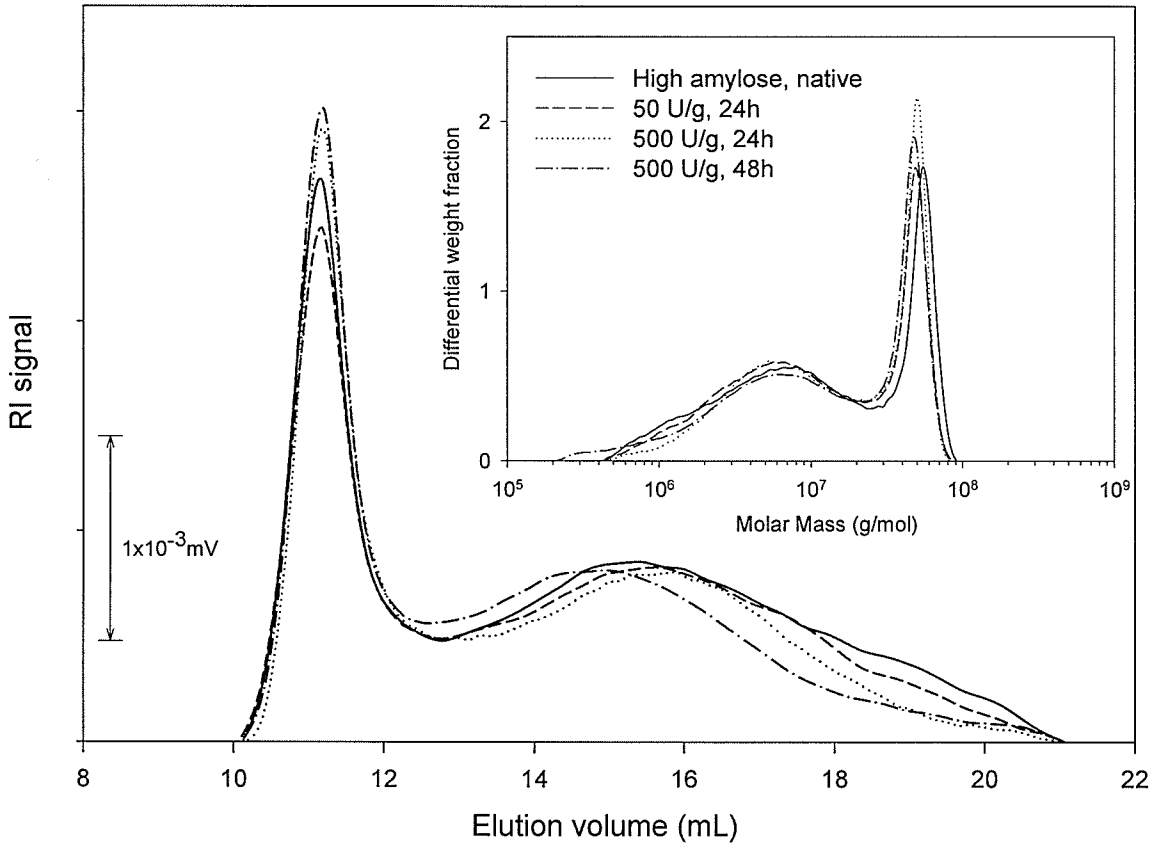

Figure. 5.7b. HPSEC elution profiles of native and α-amylase-treated high amylose barley starches. Weight average molecular weight (M_w) distributions of native and enzyme-treated barley starches (inserts).

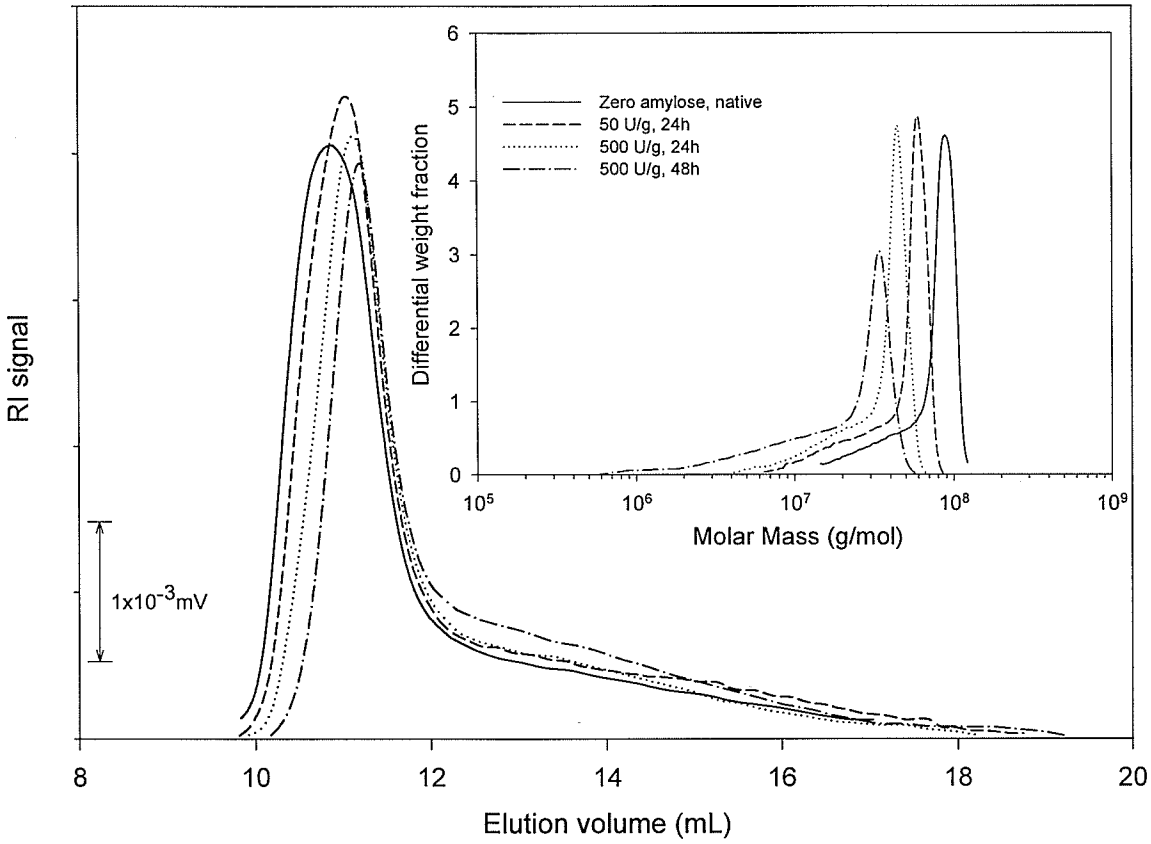

Figure. 5.7c. HPSEC elution profiles of native and α-amylase-treated zero amylose barley starches. Weight average molecular weight (M_w) distributions of native and enzyme-treated barley starches (inserts).

Table 5.1. Effect of α-amylolysis on solubilization, M_w, and R_g of various barley starches

Enzyme treatment	Normal starch					High amylose starch					Zero amylose starch				
	Solubili-zation (%)	High M_w fraction (V_e:10-12 mL)		Low M_w fraction (V_e:12-20 mL)		Solubili-zation (%)	High M_w fraction (V_e:10-12 mL)		Low M_w fraction (V_e:12-20 mL)		Solubili-zation (%)	High M_w fraction (V_e:10-12 mL)		Low M_w fraction (V_e:12-20 mL)	
		$M_w\times10^{-6}$ (g/mol)	R_g (nm)	$M_w\times10^{-6}$ (g/mol)	R_g (nm)		$M_w\times10^{-6}$ (g/mol)	R_g (nm)	$M_w\times10^{-6}$ (g/mol)	R_g (nm)		$M_w\times10^{-6}$ (g/mol)	R_g (nm)	$M_w\times10^{-6}$ (g/mol)	R_g (nm)
Native starch		114±1.4	161±0.7	9.8±0.4	124±7.5		82±0.7	121±3.5	3.8±0.7	93±2.8		147±8.5	186±8.5	31±2.8	141±15
Enzyme-treated															
50U/g, 24h	24	87±5.6	146±4.2	5.5±0.3	112±2.1	13	79±6.2	135±8.4	3.6±0.7	95±4.2	36	110±2.8	165±2.1	21.8±7.3	109±8.4
50U/g, 48h	25	78±8.9	151±13	6.5±0.6	112±3.5	13	82±7.1	120±7.8	3.4±0.3	82±0.7	42	96±9.1	159±9.2	18.1±1.6	105±13
500U/g, 24h	29	83±4.2	145±2.8	4.6±0.3	106±0.0	18	87±5.9	119±6.3	3.5±0.6	84±2.8	44	75±1.4	140±8.4	15.8±4.5	84±0.7
500U/g, 48h	39	82±6.3	148±22	4.7±2.8	104±18	20	76±9.3	115±5.6	3.1±0.3	73±4.2	56	50±0.3	115±0.0	5.9±1.7	68.5±6.4

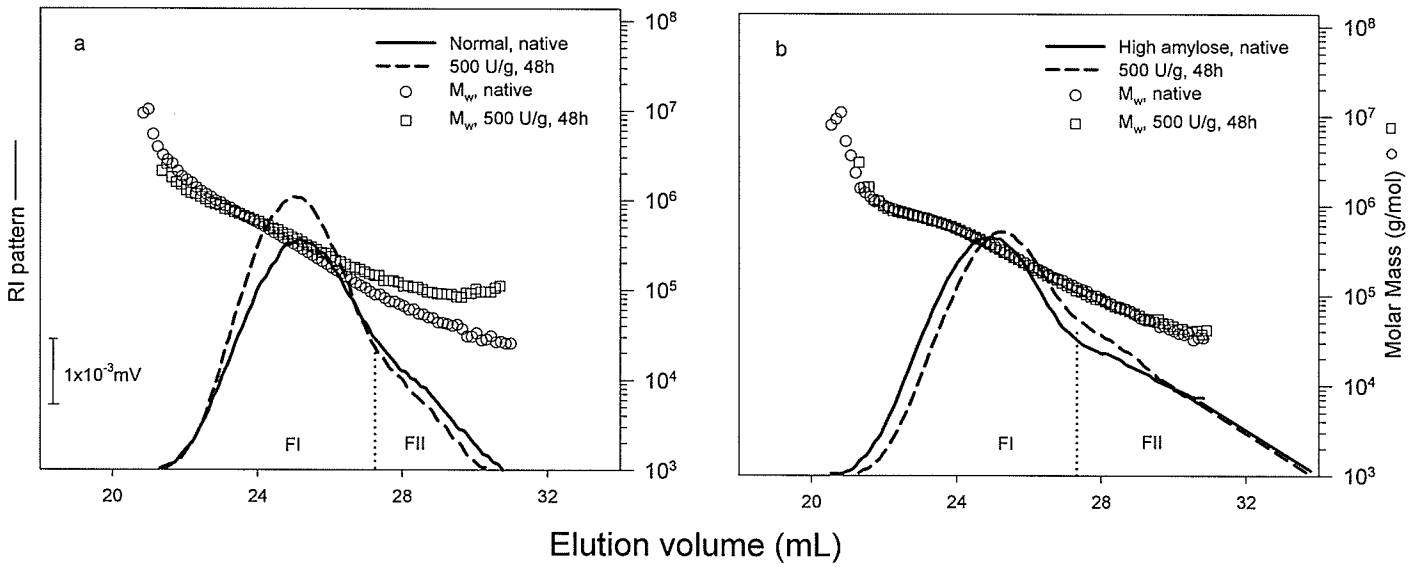

Figure. 5.8. HPSEC elution profiles and weight average molecular weights (M_w) of debranched native and enzyme-treated normal (a), and high amylose (b) barley starch polymers.

exhibits a certain degree of branching and after treatment with debranching enzymes elutes in two populations: fraction I (FI) at V_e: 22-27mL and fraction II (FII) at V_e: 27-32mL. Only small changes in the M_w of both amylose fractions were observed after α-amylolysis, although the M_w of FI in high amylose starch was slightly lower after α-amylolysis (Table 5.2). These results confirmed that amylose is not preferentially hydrolyzed during α-amylolysis. Similar observations were made for wheat, corn, and sorghum starches (Colonna et al. 1988; Leach and Schoch 1961).

The relative distribution of linear chains (DP 3-50) in amylopectin of native and partially hydrolyzed starches is shown in Fig. 5.9a-c. Some differences in the relative amount of linear chains were observed especially in amylopectin of the zero amylose starch. After hydrolysis, the amount of longer chains with DP≥35 decreased, whereas the amount of chains with DP<34 slightly increased. It is possible that the increase of shorter chains originated from the scission of longer chains. However, the differences were very small, and it appears that the primary molecular structure of linear chains in amylopectin, after partial α-amylolysis, was not significantly affected.

Our results clearly indicate that the susceptibility and extent of hydrolysis of barley starches were substantially affected by the presence and the amount of amylose in starch granules. Surprisingly, despite the extensive physical erosion and fragmentation of the zero amylose starch granules, the polymers remaining in the granule residues retained their macromolecular size. Our observations are in agreement with several previous reports. Leach and Schoch (1961) demonstrated that the intrinsic viscosities of corn and potato starches remaining after α-amylase attack (56-58% solubilization) were only slightly lower than those of the parent starches. They postulated that α-amylase does not penetrate freely into the molecular lattice of the granule, but limits its action to

Table 5.2. Weight average molecular weights (M_w) of amylose after debranching of native and enzyme-treated barley starches.

Sample	Amylose	
	F I[a] $M_w \times 10^{-3}$ (g/mol)	F II[a] $M_w \times 10^{-3}$ (g/mol)
Normal Starch		
Native	423 ± 1.5	74 ± 3.1
Enzyme-treated (500U/g, 48h)	452 ± 1.4	88 ± 5.3
High amylose starch		
Native	423 ± 14.9	70 ± 7.2
Enzyme-treated (500U/g, 48h)	373 ± 23.8	71 ± 6.3

[a] Fractions of amylose as indicated in Fig. 5.8.

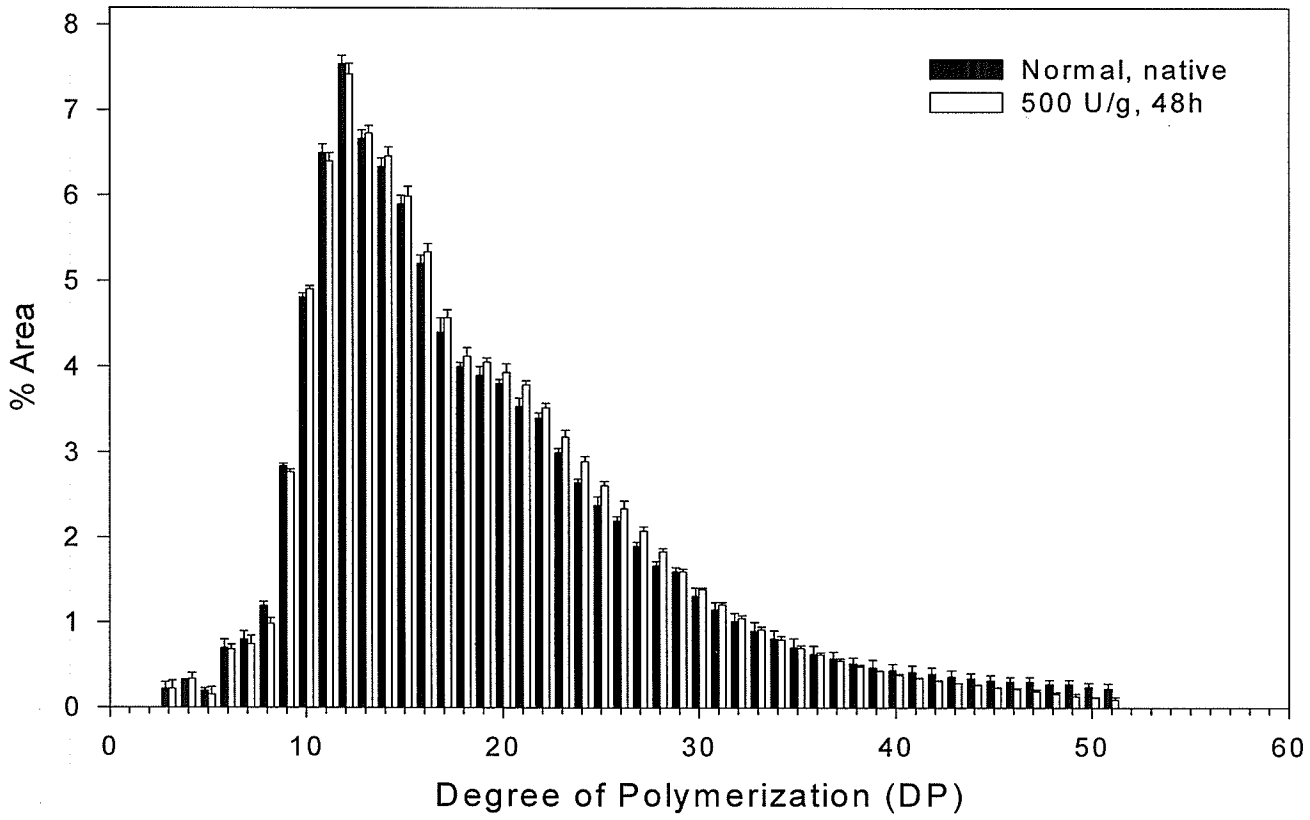

Figure. 5.9a. HPAEC profiles of debranched linear chains of native and enzyme-treated normal barley starches.

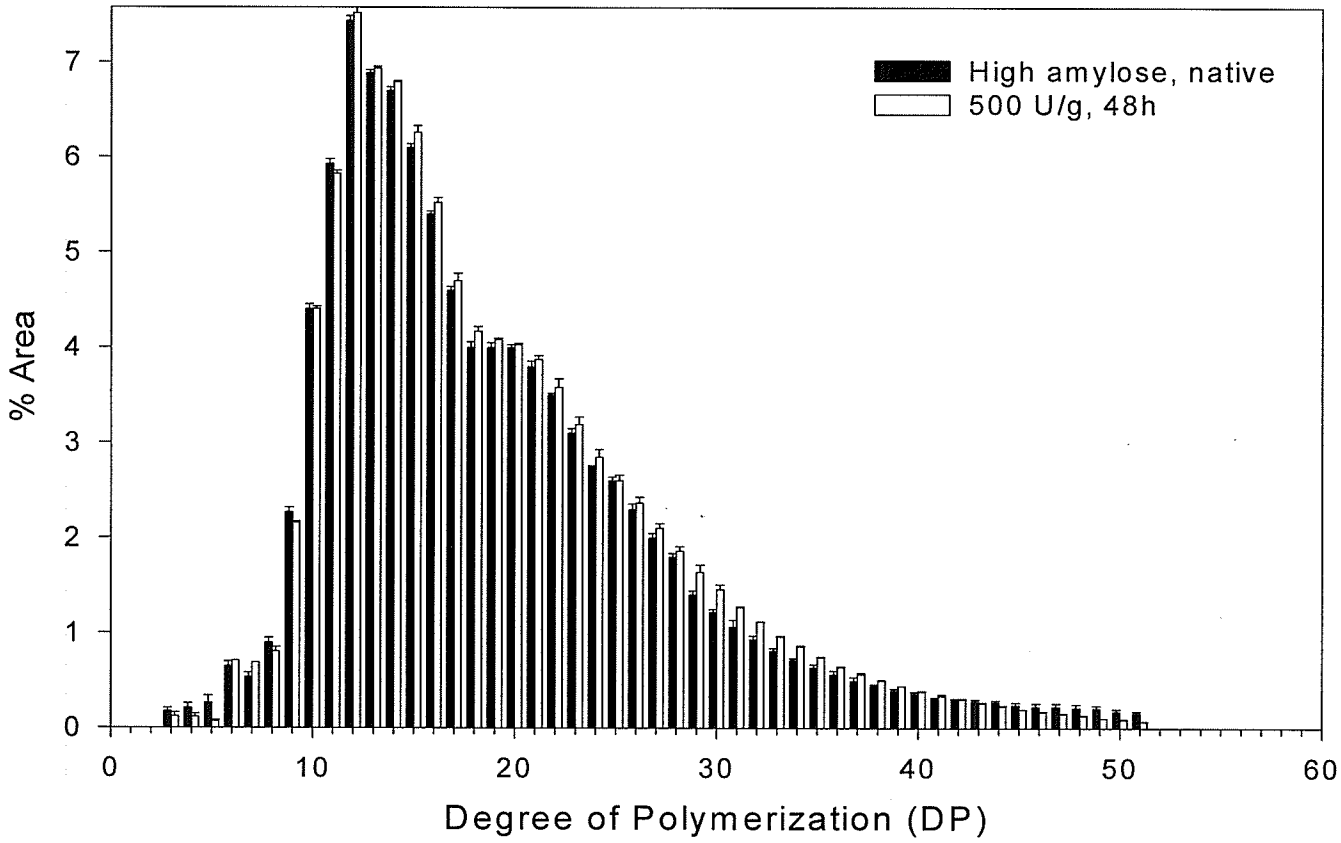

Figure. 5.9b. HPAEC profiles of debranched linear chains of native and enzyme-treated high amylose barley starches.

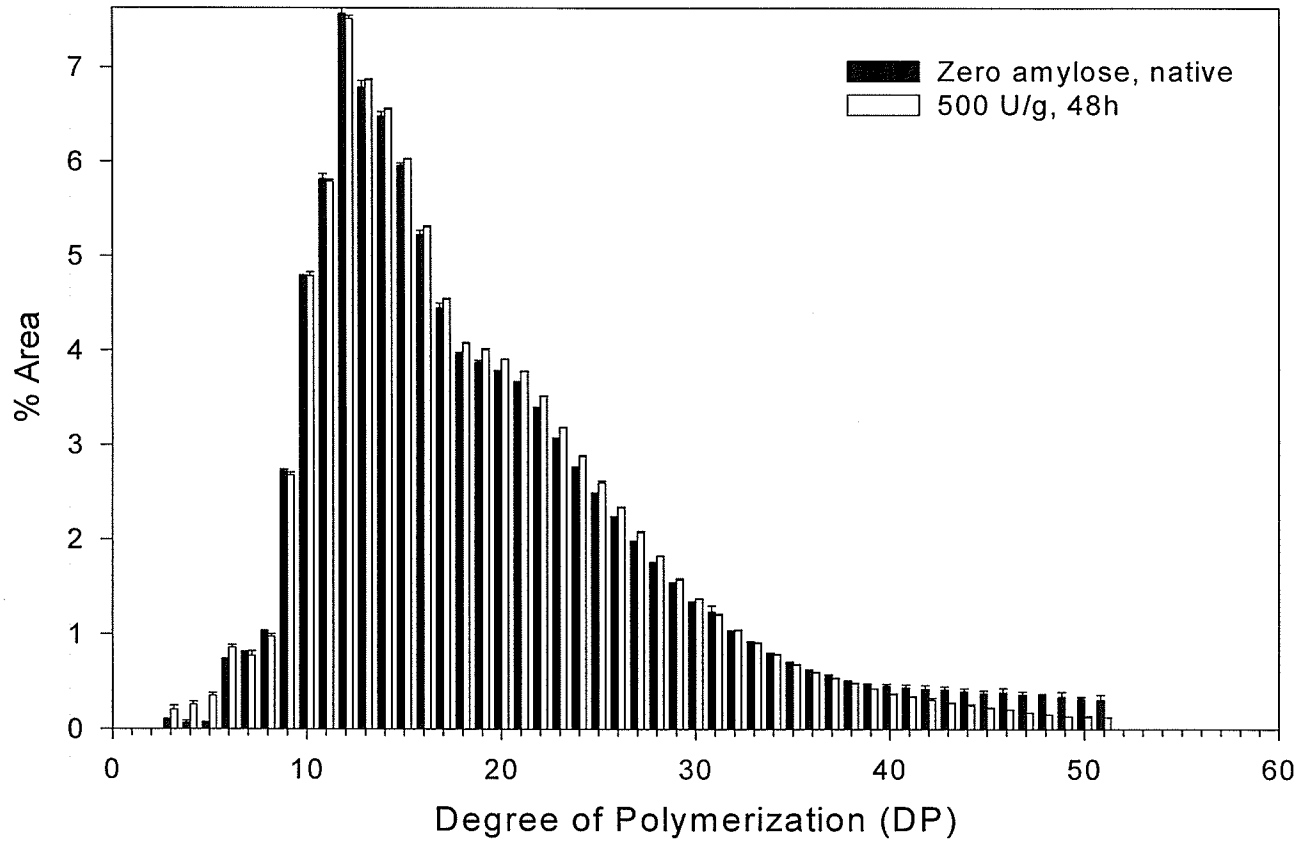

Figure. 5.9c. HPAEC profiles of debranched linear chains of native and enzyme-treated zero amylose barley starches.

certain accessible regions only. Colonna et al. (1988) inferred that the α-amylase molecule, due to its size (diameter of 6 nm), may be unable to diffuse readily through the native granule. It was demonstrated recently that molecules with hydrodynamic radius above 0.6 nm cannot penetrate starch granules, and therefore, the free movement of α-amylase within the starch granules is limited (Planchot et al. 2000). Contrary to our results, Lauro et al. (1999) reported that when half of the barley large granules were solubilized, the high molecular weight amylopectin peak disappeared from the HPSEC profile. According to Colonna et al. (1988), even after 91% solubilization, the molecular size distribution of wheat starch polymers was similar to that of the original starch. The authors suggested, however, that unequal susceptibility of wheat starch granules to α-amylolysis and the granule-by-granule hydrolysis mechanism may partially explain the unchanged molecular size distribution of starch polymers. Lauro and co-workers (1999) reported more uniform α-amylolysis of large barley starch granules, even though they also observed some intact granules remaining after extensive hydrolysis. In our studies, the normal starch granules exhibited somewhat unequal susceptibility to hydrolysis, but the zero amylose waxy granules were uniformly eroded (Fig. 5.3). The relatively high molecular weights as well as the intact molecular structure of the starch polymers remaining in the fragmented granules confirm that mobility and diffusion of α-amylase inside the granule are restricted and that the hydrolysis reactions proceed only in localized regions in the granules. Clearly, the presence of amylose affects the granule's morphology (ultrastructure, crystalline size, and interactions between amorphous and crystalline regions) and, consequently, the access and migration patterns of the enzyme inside the granule. Using transmission electron microscopy (TEM), Planchot et al. (1995) and Evans and Thompson (2004) showed that normal and waxy maize starch

granules exhibit a simultaneous tangential and radial hydrolysis pattern, whereas the high amylose maize granules exhibit mostly radially-oriented patterns. Our SEM results (Fig. 5.4) also show very different hydrolysis pattern for high amylose barley starch compared to waxy or normal starches.

Thermal properties

The DSC profiles of native and enzyme-treated starches during heating are shown in Fig. 5.10a-c, and the characteristic melting transitions are given in Table 5.3. The first endothermic peak at lower temperature (~65°C) represents the melting of amylopectin crystallites, while the peak at higher temperature (~100°C) corresponds to the melting of amylose-lipid complexes.

The thermograms of the native and enzyme-treated normal and high amylose starches were generally similar, but the melting enthalpy values (ΔH) for amylopectin and amylose-lipid complexes for partially hydrolyzed samples were higher than for the intact starches (Table 5.3). No differences in the peak melting temperatures (T_p) of amylopectin were recorded but the completion temperatures (T_c) were slightly higher for the partially hydrolyzed samples. According to Cooke and Gidley (1992), the ΔH values correlate mainly with the amount of double helices that unravel and melt during gelatinization. Our results may indicate, therefore, that α-amylase preferentially hydrolyzed the weakly organized regions, leaving the regions enriched in double-helical order intact. It is also possible that some re-ordering and re-structuring of starch polymers within the granule may have also occurred during amylolysis. In addition to higher endothermic enthalpy values for amylopectin, the partially hydrolyzed normal and high amylose starches also exhibited higher ΔH values for amylose-lipid complexes.

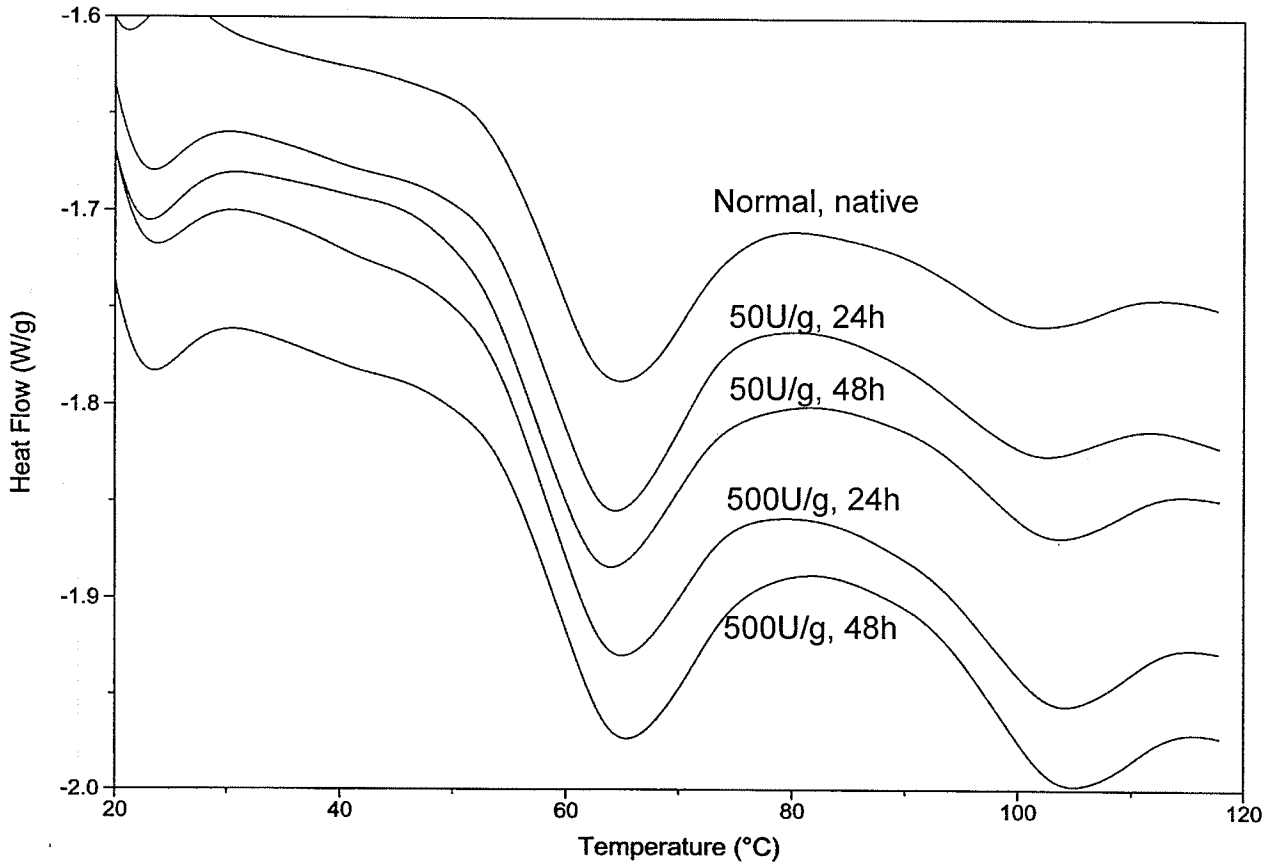

Figure. 5.10a. DSC thermograms of native and enzyme-treated normal barley starches (40% w/w).

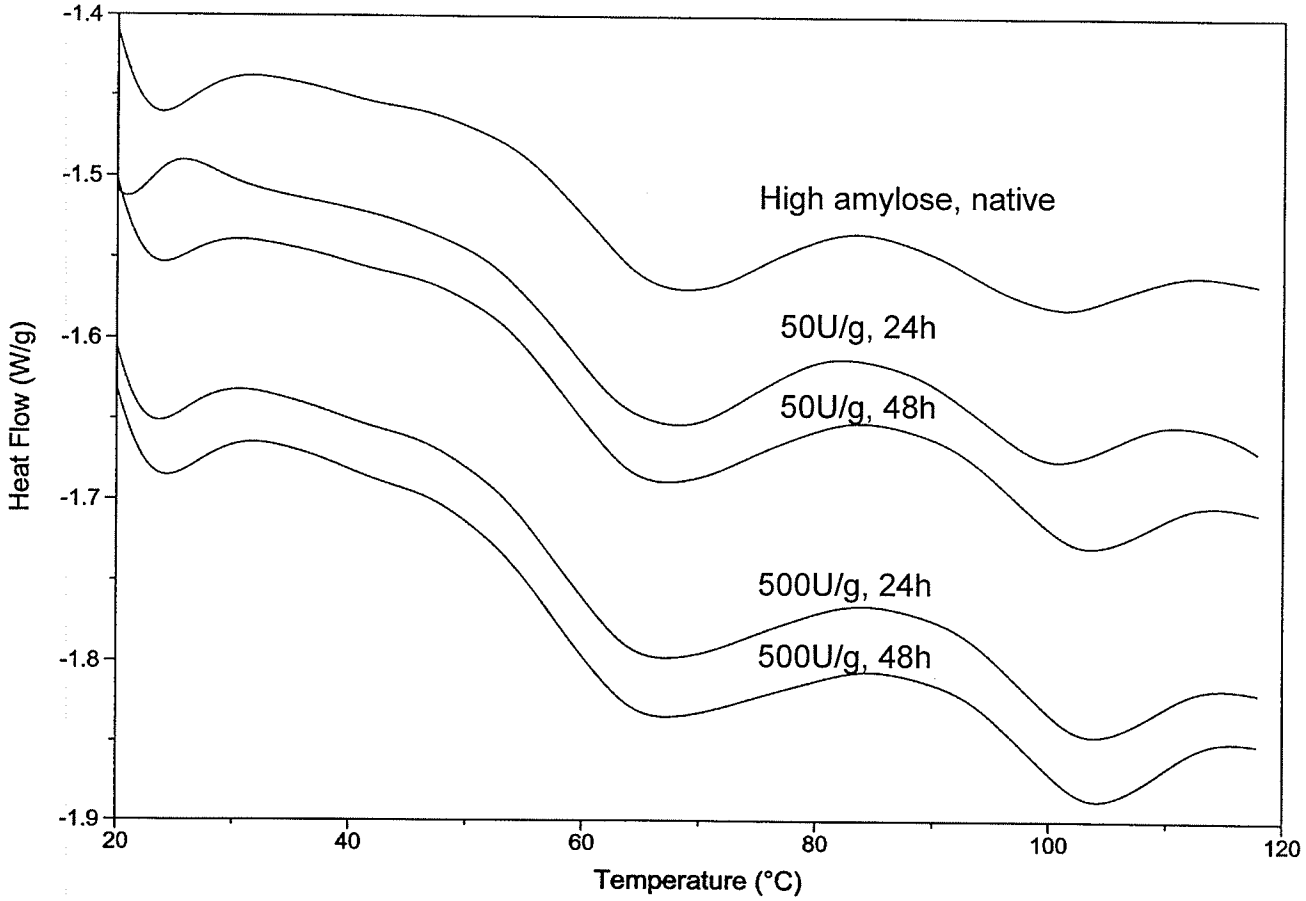

Figure. 5.10b. DSC thermograms of native and enzyme-treated high amylose barley starches (40% w/w).

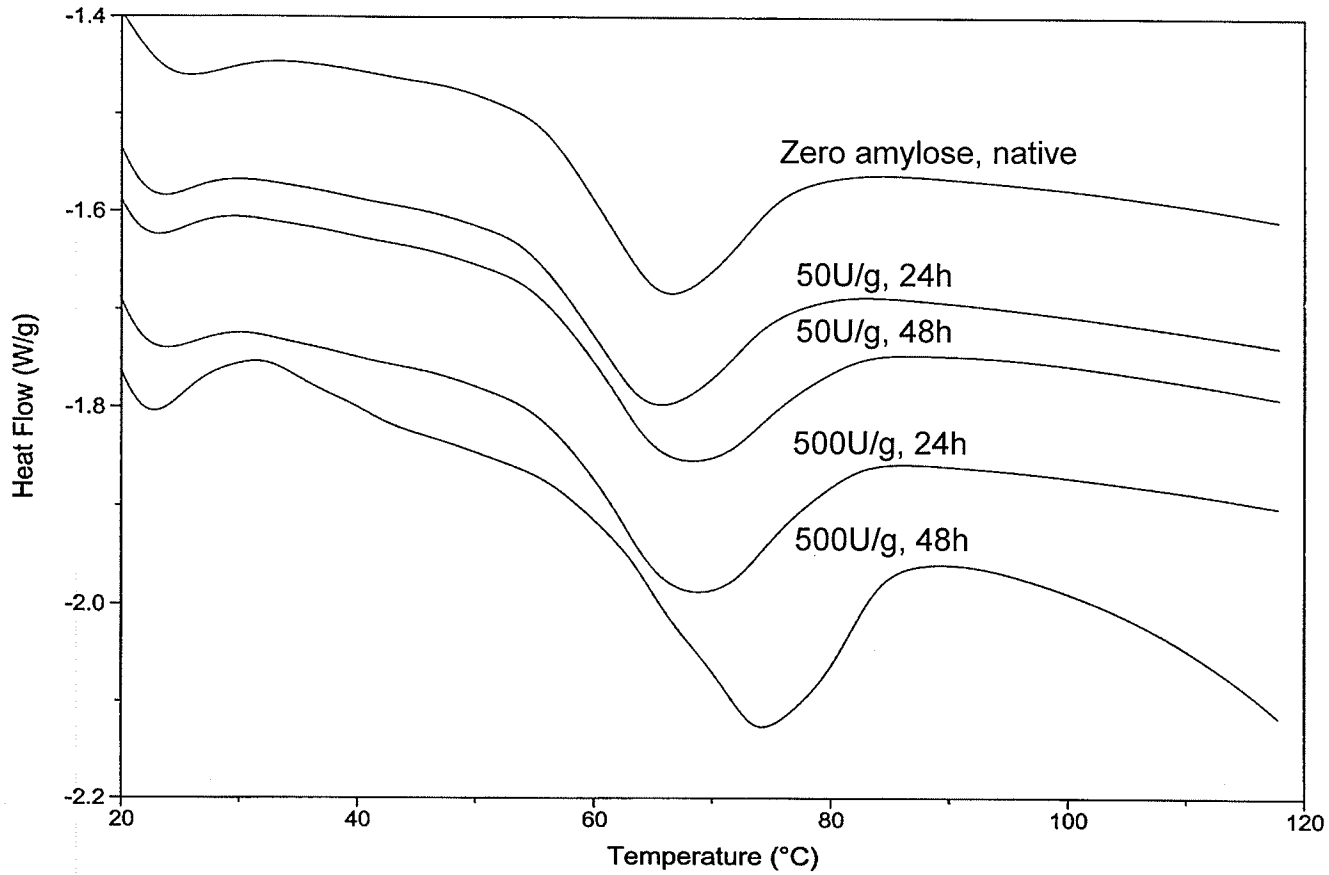

Figure. 5.10c. DSC thermograms of native and enzyme-treated zero amylose barley starches (40% w/w).

Table 5.3. DSC gelatinization temperatures and enthalpies of native and α-amylase-treated starches

Sample	Amylopectin				Amylose-lipid	
	T_o(°C)	T_p(°C)	T_c(°C)	ΔH (J/g)	T_p (°C)	ΔH (J/g)
Normal starch						
Native	53.8±0.2	64.2±0.2	80.1±0.2	9.7±0.2	101.3±0.6	1.9±0.3
Enzyme-treated						
50 U/g, 24h	52.1±0.4	63.7±0.3	80.2±0.3	11.6±0.9	102.2±1.4	2.8±0.3
50 U/g, 48h	53.3±0.3	63.7±0.4	82.4±0.1	12.2±0.1	102.9±0.2	3.0±0.1
500 U/g, 24h	52.9±0.2	63.7±0.4	81.1±0.9	12.2±0.1	102.9±0.2	3.1±0.0
500 U/g, 48h	53.6±0.0	64.9±0.1	82.9±0.6	11.9±0.5	103.8±0.4	4.6±0.0
High amylose starch						
Native	54.0±0.1	66.9±0.2	83.4±0.3	6.9±0.01	100.5±0.2	2.3±0.5
Enzyme-treated						
50 U/g, 24h	52.3±0.2	65.6±0.5	82.6±0.0	7.8±0.1	99.9±0.2	2.6±0.3
50 U/g, 48h	52.0±0.3	65.3±0.4	84.2±0.5	8.8±0.4	102.8±0.1	3.3±0.2
500 U/g, 24h	51.4±0.0	65.4±0.4	85.3±0.3	8.5±0.2	102.9±0.3	3.5±0.1
500 U/g, 48h	52.2±1.3	65.2±0.0	84.4±0.2	9.6±0.1	103.5±0.0	4.2±0.1
Zero amylose starch						
Native	55.2±0.4	65.9±0.5	85.6±1.3	14.3±0.7		
Enzyme-treated						
50 U/g, 24h	53.8±0.3	65.1±0.2	84.0±0.2	13.8±0.1		
50 U/g, 48h	56.1±1.2	67.8±0.7	88.4±1.1	17.1±0.4		
500 U/g, 24h	58.1±3.2	67.9±0.7	86.2±1.4	16.8±0.3		
500 U/g, 48h	57.8±1.6	73.9±0.1	88.1±2.7	20.2±0.3		

These results are in accordance with the X-ray crystallography and CP/MAS ^{13}C NMR data (Fig. 5.5 and 5.6).

For the zero amylose barley starches, which underwent much greater solubilization than normal and high amylose samples, a significant increase in the T_p and ΔH values was observed. These results, supported by data obtained from the X-ray studies, would suggest that the overall crystalline order in zero amylose starch increased due to partial α-amylolysis. This could be either due to more extensive degradation of chains in the less dense amorphous regions of zero amylose starch granules compared with high amylose or normal granules, or due to perfection of the crystalline regions facilitated by plasticization and increased chain mobility in regions affected by α-amylase. To date, there is no agreement as to the effects of enzymic hydrolysis on the thermal properties of starches. Lauro and co-workers (1999) observed large increases in T_p, and decreases in ΔH with increasing solubilization rate of large barley starch granules, whereas, Colonna et al. (1988) reported no changes in the DSC profiles of wheat starches even after 91% solubilization.

Digestibility of hydrolyzed starches

The previously partially hydrolyzed barley starches were again subjected to α-amylolysis to determine whether their susceptibility to hydrolysis changed compared to the native samples. Partially hydrolyzed normal and high amylose samples exhibited slightly lower susceptibility to subsequent α-amylolysis than the native starches (Fig. 5.11). The degree of solubilization also slightly decreased with the increasing extent of previous hydrolysis, indicating densely packed ultrastructure remaining in the granules after initial hydrolysis. Interestingly, the partially hydrolyzed waxy starch granules,

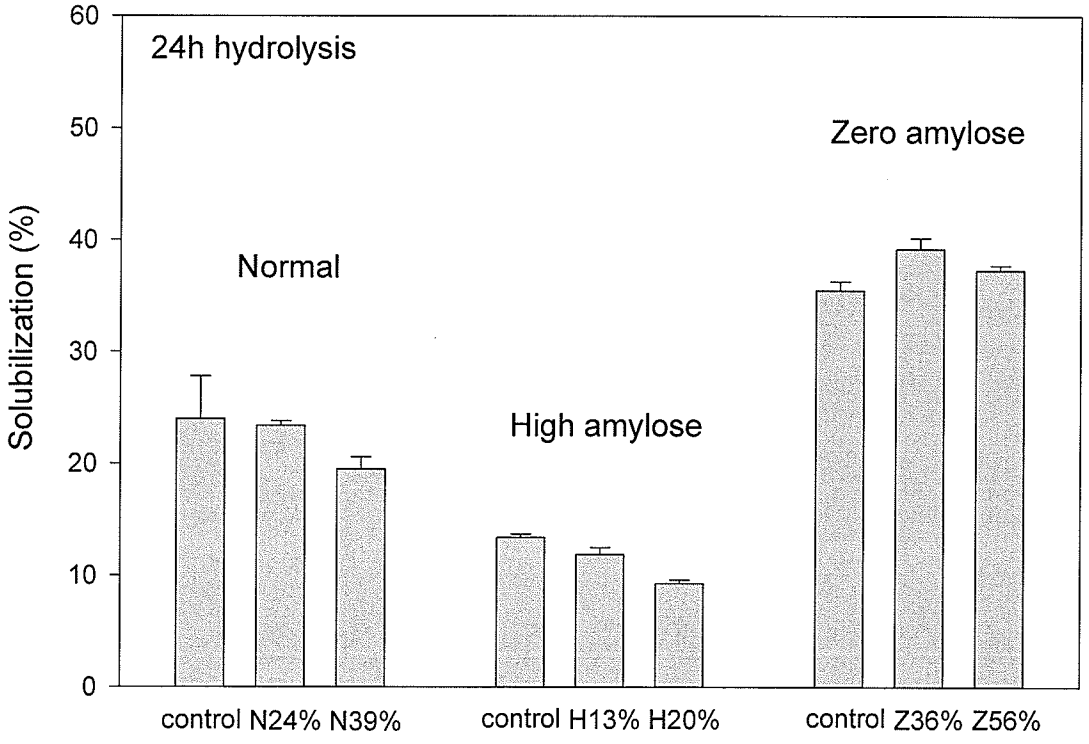

Figure. 5.11. The extent of solubilizations of native and previously hydrolyzed barley starches after 24h of α-amylolysis (N24% and N39%, normal starches previously solubilized to 24% and 39%, respectively; H13% and H20%, high amylose starches previously solubilized to13% and 20%; Z36% and Z56%, zero amylose starches previously solubilized to 36% and 56%, respectively).

despite having a slightly higher degree of crystallinity, showed similar enzyme susceptibility as native starches. It seems probable that the highly corroded surface and numerous channels penetrating the interior of the waxy granules, as well as the presence of loosely organized amorphous regions, facilitated the subsequent hydrolysis. It appears that once the enzyme is able to penetrate the loosely packed regions in the granules, its action will eventually lead to disrupting and disarranging of the crystallites and their subsequent hydrolysis. The presence of amylose in the amorphous regions of the granule (either intertwined in the branching regions of amylopectin, or in the helical complexes with lipids) increases their density and reduces formation of effective enzyme-substrate complexes.

Rheological properties of starches

The viscoelastic properties of native and enzyme-treated starch solutions (40% w/w) during cooling (50°C to 5°C) and storage for 20h (5°C) are shown in Fig. 5.12 and 5.13, respectively. Upon cooling, the native normal and high amylose starch solutions exhibited greater development of the elastic (G') than viscous (G") modulus, indicating a formation of stronger three-dimensional networks with decreasing temperature (Fig. 5.12). The tan δ values decreased from 0.19 to 0.13 for normal starch and from 0.14 to 0.09 for the high amylose sample. These results clearly indicate that high amylose starch formed stronger gels than normal starch. The native zero amylose starch solution showed substantially lower G' values during cooling and storage than normal and high amylose samples. Although the G' slightly increased, especially between the 8 and 16h storage, the overall very low values of G' and a relatively high tan δ value after storage (0.3) indicate formation of a paste rather than a gel.

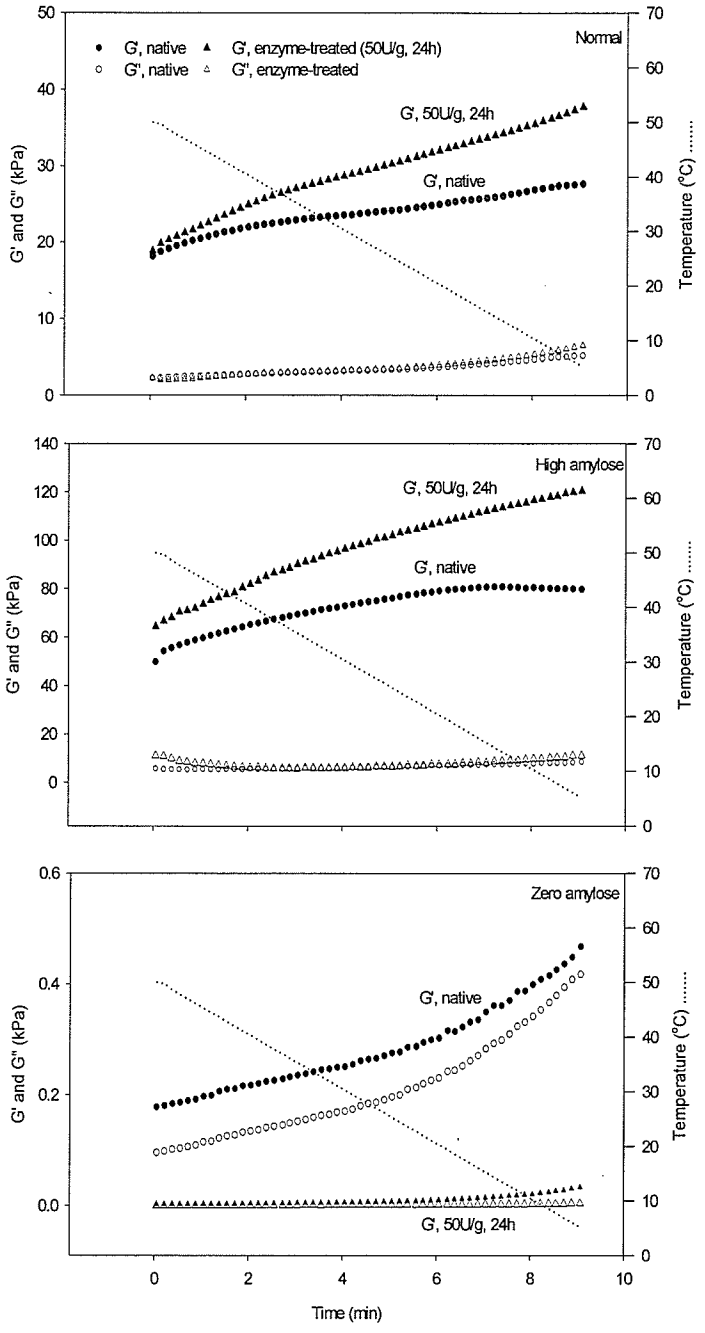

Figure. 5.12. The development of G' and G" moduli in native and enzyme-treated barley starches (40% w/w) upon cooling from 50°C to 5 °C (cooling rate of 5 °C/min).

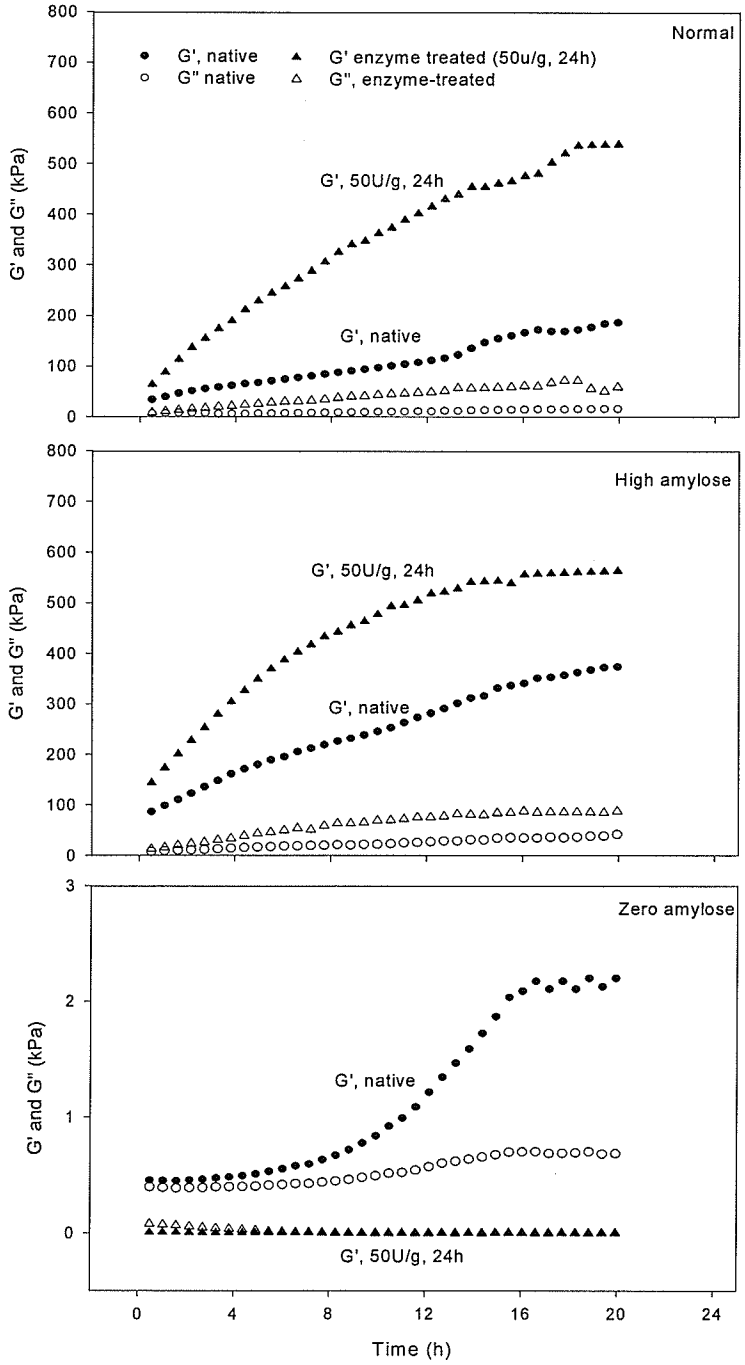

Figure. 5.13. The network development of native and enzyme-treated barley starches (40% w/w) during storage for 20h at 5 °C.

Starch gel can be regarded as "a polymer composite in which swollen granules are embedded in and reinforce a continuous matrix of entangled amylose molecules" (Ring 1985). Therefore, the amylose gel matrix, the volume fraction and rigidity of swollen granules as well as the interactions among the starch components are all major factors affecting the viscoelastic properties of starch gels (Eliasson 1986). The amylose gel matrix can be influenced by the amylose content of starch. Gelation of amylose is a rapid process associated with conformational ordering (formation of double helices) and formation of crosslinks. High amylose barley starch is likely to have a more rigid matrix due to a higher amylose content than normal starch. Gelation of pure amylopectin is a much slower process than gelation of pure amylose, and it is associated not only with coil to double helix transitions of short amylopectin side chains, but also with aggregation and recrystallization. Substantial increases in gel stiffness and strength are due to formation of crystalline domains detectable by X-ray or DSC analysis. Very slow retrogradation of waxy barley starch indicates rather unique properties of this starch. Czuchajowska et al. (1998) also reported that no recrystallization was observed in waxy barley during storage when probed with the DSC technique. These poor gelation and retrogradation properties of waxy barley starches may be associated with the relatively short length of linear chains in amylopectin of these starches (Chapter 3).

To determine the effects of enzymatic modification on the gelation properties of various barley starches, we chose only the least hydrolyzed samples (50 U α-amylase/g of starch, 24h hydrolysis). The relatively high yield of modified starches obtained after this mild hydrolysis was the main factor justifying this choice. The enzyme-treated normal and high amylose barley starches exhibited greater increases in G' values during

cooling and storage (Fig. 5.12 and 5.13). It appears that the partial depolymerization of starch polymers increased the mobility and diffusion of chains, and therefore increased the rate and extent of crosslink formation, leading to formation of stronger gel networks. Clark and co-workers (1989) showed that the molecular size of amylose chains significantly affected the kinetics of gelation and rheological properties of amylose gel. For long amylose chains (DP 2550 and 2800), it was shown that the initial formation of relatively few crosslinks retarded chain mobility and slowed down subsequent crosslinking and increases in G' values. In our case, small decreases in the molecular weight of amylose and amylopectin in both barley starches facilitated faster and stronger gel formation in both cases. The enzyme-treated zero amylose starch, on the other hand, exhibited, upon cooling, properties of viscous solutions with G" values slightly higher than G'. During storage for 20h at 5°C, the modified zero amylose starch solution did not show any evidence of network development either (Fig. 5.12 and 5.13).

Conclusion

The rate and pattern of hydrolysis of barley starches are clearly affected by the amount of amylose in starch granules. The amount of solubilized carbohydrates after 48h of α-amylolysis ranged from 13 -20% for high amylose, 25-39% for normal, and from 42-56% for zero amylose waxy samples, depending on the amount of enzyme used for hydrolysis. Despite quite extensive physical erosion and fragmentation of barley starches, the polymers remaining in granules after α-amylolysis retained their macromolecular form. After 56% solubilization of zero amylose starch granules, only a three-fold decrease in the molecular weight of amylopectin was observed. Very small changes in the molecular weight of amylose in normal and high amylose starches after hydrolysis indicate that amylose is not preferentially hydrolyzed during α-amylolysis. The normal and high amylose barley starches showed very little change in the degree of crystallinity after α-amylolysis, indicating that both amorphous and crystalline regions inside the granules were hydrolyzed concurrently. On the other hand, a small increase in the crystallinity observed for the zero amylose waxy starch after hydrolysis could be associated with preferential hydrolysis of less dense and/or weakly organized regions in waxy granules to which the enzyme appears to have an easier access. The results of this study clearly showed that the presence of amylose in barley granules most likely increases their density and, therefore, reduces the enzyme accessibility to the inside of the granules and formation of the effective enzyme-substrate complexes.

CHAPTER 6

Physicochemical properties and molecular structure of modified barley starch granules with various amylose contents. Part II: Acid/alcohol hydrolysis.

Abstract

Isolated hulless barley starches with varying amylose contents (0-40%) were subjected to partial acid hydrolysis (0.36% or 2% HCl; 10 and 96h) in various alcohols (methanol, ethanol and 1-butanol). In general the acid hydrolysis caused very little solubilization (<9%) of starch granules. Despite an intact appearance of the modified granules, as made evident by the scanning electron microscopy, starch polymers were substantially degraded by acid. The high-performance size exclusion chromatography indicated that the greatest depolymerization always occurred when the hydrolysis was carried out in 1-butanol. The waxy samples produced a slightly higher amount of solubilized carbohydrates but a close examination of the starch polymers inside the granules after hydrolysis has not indicated significant differences between waxy and high amylose starches in their susceptibility to hydrolysis. The acid/alcohol-treated starches showed increased intensity of peaks in the X-ray diffractogram, indicating an increase in crystallinity and ordering of crystallites due to preferential hydrolysis of amorphous regions inside starch granules. The peak melting temperature (T_p) of all partially hydrolyzed samples decreased the most after 10h but started to slightly increase after longer hydrolysis time (96h). The peak width generally broadened due to the hydrolysis. The enthalpy values (ΔH) of normal and high amylose samples decreased

somewhat upon hydrolysis. The ΔH of both waxy samples did not substantially change upon hydrolysis. During the long time storage, the partially hydrolyzed high amylose starch (2% HCl/MeOH, 10h) showed significantly higher values of G' compared to the native sample, whereas the partially hydrolyzed normal starch exhibited the G' development similar to its native counterpart. Both normal and high amylose starches, hydrolyzed for 96h, exhibited a rapid rise in G' upon cooling but very little network development thereafter.

Introduction

Acid hydrolysis has been used traditionally to modify native starches and to create products with altered solubility, viscosity, and/or gelation properties. Acid-modified starches are used in food, paper, textile, and other industries (Atichokudomchai et al. 2001; Hoover 2000; Virtanen et al. 1993; Wang and Wang 2001). During acid hydrolysis, the hydroxonium ion (H_3O^+) carries out an electrophilic attack on the oxygen atom of the α-(1→4) glycosidic bond, which leads eventually to the bond cleavage. Since the α-(1→4) linkages are preferentially hydrolyzed over the α-(1→6) ones, acid hydrolysis causes substantial reduction in the chain length of starch polymers (Atichokudomchai et al. 2001; Virtanen et al. 1993; Wang and Wang 2001). Starches generally undergo a two-stage hydrolysis process. An initially fast hydrolysis of starch polymers, occurring in the amorphous regions of starch granules, is followed by a slower hydrolysis of the densely packed crystalline regions (Biliaderis et al. 1981; Jacobs et al. 1998; Kainuma and French 1971; Li et al. 2001; Robin et al. 1974; Shi and Seib 1992; Wang and Wang 2001). Dense packing of chains within the starch crystallites and sterical constraints preventing the required change in conformation (chair→half chair) of the D-Glc*p* units prior to hydrolysis, have been proposed to account for the slower hydrolysis rate of the crystalline portion of the starch granule.

The differences in the rate and degree of acid hydrolysis of granular starch have been attributed to differences in granular size, extent and type of chain interactions within the granule (i.e. degree and type of crystallinity) and starch composition (amylose content, degree of phosphorylation). For example, small granules in barley starches were reported to have a higher rate of acid hydrolysis than large ones, presumably due to their

larger surface area per unit weight (Vasanthan and Bhatty 1996). Also, high amylose barley starch was reported to be less susceptible to acid hydrolysis than normal and waxy barley starches. It was suggested that the highly compact amorphous regions in high amylose starch granules, resulting from extensive inter-chain associations of amylose polymers, prevent penetration of acid into the granules (Vasanthan and Bhatty 1996). The X-ray crystallinity pattern (A, B and C types) also determines the rate of acid hydrolysis of granular starches (Gerard et al. 2002; Jane et al. 1997). Jane et al. (1997) postulated that the branching points of amylopectin in the A-type starches, present inside the crystalline regions, weaken the crystallites, and result in a greater susceptibility to acid hydrolysis of A-type than B-type starches.

Robin et al. (1974) reported that extensive acid hydrolysis of potato and waxy maize starches resulted in residues composed of a mixture of low molecular weight, linear and singly branched molecules. These results confirmed the cluster model of amylopectin polymers proposed by Kainuma and French (1971). It was implied that the branching points in amylopectin molecules are mainly located in the intercrystalline areas within the starch granules, and the crystalline regions inside the granule consists mostly of clusters of short linear chains (60 Å in length), which are resistant to the acid hydrolysis (Robin et al. 1974). Therefore, the acid hydrolysis of starch granules has been used not only to modify the properties of starches to widen their applications, but also to elucidate the structures of starch polymers and their organizations inside the granule.

The most traditional acid hydrolysis procedures used for modification of starch include those reported by Nageli (1874) and Lintner (1886). The Nageli procedure involves treatment of native starch with 15% sulfuric acid for one month at room temperature. The hydrolyzate, called "Nageli amylodextrin", is readily soluble in hot

water and contains a mixture of low molecular weight (M_w) linear and branched dextrins with an average degree of polymerization (DP) of 25-30. The Lintner procedure involves hydrolysis of native granules in 7.5% (w/v) HCl for one week and results in a product with a high molecular weight. In industry, the acid-modified starches are prepared by treating starch slurries with dilute HCl or H_2SO_4 at 25 - 55°C for various periods of time.

Recently, Robyt and co-workers (1996) conducted acid hydrolysis of potato and waxy maize starch in various alcohols. The products were soluble in hot water and gave clear solutions. It was shown that the DP and molecular weight distribution of the hydrolysis products could vary widely depending on the type of alcohol used. Compared with the Lintner procedure, the time required to produce soluble starch by the acid/alcohol treatment was substantially reduced (from 1 week to 1 hour).

In the present study, isolated hulless barley starches with various amylose content (0-40%) were subjected to partial acid hydrolysis in various alcohols. The objectives of this work were (1) to elucidate the effects of various acid/alcohol treatments and amylose content on the degree and rate of the acid hydrolysis, and (2) to examine the physical and molecular characteristics of the starch material remaining after partial acid hydrolysis.

Materials and Methods

Materials

Four types of barley starch: normal, high amylose, waxy and zero amylose, were isolated from four hulless barley genotypes; Falcon, CDC 92-55-06-48, SR 93139 and CDC Alamo, respectively, according to the previously reported procedure (Chapter 3). The chemicals used were all reagent grade.

Acid/alcohol modification of starch granules

Starch samples (6g) were suspended separately in methanol, ethanol or 1-butanol (24mL) and concentrated HCl was added to achieve 0.36% and 2% acid concentration. Samples were modified for 10h and 96h at 20°C. After modification, the starch suspensions were washed with 70% ethanol and filtered on a 0.45μm membrane (HVLP) to neutralize the samples. The acid- treated starch residues were washed with acetone and dried overnight at room temperature.

Starch solubilization

The amount of solubilized carbohydrates during acid/alcohol treatment of starch granules was determined by the phenol-sulfuric acid method (Dubois et al. 1956). Due to the incompatibility of 1-butanol and the phenol-sulfuric mixture, the determination of solubilized carbohydrates was performed only for starches modified in methanol and ethanol. Starch (0.25g) was suspended in methanol or ethanol (1mL) containing 0.36% HCl or 2% HCl for 10, 48, and 96h at 20°C. After the desired period of modification, 19mL of distilled water was added and the suspensions were centrifuged for 10min at

1,200*g*. The supernatant was used to determine the amount of solubilized carbohydrates. For the 2% HCl/1-butanol treated starches, the yields of the residual granules were used to determine the degree of solubilization.

M_w analysis of starch polymers

The acid/alcohol-modified starches (3mg) were dissolved in boiling water (10mL) for 10 min. Native starches were dissolved in DMSO first, precipitated with ethanol, dried, and then redissolved as previously described (Chapter 3). The dissolved native and modified starches were filtered through a 3.0μm cellulose acetate membrane, and then injected into the high-performance size exclusion chromatography column coupled with multi-angle light scattering and refractive index detection system (HPSEC-MALS-RI). The M_w of native and acid/alcohol-treated starches was determined as previously described (Chapter 3).

Debranching of acid treated starches

The native and acid/alcohol-modified starches (25mg) were suspended in ethyl alcohol (0.1mL), dissolved in 1N NaOH (1mL), diluted with water (3mL) and then neutralized with 1N HCl. Native starches were also autoclaved (20min at 121°C). The solubilized starches (3mL) were mixed with 1mL acetate buffer (0.1M, pH 3.5) and incubated with isoamylase (500U/g, Hayashibara Biochemical Laboratories Inc., Okayama, Japan) for 24h at 40°C. The digested starches were neutralized (1N NaOH), heated in a boiling water bath for 5min to stop the enzyme activity, filtered through a 0.45μm membrane, and then injected into HPSEC-MALS-RI and high-performance anion exchange chromatography with a pulsed amperometric detector (HPAEC-PAD)

systems, as described previously (Chapter 5).

Other physical and rheological measurements of starches

Scanning electron microscopy, X-ray diffractometry, solid-state CP/MAS ^{13}C NMR, thermal analysis, and digestibility to α-amylase as well as viscoelastic properties of native and acid/alcohol-modified starch samples were determined by the previously reported instrumental and sample preparation methods (Chapter 5).

Results and Discussion

Solubilization and morphology of acid/alcohol-treated barley starches

The amounts of solubilized carbohydrates obtained as a result of acid/alcohol treatments of various barley starches are shown in Fig 6.1. In general, very little solubilization of barley starches occurred during hydrolysis. After 10h of hydrolysis, the amount of solubilized carbohydrates from all starch samples was below 0.6%, irrespective of the acid concentration or the alcohol type (Fig. 6.1). After 96h of hydrolysis in either methanol or ethanol, the largest amount of carbohydrates was released from the zero amylose starches, while the smallest was released from the high amylose samples; the differences, however, were very small (Fig. 6.1). At 2% HCl, slightly higher amounts of solubilized carbohydrates were obtained for hydrolysis conducted in methanol than in ethanol. This was particularly evident for the zero amylose starches. The 2% HCl digested starches in 1-butanol yielded over 91% of the residual material indicating less than 9% solubilization (Table 6.1).

The appearance, shape and size distribution of barley starch granules were not affected to any great extent by the hydrolysis, as indicated in the scanning electron microscopy (SEM) photographs (Fig. 6.2). Among all barley starches, only the waxy and zero amylose starches showed some evidence of acid modification. It is possible that the pores observed on the surface of native waxy and zero amylose starch granules might have been responsible for the greater penetration of acid and consequently the more extensive hydrolysis of these starches compared to normal and high amylose starches. Much greater solubilization and corrosion of granules were previously observed as a consequence of partial α-amylolysis of barley starches (Chapter 5). Harsher conditions

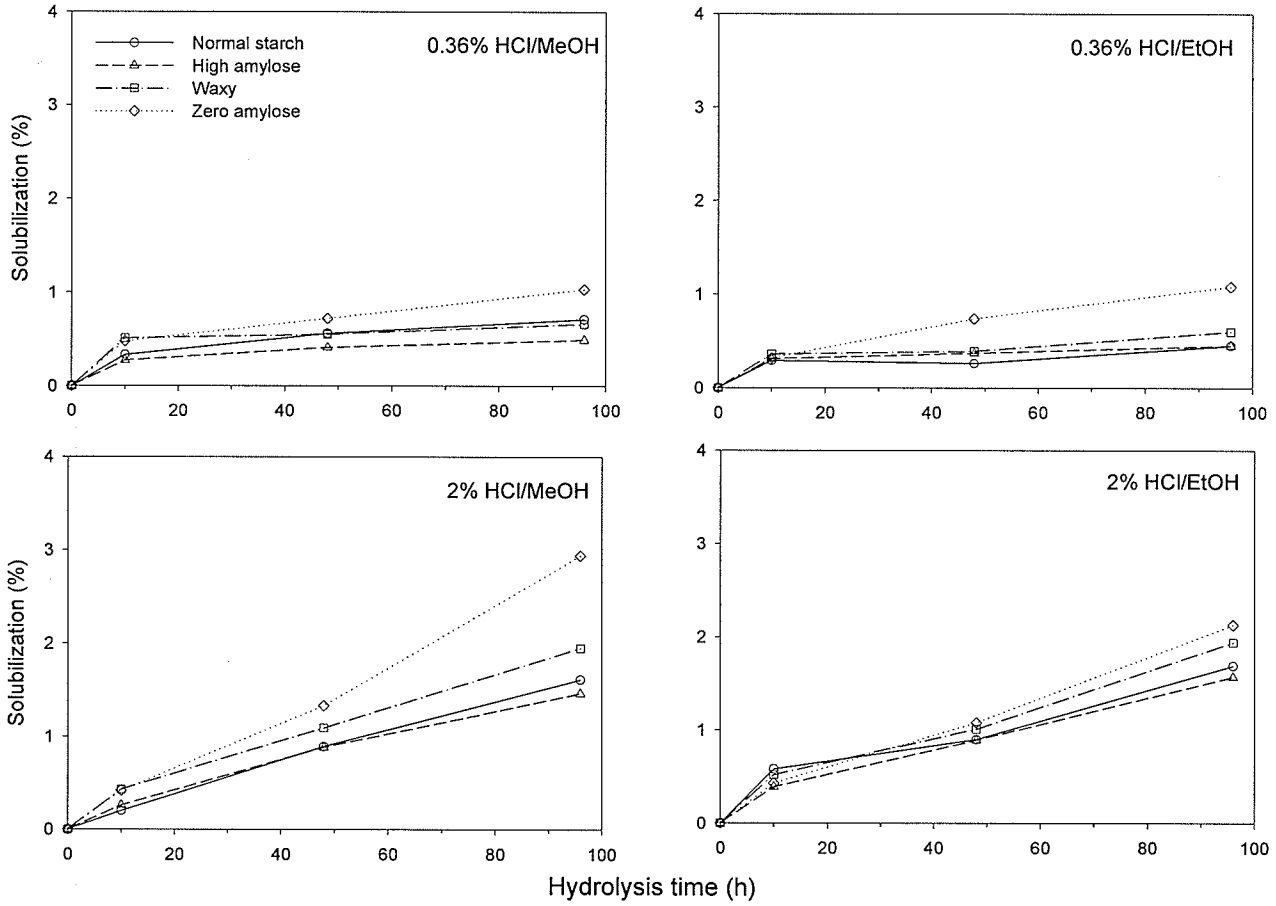

Figure. 6.1. Starch solubilization during acid/alcohol hydrolysis in the two different acid concentrations (0.36% and 2% HCl/MeOH and EtOH).

Table 6.1. Yields of acid-treated (2% HCl) starch residues in 1-BuOH after 96h hydrolysis.

Starch	Yield
Normal	91.5% ± 1.8
High amylose	92.3% ± 2.2
Waxy	93.1% ± 0.7
Zero amylose	92.9% ± 2.8

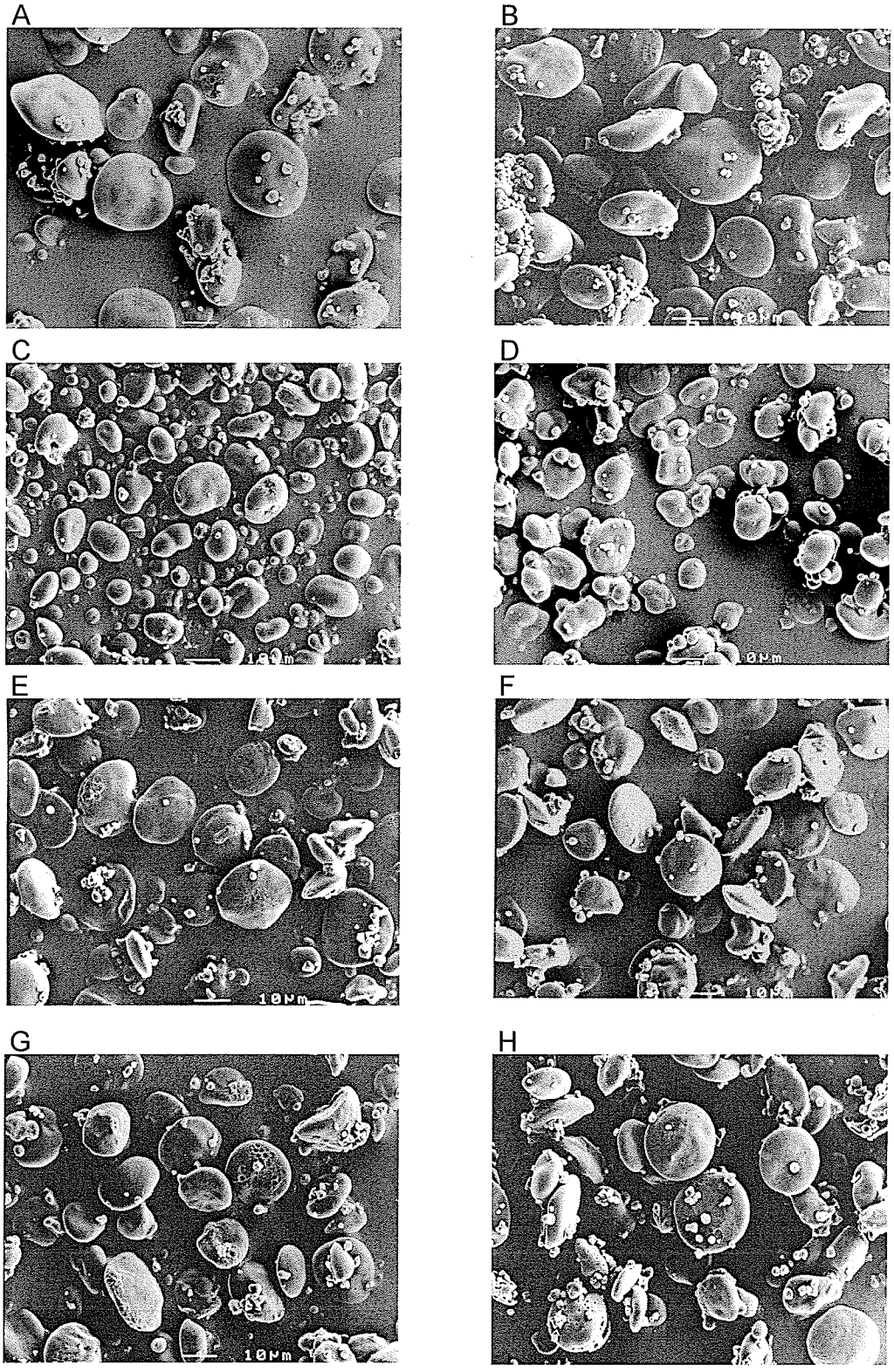

Figure. 6.2. Scanning electron photomicrographs of native and acid/alcohol-treated (2% HCl/BuOH, 96h) normal (A,B), high amylose (C,D), waxy (E,F), and zero amylose (G,H) barley starches, respectively.

of acid hydrolysis, such as those normally applied during the lintnerization process (2.2N HCl, 35°C, 17 days) can also lead to substantial solubilization of barley starches (up to 100%) as reported by Vasanthan and Bhatty (1996).

Molecular weight of partially hydrolyzed starches

Figures 6.3a-d show the HPSEC profiles of native and partially hydrolyzed barley starches as influenced by different hydrolysis conditions. Substantial depolymerization of starch polymers occurred during hydrolysis as shown by significant shifts of the eluting species after hydrolysis. The degree of depolymerization and the distribution of molecular weights in hydrolyzed starches were affected not only by the acid strength and hydrolysis time but also by the type of alcohol in which the hydrolysis was carried out. The average molecular weights of starch polymers produced by acid hydrolysis of granular barley starches are presented in Table 6.2. Generally with increasing hydrolysis time and acid concentration, the M_w of all starches substantially decreased. The M_w of starches treated for 96h at a lower acid concentration (0.36%) were lower than those treated for 10h but at a higher acid concentration (2%). This indicates that hydrolysis time had a greater effect on the extent of hydrolysis than acid concentration. The greatest depolymerization always occurred when the hydrolysis was conducted in 1-butanol. Methanol and ethanol produced similar starch hydrolyzates, although small differences were noticeable. For most samples, when the hydrolysis was carried out for 10h, the starches hydrolyzed in methanol had higher average M_w than those hydrolyzed in ethanol. However, when the hydrolysis was carried out for 96h, an opposite trend was observed; the starches hydrolyzed in ethanol were somewhat less affected and exhibited slightly higher M_w than those hydrolyzed in methanol.

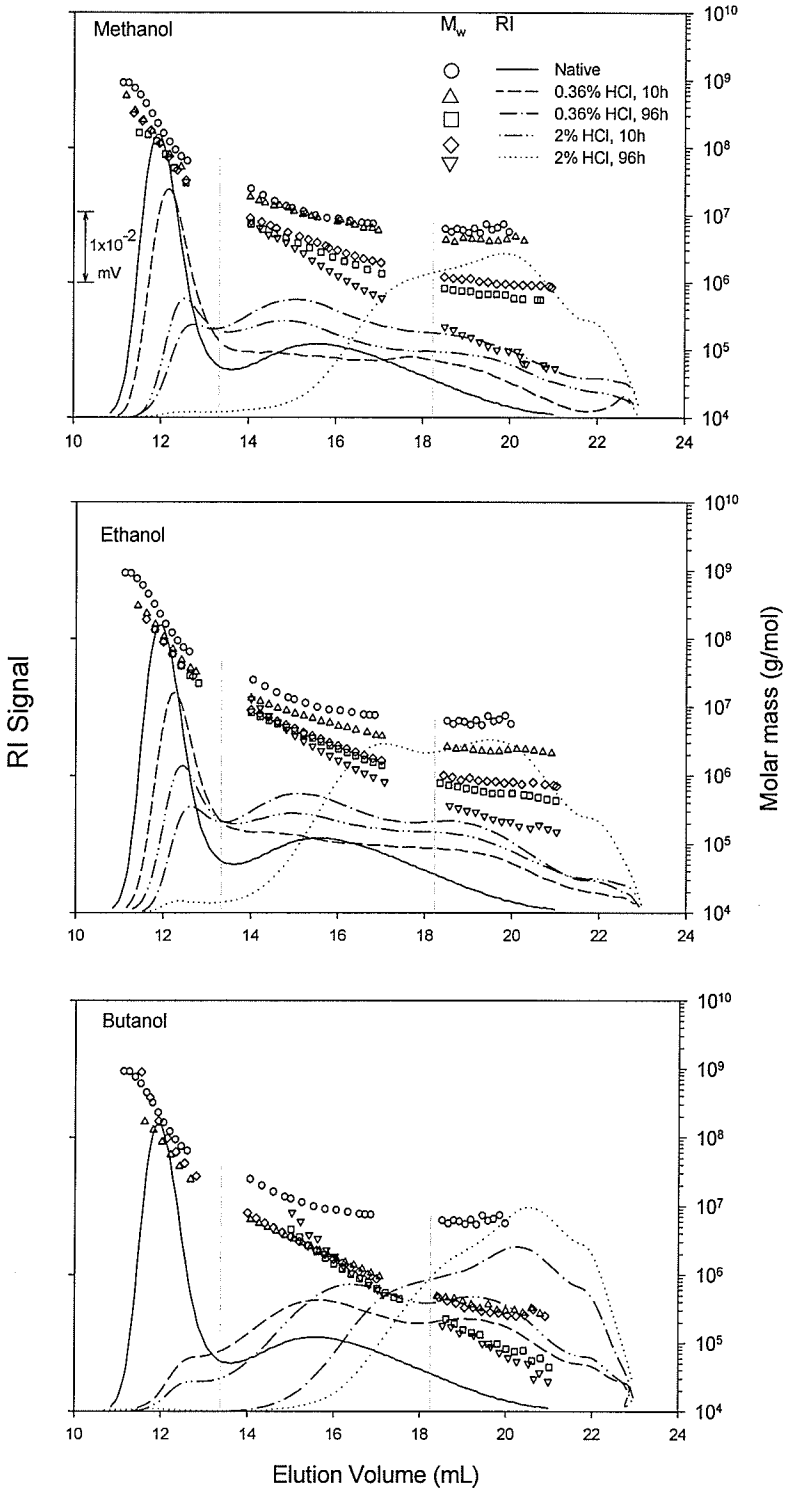

Figure. 6.3a. HPSEC profiles and weight average molecular weight (M_w) distributions of native and acid/alcohol-treated normal barley starches (0.36% and 2% HCl/MeOH, EtOH and BuOH, 10h and 96h).

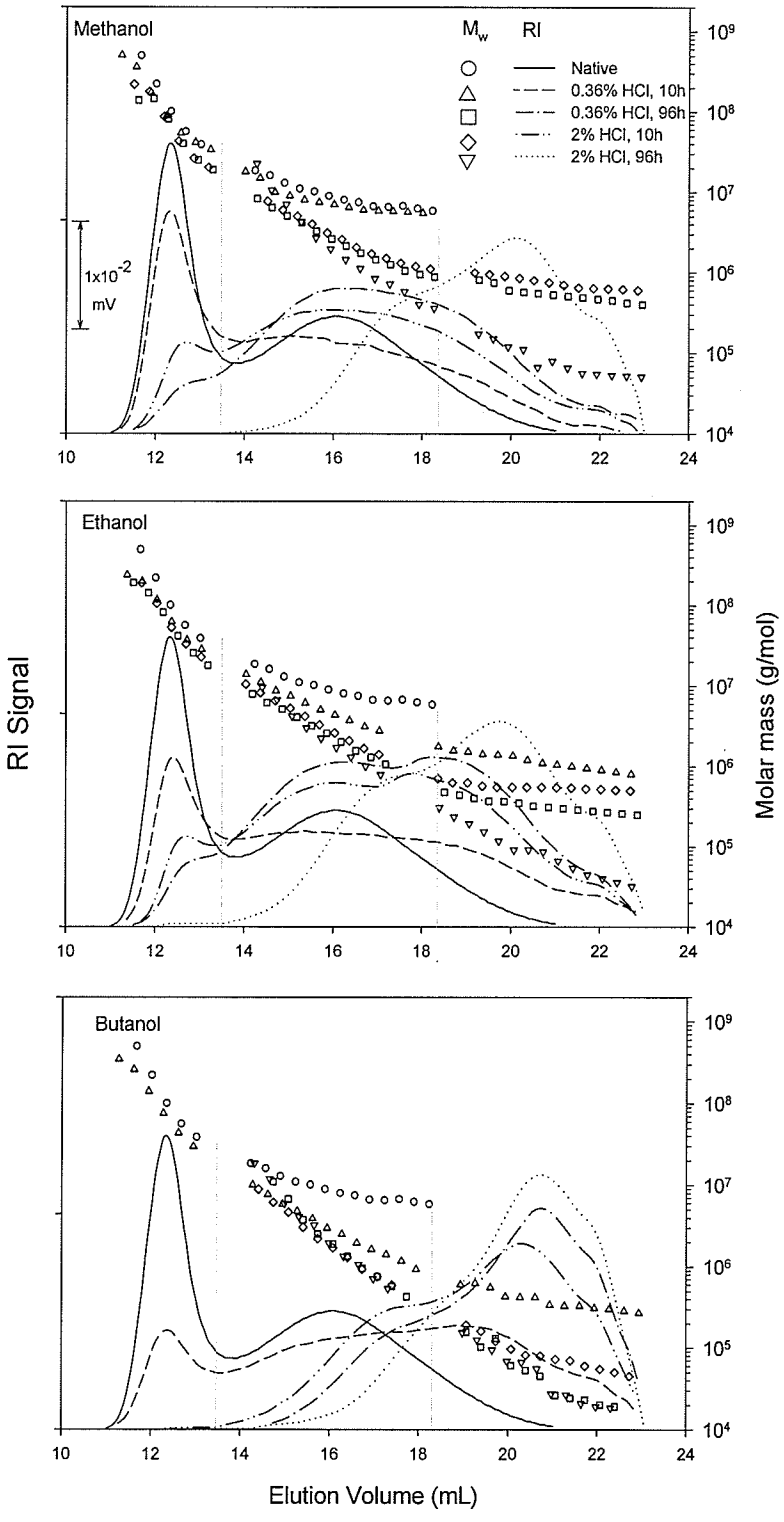

Figure. 6.3b. HPSEC profiles and weight average molecular weight (M_w) distributions of native and acid/alcohol-treated high amylose barley starches (0.36% and 2% HCl/MeOH, EtOH and BuOH, 10h and 96h).

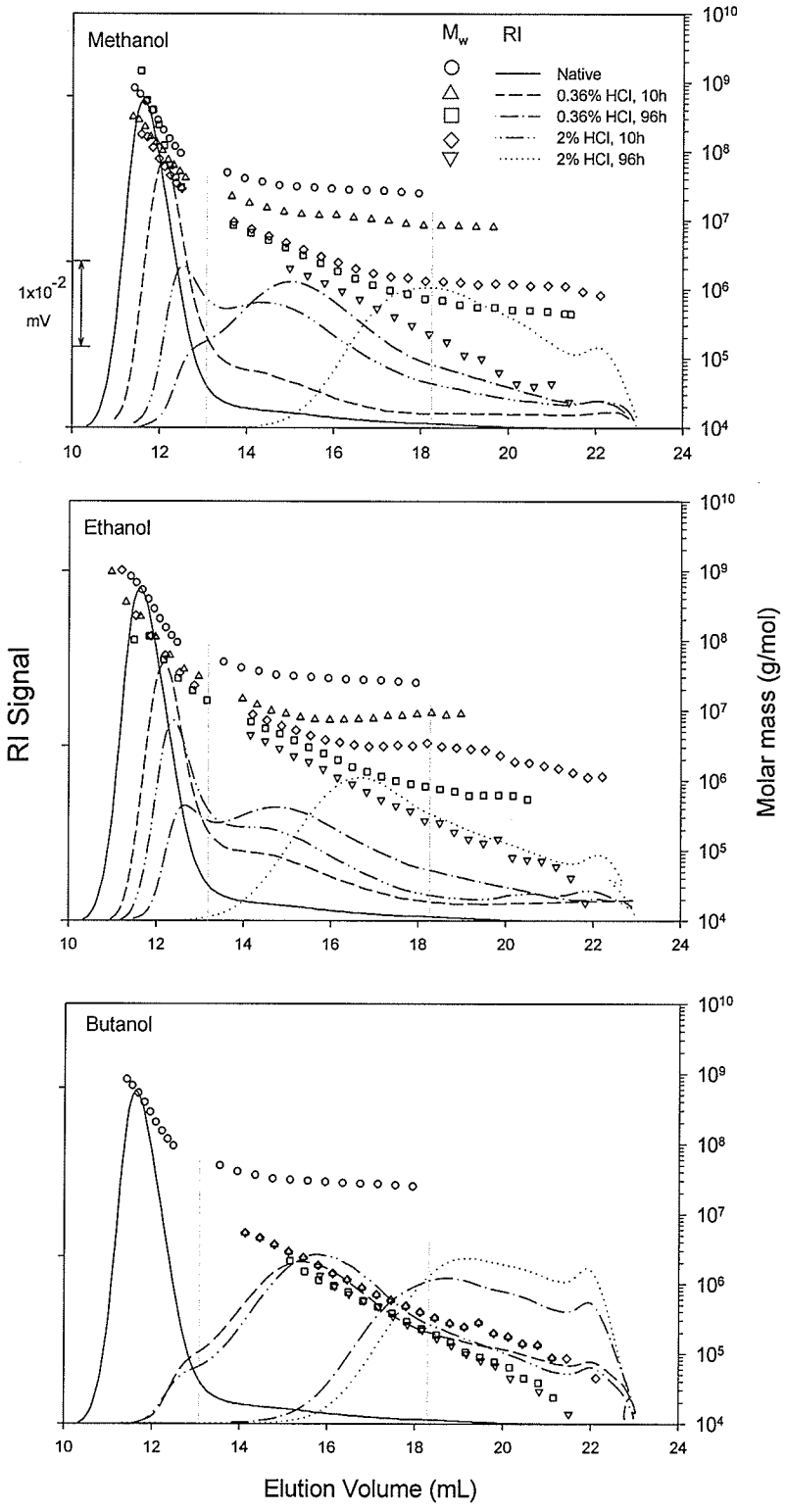

Figure. 6.3c. HPSEC profiles and weight average molecular weight (M_w) distributions of native and acid/alcohol-treated waxy barley starches (0.36% and 2% HCl/MeOH, EtOH and BuOH, 10h and 96h).

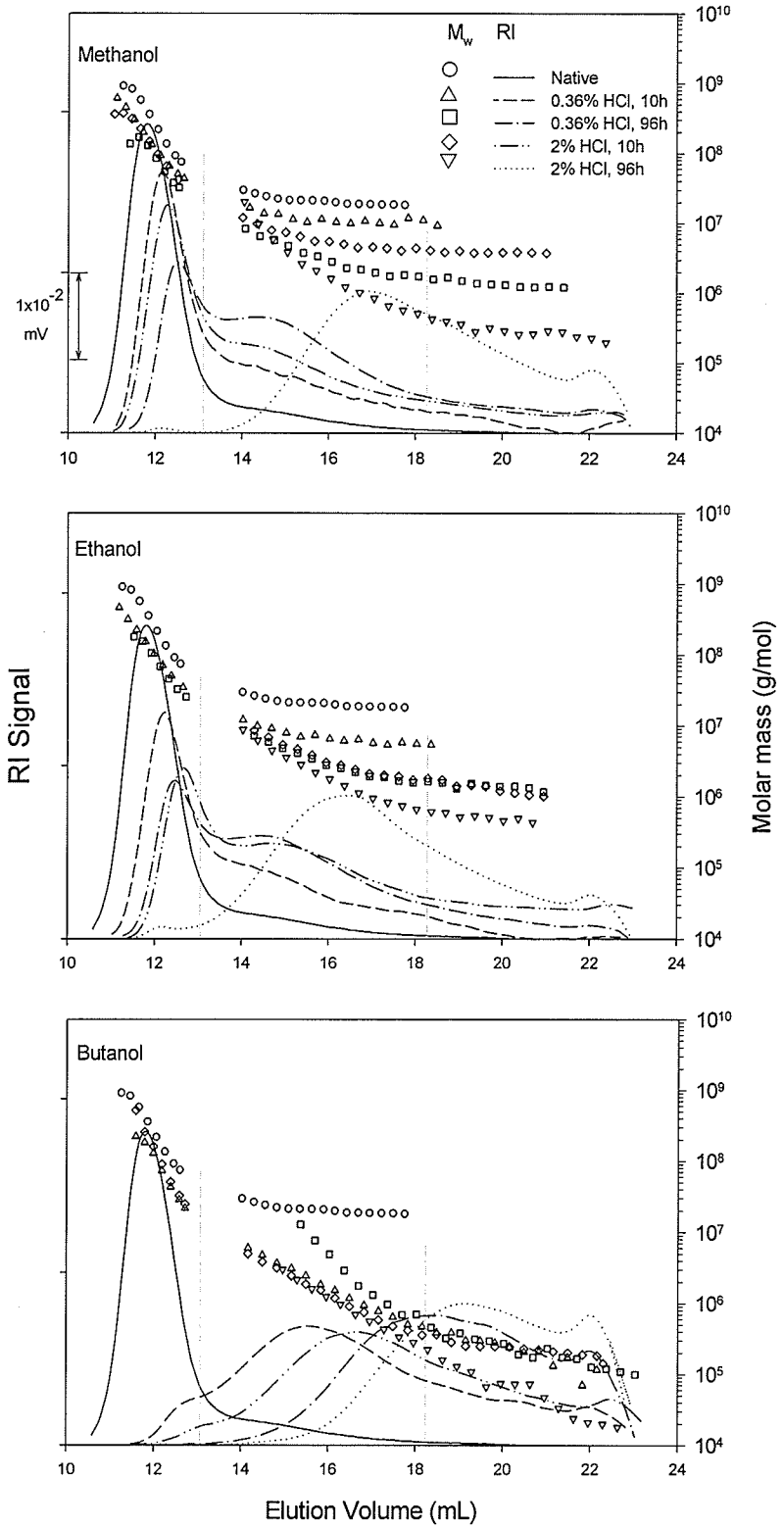

Figure. 6.3d. HPSEC profiles and weight average molecular weight (M_w) distributions of native and acid/alcohol-treated zero amylose starches (0.36% and 2% HCl/MeOH, EtOH and BuOH, 10h and 96h).

Table 6.2. Weight average molecular weights (M_w) of native and acid/alcohol-treated starches.

Acid treatment	Weight average molecular weight ($M_w \times 10^{-6}$)[a]			
	Normal	High amylose	Waxy	Zero amylose
Native	50±2.3	30±1.1	76±3.1	80±3.2
0.36% HCl				
10h				
MeOH	31±1.3	27±0.7	44±1.5	41±0.3
EtOH	21±1.1	15±0.2	36±1.3	31±0.8
BuOH	3.0±0.2	9.5±0.4	2.7±0.1	3.2±0.3
96h				
MeOH	4.8±0.8	3.7±0.2	4.1±0.5	9.3±0.1
EtOH	5.6±0.2	3.5±0.1	6.2±0.2	10±0.3
BuOH	0.3±0.0	0.3±0.1	0.2±0.1	0.6±0.0
2% HCl				
10h				
MeOH	7.7±0.2	6.8±0.1	7.9±0.2	20±0.5
EtOH	8.1±0.3	4.7±0.1	14±0.3	12±0.2
BuOH	2.0±0.1	0.6±0.1	2.6±0.1	2.0±0.1
96h				
MeOH	0.5±0.1	0.4±0.1	0.3±0.1	1.0±0.0
EtOH	1.0±0.1	0.6±0.0	0.8±0.1	2.3±0.1
BuOH	0.3±0.0	0.2±0.1	0.2±0.1	0.3±0.1

[a]Weight average molecular weight of polymers eluting between Ve:11-23mL as shown in Fig. 6.3a-d.

When the hydrolysis was carried out in methanol or ethanol, the hydrolyzed starch granules still contained a considerable amount of very high molecular weight species corresponding to the M_w (5×10^7-1×10^9) of intact amylopectin fractions (Ve: 11-13.5 mL). The amount of this fraction decreased, however, with increasing hydrolysis time or acid concentration, and samples hydrolyzed for 96h in 2% HCl were almost totally devoid of the high M_w population (Ve: 11-13.5mL). This was observed for all four types of barley starch (Fig 6.3a-d). When the hydrolysis was carried out in 1-butanol, most of the 'intact amylopectin' fraction diminished even if the reaction was conducted under the mildest conditions (0.36% HCl, 10h). These results indicate that in the presence of 1-butanol, acid penetration throughout the granule occurred very quickly and uniformly, affecting the whole population of starch polymers. Robyt and co-workers (1987; 1996) suggested that higher alcohols might increase the actual concentration of acid inside the granules and/or assist in dissolution of the amylose double helices or amylose-amylopectin complexes and thus increase the overall hydrolysis rate and extent. This suggestion can be supported also by the fact that 1-butanol is less miscible with water than methanol and ethanol. 1-BuOH might form complexes with amylose polymers inside the granules. The amylose-BuOH complexes appeared to be also highly susceptible to acid hydrolysis.

The species eluting in the intermediate (Ve: 13.8 -18 mL) and low M_w (Ve: 18-23 mL) regions contained a mixture of partially depolymerized amylopectin and amylose chains. For all partially hydrolyzed samples, the species eluting in these regions had lower M_w than those originating from the intact starches. This may indicate more linear and extended conformation of the hydrolyzate chains compared with the relatively compact and branched structure of the intact starch polymers eluting in the same regions.

When the hydrolysis of normal or high amylose starches was carried out in methanol or ethanol, the hydrolyzed material retained in the granules consisted of three

populations of polymers: the high M_w amylopectin, the intermediate, and the low M_w amylose and amylopectin chains. The relative proportions of these populations as well as their M_w were influenced by the hydrolysis time and acid concentration. The samples hydrolyzed at 2% HCl for 96h, however, were lacking the high amylopectin fraction. Waxy and zero amylose waxy samples, hydrolyzed in methanol or ethanol, eluted mostly in the high and intermediate M_w regions, except when the hydrolysis was carried out at 2% HCl for 96h; in this case, a considerable amount of material eluted in the low M_w region.

When the hydrolysis of all four types of starches was carried out in 1-butanol, the hydrolyzates contained mostly the intermediate and low M_w populations. After prolonged hydrolysis (96h) in both acid concentrations, the low M_w population predominated in all samples. Our results are in good agreement with those of Robyt and co-workers (1987; 1992; 1996) who showed that by selecting different alcohols, concentration of acid and/or starch substrate, and temperature of hydrolysis reactions, partially hydrolyzed starches with a wide range of DP can be produced. Our results also indicate that the M_w and the mode of distribution of various M_w species can be tailored to specific needs.

The M_w and the M_w distribution profiles of starch populations obtained after hydrolysis did not indicate that the high amylose starch was less affected by hydrolysis than normal or waxy starches. This is contrary to previous reports (Li et al. 2001; Vasanthan and Bhatty 1996) indicating that the extent of acid hydrolysis follows the order: waxy>normal>high amylose starch. However, the susceptibility of starches to hydrolysis has often been inferred from the amount of material solubilized and leached out of granules and not from the properties of the material remaining in the granules after hydrolysis. In our study, the waxy samples have also produced a slightly higher

amount of solubilized carbohydrates but a close examination of the starch polymers inside the granules after hydrolysis has not indicated significant differences between waxy and high amylose starches in their susceptibility to hydrolysis under mild conditions as conducted in this study.

Despite the intact appearance of granules after partial acid hydrolysis, the SEC revealed that substantial modification of starch polymers occurred inside the granules. This is contrary to very small changes in the M_w brought about by partial α-amylolysis of barley starches (Chapter 5). As previously suggested, acid seems to freely penetrate the entire granule and to attack the more susceptible glycosidic linkages located in the amorphous region, causing substantial decrease in M_w of starch polymers (Biliaderis et al. 1981; Kainuma and French 1971; Robin et al. 1974). α-Amylase, because of its large size, cannot easily diffuse into the granule and its action is confined to localized regions only, where both amorphous and crystalline regions are hydrolyzed concomitantly (Colonna et al. 1988; Leach and Schoch 1961).

Debranching of partially hydrolyzed starches

The HPSEC elution profiles of native and acid/alcohol-hydrolyzed normal and high amylose starches after debranching with isoamylase are shown in Fig. 6.4a-b. The high molecular weight peaks (Ve: 21-32 mL) represent debranched amylose polymers, while the lower molecular weight peaks (Ve: 32-37 mL) are derived from debranched amylopectin chains. It is evident that the degradation of amylose depended on the alcohol medium in which the hydrolysis was conducted. The most severe depolymerization occurred when the hydrolysis was conducted in 1-butanol/HCl (Fig.

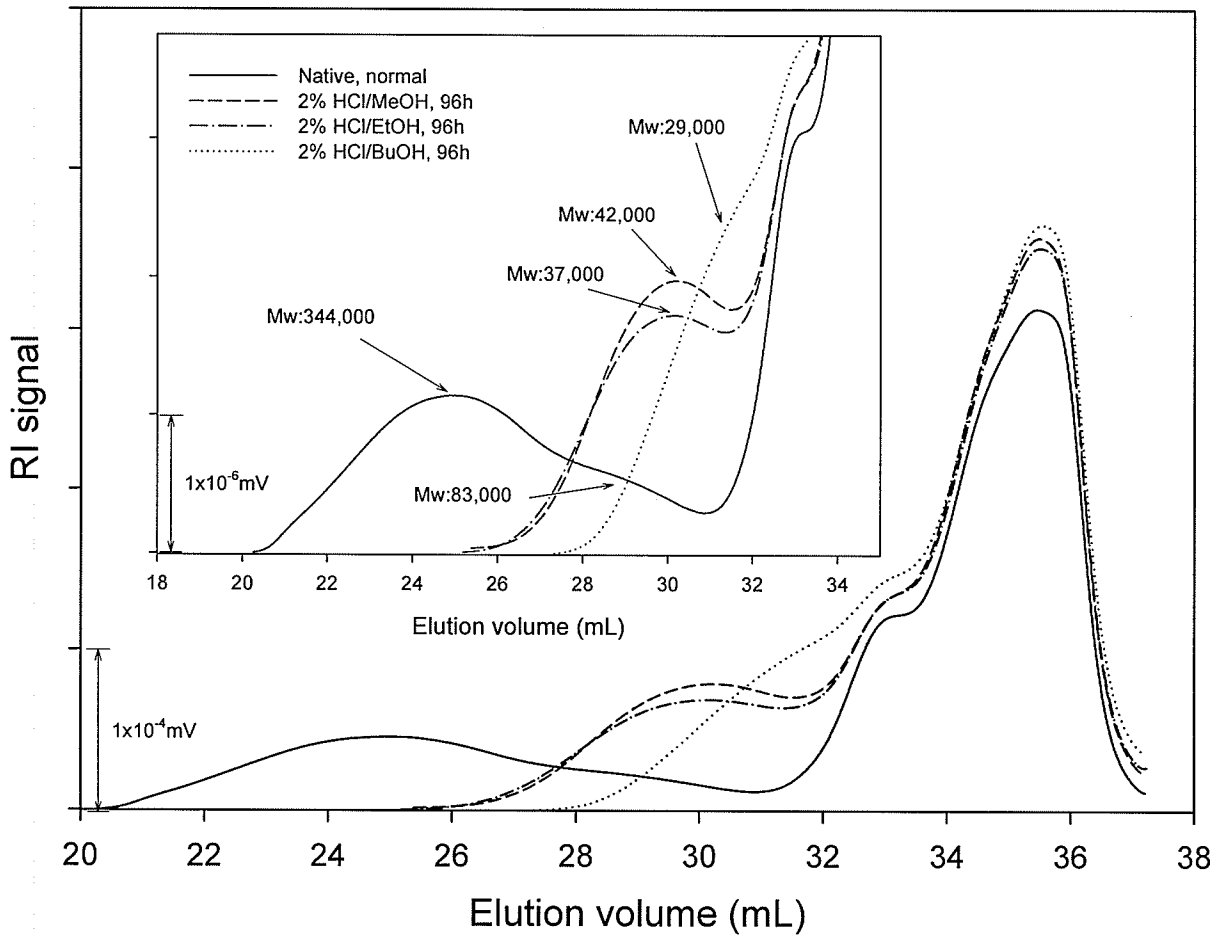

Figure. 6.4a. HPSEC debranched chain length profiles of naive and acid/alcohol-treated normal starches. Insert; HPSEC debranched amylose chain length profiles and weight average molecular weights (M_w) in peaks.

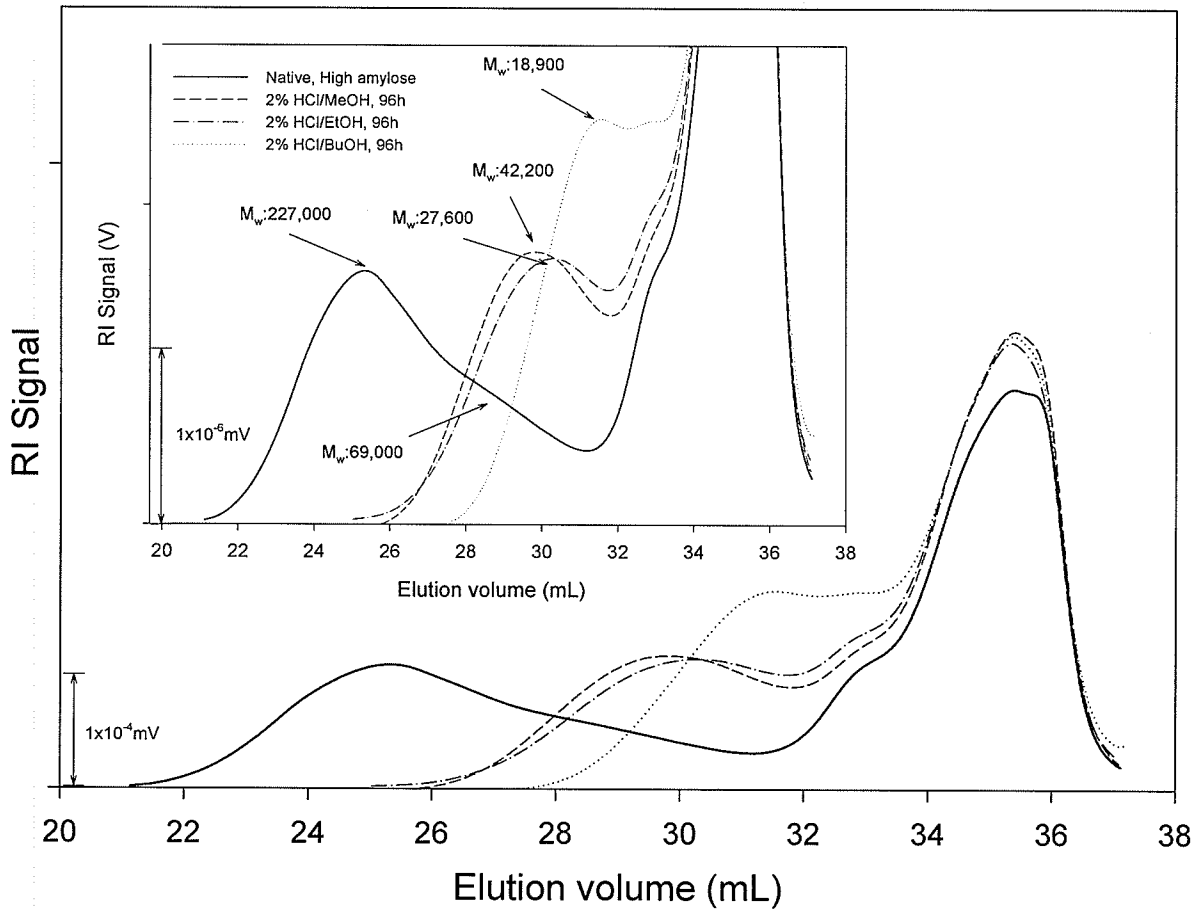

Figure. 6.4b. HPSEC debranched chain length profiles of naive and acid/alcohol-treated high amylose starches. Insert; HPSEC debranched amylose chain length profiles and weight average molecular weights (M_w) in peaks.

Table 6.3. Weight average molecular weights (M_w) and relative content of debranched amylose fractions in native and acid/alcohol-treated normal and high amylose starches.

Acid treatments	Ve: 21-32 mL ($M_w \times 10^{-3}$)	Amylose content (%)
Normal		
Native	337±1.7	24.1±0.3
2% HCl/MeOH, 96h	53±0.2	21.0±0.2
2% HCl/EtOH, 96h	50±0.3	19.7±0.1
2% HCl/BuOH, 96h	31±0.1	18.9±0.2
High amylose		
Native	191±0.6	41.8±0.2
2% HCl/MeOH, 96h	54±0.3	29.6±0.5
2% HCl/EtOH, 96h	75±0.2	28.2±0.4
2% HCl/BuOH, 96h	30±0.2	27.5±0.1

6.4a-b and Table 6.3). The substantial decrease in the M_w of amylose chains during acid/alcohol hydrolysis indicates pronounced susceptibility of amylose to hydrolysis. However, a considerable portion of amylose remained in the polymeric form. Ma and Robyt (1987) reported a significant decrease in DP of amylose polymers in potato starches hydrolyzed (0.36% HCl, 1h, 65°C) in methanol and ethanol and a complete depolymerization of amylose when the hydrolysis was conducted in 2-propanol or 1-butanol. Based on these observations the authors questioned the presence of amylose chains in the crystalline regions of starch granules.

The content of amylose fraction determined from the integration of high (Ve: 21-32 mL) and low M_w peaks (Ve: 32-37 mL) is presented in Table 6.3. As previously mentioned (Chapter 3), these values are in a good agreement with the amylose content determined by the iodine potentiometric method, and they indicate the changes in the content of amylose fraction in native and acid/alcohol-modified starches. Relatively

small differences in the amylose content between native and acid/alcohol-hydrolyzed starches indicate that despite substantial depolymerization, the amylose fraction remained in the granules after hydrolysis. These results are also in good agreement with the very low solubilization of barley starches observed after acid/alcohol treatments (Fig. 6.1).

The HPSEC chromatograms of debranched amylopectin fractions (long B, intermediate B, short B+A chains) of the zero amylose starch are shown in Fig. 6.5. A decrease in the amount of the long B chain fraction and an increase in the amount of short B+A chains were observed for the treated samples. The average M_w of the linear chains decreased from 4,275 for the zero amylose samples to 4,217, 3,757, and 3,480 for the acid-treated samples (2% HCl) in methanol, ethanol, and 1-butanol, respectively. The decrease in the M_w can likely be attributed to the depolymerization of the long B chains. The length and distribution of the debranched linear chains in native and acid/alcohol-hydrolyzed samples was also determined by the HPAEC-PAD (Fig. 6.6). Small changes in the distribution of linear chains after hydrolysis were observed. In agreement with the HPSEC results, the amount of chains with DP 17-35 slightly decreased, whereas the amount of short chains with DP ≤15 slightly increased after hydrolysis. The small increases in the amount of shorter chains (DP ~14) could have resulted from the scission of longer chains, either those connecting two neighboring crystalline clusters or those originating from defective crystallites. Small increases in the amount of very short chains (DP <7) could indicate hydrolysis in the amorphous regions enriched in branch linkages. All four types of acid/alcohol-treated starches showed similar changes in linear chain length distributions, indicating that the debranched amylose had much higher DP

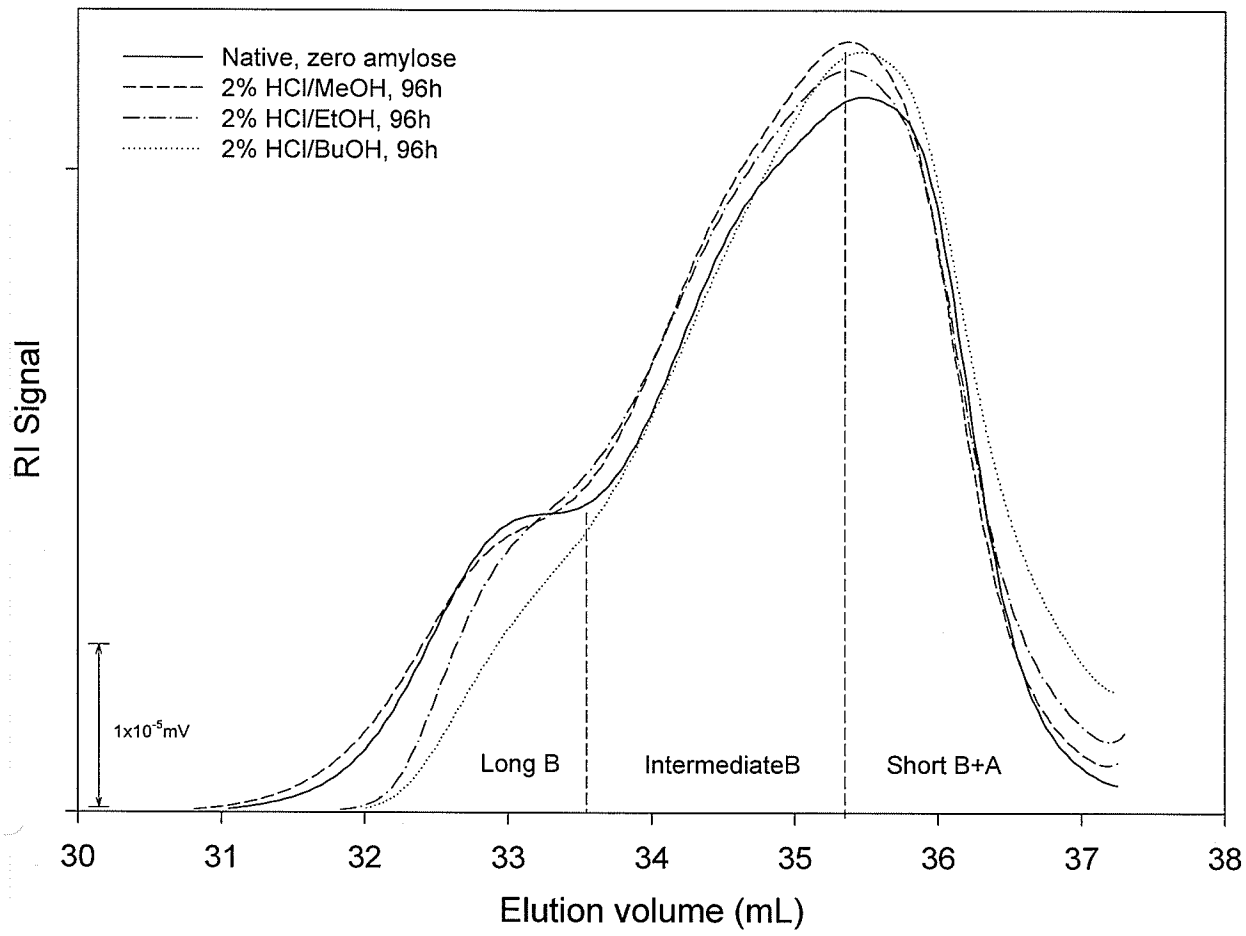

Figure. 6.5. HPSEC debranched chain length profiles of native and acid/alcohol-treated zero amylose starch (2% HCl/MeOH, EtOH and BuOH, 96h).

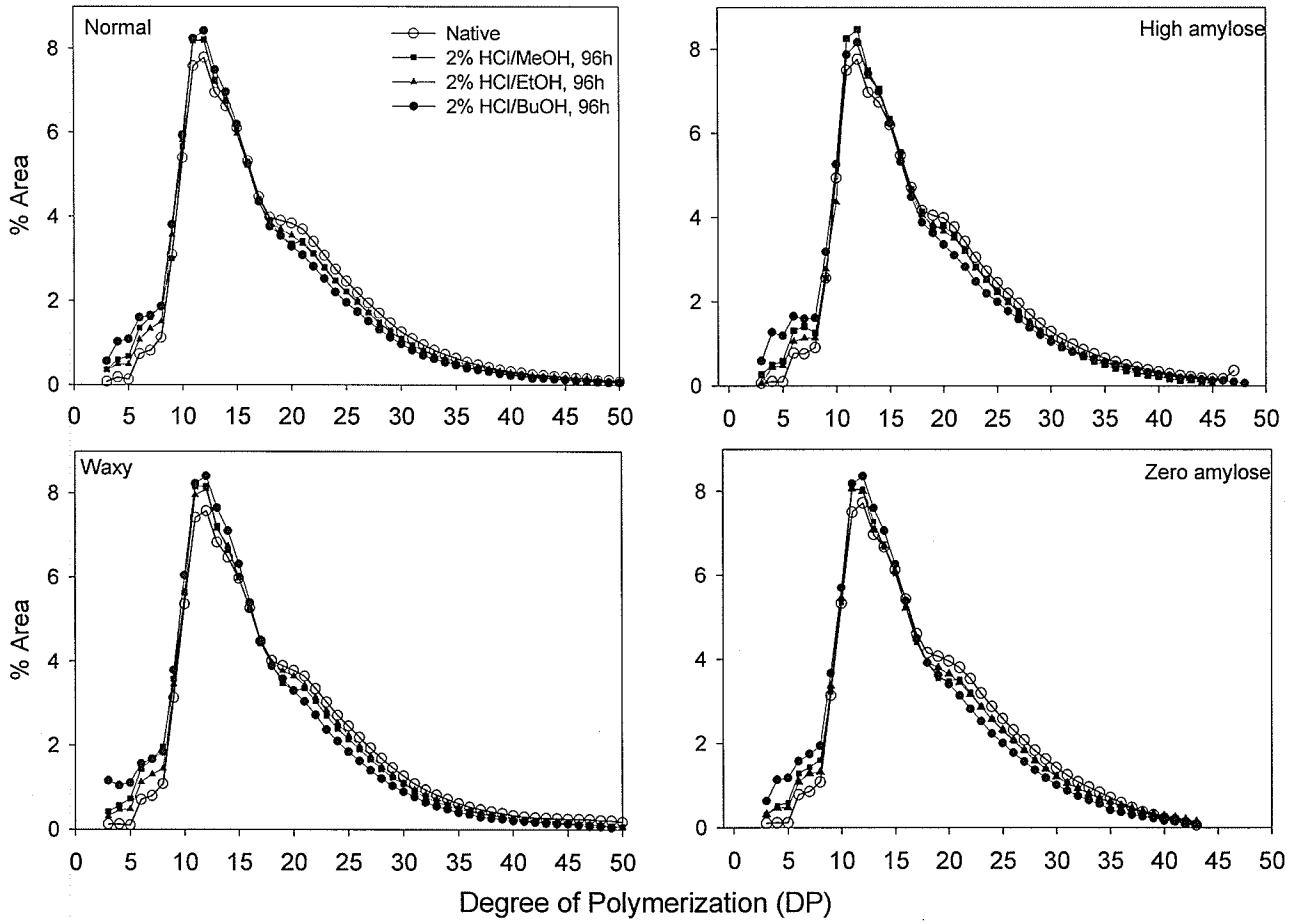

Figure. 6.6. HPAEC debranched chain length profiles of native and acid/alcohol-treated barley starches (2% HCl/MeOH, EtOH and BuOH, 96h).

than the debranched amylopectin chains and did not affect the profile of linear amylopectin chains.

These results are in good agreement with the current understanding of the mechanism of acid action inside the granule (Biliaderis et al. 1981; Jacobs et al. 1998; Kainuma and French 1971; Li et al. 2001; Robin et al. 1974; Shi and Seib 1992; Wang and Wang 2001). It is thought that acid hydrolysis initially occurs in the amorphous regions, located between crystalline regions and consisting of (1) branching points, (2) B chains connecting two or more clusters (Hizukuri 1986), and (3) linear amylose chains (Robin et al. 1974). In addition, the proposed lamellar structure (Robin et al. 1974) of amorphous and crystalline regions within starch granules is well supported by the above results. The densely packed crystalline regions consisting of short B and A chains (French 1984; Robin et al. 1974) were not affected by the acid hydrolysis.

Internal structures of partially hydrolyzed starches

The X-ray diffraction patterns of acid/alcohol-treated barley starches (2% HCl/BuOH, 96h) and of their native counterparts are shown in Fig. 6.7. Despite the varying amylose contents, all starches showed the A-crystalline pattern, indicating an identical packing geometry of double helices (Song and Jane 2000; Yoshimoto et al. 2000; 2002).

The acid/alcohol-treated starches showed increased intensity of peaks in the X-ray diffractogram (Fig. 6.7), indicating that the acid treatment induced an increase in crystalline regions and ordering of crystallites (Atichokudomchai et al. 2001). The hydrolysis of starch chains near the branching points, which are located in the amorphous regions, may induce reordering of the helix-helix structures, leading to more

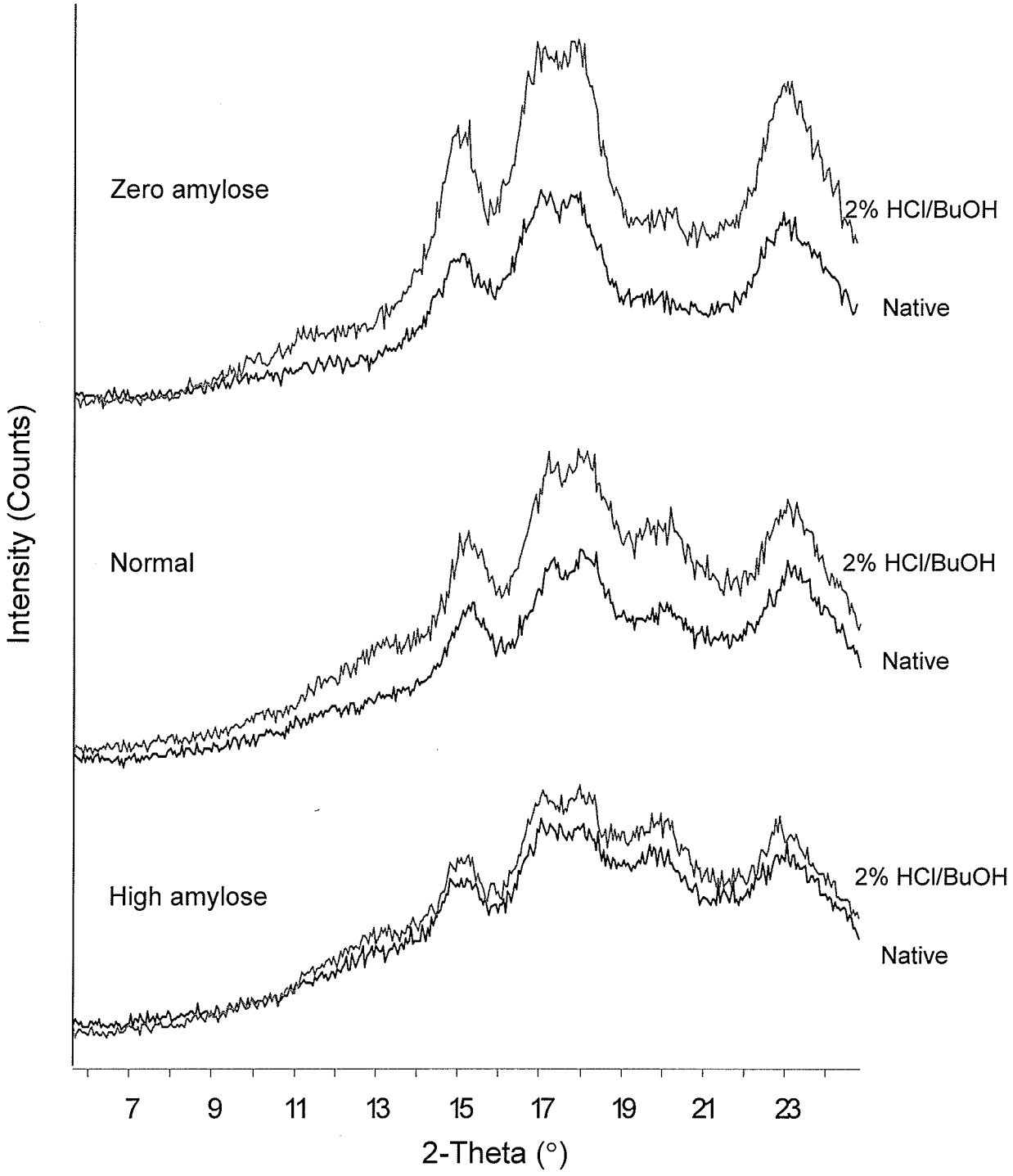

Figure. 6.7. X-ray diffraction patterns of native and acid/alcohol-treated barley starches (2% HCl/BuOH, 96h); upper lines: acid/alcohol-treated starches, lower lines: native starches.

perfect and stable crystallites (Atichokudomchai et al. 2001; Biliaderis et al. 1981; Wang and Wang 2001).

Among the various types of starches, the acid/alcohol-modified zero amylose starch showed the most significant increase in peak intensity in the X-ray diffractogram, whereas the high amylose starch the least (Fig. 6.7). It can be suggested that the amorphous region of zero amylose starch is less dense than that of high amylose starch due to the absence of amylose polymers. Therefore, the reordering of the double helices as well as the restructuring of the crystallites might have occurred more favorably in zero amylose starch than in high amylose starch during acid hydrolysis.

The solid-state CP/MAS ^{13}C NMR spectra of native and acid/alcohol-treated starches also indicated changes in the internal structures (Fig. 6.8). The narrowing of the C-1 peak and the more pronounced appearance of C-6 peak in the acid/alcohol-treated starches confirmed structural changes leading to higher crystalline orders due to substantial hydrolysis of the amorphous regions (near branching points).

Thermal properties

The DSC profiles and melting parameters of native and partially hydrolyzed barley starches are presented in Fig. 6.9a-d and Table 6.4. The peak melting temperature (T_p) of the gelatinization endotherms of all partially hydrolyzed samples decreased the most after 10h but started to slightly increase after longer hydrolysis time (96h). The peak width (T_c-T_o) generally broadened due to the hydrolysis. The enthalpy values (ΔH) of normal and high amylose samples decreased somewhat upon hydrolysis.

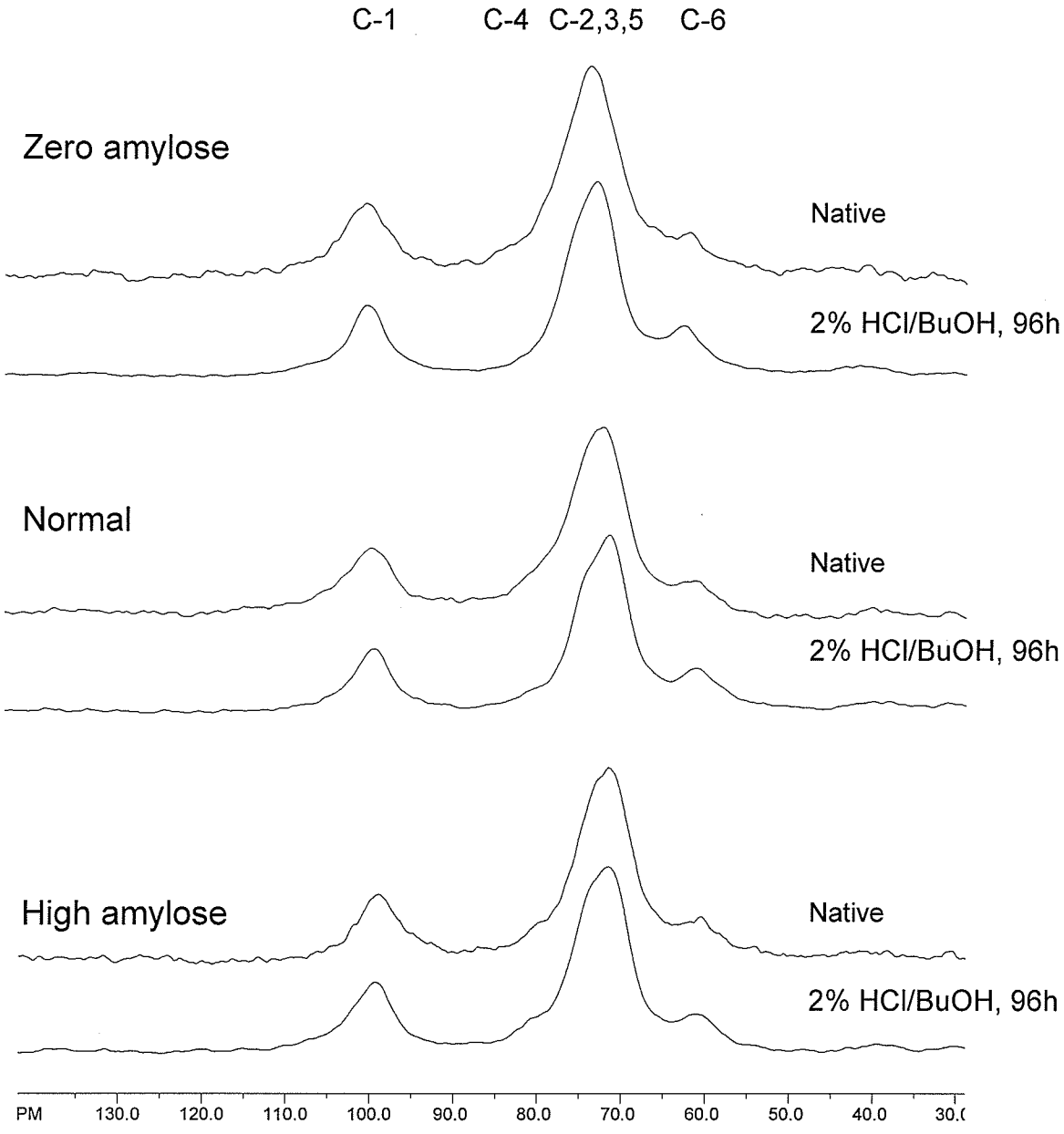

Figure. 6.8. Solid-state CP/MAS ^{13}C NMR spectra of native and acid/alcohol-treated barley starches (2% HCl/BuOH, 96h).

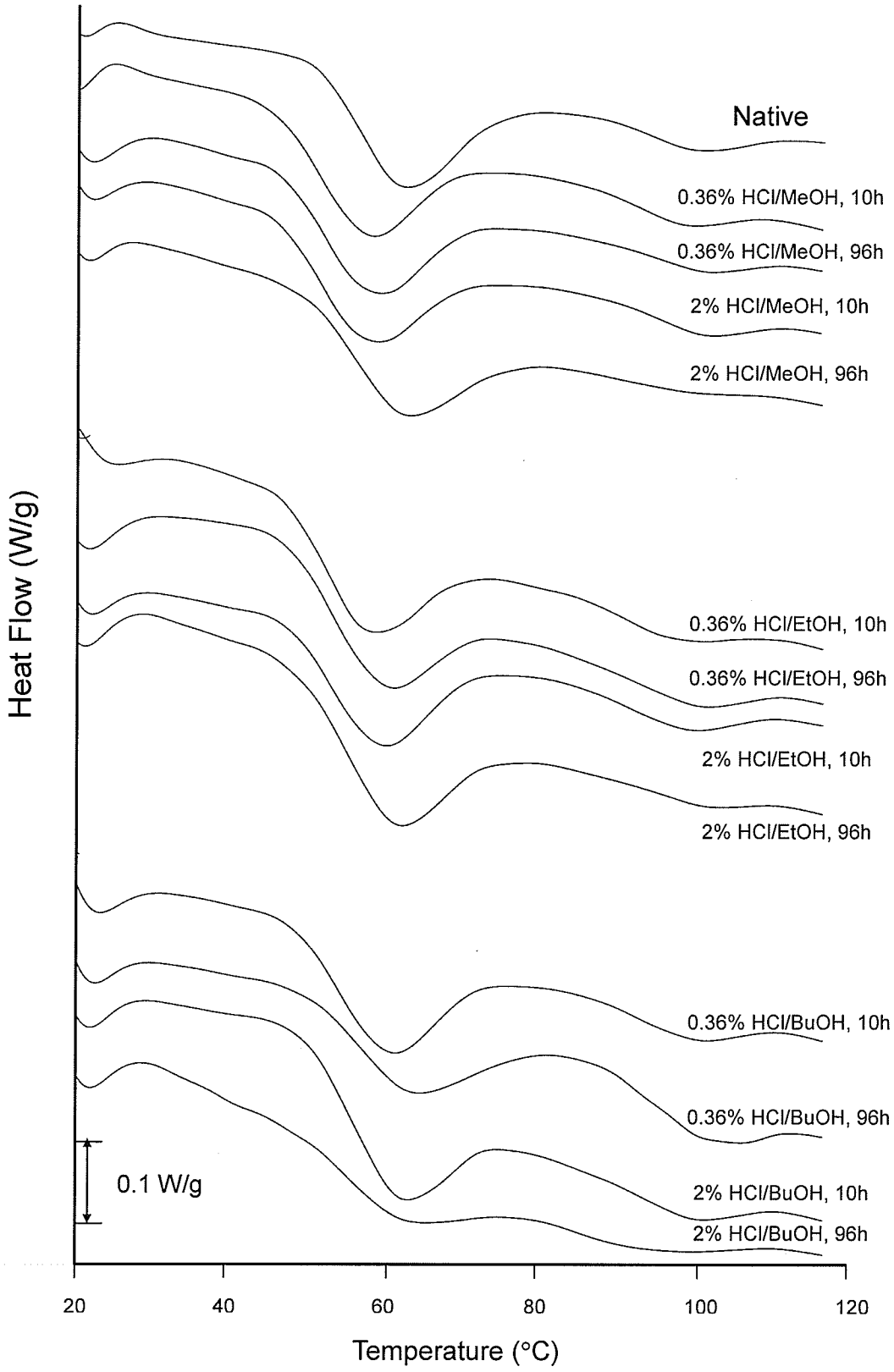

Figure. 6.9a. DSC endothermic profiles of native and acid/alcohol-treated normal starches (0.36% and 2% HCl/MeOH, EtOH, BuOH, 10h and 96h).

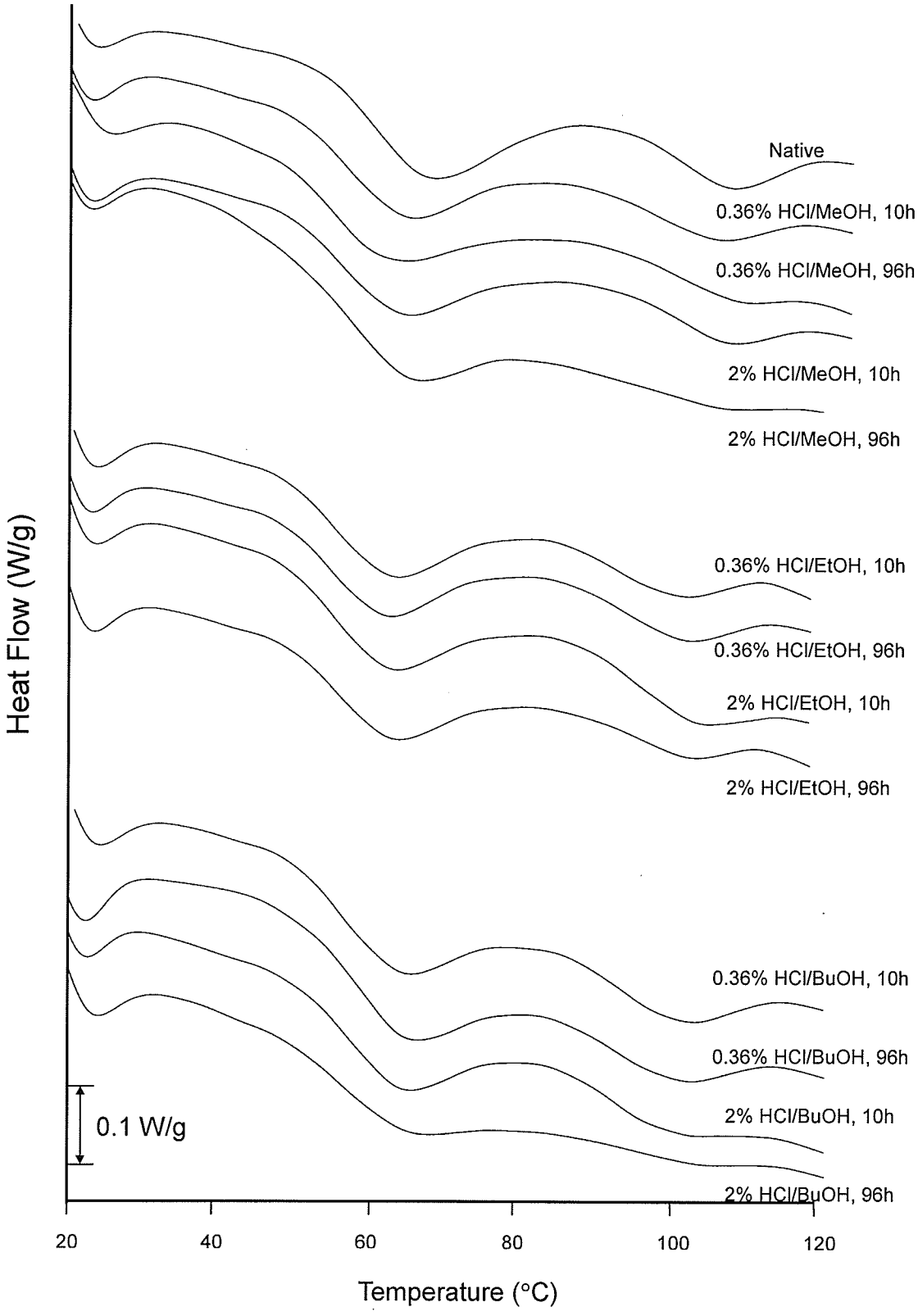

Figure. 6.9b. DSC endothermic profiles of native and acid/alcohol-treated high amylose starches (0.36% and 2% HCl/MeOH, EtOH, BuOH, 10h and 96h).

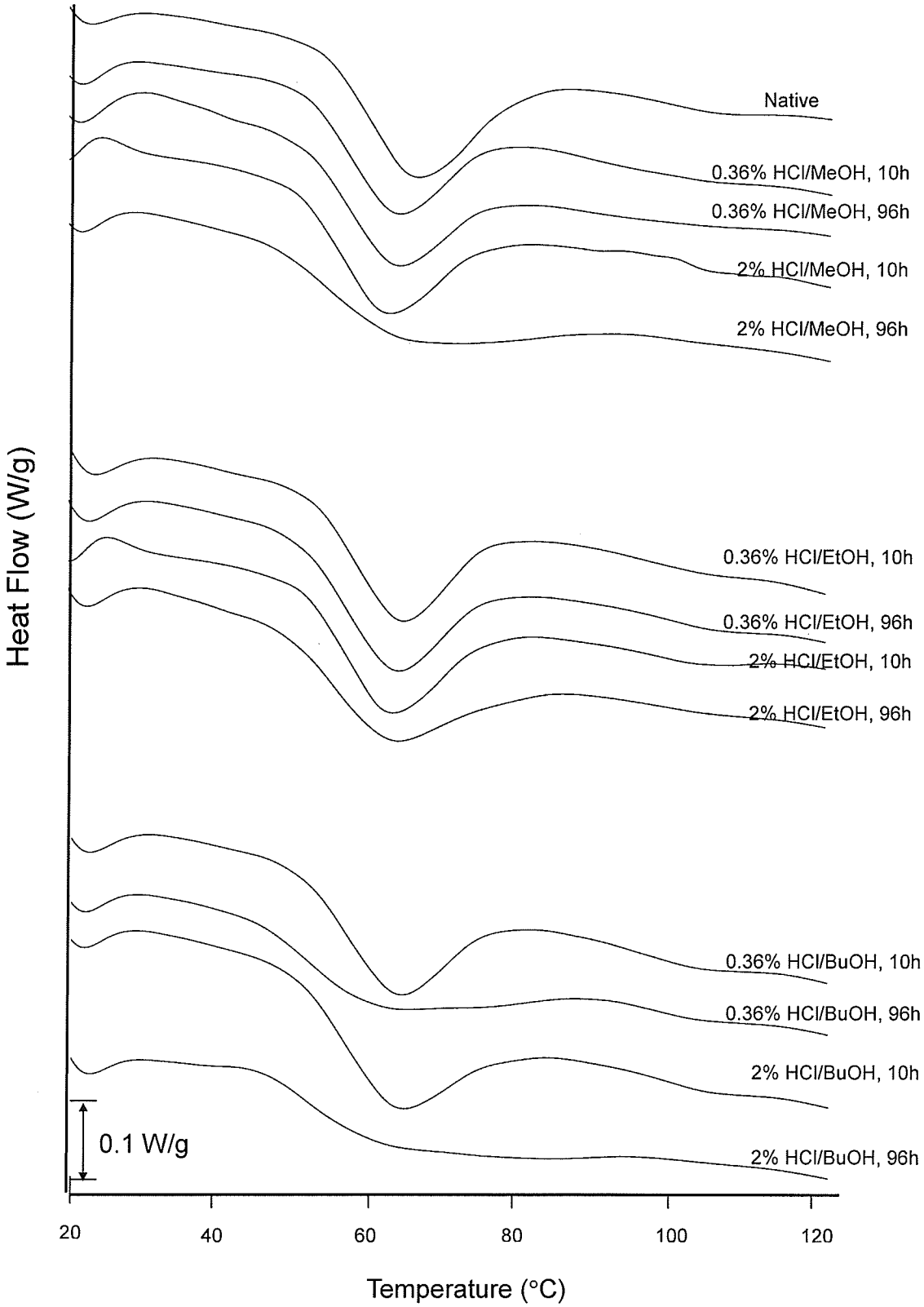

Figure. 6.9c. DSC endothermic profiles of native and acid/alcohol-treated waxy starches (0.36% and 2% HCl/MeOH, EtOH, BuOH, 10h and 96h).

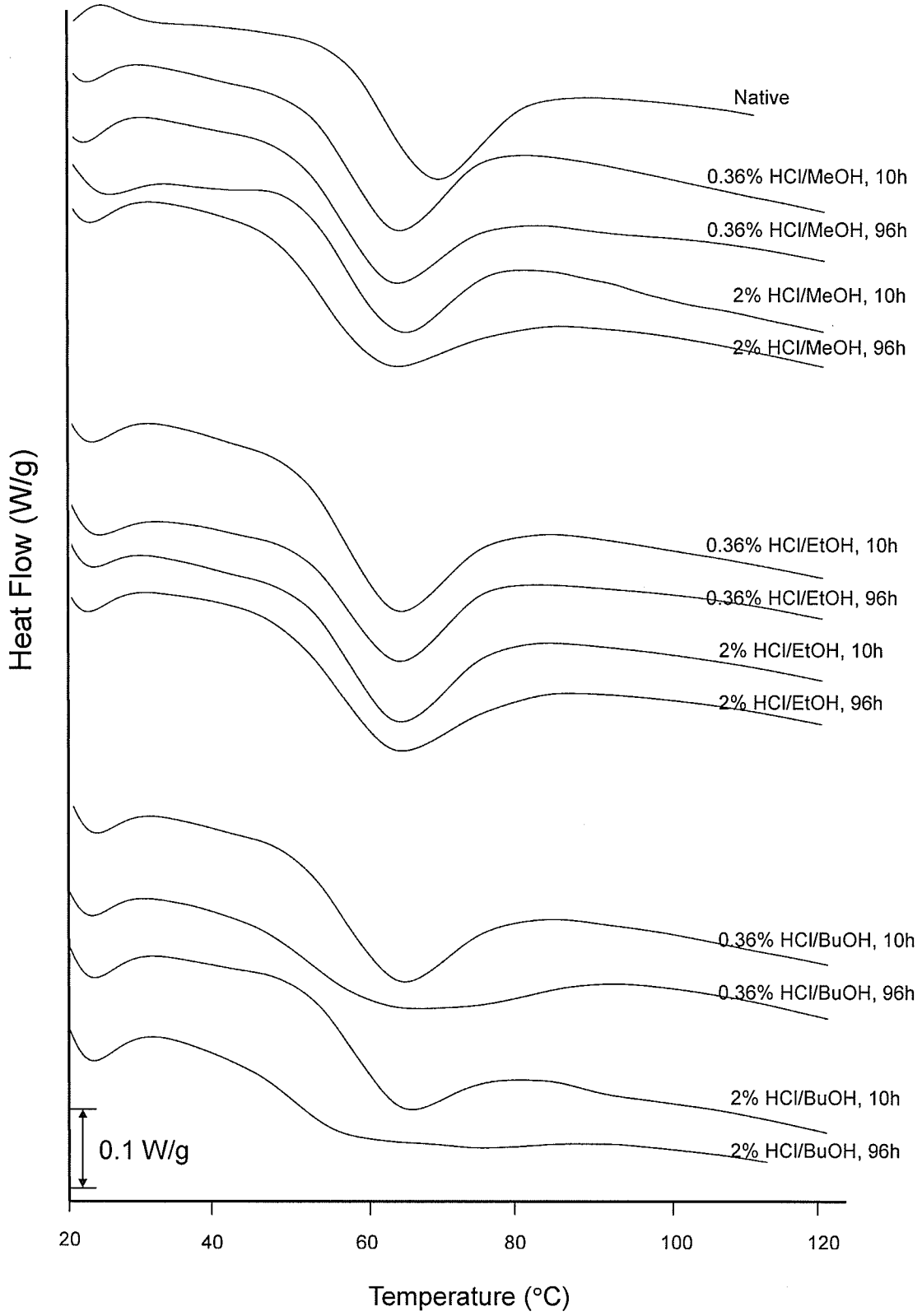

Figure. 6.9d. DSC endothermic profiles of native and acid/alcohol-treated zero amylose starches (0.36% and 2% HCl/MeOH, EtOH, BuOH, 10h and 96h).

Table 6.4. DSC transition characteristics of native and acid/alcohol-treated starches

Acid treatment	Normal					High amylose				
	ΔH (J/g)	T_p(°C)	T_c-T_o (°C)	ΔH (J/g) (AM-Lipid)	T_p(°C) (AM-Lipid)	ΔH (J/g)	T_p(°C)	T_c-T_o (°C)	ΔH (J/g) (AM-Lipid)	T_p(°C) (AM-Lipid)
Native	11.5±0.2	64.0±0.7	30.3±0.2	2.0±0.0	101.7±0.7	9.1±0.1	65.6±0.4	32.9±0.4	3.2±0.0	102.0±0.2
0.36% HCl										
10h MeOH	10.3±0.2	59.3±0.0	36.7±1.4	2.0±0.0	100.5±1.1	7.0±0.3	63.6±0.9	36.8±2.7	3.0±0.1	100.7±0.5
EtOH	10.1±0.3	59.5±0.4	30.8±0.4	2.5±0.4	98.1±0.1	7.5±0.2	62.0±1.1	33.1±3.3	3.1±0.2	100.5±0.3
BuOH	9.9±0.3	61.6±0.4	33.3±0.7	2.9±0.3	101.1±0.4	6.8±0.1	63.0±0.5	33.3±0.1	4.1±0.2	99.5±0.3
96h MeOH	10.1±0.1	60.2±0.4	35.3±0.3	1.6±0.1	102.4±0.1	8.0±0.1	60.8±0.9	39.1±3.0	1.5±0.2	102.9±0.5
EtOH	9.7±0.1	61.4±0.0	30.3±0.2	2.8±0.0	101.3±0.0	7.7±0.1	62.0±1.1	35.9±0.1	3.2±0.1	101.2±0.1
BuOH	8.5±0.0	64.6±0.0	37.2±2.5	3.0±0.2	101.3±1.4	6.2±0.0	64.1±0.5	33.7±2.4	3.6±0.1	99.6±0.2
2% HCl										
10h MeOH	10.0±0.3	60.0±0.4	34.7±0.2	1.8±0.1	102.3±0.1	7.3±0.5	61.5±1.0	36.2±1.0	2.2±0.1	101.3±1.1
EtOH	10.1±0.1	61.0±0.0	31.4±1.7	2.7±0.2	100.2±0.2	8.1±0.1	62.7±0.0	36.4±0.4	3.3±0.1	101.8±1.3
BuOH	9.3±0.6	63.0±0.3	30.9±0.8	3.1±0.1	100.7±0.1	4.1±0.6	63.2±0.4	32.4±4.8	2.2±0.3	98.2±0.9
96h MEOH	9.9±0.2	63.8±0.0	37.8±1.1	0.7±0.4	100.7±0.7	7.0±1.0	62.8±0.2	35.1±2.3	0.9±0.6	101.3±0.2
EtOH	9.8±0.7	62.2±1.1	37.2±3.7	1.5±0.1	101.5±1.6	6.8±0.2	62.9±0.0	33.8±1.7	2.4±0.1	101.2±0.9
BuOH	5.5±0.5	64.0±1.0	32.5±3.3	1.6±0.2	93.5±1.9	4.6±0.1	63.9±0.1	34.5±3.2	0.9±0.1	100.4±0.8

Acid treatment	Waxy					Zero amylose				
	ΔH (J/g)	T_p(°C)	T_c-T_o (°C)	ΔH (J/g) (AM-Lipid)	T_p(°C) (AM-Lipid)	ΔH (J/g)	T_p(°C)	T_c-T_o (°C)	ΔH (J/g) (AM-Lipid)	T_p(°C) (AM-Lipid)
Native	15.1±0.1	65.5±0.2	31.4±0.4	0.8±0.0	103.1±0.1	15.3±0.2	67.0±1.2	29.4±0.1		
0.36% HCl										
10h MeOH	14.7±0.3	62.8±0.5	35.7±0.1	1.0±0.0	101.2±0.5	15.9±0.6	62.9±0.0	37.6±0.7		
EtOH	14.8±0.2	63.3±0.0	35.0±1.8	0.5±0.0	101.4±0.9	15.8±0.7	63.0±0.1	38.3±0.6		
BuOH	14.4±0.5	63.0±0.1	37.1±1.8	0.7±0.7	101.3±0.8	14.9±0.6	62.8±0.1	39.1±1.9		
96h MeOH	14.6±0.5	62.8±0.1	36.4±0.2	0.7±0.1	97.1±0.6	15.7±0.9	62.7±0.0	40.4±2.4		
EtOH	15.0±0.1	62.6±0.1	35.6±0.7	0.8±0.1	102.7±0.0	15.3±0.5	62.9±0.8	38.2±0.8		
BuOH	14.4±0.6	60.9±0.6	46.9±1.1	0.4±0.2	99.1±2.3	15.4±0.4	62.0±0.1	57.7±0.3		
2% HCl										
10h MeOH	14.4±0.6	61.5±0.2	38.4±0.4	0.5±0.1	103.3±0.5	14.4±0.7	62.9±0.4	36.2±2.4		
EtOH	14.8±0.1	62.3±0.8	37.6±1.2	0.9±0.1	101.4±0.4	14.6±0.5	63.2±0.4	37.6±2.3		
BuOH	14.6±0.5	62.6±0.2	37.2±2.6	0.5±0.1	101.9±0.4	14.4±0.3	62.8±0.7	38.1±2.8		
96h MeOH	14.4±0.4	63.4±1.1	47.9±1.3			15.8±0.2	62.1±0.1	47.0±3.5		
EtOH	14.8±0.2	62.3±0.1	40.2±0.4			15.5±0.3	63.2±0.1	45.5±4.0		
BuOH	13.9±0.7	62.4±0.3	49.5±0.9			13.6±0.4	58.1±1.7	59.1±0.2		

The ΔH of both waxy samples did not substantially change upon hydrolysis. In general, upon extensive lintnerization of starches, a shift of the endotherms to higher temperature and a peak broadening but no changes in enthalpy of gelatinization are expected (Biliaderis et al. 1981; Jacobs et al. 1998; Shi and Seib 1992). These changes are attributed to the selective removal of the amorphous region in a granule by acid, as previously suggested by the results of X-ray crystallography and NMR spectroscopy. It is believed that the amorphous region can uptake water and therefore, facilitate cooperative melting of the crystalline parts. In the absence of the amorphous regions, the crystallites melt at a higher temperature and the transition is broader because of variations in their stability. Under the mild acid hydrolysis conditions (as conducted in this experiment), the amorphous regions may still be present inside the granule, although they may be partially degraded and/or decoupled from the crystallites. As a result of the partial modification of the amorphous region, the diffusion of water into the granule and hydration-facilitated melting of crystallites may be amplified resulting in the initial decrease in T_p observed for all partially hydrolyzed barley starches. Shi and Seib (1992) also reported that the T_p of lintnerized waxy rice starches decreased during the first 2 days of hydrolysis and only then started to increase. The small decreases in the ΔH values, observed in the partially hydrolyzed normal and high amylose samples, may indicate degradation of some amylose chains involved in double helical structures with either other amylose or amylopectin chains. No decreases in enthalpy were observed in the partially hydrolyzed waxy starches, containing very little or no amylose.

The second melting endotherm ($T_p \sim 100^{\circ}C$) in the DSC thermograms of normal and high amylose can be attributed to melting of the amylose-lipid complexes. Mild acid

hydrolysis, especially in butanol, slightly increased the ΔH values (Table 6.4). The newly formed amylose-butanol complexes could have contributed to these increased ΔH values. Upon stronger hydrolysis conditions (2% HCl, 96h), the ΔH of amylose-lipid complexes decreased, indicating extensive depolymerization of amylose chains.

α-Amylase digestibility of acid/alcohol treated starches

The digestibility of native and acid/alcohol-treated starches was determined from the amounts of carbohydrates solubilized and leached out of the granules during α-amylolysis. (Fig. 6.10). Partial acid hydrolysis significantly increased the rate and extent of α-amylolysis of all four types of barley starches. The rate of solubilization during the first 8h of α-amylolysis was equally high for all modified samples and significantly greater than for the native counterparts (results shown only for samples treated with 2% HCl in 1-butanol for 96h). During the second stage of α-amylolysis, the rate and extent of solubilization was much higher for the waxy samples than for the normal and high amylose starches. It appears that the partial acid degradation of the amorphous regions in the granules facilitated a better diffusion and penetration of the enzyme inside the granule. The initial high rate of solubilization probably indicates fast hydrolysis and release of the oligosaccharides from the depolymerized internal starch polymers. The slower rate of solubilization observed after the first 8h of α-amylolysis may be attributed to the inhibitory effect of the released oligosaccharides on the enzymes (Hill and MacGregor 1988).

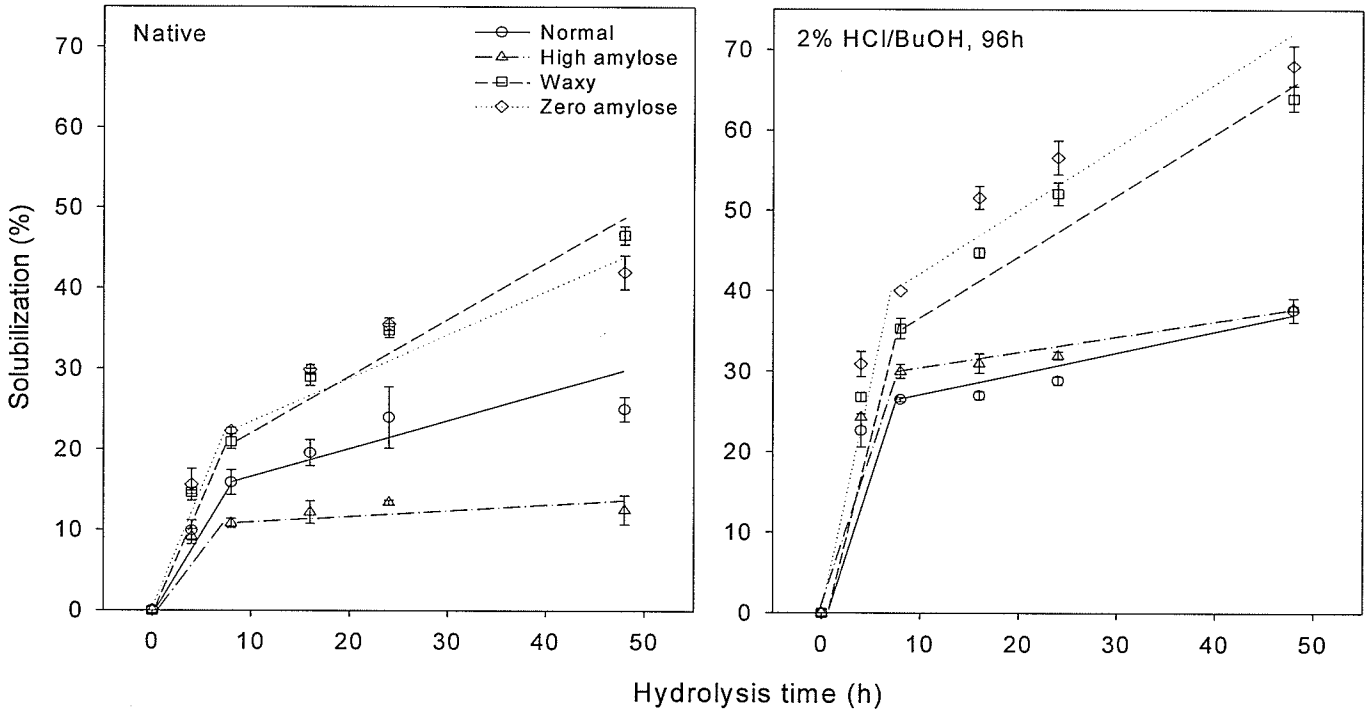

Figure. 6.10. The α-amylase digestibility of native and acid/alcohol-treated barley starches (2% HCl/BuOH, 96h).

Dynamic viscoelasticity

The viscoelastic properties of native and acid/alcohol-treated barley starch solutions (40% w/w) during cooling and storage (5°C, 20h) are shown in Figures. 6.11 and 6.12. During the initial cooling, normal and high amylose starch samples hydrolyzed for 10h in 2% HCl/MeOH showed slightly lower G' values than their native counterparts (Fig. 6.11). During the long time storage, the partially hydrolyzed high amylose starch showed significantly higher values of G' compared to the native sample, whereas the partially hydrolyzed normal starch exhibited G' development similar to its native counterpart (Fig. 6.12). Both normal and high amylose starches, hydrolyzed for 96h, exhibited a rapid rise in G' upon cooling but very little network development thereafter (Fig. 6.11 and 6.12). As a consequence, the final G' values of both normal and high amylose samples hydrolyzed for 96h were much lower compared to their native and 10h- hydrolyzed counterparts. The substantial differences in the molecular weight of the 10h- vs. 96h-hydrolyzed samples (Table 6.2) are probably responsible for the observed effects. These results indicate that the optimum gelation potential of amylose-containing starches can be obtained by appropriate modification of their molecular weight.

The initial stage of starch gelation is dominated by the interactions of leached amylose chains, while re-crystallization of short amylopectin chains (DP 15) contributes to stiffness development of starch gel during a long time storage (Miles et al., 1985a). The DP of amylose chains is an important factor in determining the aggregation kinetics of amylose polymers and the final G' value of amylose gels after storage (Clark et al., 1989). It was reported that amylose chains with DP<1100 can reach the maximum G' values more rapidly than the longer chains (with DP 2550). However, the shorter chains exhibited lower final G' values than their longer counterparts (Clark et al., 1989).

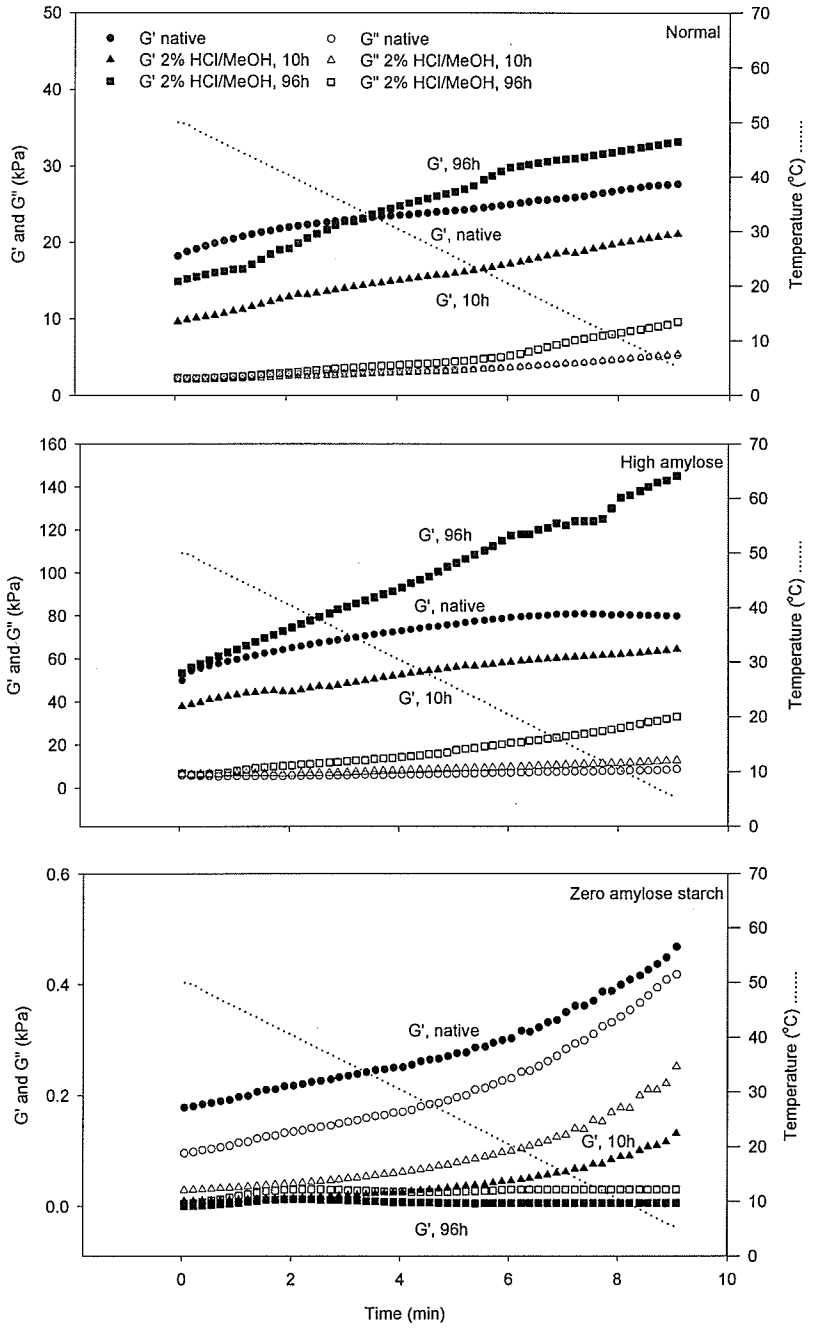

Figure. 6.11. The temperature dependence of initial network formations (G' and G") of native and acid/alcohol-treated barley starches (40% w/w) upon cooling from 50°C to 5 °C (cooling rate of 5 °C/min).

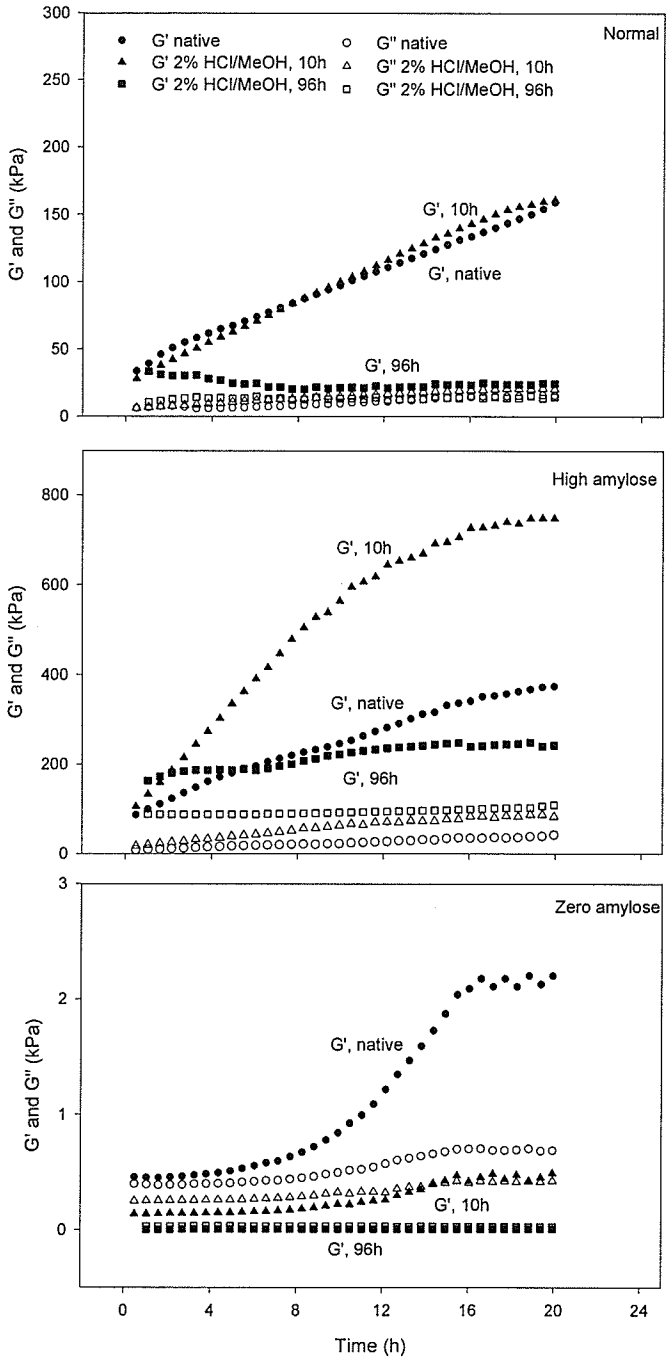

Figure. 6.12. The time dependence of network developments of native and acid/alcohol-treated barley starches (40% w/w) during storage for 20h at 5 °C.

In addition, the longer amylose chains (DP 2550) exhibited a continuous increase in the G' values during storage for 58h without reaching a definite plateau. This behaviour was attributed to a low diffusion rate of longer amylose chains, which slowed down cross-linking and increases in G' (Clark et al., 1989). In this study, the native high amylose starch exhibited a gradual increase in G' throughout the entire storage period, whereas the modified high amylose sample (10h) exhibited a greater development of G' during the first few hours of storage, followed by an attainment of plateau values after ~16 hours of storage. These effects are probably associated with the increased diffusion of polymer chains and consequently higher rates of cross-linking of somewhat truncated amylose chains in the modified sample. The 96h-modified high amylose starch showed the most rapid development of G' during cooling, but achieved relatively low G' values during the long time storage, most likely due to the substantially reduced molecular weight of this sample.

In contrast to amylose, partial degradation of amylopectin chains, in the zero amylose starch samples, appears to substantially decrease their potential to form elastic cross-linked networks even upon long time storage (Fig. 6.11 and 6.12). Lauro et al. (1997) also reported that stiffness of amylopectin gels decreased substantially with increasing hydrolysis of amylopectin. In our studies, the partially hydrolyzed zero amylose waxy starch samples exhibited mostly viscous properties during cooling and storage experiments. Despite a relatively high molecular weight (Table 6.2), the 10h-hydrolyzed zero amylose starch sample showed very low G' values compared to those of partially hydrolyzed normal and high amylose samples.

As explained before, the uniquely slow gelation and retrogradation properties of

zero amylose waxy barley starches may be associated with the relatively short length of the linear chains in amylopectin of waxy starches compared to high amylose barley starches. The additional fragmentation of amylopectin polymers during partial acid hydrolysis completely diminished their potential for gelation and retrogradation. These results indicate that partially modified waxy barley starches are resistant to retrogradation. This property may be particularly useful in certain food applications and should be further investigated.

Conclusion

Despite a very low degree of solubilization (< 9%) and almost intact granular morphology, substantial degradation of starch polymers occurred inside the granules. In addition to hydrolysis time and acid concentration, the type of alcohol in which the hydrolysis was carried out had a great effect on the extent of hydrolysis. The greatest depolymerization was always found in starches hydrolyzed in 1-butanol, which seemed to facilitate the penetration of acid inside starch granules. The waxy samples have produced a slightly higher amount of solubilized carbohydrates but a close examination of the starch polymers inside the granules after hydrolysis has not indicated significant differences between waxy and high amylose starches in their susceptibility to hydrolysis. Acid hydrolysis significantly increased the crystallinity of starches, indicating that acid preferentially hydrolyzed the amorphous regions. The significant increases in the rate and extent of α-amylolysis of acid-treated starches indicated that partial acid degradation of the amorphous regions in the granules might facilitate a diffusion and penetration of α-amylase inside the starch granule. The results of this study are in good agreement with the current understanding of the mechanism of acid action inside starch granules, and support well the proposed lamellar structure of amorphous and crystalline regions within starch granules. The rheology results revealed that amylose content as well as the hydrolysis conditions (alcohol type, hydrolysis time, and acid concentration) significantly affected the gelation potential of barley starches. The rheological properties of starch solutions can be controlled by selection of hydrolysis conditions.

CHAPTER 7

Flow and Viscoelastic Properties of High Amylose Hulless Barley Starch and β-Glucan Blends

Abstract

Steady shear viscosity and small deformation oscillatory measurements were used to characterize the rheological properties of blends of high amylose (HA) barley starch and β-glucans (BG). The experiments were conducted at various ratios of the two polymers and at different concentrations of total carbohydrates (5% and 15% w/w). Both high and low molecular weight β-glucan preparations were used in this study (HMW-BG and LMW-BG, respectively). The apparent viscosity of the blends (5% w/w total concentrations) was influenced by the molecular weight of β-glucan. The addition of HMW-BG generally increased, whereas LMW-BG decreased the viscosity of blends compared to 5% starch alone. HMW-BG appeared to inhibit the mobility and diffusion of starch polymers in the solutions. The addition of HMW-BG also affected the viscoelastic properties of the blends, especially increasing the viscous properties of the blends, compared to that of the pure starch sample (5% w/w). The starch and HMW-BG blends (5% w/w total carbohydrate concentration; ratio of starch:β-glucan - 100:0, 85:15, 70:30, 55:45), however, exhibited improved viscoelastic properties, compared to the individual polymer solutions at corresponding concentrations, indicating that the starch-starch junction zones might be replaced by BG-BG or starch-BG entanglements. On the other hand, the addition of LMW-BG did not improve the viscoelasticity of the blend networks (5% w/w total carbohydrate concentration). In a high concentration system (15% w/w total carbohydrate concentration; ratio of starch:β-glucan - 100:0, 95:5,

90:10), both HMW- and LMW-BG had relatively little effect on the G' and tan δ values of the blends, indicating that the blend networks at higher concentration were governed mostly by the strong junction zones formed by the starch polymers. However, some interactions and/or entanglements between starch and β-glucan polymers were also evident in the modified high amylose starch and β-glucan blend systems (95:5 blends). It appeared that the starch digestibility of the blends was inversely proportional to the elastic properties of the networks.

Introduction

The rheological behavior of starch dispersions/gels can be influenced and thus controlled by several factors, including concentration of starch polymers, amylose/amylopectin ratio, molecular weight (M_w) of amylose and amylopectin, and dissolution methods (Biliaderis 1992; Eliasson 1986; Ring 1985). The use of native starch in processed food, however, is limited because of its time-dependent structural changes (gelation, retrogradation, and syneresis), which makes the starch-containing food products difficult to control (Kulicke et al. 1996). Furthermore, viscosities of native starch gels are often too high for industrial applications (Rosalina and Bhattacharya 2002). In order to overcome these shortcomings, native starches are often modified by chemical and/or physical methods, to change their rheological behaviour, and to improve their processing, storage stability, and resistance to pH, acid, and thermal and/or shear treatments (Wurzburg 1986).

An alternative way of improving the properties of starches is through blending with other polysaccharide polymers. The flow and viscoelastic behaviour of maize starch and galactomannan blends (Alloncle et al. 1989, Eidam et al. 1995, Yoshimura et al. 1998), of wheat starch and xanthan gum blends (Alloncle et al. 1991; Christianson et al. 1981; Yousria et al. 1994), of cross-linked waxy corn starch and κ-carrageenan blends (Tecante and Doublier 1999), of waxy maize starch and galactoxyloglucan blends (Freitas et al. 2003), and of wheat or rice starch and yellow mustard mucilage (YMM) blends (Liu et al. 2003) have been reported. One of the appealing aspects of starch/hydrocolloid blends is that they show a variety of rheological and texture-imparting properties, which are suitable for broad applications in food products.

The addition of hydrocolloids usually results in a noticeable increase in viscosity

relative to starch alone (Alloncle et al. 1989; Christianson et al. 1981; Kulicke et al. 1996; Liu et al. 2003; Sajjan and Rao 1987). Hot starch-galactomannan dispersions exhibited a dramatic increase in viscosity compared with starch or galactomannan alone (Christianson et al. 1981; Sajjan and Rao 1987). The authors suggested that the increased viscosity of starch-galactomannan blends was attributable to the physical interaction between hydrocolloid and amylose polymers. Starch pastes have been described as a suspension of swollen granules dispersed in a macromolecular medium (Doublier et al. 1987; Ring 1985). Based on the biphasic system of starch pastes, Alloncle et al. (1989) proposed that the increase in viscosity of starch-galactomannan blends resulted from the increase in the concentration of galactomannan polymers in the continuous phase, which was induced by starch granule swelling. The viscoelastic properties of starch gels are also significantly influenced by the addition of hydrocolloids (Eidam et al. 1995; Freitas et al. 2003; Kulicke et al. 1996; Liu et al. 2003; Yoshimura et al. 1998, 1999). In blends of konjac-glucomannan and corn starch, substantial increases in both storage (G') and loss (G") moduli were observed, with a more pronounced increase in G" (Yoshmura et al. 1998). Blends of starch and galactomannans, and of starch and κ-carrageenan also significantly increased the viscous properties of the systems (Eidam et al. 1995). It was suggested that the increase in G" values in the starch/hydrocolloid blends was attributed to the thermodynamic incompatibility between starch and hydrocolloid polymers (Eidam et al. 1995; Kulicke et al. 1996; Yoshimura et al. 1998). On the other hand, in a blend of ι-carrageenan and maize starch, the elastic property was improved, compared to the starch gel alone (Eidam et al. 1995), indicating that intermolecular interaction occurred between starch and ι-carrageenan polymers. The addition of YMM to wheat and rice starches increased hardness, adhesiveness, chewiness, and springiness of their gel textures, also indicating

the occurrence of interaction between YMM and starch polymers (Liu et al. 2003).

Despite the increasing interest in β-D-glucans during the last two decades due to their nutritional benefits (Inglett 1997), only a few studies have focused on the rheological behaviour of starch and β-D-glucan blends (Carriere and Inglett 1998; 1999). Cereal β-D-glucans are linear homopolysaccharides composed of D-glucopyranosyl residues linked via a mixture of β-(1→3) and β-(1→4) linkages (Wood et al. 1991; Woodward et al. 1983). Rheologically, cereal β-D-glucans behave similarly to random coil polysaccharides. However, some β-D-glucans can form gels under certain conditions (Bohm and Kulicke 1999). It has been suggested that the ratio of cellotriosyl to cellotetraosyl units in the cereal β-D-glucan structure affects gelling ability (Bohm and Kulicke 1999; Cui and Wood 2000). In addition to structural features, it has also been reported that molecular size plays an important role in the gelation potential of cereal β-D-glucans (Bohm and Kulicke 1999; Cui and Wood 2000; Lazaridou et al. 2003).

The aim of the present investigation was to study the rheological behaviour of high amylose barley starches (native and enzyme-modified) and barley β-glucan blends. The effects of different polymer ratios, molecular weights of β-glucans as well as different total carbohydrate concentrations in the blends on the flow and viscoelastic properties of the mixed systems were investigated.

Materials and Methods

Materials

High amylose (HA) starch was isolated from hulless barley (cv. CDC 92-55-06-48), according to a previously reported procedure (Chapter 3). The enzyme-modified starch was obtained by partial hydrolysis of HA starch with α-amylase (*Bacillus licheniformis*, 3000 U/mL, Megazyme, Bray, Ireland). HA starch was digested with α-amylase (50 U per gram of starch) for 24 hours (Chapter 5). The β-glucans (BG) were extracted from ground hulless barley according to the method of Izydorczyk et al. (1998). A portion of the isolated BG was subjected to partial hydrolysis with a malt extract to reduce its molecular weight. The molecular weight of native and partially digested BG was determined by high-performance size exclusion chromatography (HPSEC) coupled with multi-angle light scattering (MALS) and refractive index (RI) detectors (Chapter 3). The weight average molecular weight of the native BG fraction was $1.29\times10^{6}\pm0.02$ and it is designated as high molecular weight BG (HMW-BG). The weight average molecular weight of the partially hydrolyzed BG was $0.446\times10^{6}\pm0.02$, and it was designated as the low molecular weight BG (LMW-BG).

Preparation of mixed systems

Starch and BG solutions were prepared by dissolving those polymers separately at various concentrations (Table 7.1) in water by heating and stirring at 100°C. The blends of HA starch and BG were prepared by adding appropriate amounts of HA starch to solutions of BG (Table 7.1) and boiling the mixtures for 10 min in closed vials to avoid any evaporation.

Table 7.1. Concentrations and compositions of starch and β-glucan blends.

Total carbohydrate concentration in blends (%)	Ratio of starch : BG	Concentration of starch in blends (%)	Concentration of BG in blends (%)
5	100 : 0	5	0
	85 : 15	4.25	0.75
	70 : 30	3.5	1.50
	55 : 45	2.75	2.25
15	100 : 0	15	0
	95 : 5	14.25	0.75
	90 : 0	13.5	1.50

Rheological measurements

All the rheological tests were performed with a stress-controlled rheometer (AR-2000, TA Instruments, New Castle, DE), using a cone and plate geometry (40 mm diameter, 4°, 119 μm truncation). The hot HA starch and BG solutions were transferred from vials to the bottom plate of the geometry. After lowering the upper cone of the geometry, the solutions were allowed to cool to 20°C. In order to minimize the moisture loss in the samples, the entire geometry was covered by a moisture trap (TA Instruments, New Castle, DE). Steady shear measurements were conducted by applying continuous-ramp shear rates in the range of 0.0013 – 100 s^{-1} at 20°C. The shearing time was 30 min for both the ascending and descending shear cycles. Oscillatory measurements were performed by applying a constant strain (0.2%) at 0.01 - 50 Hz frequency range. The development of viscoelastic properties of blends was examined by monitoring the storage and loss moduli changes at a frequency of 0.5 Hz and a constant 0.2% strain at 20°C for 2 h.

α-Amylase digestibility of mixed systems

The blends of HA starch and HMW- and LMW-BG were subjected to α-amylase (10U/g, porcine pancreas, Sigma) hydrolysis for 5 to 30 min at 35°C. In order to stop the hydrolysis reaction, 20 μL of 1M-HCl was added into the solution. The solution was centrifuged (6940*g*, 10 min) and the amount of reducing sugars present in the supernatants was determined by the modified Park-Johnson method (Hizukuri et al 1981).

Results and Discussion

Low concentration system (5% w/w)

Steady shear rheological properties. Figure 7.1(a, b) shows the steady shear viscosity profiles of freshly prepared native and enzyme-modified HA starch pastes in concentrations ranging from 2.75% to 5%. All samples exhibited a shear thinning behaviour with increasing shear rates. The viscosity profiles obtained with increasing and then decreasing shear rates did not overlap completely, indicating some thixotropic properties of starch samples, the extent of which was independent on the polymer concentrations. The shear thinning behaviour and the thixotropy are typical for cereal starch pastes (Alloncle et al. 1989; Doublier 1981). Despite a decrease in molecular weight of HA starch during α-amylolysis, the modified HA starch solutions showed similar or even slightly higher viscosity values than native HA starch (Fig. 7.1b). It appears that mild depolymerization of starch polymers increased chain diffusion and thus improved their interactions and entanglements in solution.

Steady shear viscosity profiles of freshly prepared HMW-BG and LMW-BG solutions are shown in Figure 7.2. The viscosity of BG solutions increased with molecular weight and concentration of polymer. The viscosity profiles obtained with subsequent increasing and decreasing shear rates overlapped, indicating that the BG solutions had no thixotropic properties. These results are in good agreement with previous studies that revealed no thixotropic properties for purified oat beta-glucan dispersions (Lazaridou et al. 2003; Zhang et al. 1998).

Figure 7.3 shows the steady shear viscosity profiles of native HA starch and HMW-BG blends in various ratios at a total polymer concentration of 5% (w/w). The apparent

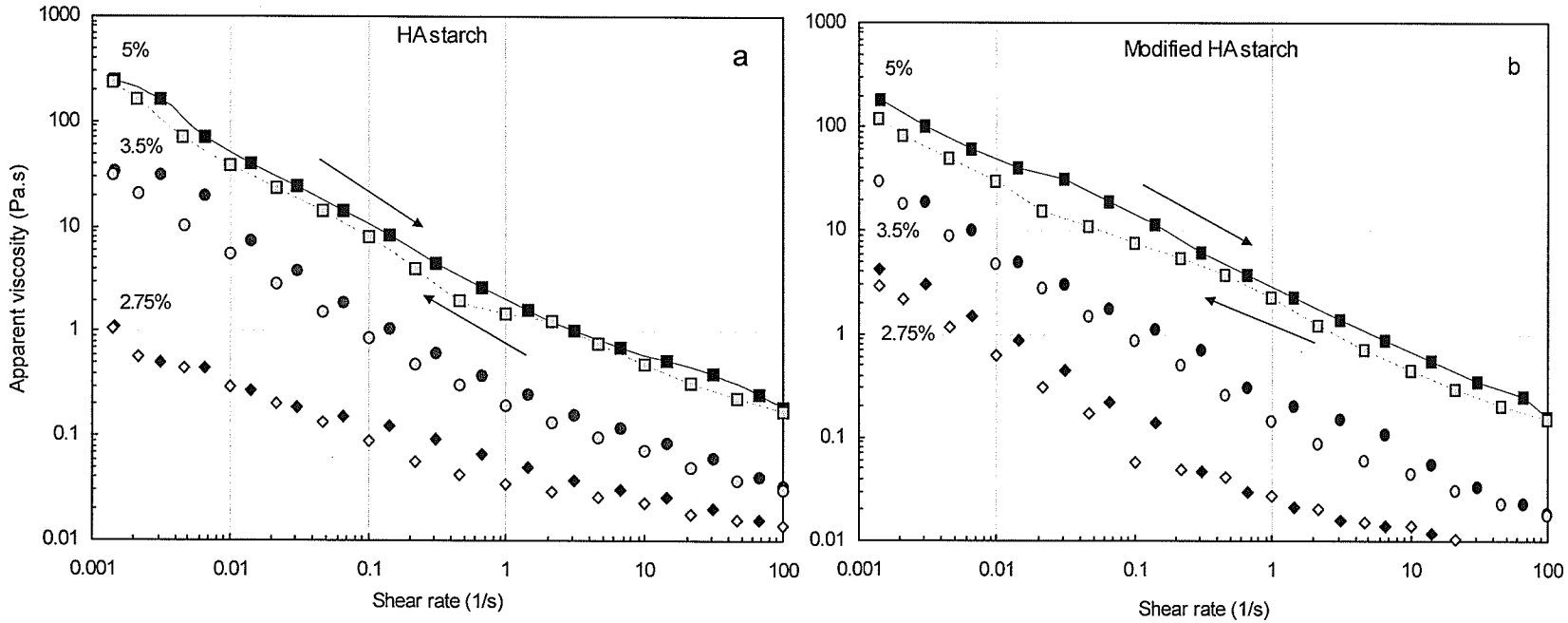

Figure 7.1. Steady shear viscosity profiles of freshly prepared HA starch (a) and enzyme-modified HA starch (b) (50U/g, 24h) at concentrations ranging from 2.75% to 5% (w/w).

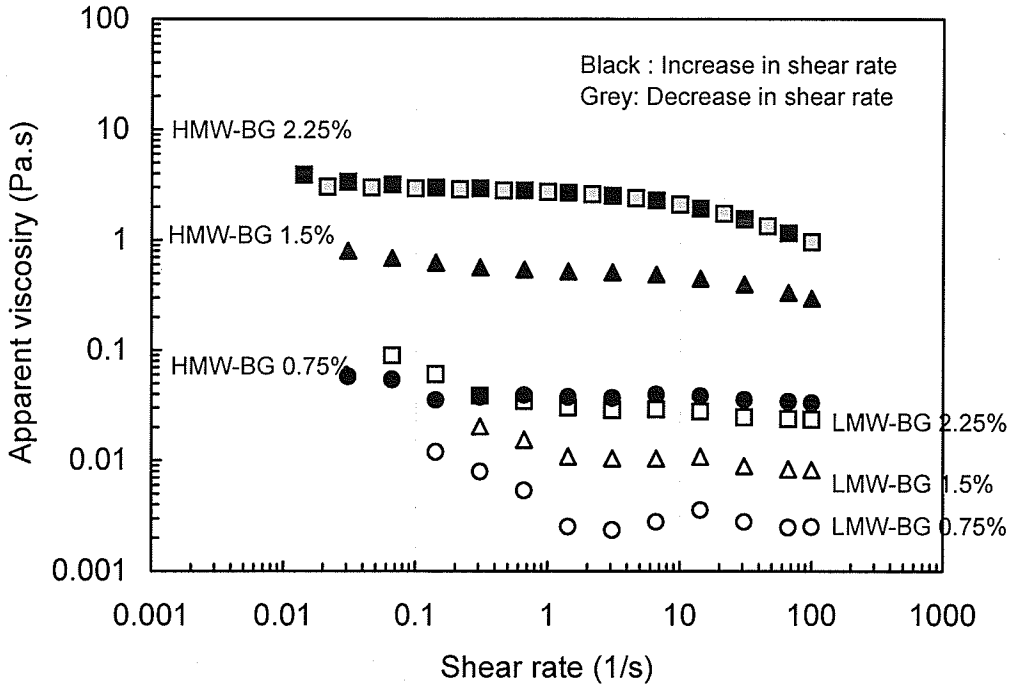

Figure 7.2. Steady shear viscosity profiles of freshly prepared HMW-BG and LMW-BG solutions at concentrations ranging from 0.75% to 2.25% (w/w).

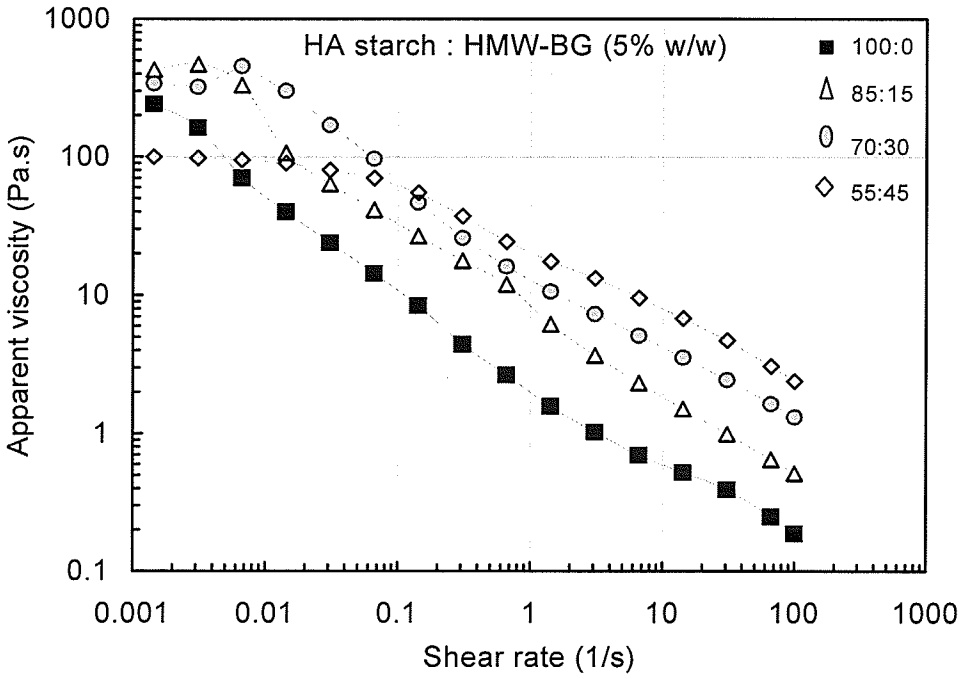

Figure 7.3. Steady shear viscosity profiles of HA starch and HMW-BG blends at a total polymer concentration of 5% (w/w).

viscosity values of the blends were generally higher than those of HA starch sample (5% w/w) alone, and much higher than the viscosity of individual polymer solutions at corresponding concentrations (Table 7.1, Fig 7.1a, Fig. 7.2). At the high shear rates, the apparent viscosity increased with increasing ratios of HMW-BG in the blends. At low shear rates, the effect was opposite; i.e., the blend containing the highest amount of BG exhibited the lowest viscosity. The shear thinning behaviour also slightly decreased with increasing HMW-BG content in the blends. It appears that the addition of long chains of β-glucans substantially affected the mobility of starch chains in solutions. At the very low shear rates, when there is normally enough time for the polymer chains to re-establish new entanglements, the presence of BG appeared to interfere with this process, probably by decreasing the mobility and diffusion of polymer chains. As the shear rate increased, on the other hand, the HMW-BG seemed to inhibit chain disentanglement, thus reducing the shear thinning behaviour.

The apparent viscosity of blends containing LMW-BG was generally lower compared to the viscosity of HA starch (5% w/w) alone (Fig. 7.4). The decrease in viscosity was proportional to the amount of LMW-BG in the blends. However, the apparent viscosity of the 55:45 (HA starch : LMW-BG) blend was higher than the viscosity of individual polymer solutions at corresponding concentrations (i.e., 2.75% HA starch and 2.25% LMW-BG) (Fig. 7.1a and 7.2). Similar observations were made for the 70:30 and 85:15 blends. It appears therefore that blending of HA starch and BG polymers induced some interactions and co-entanglements of these polysaccharides causing substantial increases in solution viscosity upon mixing. The molecular weight of BG polymers had a direct effect on the apparent viscosity of the blends. The blends of modified HA starch with BG (Figs. 7.5 and 7.6) exhibited similar viscous properties to

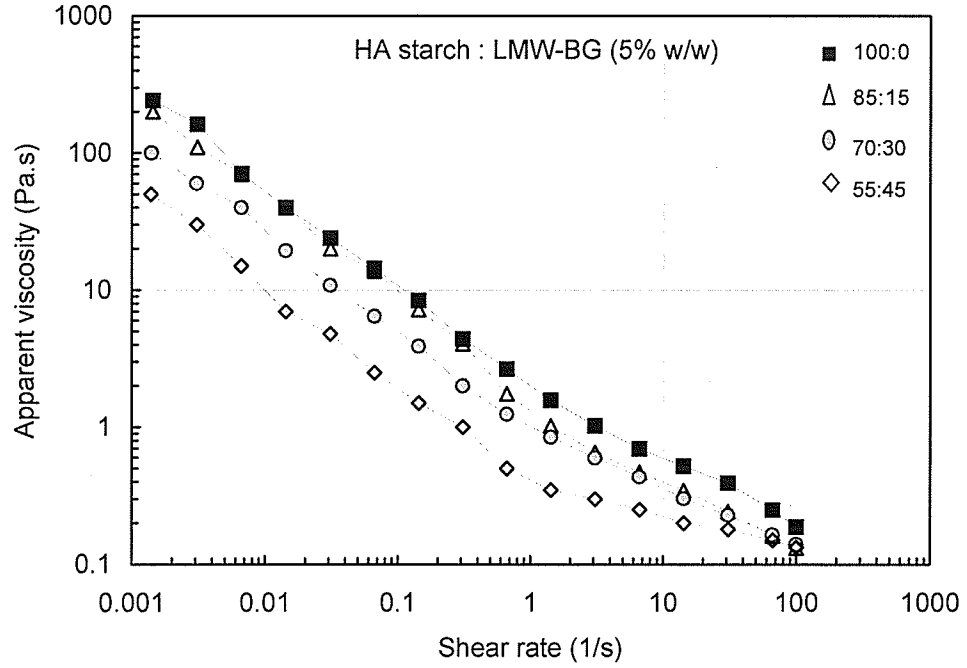

Figure 7.4. Steady shear viscosity profiles of HA starch and LMW-BG blends at a total polymer concentration of 5% (w/w).

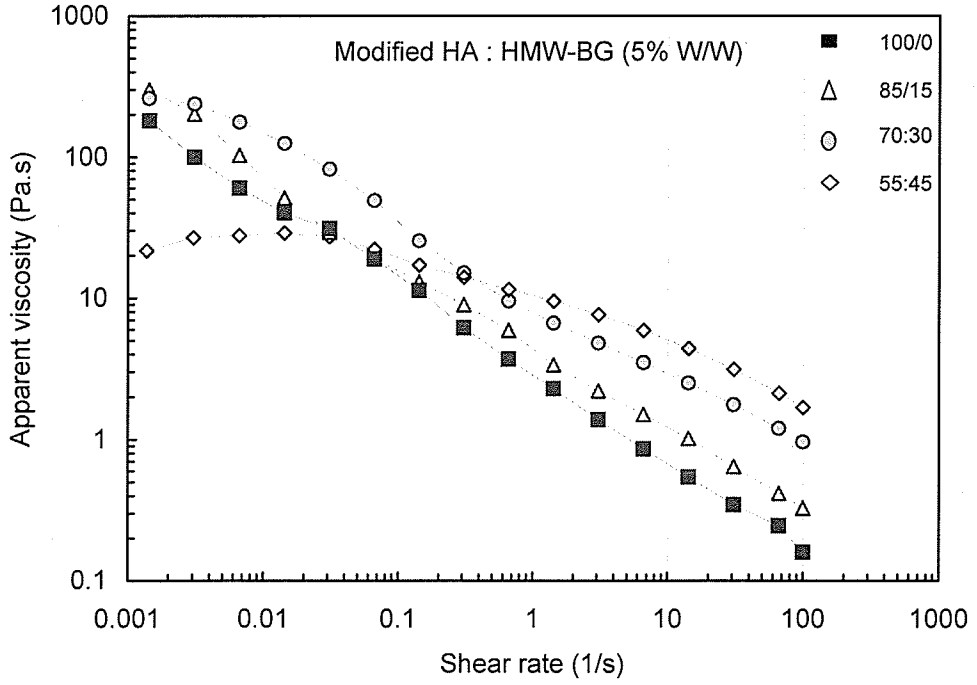

Figure 7.5. Steady shear viscosity profiles of modified HA starch and HMW-BG blends at a total polymer concentration of 5% (w/w).

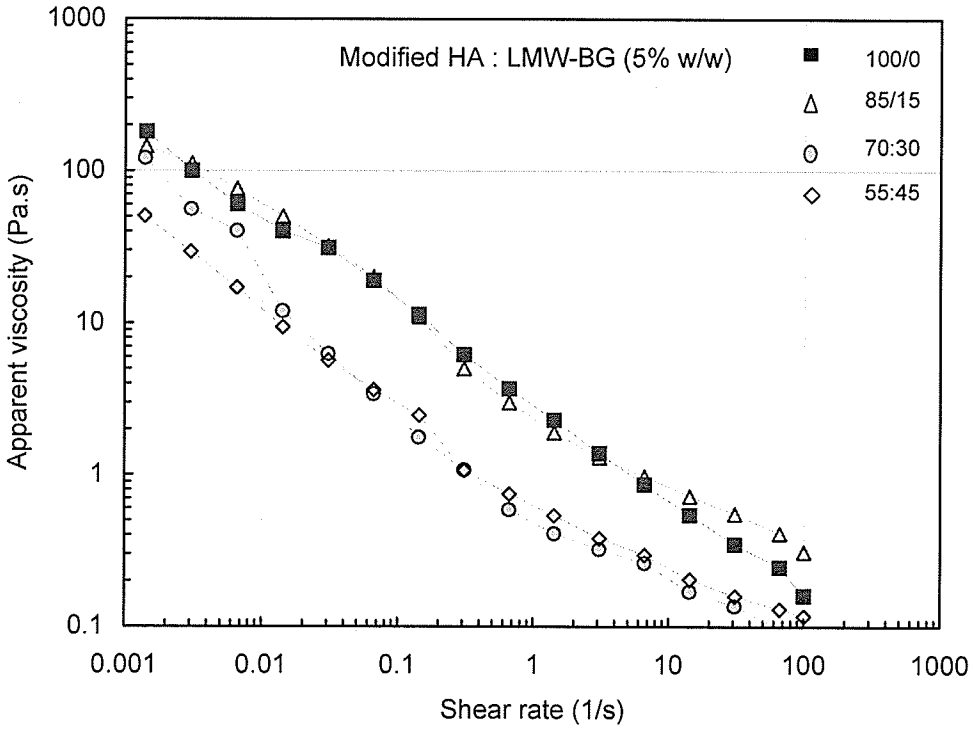

Figure 7.6. Steady shear viscosity profiles of modified HA starch and LMW-BG blends at a total polymer concentration of 5% (w/w).

blends containing native starch. The addition of the HMW-BG generally increased, whereas the LMW-BG decreased the viscosity of blends compared to 5% modified HA starch alone. As pointed out before, the increased chain mobility probably improved the chain interactions and compensated for the normally occurring decrease in viscosity due to reduction of molecular size of polymer chains.

Viscoelastic properties. Figures 7.7 a and b show the plots of G' and G" moduli against frequency of freshly prepared native HA starch solutions. At 5% and 4.25% (w/w) polymer concentrations, the G' and G" showed little dependence on frequency. Although the G' was higher than G" for both concentrations, the tan δ values ranged from 0.22 to 0.96, and from 0.22 to 1.11, respectively, indicating rheological behaviour of rather weak gel systems (Clark and Ross-Murphy 1987). At 3.5% and 2.75% (w/w) starch concentrations, the G" was higher than G' at the lower frequency range. In addition, both moduli were highly dependent on increasing frequency, thus exhibiting behaviour of concentrated polymer solutions (Clark and Ross-Murphy 1987). The mechanical spectrum of a 5% (w/w) solution prepared from partially modified HA starch (Fig. 7.8) also indicated properties of a concentrated solution with G' values lower than G" at lower frequencies, but exceeding G" at higher frequencies.

The development of storage and loss moduli during storage for 2h at 20°C for native and enzyme-modified starch pastes is shown in Fig. 7.9 and 7.10. For native starch samples, both moduli increased with increasing starch concentration. At 4.25% and 5% starch concentrations, the G' slightly increased with time, and tan δ decreased from 0.38 to 0.22, and from 0.32 to 0.13, respectively, indicating slight increases in the

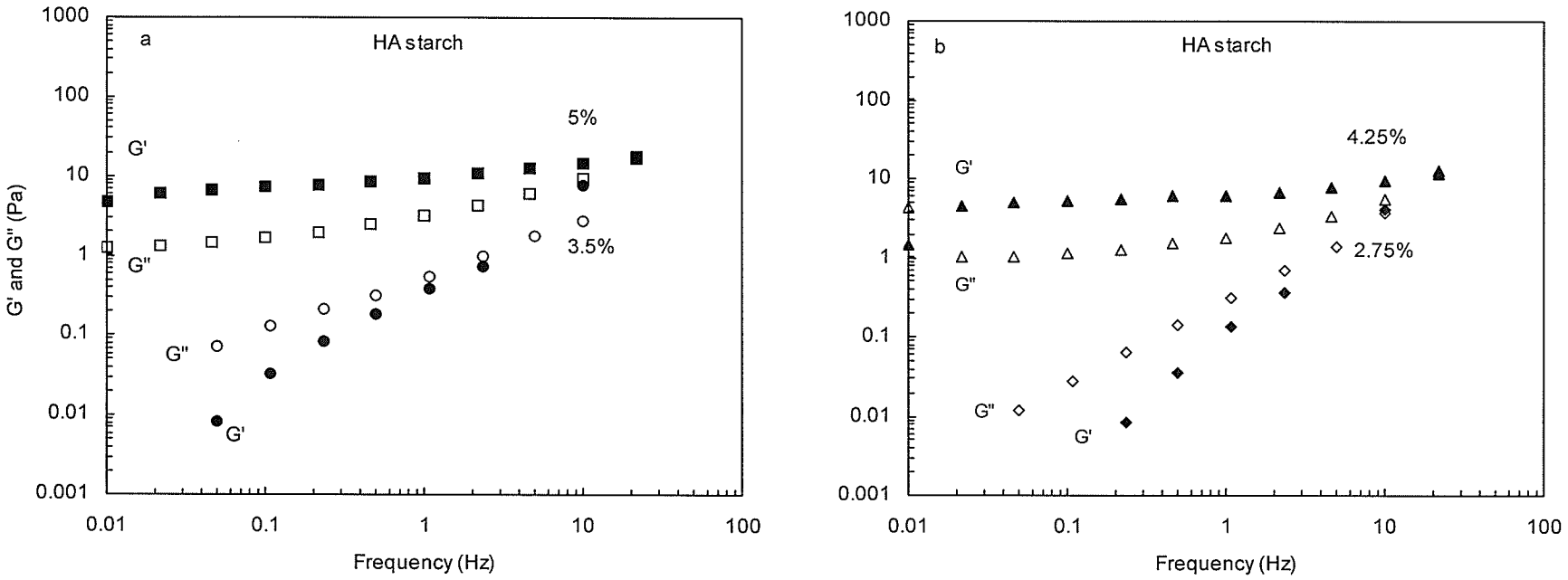

Figure 7.7. The mechanical spectra of G' and G" against frequency of freshly prepared HA starch at 5%, 4.25%, 3.5%, and 2.75% (w/w).

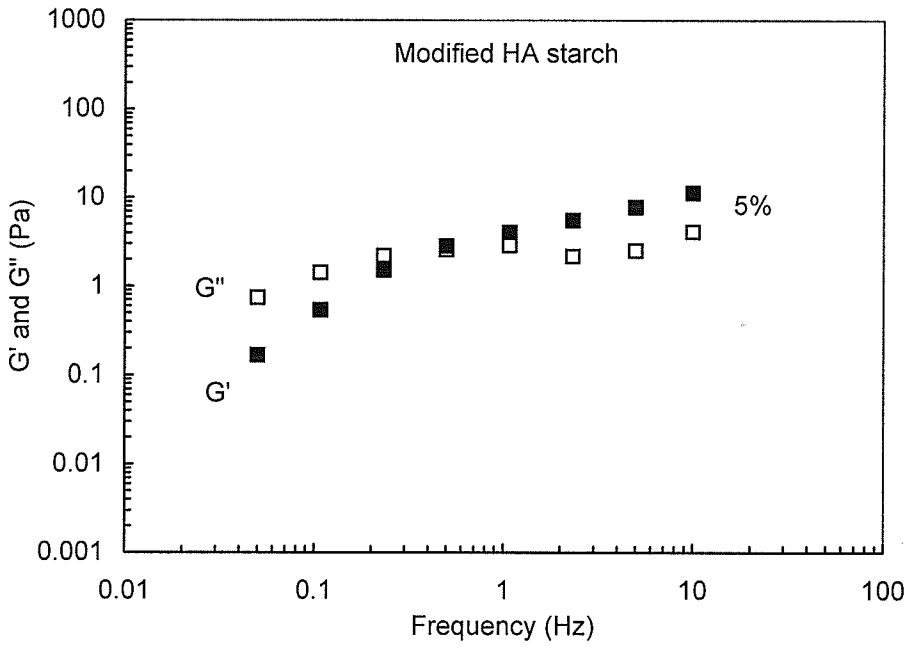

Figure 7.8. The mechanical spectrum of G' and G" against frequency of freshly prepared modified HA starch at 5% (w/w).

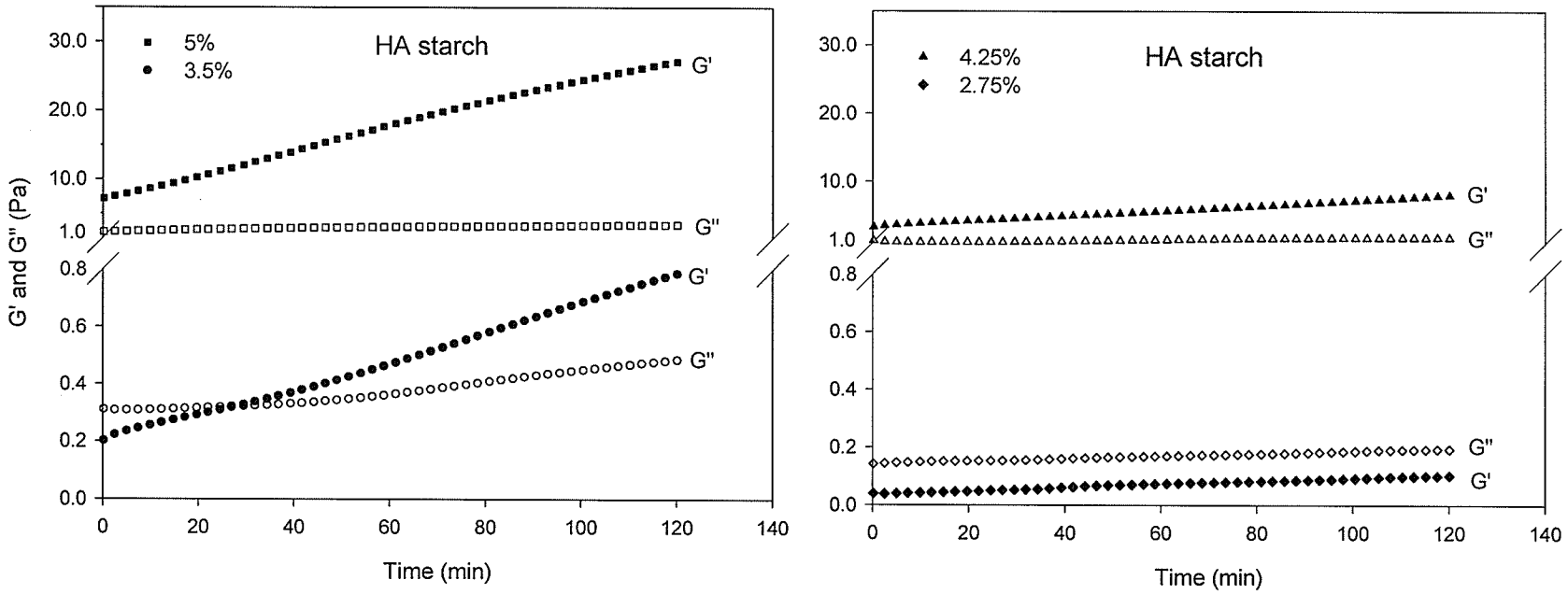

Figure 7.9. The development of G' and G" during storage for 2h at 20°C for native HA starch at 5%, 4.25%, 3.5%, and 2.75% (w/w).

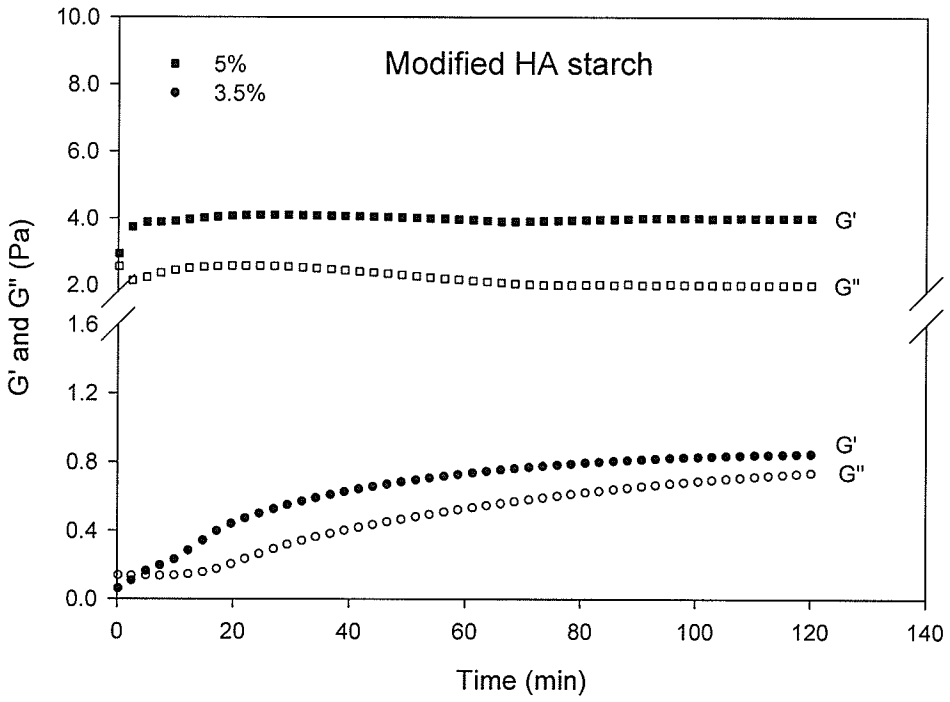

Figure 7.10. The development of G' and G" during storage for 2h at 20°C for modified HA starch at 5% and 3.5% (w/w).

gels' elasticity. At 3.5% starch concentration, the G' exceeded G" after 30 min of storage, whereas, at 2.75% concentration, G" was higher than G' throughout the entire storage time. The enzyme-modified starch (5% w/w) showed a substantially weaker gel network compared to the native starch at the same concentration (Fig. 7.10).

Figure 7.11a shows the mechanical spectra of HMW-BG solutions. At all BG concentrations (0.75% and 2.25% shown in Fig. 7.11), the G" was higher than G', although, at higher frequencies, the G' values approached those of G". No differences in G' and G" were observed upon storage for 2h at 20°C (Fig. 7.11b), indicating the lack of network formation under the conditions tested. As expected, the LMW-BG exhibited very weak viscoelastic properties with very low G' and G" values (results not shown).

The mechanical spectra of HA starch and HMW-BG blends at various ratios of these polysaccharides and a total polymer concentration of 5% (w/w) are shown in Fig. 7.12(a, b). With an increasing amount of HMW-BG in the blends, the moduli became more dependent on the frequencies. For the 85:15 (HA starch : HMW-BG) blend, the values of G' and G" were slightly higher than for the HA starch at 5% (w/w). For the 70:30 and 55:45 blends, at frequencies > 0.1 Hz, the G' values exceeded the G' of starch alone, but were more dependent on frequencies compared to the pure starch system at 5% concentration. As can be seen in Fig. 7.12b, the fractions of HMW-BG as part of the mixture with HA starch resulted in a significant increase in viscous properties (high tan δ values). Especially the 70:30 and 55:45 HA starch and HMW-BG blends exhibited higher tan δ values than starch alone. Interestingly, however, the tan δ values were very dependent on frequencies, and first, there was an increase in tan δ with increasing frequency, but above the frequency of 0.5 Hz, the tan δ started to decrease.

Figure 7.13a shows the development of G' for blends of HA starch and HMW-BG

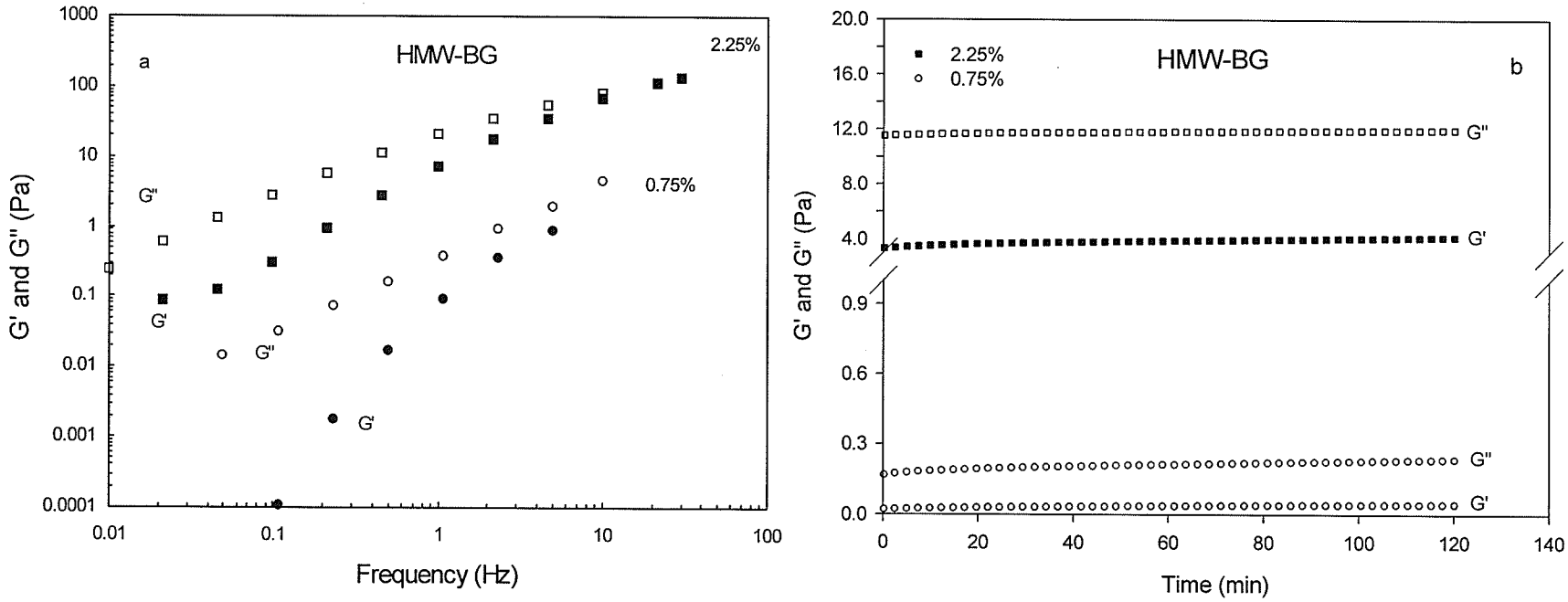

Figure 7.11. The mechanical spectra of G' and G" against frequency (a), and the development of G' and G" during storage for 2h at 20°C (b) for HMW-BG solutions at 2.25% and 0.75% (w/w).

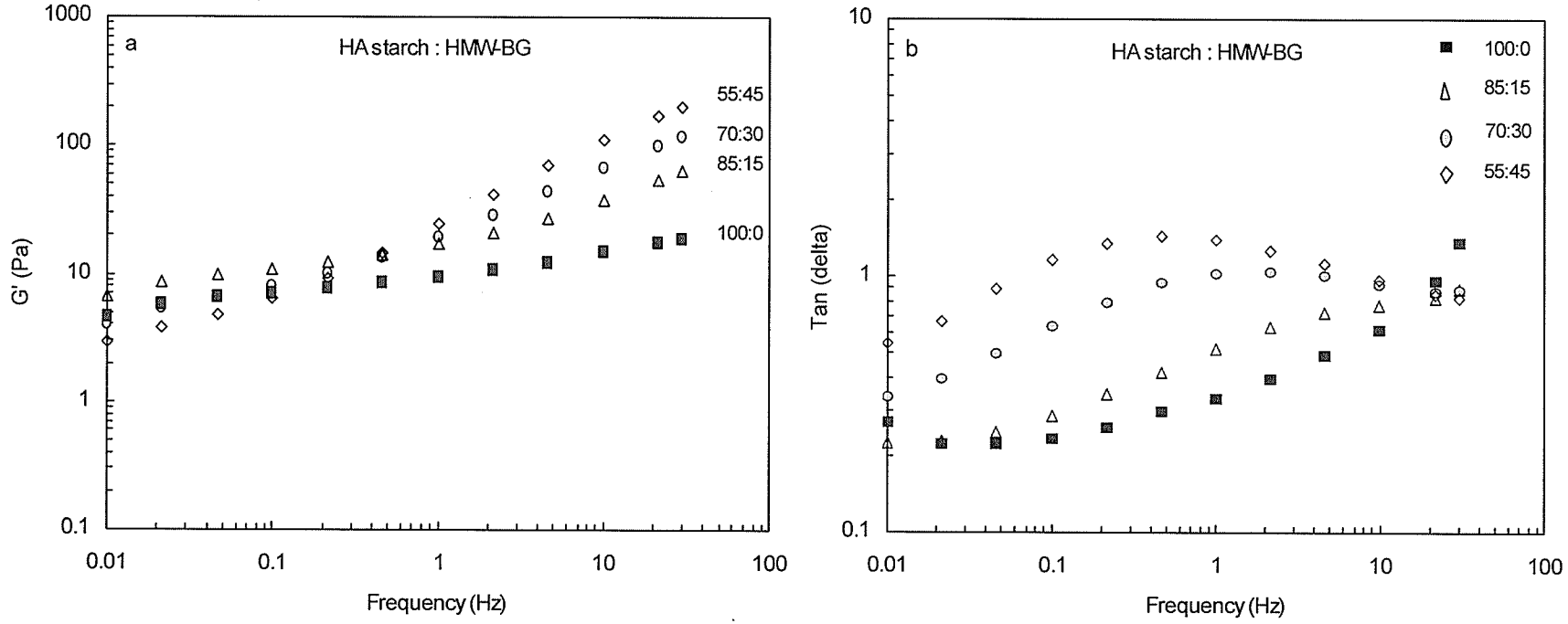

Figure 7.12. The mechanical spectra of G' (a), and tan δ (b) against frequency of freshly prepared HA starch and HMW-BG blends at a total concentration of 5%.

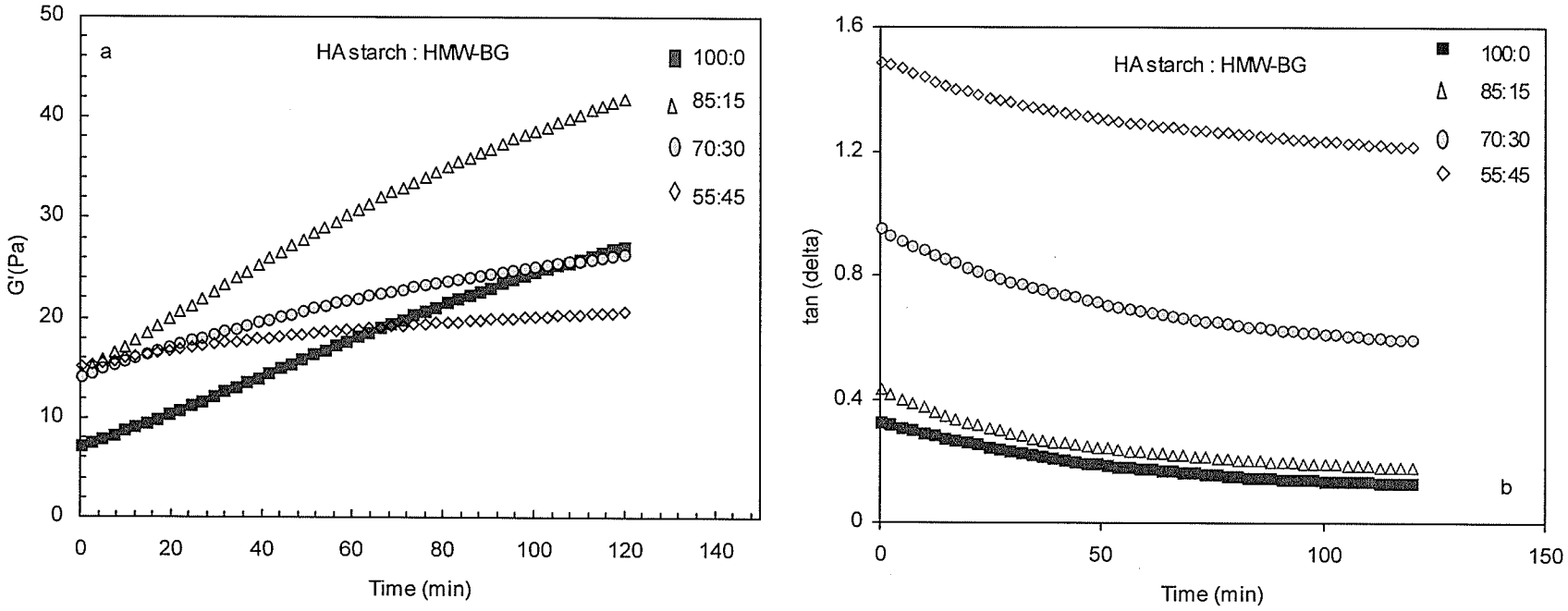

Figure 7.13. The development of G' (a), and tan δ (b) during storage for 2h at 20 °C for HA starch and HMW-BG blends at a total concentration of 5%.

during storage. Some structure formation occurred during the storage as indicated by increasing G' and decreasing tan δ values with time. All blends exhibited slightly higher G' and considerably higher G" compared to the HA starch alone at 5% (w/w). As a result, the tan δ values for the blends were much higher than those for the 5% starch solution alone (Table 7.2). However, the blend exhibited stronger viscoelastic properties (higher G' and lower tan δ values) than individual polymer solutions at corresponding concentrations (Table 7.2). These results indicate that some interactions between BG and HA starch polymers might be occurring in the dilute solutions. The BG-BG or starch-BG entanglements most likely replace some of the specific starch-starch interactions. These new chain entanglements, however, appear to be slightly weaker than the starch-starch junction zones, resulting in considerably higher G" and tan δ values of the blends compared to the pure HA starch system at 5% of the total polymer concentration. The addition of HMW-BG to HA starch resulted, therefore, in formation of a viscoelastic network with quite different rheological properties than these obtained with pure starch at the total polymer concentration of 5%. The HMW-BG-containing networks were characterized by greater viscosity compared to the more elastic and rigid pure starch networks. Kulicke et al. (1996) and Yoshimura et al. (1998) reported significant increases in viscosity but no improvements in elasticity for the blends of starch and galactomannan, and concluded that no specific interactions occurred between these polymers. On the other hand, Eidam et al. (1995) reported that the elastic properties of starch polymers are significantly improved by addition of ι-carrageenans.

The blends of HA starch with LMW-BG exhibited weaker elastic properties than the blends with HMW-BG (Fig. 7.14, Table 7.3). The replacement of starch with LMW-BG progressively weakened the networks with increasing proportions of LMW-

Table 7.2. Rheological properties of blends, and HA starch and HMW-BG solutions alone after 2 hours of storage.

Ratio HA starch : HMW-BG	**Blends**			**HA starch**			**HMW-BG**		
	Total polymer conc.(%)	G' (Pa)	tan δ	*Starch conc.(%)*	G' (Pa)	tan δ	*BG conc.(%)*	G' (Pa)	tan δ
100:0	-	-	-	*5*	27.1	0.13	-	-	-
85:15	*5 (4.25[a] + 0.75[b])*	41.8	0.18	*4.25*	8.0	0.22	*0.75*	0.04	5.39
70:30	*5 (3.5 + 1.5)*	26.3	0.59	*3.5*	0.8	0.62	*1.5*	0.47	5.08
55:45	*5 (2.75 +2.25)*	20.6	1.21	*2.75*	0.1	1.90	*2.25*	4.2	2.88

[a]Concentration of HA starch in blends.

[b]Concentration of BG in blends.

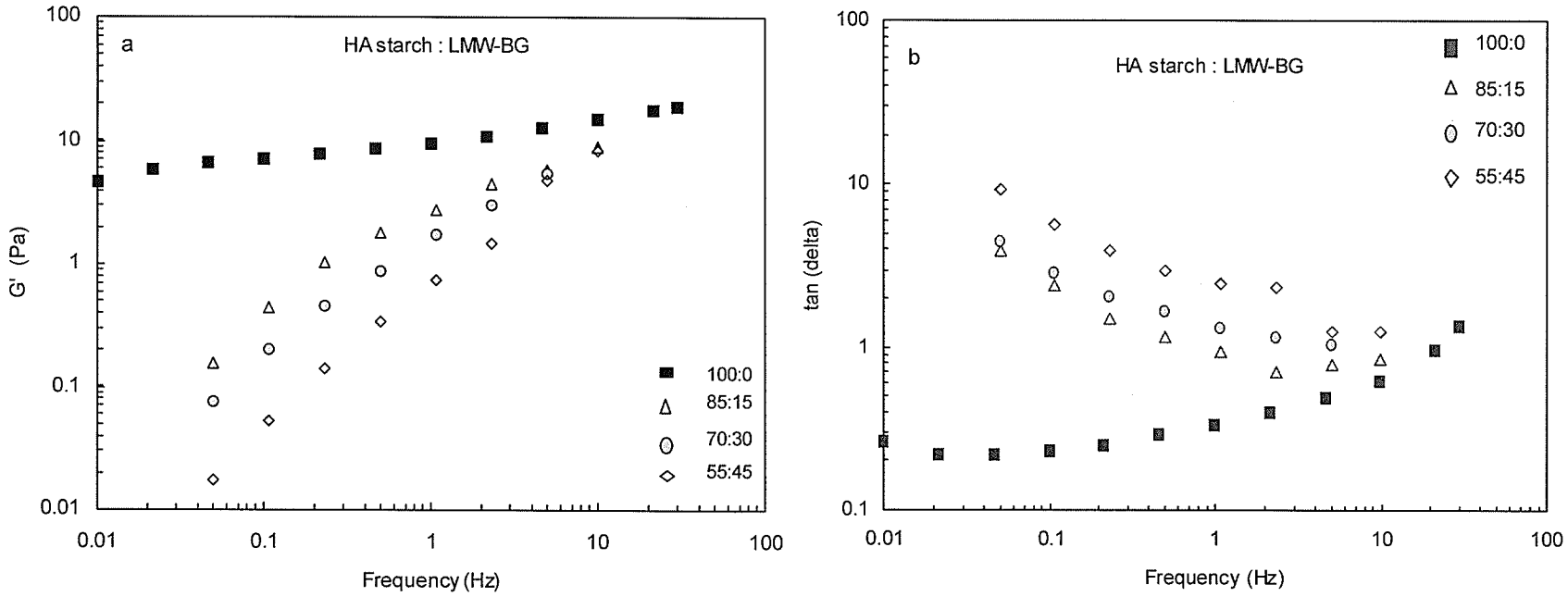

Figure 7.14. The mechanical spectra of G' (a) and tan δ (b) against frequency of freshly prepared HA starch and LMW-BG blends at a total concentration of 5%.

Table 7.3. Rheological properties of blends, and HA starch and LMW-BG solutions alone after 2 hours of storage.

Ratio HA starch : LMW-BG	**Blends**			**HA starch**			**LMW-BG**		
	Total polymer conc.(%)	G' (Pa)	tan δ	*Starch conc.(%)*	G' (Pa)	tan δ	*BG conc.(%)*	G' (Pa)	tan δ
100:0	-	-	-	*5*	27.1	0.13	-	-	-
85:15	*5 (4.25[a] + 0.75[b])*	4.5	0.52	*4.25*	8.0	0.22	*0.75*	nd[c]	nd
70:30	*5 (3.5 + 1.5)*	4.0	0.51	*3.5*	0.8	0.62	*1.5*	nd	nd
55:45	*5 (2.75 +2.25)*	1.3	0.94	*2.75*	0.1	1.90	*2.25*	0.01	7.42.

[a]Concentration of HA starch in blends.

[b]Concentration of BG in blends.

[c]Not determined because of too low values.

BG in the blends (Table 7.3). It appears that the network junction zones formed by HMW-BG were capable of at least partial replacement of the permanent starch-starch junction zones in the network, resulting in formation of weak mixed gels. On the other hand, the LMW-BG did not exhibit such properties. These results confirmed the importance and contribution of the molecular weight of BG to formation of strong mixed networks.

The partial replacement of modified HA starch with HMW-BG (85:15 blend) improved the viscoelastic properties of the mixed networks by increasing the G' and decreasing tan δ values (Fig. 7.15, Table 7.4). However, the blends containing higher proportions of BG exhibited properties of viscous solutions rather than gels. The blends of modified HA starch and LMW-BG exhibited very poor viscoelastic properties, and were not investigated further.

High concentration system (15% w/w)

Figure 7.16 shows the frequency sweeps of native HA starch samples in concentrations ranging from 13.5% to 15%. The networks exhibited properties of strong gels with very high G' and very low tan δ values. The modified HA starch was capable of forming even stronger gel networks with G' values being approximately twice as high as those of native HA starch at corresponding concentrations (Fig 7.17; Table 7.5 and 7.6). The partial replacement of either native or modified HA starch with HMW-BG (95:5 and 90:10 blends of starch and BG) only slightly decreased the G' compared to starch alone at 15% (w/w) concentration (Fig. 7.18 and 7.19). However, the tan δ values of the blends were higher and more dependent on frequency. Relatively small differences between the effects of partial replacement of starch with HMW-BG

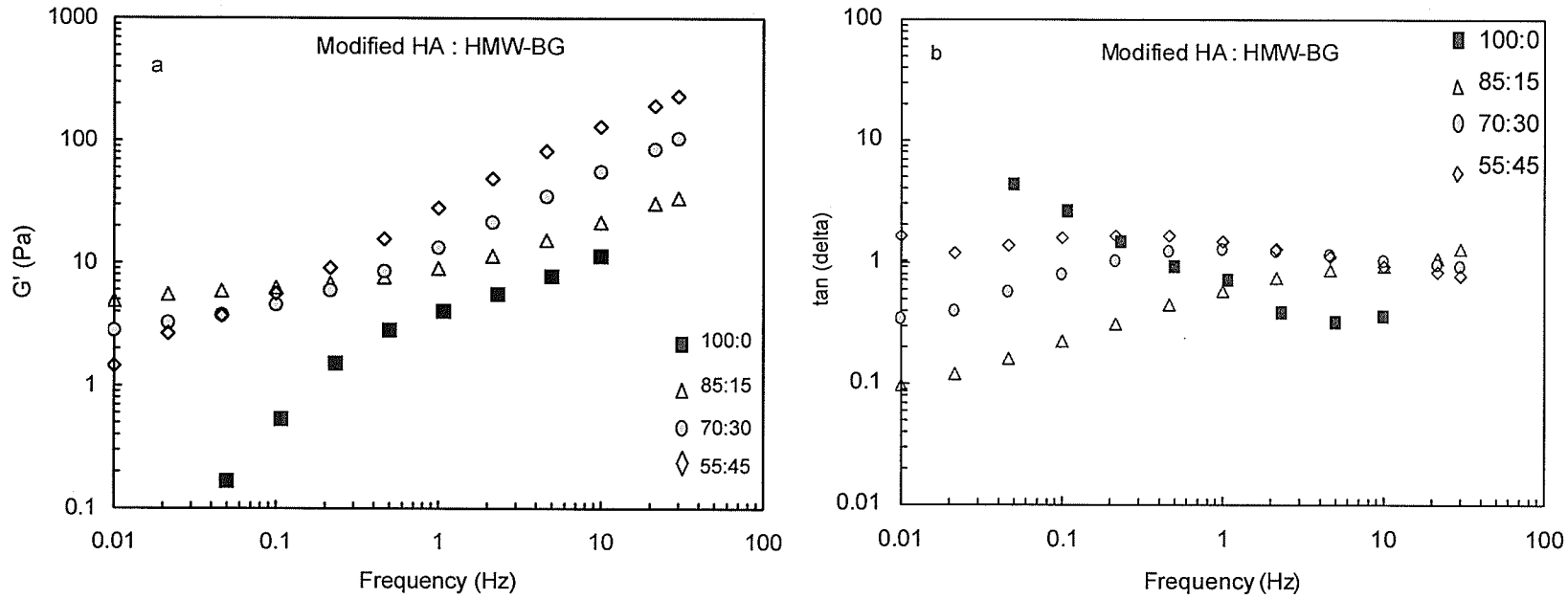

Figure 7.15. The mechanical spectra of G' (a) and tan δ (b) against frequency of freshly prepared modified HA starch and HMW-BG blends at a total concentration of 5%.

Table 7.4. Rheological properties of blends, and modified HA starch and HMW-BG solutions alone after 2 hours of storage.

Ratio Modified HA starch : HMW-BG	**Blends**			**Modified HA starch**			**HMW-BG**		
	Total polymer conc.(%)	G' (Pa)	tan δ	*Starch conc.(%)*	G' (Pa)	tan δ	*BG conc.(%)*	G' (Pa)	tan δ
100:0	-	-	-	*5*	4.0	0.50	-	-	-
85:15	*5 (4.25[a] + 0.75[b])*	12.7	0.35	*4.25*	4.0	0.25	*0.75*	0.04	5.39
70:30	*5 (3.5 + 1.5)*	14.1	1.07	*3.5*	0.85	0.87	*1.5*	0.47	5.08
55:45	*5 (2.75 +2.25)*	21.1	1.47	*2.75*	0.009	6.14	*2.25*	4.2	2.88

[a]Concentration of modified HA starch in blends.

[b]Concentration of BG in blends.

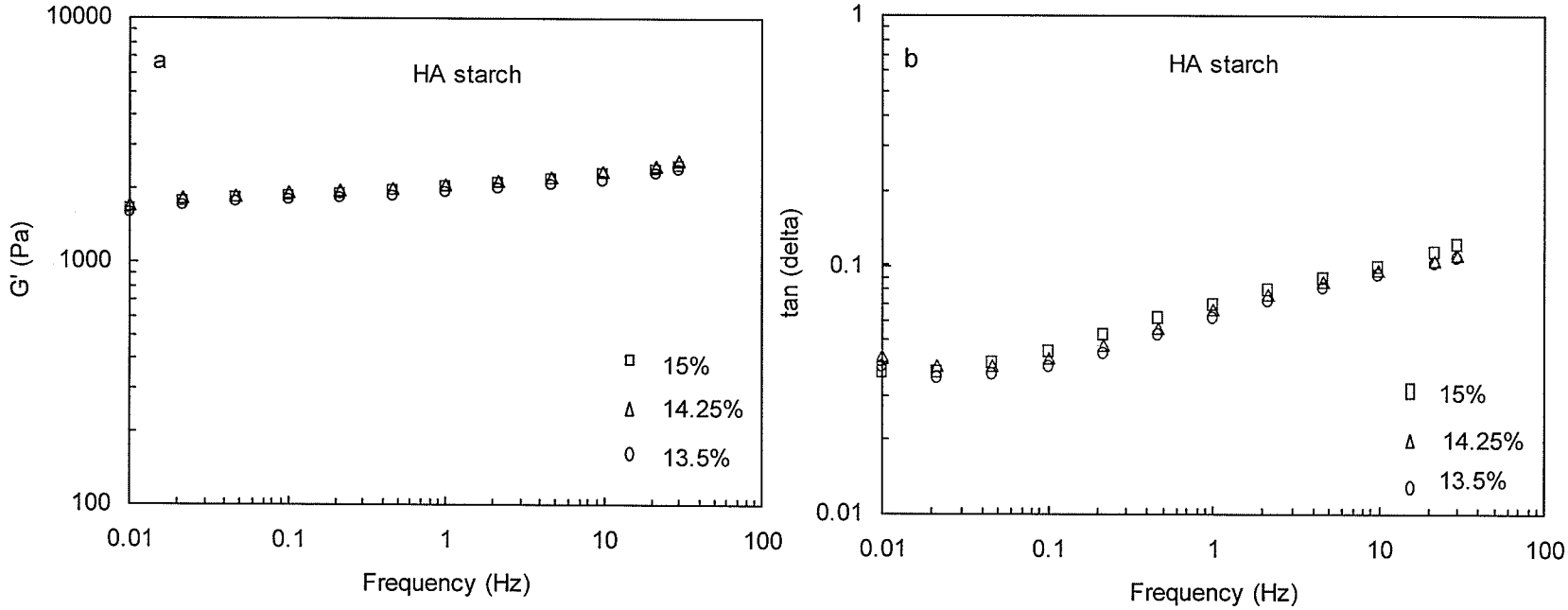

Figure 7.16. The mechanical spectra of G' (a) and tan δ (b) against frequency of freshly prepared HA starch at concentrations of 15%, 14.25%, and 13.5% (w/w).

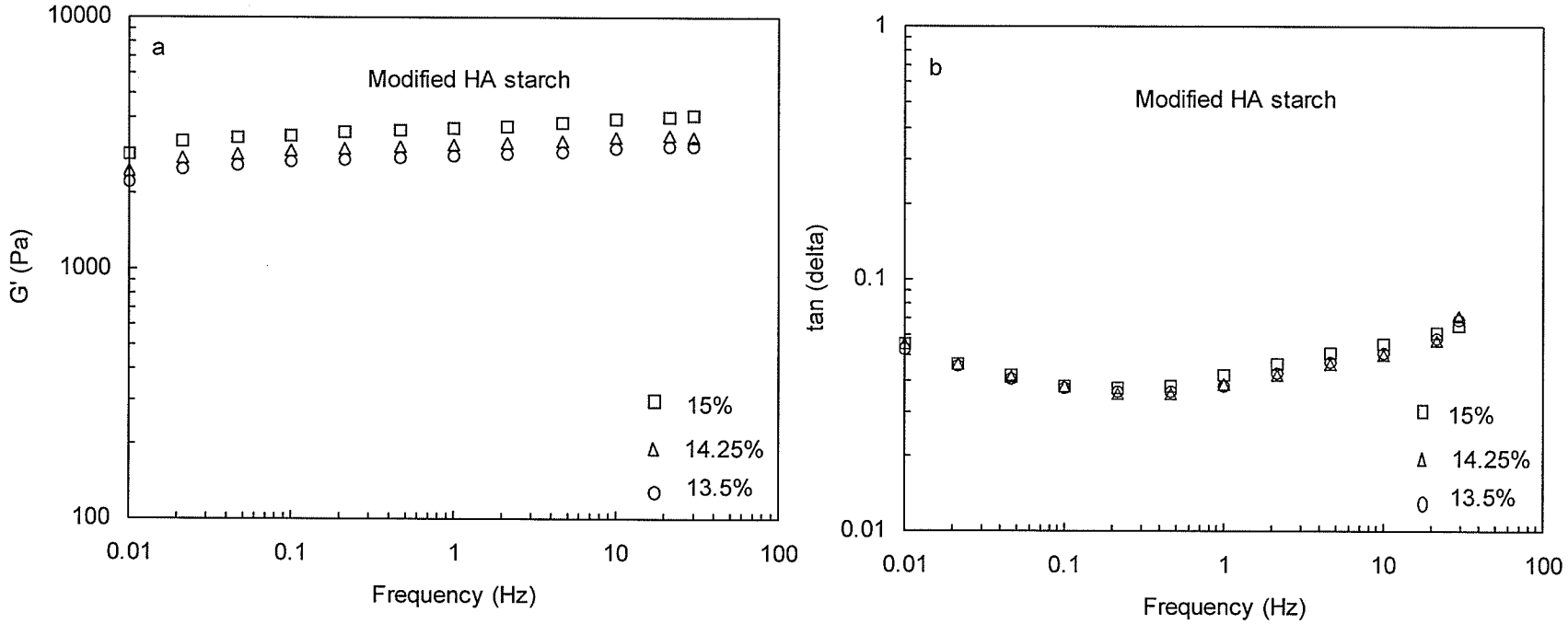

Figure 7.17. The mechanical spectra of G' (a) and tan δ (b) against frequency of freshly prepared modified HA starch at concentrations of 15%, 14.25%, and 13.5% (w/w).

Table 7.5. Rheological properties of blends, and HA starch gels after 2 hours of storage.

Ratio HA starch : HMW-BG	Blends			HA starch		
	Total polymer conc.(%)	G' (Pa)	tan δ	*Starch cocn.(%)*	G' (Pa)	tan δ
100:0	-	-	-	*15*	2351	0.05
95:5	*15 (14.25[a] + 0.75[b])*	2098	0.09	*14.25*	2367	0.05
90:10	*15 (13.5 + 1.5)*	1714	0.16	*13.5*	2208	0.05

Ratio HA starch : LMW-BG	Blends			HA starch		
	Total polymer conc.(%)	G' (Pa)	tan δ	*Starch cocn.(%)*	G' (Pa)	tan δ
100:0	-	-	-	*15*	2351	0.05
95:5	*15 (14.25 + 0.75)*	1849	0.06	*14.25*	2367	0.05
90:10	*15 (13.5 + 1.5)*	1359	0.07	*13.5*	2208	0.05

[a]Concentration of HA starch in blends.

[b]Concentration of BG in blends.

Table 7.6. Rheological properties of blends, and modified HA starch gels after 2 hours of storage.

Ratio Modified HA starch : HMW-BG	**Blends**			**Modified HA starch**		
	Total polymer conc.(%)	G' (Pa)	tan δ	*Starch cocn.(%)*	G' (Pa)	tan δ
100:0	-	-	-	*15*	5023	0.03
95:5	*15* *(14.25[a] + 0.75[b])*	4734	0.10	*14.25*	3956	0.05
90:10	*15* *(13.5 + 1.5)*	3581	0.15	*13.5*	3706	0.04

Ratio Modified HA starch : LMW-BG	**Blends**			**Modified HA starch**		
	Total polymer conc.(%)	G' (Pa)	tan δ	*Starch cocn.(%)*	G' (Pa)	tan δ
100:0	-	-	-	*15*	5023	0.03
95:5	*15* *(14.25 + 0.75)*	4490	0.10	*14.25*	3956	0.05
90:10	*15* *(13.5 + 1.5)*	3461	0.07	*13.5*	3706	0.04

[a]Concentration of modified HA starch in blends.

[b]Concentration of BG in blends

compared to the effects exerted by LMW-BG were observed in the high concentration (15% w/w) mixed systems (Fig. 7.18, 7.19, and 7.20, 7.21). Tables 7.5 and 7.6 show the G' and tan δ values of HA starch gels alone and HA starch and BG mixed gels. The G' values of blends of native HA starch with BG (both HMW and LMW) were lower than HA starch alone at 15% (w/w) or at starch concentrations corresponding to those in the blends (i.e., 14.25% and 13.5% in 95:5 and 90:10 blends, respectively). It appears, therefore, that the elastic properties of mixed networks at higher concentrations are governed mostly by the strong junction zones formed by the starch polymers. The decrease in the elastic properties of blends is caused by the decrease of starch concentration as well as by the presence of BG polymer chains, which appear to interfere with the molecular association among starch polymers (most likely by increasing the viscosity of the continuous phase thus decreasing the mobility of starch polymers and their chances to form effective junction zones). Interestingly, however, the G' of 95:5 blends of modified HA starch with BG (both HMW and LMW) were lower than G' of modified HA starch alone at 15% (w/w), but higher than G' of modified HA starch alone at concentrations of 14.25% (corresponding to the concentration starch in 95:5 blends). As pointed out before, the increased mobility of partially depolymerized starch polymers probably counterbalanced the increased viscosity of the continuous phase due to the presence of BG. These results, however, indicate that BG might have also contributed to the overall elastic properties of the networks either through formation of BG-BG and/or BG-starch entanglements.

Digestibility of starch/β-glucan blends

The α-amylase digestibility of blends of HA starch with HMW- and LMW-BG is

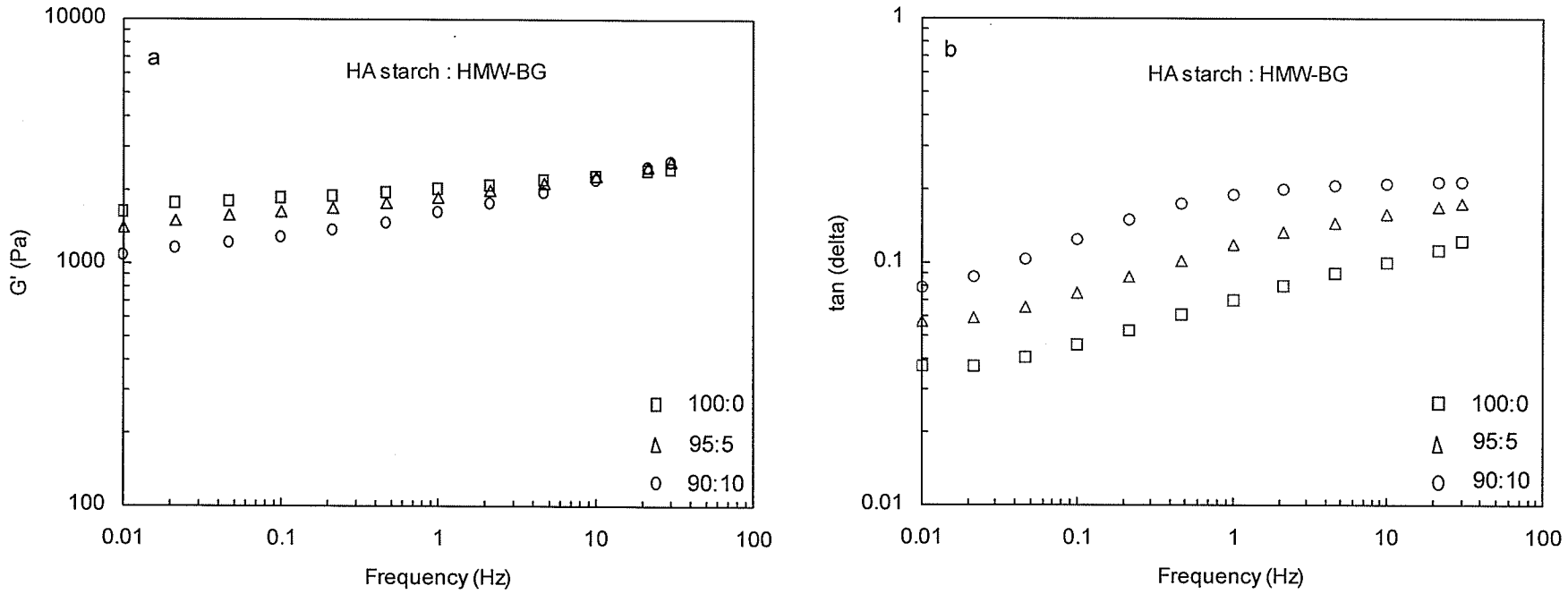

Figure 7.18. The mechanical spectra of G' (a) and tan δ (b) against frequency of freshly prepared HA starch and HMW-BG blends at a total concentration of 15% (w/w).

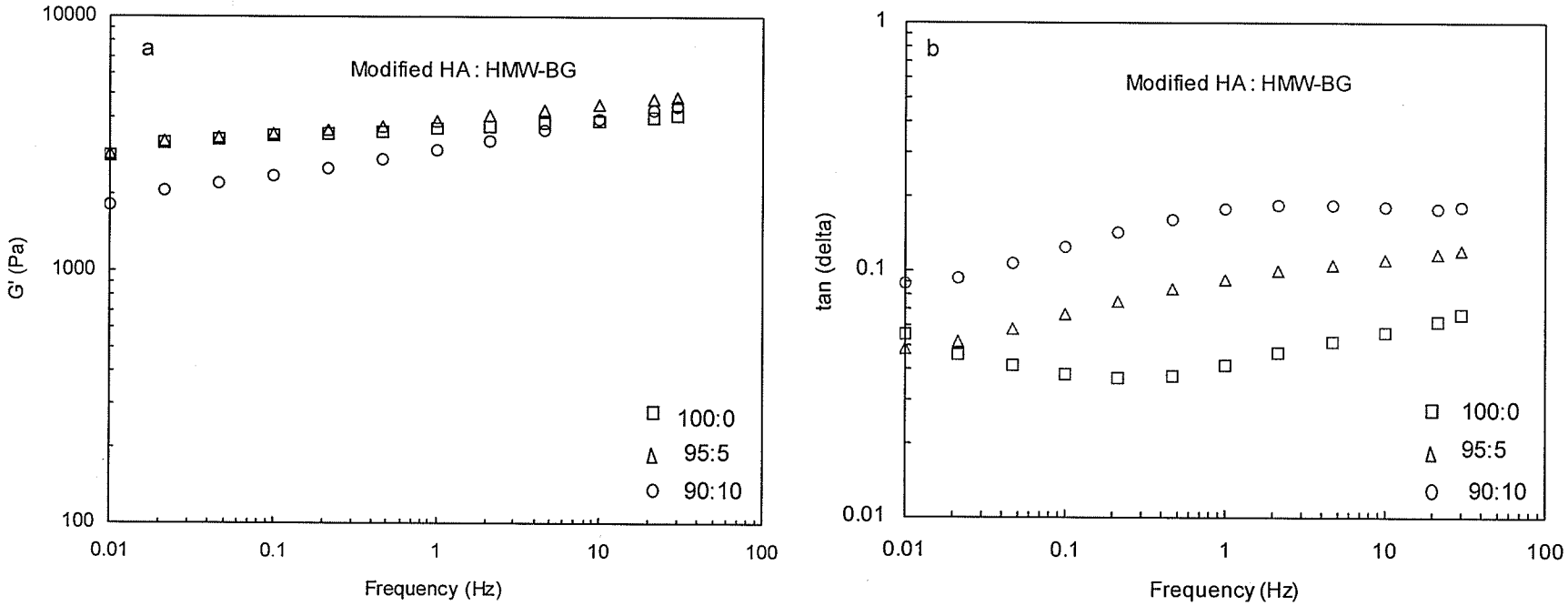

Figure 7.19. The mechanical spectra of G' (a) and tan δ (b) against frequency of freshly prepared modified HA starch and HMW-BG blends at a total concentration of 15% (w/w).

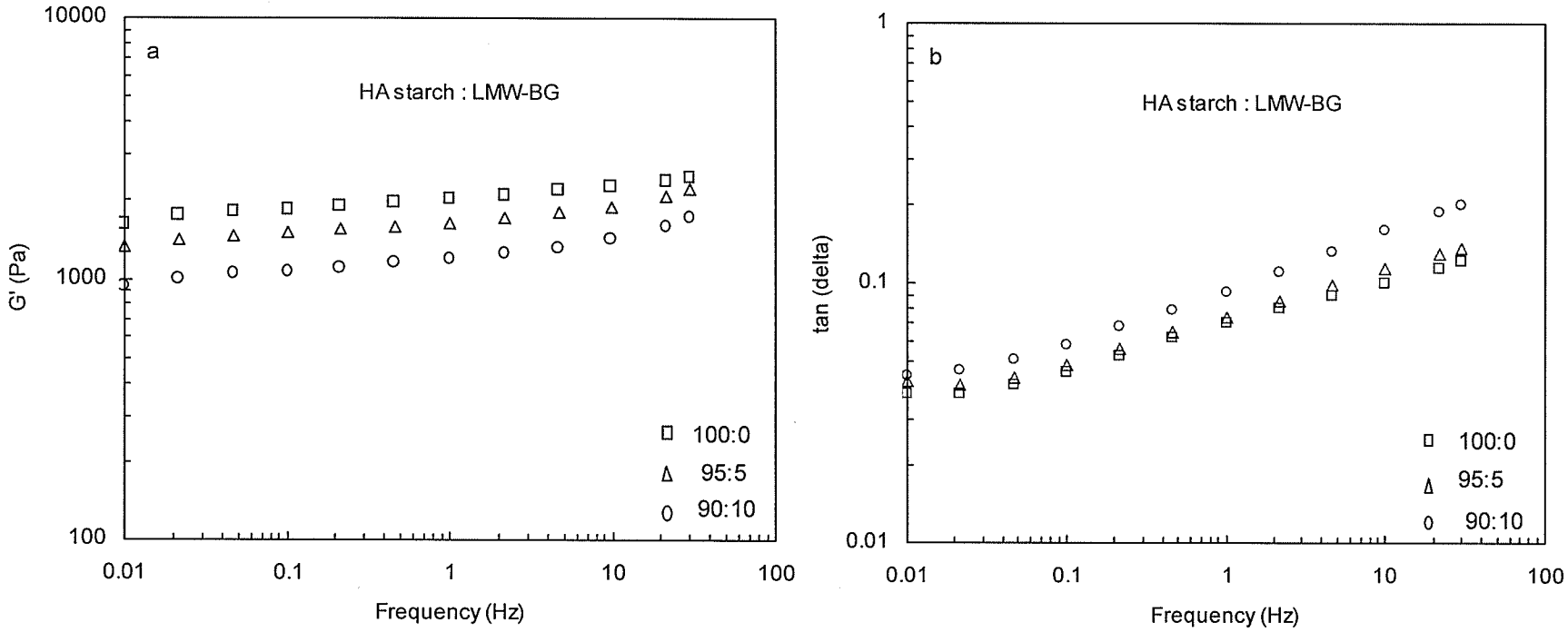

Figure 7.20. The mechanical spectra of G' (a) and tan δ (b) against frequency of freshly prepared HA starch and LMW-BG blends at a total concentration of 15% (w/w).

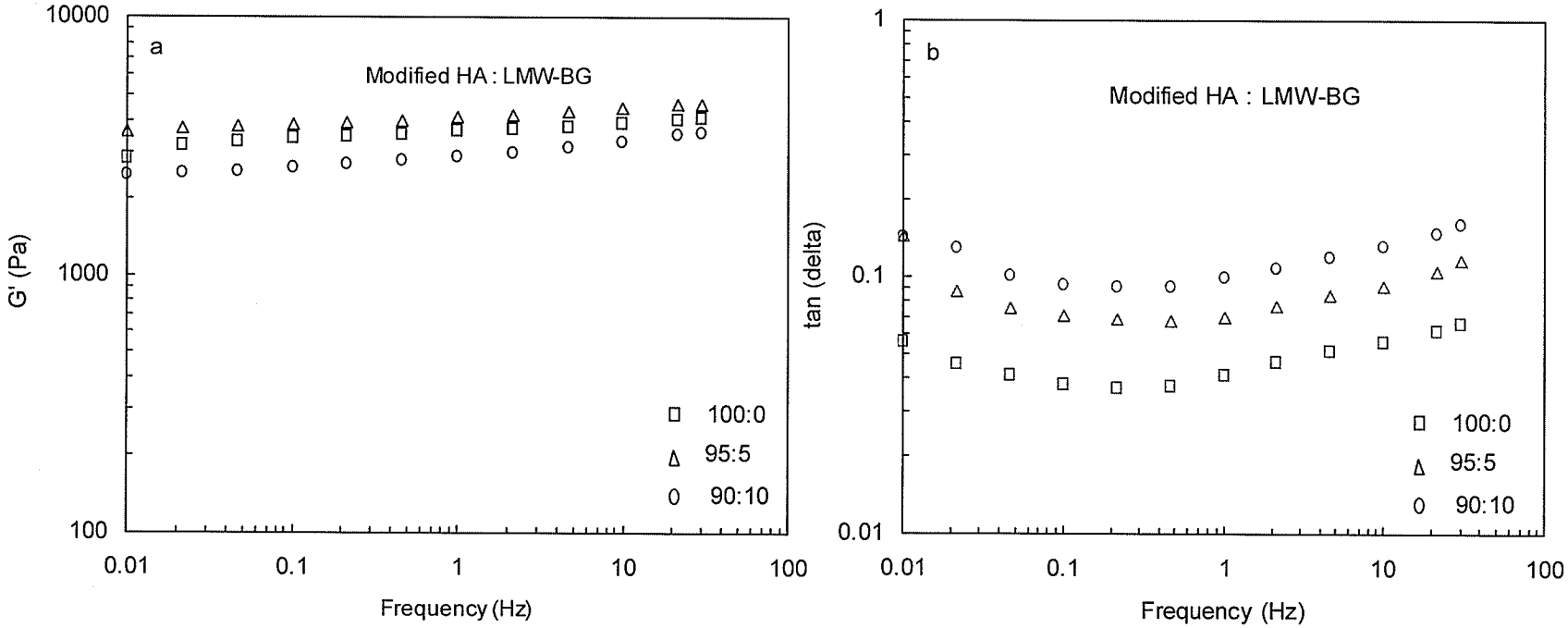

Figure 7.21. The mechanical spectra of G' (a) and tan δ (b) against frequency of freshly prepared modified HA starch and LMW-BG blends at a total concentration of 15% (w/w).

shown in Table 7.7. The amount of reducing sugar generated during α-amylolysis was assumed to indicate the degree of starch digestibility. For the low concentration blends (5% w/w total carbohydrate), the addition of HMW-BG decreased, whereas the addition of LMW-BG increased the digestibility of starch. The results seem to correspond well to the viscoelastic properties of the networks. For the 85:15 blend, the addition of HMW-BG significantly increased the elastic properties of the gel network compared to those of HA starch alone at an equivalent starch concentration (4.25% w/w) (Table 7.2). However, the addition of LMW-BG substantially weakened the strength of the gel (Table 7.3). Similar experiments were conducted for the high concentration blends (15% w/w total carbohydrate) of native HA starch and BG. (90:10 blends; results not shown). The mixed gels containing HMW- and LMW-BG were more digestible than HA starch gel alone (at 13.5% w/w). As indicated in Table 7.5, the addition of BG substantially reduced the G' and increased the tan δ values of the mixed gels compared to the pure HA starch gel. These results indicate that the starch digestibility is related to the elasticity and rigidity of starch gels. The reduction of digestibility of starch upon addition of BG is possible, but highly dependent on the overall viscoelastic properties of the networks. Autio et al. (2002) also reported that the extent of α-amylolysis of HYLON VII gels was inversely proportional to the gel rigidity when the storage modulus (G') of HYLON VII gel was over 15,000 Pa. However, no clear relationship was found for weaker gels.

Table 7.7. The amount of reducing sugars liberated during α-amylase (10 U/g) hydrolysis of HA starch and blends of HA starch with BG (mg glucose/g starch).

Hydrolysis time	HA starch[a]	HA starch + HMW-BG[b]	HA starch + LMW-BG[b]
5 min	39.3± 2.7	37.6± 0.3	50.0± 0.7
15 min	87.5± 1.5	80.1± 3.3	104.5± 2.1
30 min	137.3± 1.1	127.0± 1.0	162.6± 6.1

[a]Results for 4.25% w/w HA starch

[b]Blends of HA starch (4.25% w/w) and BG (0.75% w/w)

Conclusion

Rheological examinations of mixtures prepared from HA barley starch and BG have shown that the effects of BG addition are complex and governed by various factors including the ratios of the two polysaccharides, the molecular weight of BG as well as the chain mobility and diffusion of starch polymers. Generally, the HMW-BG increased the viscosity of the continuous phase and lowered the mobility of starch chains in solutions, thus reducing their potential to form stable junction zones. This resulted in an increase of the viscous character of the networks, but reduced their elasticity and rigidity. The addition of HMW-BG might, therefore, be beneficial for optimizing gel textures. It is known that unpleasant mouth feel or swallowing problems are experienced if thickeners possess too elastic and rigid properties (Kulicke et al. 1996). The rheological properties obtained by partial replacement of HA starch with BG were unique and different than those achievable by simply lowering the concentration of starch polymers. Under certain conditions, however, the addition of HMW-BG appeared to improve the elastic properties of the networks. This was especially seen in the low concentration systems (especially for the 85:15 blend of HA and HMW-BG at the total polymer concentration of 5 % w/w) as well as in the high concentration systems of modified HA starch. It appears that HMW-BG are also capable of forming effective network points, which, although weaker than those formed by starch polymers alone, can also contribute to the viscoelastic properties of the networks and have a potential to change starch digestibility.

CHAPTER 8

General Discussion

This thesis comprises a series of investigations of the molecular, physicochemical, and rheological properties of native and modified barley starches with various amylose content. In the first stage of this research program, the granular features and molecular characteristics of barley starches with variable amylose content were investigated. Next, barley starches were hydrolyzed with acid and α-amylase, and the physicochemical properties of the hydrolyzed starch residues were examined. The mechanisms of acid and α-amylase hydrolysis of starch granules were also compared. Finally, as an alternative to chemical and enzymatic modifications, starch and β-glucan polymers were mixed, and the rheological properties of the blends were investigated.

Granular and molecular characteristics of barley starches

The diameter of barley starch granules was found to range from 2 to 26μm. The relative proportion of small and large granules differed among the different types of starches. Normal starches contained the greatest amount of large granules (74.7%), whereas high amylose starches had the smallest amount of large granules (19.4%). The waxy and zero amylose starches contained 66.4 and 43.9% of large granules, respectively. Despite the different proportions of large to small granules, normal and waxy starches showed a bimodal size distribution of starch granules. In contrast to normal and waxy starch granules, high amylose starch granules showed a unimodal size distribution, with the highest proportion being 3μm granules and a very small amount of larger granules. The granule size distributions of barley starches were different not only

among the different types of barleys but also between samples within the same starch type. These results are in good agreement with previous reports, in which normal and waxy types of barley were reported to contain starch granules consisting of a mixture of large, lenticular granules (10-25μm) and small, irregularly shaped granules (<10μm) distributed in a bimodal fashion (MacGregor and Fincher 1993; Morrison et al. 1986). On the other hand, Song and Jane (2000) reported that high amylose barley starch contained granules of relatively small size (average diameter 4 μm).

In order to investigate the molecular characteristics of barley starch polymers, amylose and amylopectin polymers were separated by either high-performance size exclusion chromatography (HPSEC) or flow-field flow fractionation (flow-FFF) techniques. The separated starch polymers were detected by a multiangle light scattering (MALS) and a refractive index (RI) detector connected online to HPSEC or flow-FFF. Using the HPSEC-MALS-RI system, the weight average molecular weight (M_w) of amylose and amylopectin polymers in various types of barley starches was determined to range from 2.70×10^6 to 5.67×10^6 (g/mol), and 136×10^6 to 305×10^6 (g/mol), respectively. The radii of gyration (R_g) values of amylose and amylopectin ranged from 64 to 107nm, and from 164 to 266nm, respectively. In general, amylopectin in waxy and zero amylose starches had the highest average molecular weight, followed by amylopectin in normal and high amylose barley starches. A good correlation ($r^2=0.96$) was found between M_w and R_g values for amylopectin in various barley starches. This study revealed significant differences in the M_w and R_g, but rather small differences in the conformation of amylopectins from different types of barley starches.

Although the HPSEC-MALS-RI system appeared to be a useful tool for investigating the molecular features of barley starch polymers, this technique is not without some limitations. Amylopectin, due to its extremely high molecular weight,

elutes in the void volume of size exclusion columns, thereby failing to provide information about the distribution of molecular weight. Another limitation of the HPSEC technique found in this study relates to the fact that amylopectin polymers coelute with amylose polymers, leading to overestimation of the M_w and the amount of amylose polymers. Possible shear degradation of large macromolecules inside the HPSEC columns as well as interaction between the sample and column-packing materials have also been reported (Yokoyama et al. 1998). These limitations of the HPSEC technique motivated us to investigate the possibility of application of the flow-FFF technique for separation and analysis of the starch polymers. Flow-FFF fractionates macromolecules by their sizes (Giddings et al. 1992; Giddings 1995). The upper size limit for flow-FFF is about 50μm. Fractionation of macromolecules takes place in a liquid medium with less shearing. Therefore flow-FFF has been proven especially applicable to separation of very high molecular weight polymers (Giddings et al. 1992; Giddings 1995; Wittgren and Wahlund 1997). In our study, with application of two different cross-flows (0.35mL/min followed by 0.1mL/min) a complete separation of amylose and amylopectin from normal barley starch was obtained.

The observed M_w of amylose and amylopectin of normal barley starch by HPSEC-MALS-RI and flow-FFF-MALS-RI systems were 5.67×10^6g/mol and 226×10^6g/mol, and 2.3×10^6g/mol and 280×10^6g/mol, respectively. Considerable difference in the M_w of the amylose fraction in particular, as estimated by HPSEC and flow-FFF, may reflect substantial differences in the efficiency of separation of starch polymers achieved by these two techniques. The M_w of amylose, as determined by the SEC-MALS-RI system, may be affected by amylopectin polymers co-eluting in the same region. This study, therefore, revealed that flow-FFF technique is a more efficient method for separation of starch polymers. In addition, the increasing rates of the second cross-flow progressively

extended the elution of amylopectin over a broader range of volume, and afforded a better insight into the distribution of molecular weights of amylopectin.

The molar masses and dimensions of barley starch polymers found in this study generally fall in the range reported for starch polymers of other botanical origin (Bello-Perez et al. 1998; Fishman and Hoagland 1994; Hansellmann et al. 1995; Roger et al. 2001). However, some differences in the reported M_w values might be attributed to different solubilization methods used in various studies. Several approaches to achieving complete starch dissolution have been attempted (microwaving, autoclaving, and steam-jet cooking), ranging from very mild to more severe treatments (Aberle et al. 1994; Bello-Perez et al. 1998; Fishman and Hoagland 1994; You and Lim 2000). It has been emphasized that in order to properly determine the M_w of starch polymers, complete solubilization of amylose and amylopectin must be ensured. Incomplete disaggregation or degradation of starch polymers would lead to overestimation or underestimation, respectively, of the true M_w of starch polymers. Autoclaving (121°C, 20min) used in this study appeared to be a good solubilization method to obtain complete dissolution of starch polymers without their degradation.

After debranching of starch polymers with isoamylase, the molecular characteristics of linear starch chains were determined using the HPSEC-MALS-RI system. The M_w of debranched amylose fractions from normal and high amylose starches were significantly lower than those determined from the elution patterns of intact starches. These results suggest a certain degree of branching in amylose fractions of barley starches.

The debranched amylopectin molecules from the four types of barley starches exhibited similar profiles, showing trimodal distributions of long B, intermediate B, and short B or A chains. These results imply that the packing geometry of double helices in

the different types of barley starches may be similar. Indeed, the X-ray diffractograms confirmed that the different types of barley starches exhibited A-type crystalline pattern. The highest M_w for the long B chains was observed for high amylose starch, followed by normal, waxy and zero amylose starches. These results are not consistent with the results reported by Song and Jane (2000). These authors reported that normal starch contained the longest linear chains with a DP value of 82. These discrepancies may be due to the differences in the origin of starches as well as to differences in the methods employed for the detection of the debranched chains.

Molecular conformations of amylose and amylopectin polymers from normal barley starch were examined by plotting log R_g vs. log M_w, which were determined by the flow-FFF-MALS-RI system. For amylose, the calculated α value of 0.6 for the slope suggested a very different conformation than that obtained for amylopectin (α=0.3). The above results are in good agreement with theoretical predictions because amylopectin, due to its branching characteristics, assumes a more compact conformation in solution than amylose.

Modifications of barley starches

Modification of native starches is often desirable because the use of native starch in various food products and/or during processing might cause certain problems due to the structural changes occurring in starch upon storage or processing conditions (e.g. gelation, retrogradation, syneresis). Therefore, native starches have been modified by enzymic, chemical and/or physical methods in order to increase their ability to withstand heat, shear, or acid associated with various processing conditions, as well as to improve their functionalities in specific applications. In the second part of this study, the molecular structure and properties of barley starches as affected by α-amylolysis and

partial acid hydrolysis were investigated.

α-Amylase-treated barley starches. Isolated hulless barley starches with varying amylose contents were subjected to α-amylase hydrolysis for up to 48h at two enzyme levels (50U/g and 500U/g of starch). Waxy starch exhibited the greatest solubilization (36-56%), followed by normal (24-39% solubilization) and high amylose starch (13-20% solubilization). α-Amylase treatments significantly affected the appearance of waxy and normal starch granules, creating sponge-like structures with large pores. The interior of waxy and normal granules exhibited both radial and tangential hydrolysis patterns; however, the endoerosion was confined only to certain areas of the granules. The high amylose starch granules showed almost no evidence of enzyme erosion up to 48h of hydrolysis. The higher granule density, lower swelling capacity, and/or higher amount of amylose-lipid complexes could have slowed down or restricted the penetration of α-amylase into the high amylose starch granules.

The X-ray diffractometry studies indicated no significant differences in the degree of crystallinity between native and enzyme-modified normal (39% solubilized) or high amylose (20% solubilized) barley starches. These results may imply that both amorphous and crystalline regions inside the granules were hydrolyzed concurrently. On the other hand, the zero amylose waxy starches exhibited a slight increase in the crystallinity level, as confirmed by X-ray diffractometry, DSC, and CP/MAS ^{13}C NMR studies. It is not entirely clear, however, whether the ordering of amylopectin crystallites is due to preferential hydrolysis of weakly organized regions or re-structuring of starch polymers during hydrolysis. The X-ray, NMR, and DSC studies provided also some evidence for the presence of larger amounts of amylose-lipid complexes in the enzyme-treated normal and high amylose starches than in their native counterparts.

All three types of barley starch showed some decrease and change in the M_w values and distribution after α-amylolysis. Surprisingly, however, despite the extensive physical erosion and fragmentation of the zero amylose starch granules, the polymers remaining in the granules retained their macromolecular size. After 56% solubilization, only about a three-fold decrease in the M_w was observed in the zero amylose waxy sample. The M_w of amylopectin in normal starch (25-39% solubilization) decreased even less drastically and very little change in the M_w was observed for the high amylose (13-20% solubilization) sample after α-amylolysis.

The examination of the debranched amylose in normal and high amylose barley starches before and after α-amylolysis revealed very small differences in the M_w values and confirmed that amylose was not preferentially hydrolyzed during the enzymic treatments. Similar observations have been reported for wheat, corn, and sorghum starches (Colonna et al. 1988; Leach and Schoch 1961). The debranching of amylopectin in barley starches before and after α-amylolysis also confirmed that the primary structure of linear chains in amylopectin was not significantly affected by the partial hydrolysis.

The results of these studies clearly indicate that the susceptibility and extent of hydrolysis of barley starches are substantially affected by the presence and the amount of amylose in starch granules. It is possible that the presence of amylose affects the structure of starch granules and consequently the access and migration patterns of enzymes inside the granules. These studies showed also that starch polymers remaining in the granules after partial α-amylolysis possess relatively high M_w values as well as relatively intact molecular structure. These observed results can be accounted for by assuming that the mobility and diffusion of α-amylase inside the granule are restricted and that the hydrolysis reactions proceed only in localized regions of the granules.

Gelatinized barley starches (40% w/w) exhibited a tendency to form three-dimensional networks upon cooling and storage. The amylose content in barley starches positively correlated with the development of the elastic modulus (G') of the networks. The high amylose barley starch formed the strongest, whereas the zero amylose barley starch the weakest gels. The enzyme-treated zero amylose barley starches lost the ability to form gel networks and exhibited properties of viscous solutions rather than gels. The enzyme-treated normal and high amylose starches, on the other hand, formed stronger gels with higher G' values than their native counterparts. These results indicate that partial hydrolysis of starch polymers increases the mobility and diffusion of chains and, therefore, improves the rate and extent of crosslinking, leading to faster and stronger gel formation. Clark et al. (1989) postulated that the molecular size of amylose chains significantly affected the kinetics of gelation and the rheological properties of amylose gel. The long amylose chains appeared to retard chain mobility and to slow down the formation of effective crosslinks.

Acid/alcohol-hydrolyzed barley starches. Hulless barley starches (normal, high amylose, waxy and zero amylose) were partially modified with 0.36% or 2% HCl in different alcohol media (methanol, ethanol and 1-butanol). In general, the acid hydrolysis caused very little solubilization of barley starches, and very few changes in the appearance of granules as indicated by the SEM. However, despite the intact appearance of granules after partial acid hydrolysis, substantial depolymerization of starch polymers inside the granules occurred as indicated by the HPSEC chromatograms. The degree of depolymerization and the distribution of molecular weights in hydrolyzed starches were affected not only by the acid strength and hydrolysis time, but also by the type of alcohol in which the hydrolysis was carried out. In general, the average M_w of

starch polymers decreased with increasing hydrolysis time and acid concentration. The greatest depolymerization always occurred when the hydrolysis was conducted in 1-butanol.

When the hydrolysis of barley starches was carried out in methanol or ethanol, the hydrolyzed starch granules still contained a considerable amount of very high molecular weight species corresponding to the M_w (5×10^7-1×10^8) of intact amylopectin. The amount of this fraction decreased, however, with increasing hydrolysis time and/or acid concentration. When the hydrolysis was carried out in 1-butanol, the majority of the intact amylopectin fraction disappeared. The presence of 1-butanol facilitated greater and more effective hydrolysis. It has been suggested (Robyt et al. 1987; 1996) that higher alcohols might increase the actual concentration of acid inside the granules and/or assist in dissolution of amylose-amylopectin complexes and double helical structures of amylose, thus increasing the overall rate and extent of hydrolysis.

The results of these studies clearly indicate that the average M_w and the mode of distribution of various M_w species in partially hydrolyzed barley starches can be tailored to specific needs by adopting particular hydrolysis conditions. Contrary to previous reports (Li et al. 2001; Vasanthan and Bhatty 1996), our studies did not indicate that the high amylose barley starch was less affected by acid hydrolysis than normal or waxy starches. The susceptibility of starches to hydrolysis is often inferred from the amount of material solubilized and leached out of granules and not from the properties of the material remaining in the granules after hydrolysis. In our studies, the waxy samples have also produced a slightly higher amount of solubilized carbohydrates, but a close examination of starch polymers inside the granules after hydrolysis did not indicate significant differences between waxy and high amylose barley starches in their susceptibility to hydrolysis under the mild conditions used in these studies.

The HPSEC elution profiles of native and acid/alcohol-treated normal and high amylose starches after debranching with isoamylase indicated that substantial depolymerization of amylose polymers occurred during the acid/alcohol hydrolysis. The most severe breakdown of amylose chains occurred when the hydrolysis was conducted in 1-butanol/HCl. Relatively small differences in the amylose content between native and acid/alcohol-hydrolyzed starches indicate that despite substantial depolymerization, the amylose fraction remained in the granules after hydrolysis. Analyses of the length and distribution of debranched linear chains in native and acid/alcohol-treated starches, as conducted by the HPSEC and HPAEC-PAD, indicated only small changes upon hydrolysis. In general, for all samples, the amount of chains with DP 17-35 slightly decreased, whereas the amount of short chains with DP $\leq$ 15 slightly increased after hydrolysis

The X-ray studies of native and acid-treated barley starches indicated increases in crystallinity due to hydrolysis. The solid-state CP/MAS ^{13}C NMR analysis also indicated changes in the internal structures of granules. The narrowing of the C-1 peak and the more pronounced appearance of C-6 peak in the acid/alcohol-treated starches confirmed structural changes leading to higher crystalline orders due to substantial hydrolysis of the amorphous regions.

The results of these studies are in good agreement with the current understanding of the mechanism of acid action inside the granule (Biliaderis et al. 1981; Jacobs et al. 1998; Kainuma and French 1971; Li et al. 2001; Robin et al. 1974; Shi and Seib 1992; Wang and Wang 2001). It is thought that acid hydrolysis initially occurs in the amorphous regions, located between crystalline regions and consisting of (1) branching points, (2) B chains connecting two or more clusters (Hizukuri 1986), and (3) linear amylose chains (Robin et al. 1974). The densely packed crystalline regions consisting of

short B and A chains (French 1984; Robin et al. 1974), on the other hand, are not affected by the acid hydrolysis.

The partially hydrolyzed high amylose barley starch (2% HCl/MeOH, 10h) showed faster G' development and higher G' values upon cooling and storage than its native counterpart. These results indicate that the slightly hydrolyzed amylose chains are able to diffuse faster and to cross-link more easily than intact amylose chains. The native and partially hydrolyzed (2% HCl/MeOH, 10h) normal barley starches, however, showed no substantial differences in the gelation kinetics during cooling and storage. It can be proposed that higher amounts of amylopectin polymers in normal barley starch, compared to high amylose starch, counterbalance the improved chain diffusion and gelation potential of the partially hydrolyzed amylose chains. The extensively hydrolyzed normal and high amylose barley starches (2% HCl/MeOH, 96h), on the other hand, showed no further network formation during storage. It appears that the extensively depolymerized starch chains were incapable of forming stronger three-dimensional networks. The acid-treated zero amylose starches (2% HCl/MeOH, 10h and 96h) showed no significant network development during storage, implying their excellent storage stability.

Starch/β-glucan blends. Steady shear viscosity and small deformation oscillatory measurements were used to characterize the rheological properties of blends of high amylose barley starch (HA) and β-glucans (BG). The experiments were conducted at various ratios of the two polymers and at different concentrations of total carbohydrates (5% and 15% w/w). Both high and low molecular weight β-glucan preparations were used in this study (HMW-BG and LMW-BG, respectively). For the low concentration systems (total carbohydrate concentration: 5% w/w), the apparent viscosity of the blends

was greatly affected by the M_w of β-glucans. The addition of the HMW-BG generally increased, whereas the LMW-BG decreased the viscosity of blends compared to 5% HA starch alone.

Rheological examinations of blends of HA barley starch and BG have shown that the effects of BG addition are complex and governed by many factors, including the molecular weight of BG, the ratio of these two polymers and the overall concentration of carbohydrate polymers in the blends. In general, the addition of HMW-BG increased the viscosity of the continuous phase, lowered the mobility and diffusion of starch chains in solution, and thus reduced their ability to form stable junction zones. This resulted in an increase of the viscous character of the networks (higher G") but reduced their elasticity (lower G'). In the low concentration system (5% w/w), some interactions between the BG chains or between starch-BG replaced the specific starch-starch interactions. However, these new chain entanglements were probably slightly weaker than the starch-starch junction zones, resulting in considerably higher G" of the blends compared to the pure HA starch system (at 5% w/w concentration).

In the high concentration blends (total carbohydrate concentration: 15% w/w), the G' values of the blends of HA starch with BG were lower than HA starch alone at 15% (w/w) or at starch concentrations corresponding to those in the blends. The decrease in the elastic properties of blends was caused by the decrease of starch concentration as well as by the presence of BG chains which appear to interfere with the molecular association among starch polymers. Interestingly, however, the rheological properties obtained by partial replacement of HA starch with BG were unique and different from those achievable by simply lowering the concentration of starch polymers. Our studies indicated also that reduction of starch digestibility upon addition of BG is possible but highly dependent on the overall viscoelastic properties of the networks.

Summary and Conclusions

1. Normal and waxy starches contained a significantly higher amount of large granules than high amylose starches.
2. Amylopectins in waxy barley starches exhibited significantly higher M_w and R_g than those in normal and high amylose starches.
3. All amylose polymers in barley starches exhibited a certain degree of branching.
4. The highest degree of polymerization of long B chains was observed in high amylose starch, followed by normal, waxy, and zero amylose starches.
5. Despite the different amylose content, all barley starches exhibited A-type crystalline pattern.
6. High amylose starch exhibited a higher gelatinization temperature than that of normal and waxy starches, which appears to be related to the higher M_w of the long B chains.
7. High amylose starch samples showed the strongest gel network formation, followed by normal and waxy starches. The strength of starch gelation appeared to be proportional to the amylose content and the M_w of linear amylopectin chains.
8. Flow-FFF technique provided more efficient separation of starch polymers, and more accurate M_w of amylose polymers than size exclusion chromatography. Using various cross-flow rates, it was possible to obtain better insight into the molecular weight distribution of amylopectin polymers.
9. α-Amylolysis substantially solubilized starch granules. The degree of solubilization was inversely proportional to the amylose content. Our studies showed that α-amylase was able to hydrolyze concurrently the amorphous and crystalline regions. Amylose and amylopectin polymers remaining in the granules after α-amylolysis

retained their macromolecular size.

10. The acid hydrolysis caused very little solubilization of barley starch granules. However, substantial depolymerization of amylose and amylopectin polymers occurred. The various types of barely starches did not show significant differences in the degree of susceptibility to acid hydrolysis.
11. Rheological examinations of starch and BG blends showed that the effects of BG addition on the starch network are very complex. They were affected by the molecular weight of BG, the ratio of these two polymers and the overall concentration of carbohydrate polymers in the blends.
12. The rheological properties obtained by partial replacement of starch with BG polymers were unique and different from those achievable by simply lowering the concentration of starch polymers.
13. Our studies also indicated that the reduction of starch digestibility upon addition of BG is possible but highly dependent on the overall viscoelastic properties of the networks.

Future studies

Further studies required for a more comprehensive understanding of physical and functional characteristics as well as enzymatic and chemical hydrolysis kinetics of starch granules include:

1. Detailed investigations of the fine structures and characteristics of starch granule surface, such as the protrusion of amylose and/or amylopectin chains, micropores, and internal channels, which would provide valuable information about how enzymes and chemicals penetrate inside the starch granules, bind and/or hydrolyze the starch polymers.

2. Investigation of the three-dimensional organization and the location of amylose and amylopectin polymers inside the starch granule, which would provide additional information on the physical and functional properties of starch, such as swelling, melting and rheological properties.
3. Elucidation of the detailed structural characteristics of crystallites, such as the size and the degree of perfection, which would be useful to elucidate the melting properties of starch granules.
4. A study of other modifications of barley starch using different enzymes and/or chemicals, as well as blending with other hydrocolloids would also be desirable to develop additional modified barley starches having unique functional and rheological properties.

CHAPTER 9

LITERATURE CITED

Aberle, T., Burchard, W., Vorwerg, W., and Radosta, S. 1994. Conformational contribution of amylose and amylopectin to the structural properties of starches from various sources. Starch/Starke. 46:329-335.

Alloncle, M., Lefebvre, J., Llamas, G., and Doublier, J.L. 1989. A rheological characterization of cereal starch-galactomannan mixtures. Cereal Chem. 66:90-93.

Alloncle, M., and Doublier, J.L. 1991. Viscoelastic properties of maize starch/hydrocolloid paste and gels. Food Hydrocol. 5:455-467.

Atichokudomchai, N., Shobsngob, S., Chinachoti, P., and Varavinit, S. 2001. A study of some physicochemical properties of high-crystalline tapioca starch. Starch/Starke. 53:577-581.

Autio, K., Vesterinen, E., and Stolt, M. 2002. Rheological properties of mixed starch-κ-carrageenan gels in relation to enzymatic digestibility. Food Hydrocol. 16:169-174.

Badenhuizen, N.P. 1965. Occurrence and Development of Starch in Plants. Pages 65-103 in: *Starch: Chemistry and Technology. Vol. 1.* Whistler, R.L., and Paschall, E.F. ed. Academic Press, New York, NY.

Baldwin, P.M., Adler, J., Davies, M.C., and Melia, C.D. 1998. High resolution imaging of starch granule surfaces by atomic force microscopy. J. Cereal Sci. 27:255-265.

Ball, S., Han, P.G., James, M., Myers, A., Keeling, P., Mouille, G., Buleon, A., Colonna, P., and Preiss, J. 1996. From glycogen to amylopectin: a model for the biogenesis of the plant starch granule. Cell. 86:349-352.

Banks, W., Geddes, R., Greenwood, C.T., and Jones, I.G. 1972. Physico-chemical studies on starches. Part 3. The molecular size and shape of amylopectins. Starch/Starke. 24:245-251.

Banks, W., Greenwood, C.T., and Muir, D.D. 1973. Studies on the biosynthesis of starch granules: Properties of starch components of normal barley, and with starch of high amylose content during growth. Starch/Starke. 25:153-158.

Banks, W., and Greenwood, C.T. 1975. *Starch and Its Components*, Edinburgh University Press. p.67

Bello-Perez, L.A., ParedesLopez, O., Roger, P., and Colonna, P. 1996. Amylopectin: properties and fine structure. Food Chem. 56:171-176.

Bello-Perez, L.A., Roger, P., Baud, B., and Colonna, P. 1998. Macromolecular features of starches determined by aqueous high-performance size exclusion chromatography. J. Cereal Sci. 27:267-278.

Benincasa, M.A. 2000. Synthetic Polymers - Water soluble. Pages 407-432 in: *Field-Flow Fractionation Handbook.* Schimpf, M., Caldwell, K., and Giddings, J.C., ed. John Wiley & Sons, Inc. New York. NY.

Bertoft, E, and Kulp, S.-E. 1986. A gel filtration study on the action of barley α-amylase isoenzyme on granular starch. J. Inst. Brew. 92:69-72.

Bertoft, E., and Avall, A.K. 1992. Structural analysis on the amylopectin of waxy-barley large starch granules. J. Inst. Brew. 98:433-437.

Bertoft, E., Manelius, R., Myllarinen, P., and Schulman, A.H. 2000. Characterization of dextrins solubilised by α-amylase from barley starch granules. Starch/Starke. 52:160-163.

Bhatty, R.S. 1993. Nonmalting uses of barley. Pages 355-418 in: *Barley Chemistry and Technology*. MacGregor, A.W. and Bhatty R.S. ed. American Association of Cereal Chemists. St. Paul. Minnesota.

Bhatty, R.S., and Rossnagel, B.G. 1998. Comparison of pearled and unpearled Canadian and Japanese barleys. Cereal Chem. 75:15-21.

Bhatty, R.S. 1999. β-glucan and flour yield of hull-less barley. Cereal Chem. 76:314-315.

Biliaderis, C.G., Grant, D.R., and Vose, J.R. 1981. Structure characterization of legume

starches. II. Studies on acid-treated starches. Cereal Chem. 58:502-507.

Biliaderis, C.G. 1989. The structure and interactions of starch with food constituents. Can. J. Physiol. Pharmacol. 69:60-78.

Biliaderis, C.G. 1990. Thermal analysis of food carbohydrates. Pages 168-220 in: *Thermal Analysis of Food.* Harwalkar, V.R., and Ma, C.-Y., ed. Elsevier Applied Sciences, London.

Biliaderis, C.G. and Zawistowski, J. 1990. Viscoelastic behaviour of aging starch gels: effects of concentration, temperature, and starch hydrolyzates on network properties. Cereal Chem. 67:240-246.

Biliaderis, C.G. 1992. Structures and phase transitions of starch in food systems. Food Technol. June. 98-110.

Biliaderis, C.G. 1998. Structures and phase transitions of starch polymers. Pages 57-168 in: *Polysaccharide Association Structures in Food. Walter*. R.H. eds. Marcel Dekker, Inc., New York.

Bohm, N., and Kulicke, W.M. 1999. Rheological studies of barley (1→3)(1→4)-β-glucan in concentrated solution: investigation of the viscoelastic flow behaviour in the sol-state. Carbohydr. Res. 315:293-301.

Buleon, A., Colonna, P., Planchot, V., and Ball, S. 1998. Starch granules: Structure and Biosynthesis. Int. J. Biol. Macromol. 23: 85-112.

Burt, D.J. and Russell, P.L. 1983. Gelatinization of low water content wheat starch mixtures. A combined study by differential scanning calorimetry and light microscopy. Starch/Starke. 35:354.

Carlson, T.L.G., Larsson, K., Miezis, Y., and Poovarodom, S. 1979. Phase equilibria in the aqueous system of wheat gluten lipids and in the aqueous salt system of wheat lipids. Cereal Chem. 56:417-419.

Carriere, C.J., and Inglett, G.E. 1998. Solution viscoelastic properties of OATRIM-10 and cooked oat bran. Cereal Chem. 75:354-359.

Carriere, C.J., and Inglett, G.E. 1999. Nonlinear viscoelastic solution properties of oat-based beta-glucan/amylodextrin blends. Carbohydr. Polym. 40:9-16.

Cheetham, N.W.H., and Tao, L. 1998. Variation in crystalline type with amylose content in maize starch granules: an X-ray powder diffraction study. Carbohydr. Polym. 36:277-284.

Christianson, D.D., Hodge, J.E., Osborne, D., and Detroy, R.E. 1981. Gelatinization of wheat starch as modified by xanthan gum, guar gum and cellulose gum. Cereal Chem. 58:513-517.

Clark, A., H., Gidley, M., J., Richardson, R., K., and Ross-Murphy, S., B. 1989. Rheological studies of aqueous amylose gel: The effect of chain length and concentration on gel modulus. Macromolecules. 22:346-351.

Clark, A.H., and Ross-Murphy, S.B. 1987. Structural and mechanical properties of biopolymer gels. Adv. Polym. Sci. 83:57-192.

Colonna, P., Buleon, A., and Lemarie, F. 1988. Action of *Bacillus subtilis* α-amylase on native wheat starch. Biotechnol. Bioeng. 31:895-904.

Cone , J.W., and Wolters, M.G.E. 1990. Some properties and degradability of isolated starch granules. Starch/Starke. 42:298-301.

Cooke, D., and Gidley, M.J. 1992. Loss of crystalline and molecular order during starch gelatinization: origin of the enthalpic transition. Carbohydr. Res. 227:103-112.

Cui, W., and Wood, P.J. 2000. Relationships between structural features, molecular weight and rheological properties of cereal β-D-glucan. Pages 159-168 in: *Hydrocolloids.* Nishinari, K. ed. Elsevier Science Publishers, Amsterdam.

Czuchajowska, Z., Klamczynski, A., Paszczynska, B., and Baik, B.-K. 1998. Structure and functionality of barley starches. Cereal Chem. 75:747-754.

Donald, A.M., Waigh, T.A., Jenkins, P.J., Gidley, M.J., Debet, M., and Smith, A. 1997. Internal structure of starch granules revealed by scattering studies. Pages 172-179 in: *Starch: Structure and Functionality.* Frazier, P.J., Donald, A.M., and Richmond, P. ed. The Royal Society of Chemistry, Cambridge, UK.

Donovan, J.W. 1979. Phase transitions of starch-water system. Biopolymers. 18:263-275.

Doublier, J.L. 1981. Rheological studies on starch-flow behaviour of wheat starch pastes. Starch/Starke. 33:415-420.

Doublier, J.L., Llamas, G., and Le Meur, M. 1987. A rheological investigation of cereal starch pastes and gels. Effect of pasting procedures. Carbohydr. Polym. 7:251-275.

Dubois, M., Gilles, K.A., Hamilton, J.K., Rebers, P.A., and Smith, F. 1956. Colorimeteric method for determination of sugars and related substances. Anal. Chem. 28:350-356.

Eidam, D., and Kulicke, W.M. 1995. Formation of maize starch gels selectively regulated by the addition of hydrocolloids. Starch/Starke. 47:378-384.

Eliasson, A.-C. 1983. Differential scanning calorimetry studies on wheat starch-gluten mixtures. II. Effect of gluten and sodium stearoyl lactylate on starch crystallization during aging of wheat starch gels. J. Cereal Sci. 1:207-213.

Eliasson, A.-C. 1986. Retrogradation of starch as measured by differential scanning calorimetry. Pages 93-115 in: *New Approaches to Research on Cereal Carbohydrates.* Hill, R.D. and Munck, L. ed. Elsevier Science Publishers, Amsterdam.

Eliasson, A.-C. and Gudmundsson, M. 1996. Starch: physicochemical and functional aspects. Pages 431-503 in: *Carbohydrates in Foods*. Eliasson, A.-C., ed. Marcel Dekker, Inc., New York. NY.

Ellis, H.S., and Ring, S.G. 1985. A study of some factors influencing amylose gelation. Carbohydr. Polym. 5:201-212.

Evans, A. and Thompson, D.B. 2004. Resistance to α-amylase digestion in four native high-amylose maize starches. Cereal Chem. 81:31-37.

Evans, I.D. and Haisman, D.R. 1982. The effects of solutes on the gelatinization temperature of potato starch. Starch/Starke. 34:224-231.

Fannon, J.E., Hauber, R.J., and Bemiller, J.N. 1992. Surface pores of starch granules.

Cereal Chem. 69:284-288.

Fannon, J.E., Shull, J.M., and BeMiller, J.N. 1993. Interior channels of starch granules. Cereal Chem. 70:611-613.

Fishman, M.L., and Hoagland, P.D. 1994. Characterization of starches dissolved in water by microwave heating in a high- pressure vessel. Carbohydr. Polym. 23:175-183.

Fishman M.L., Rodriguez L., and Chau H.K. 1996. Molar masses and sizes of starches by high-performance size-exclusion chromatography with on-line multi-angle laser light scattering detection. J. Agric. Food Chem. 44: 3182-3186.

Fox, J.D., and Robyt, J.F. 1992. Modification of starch granules by hydrolysis with hydrochloric acid in various alcohols, and the formation of new kinds of limit dextrins. Carbohydr. Res. 227:163-170.

Freitas, R.A., Gorin, P.A.J., Neves, J., and Sierakowski, M.R. 2003. A rheological description of mixtures of a galactoxyloglucan with high amylose and waxy corn starches. Carbohydr. Polym. 51:25-32.

French, D. 1972. Fine structure of starch and its relationship to the organization of the granules. J. Jpn. Soc. Starch Sci. 19:8-33.

French, D. 1984. Organization of starch granules. Page 183 in: *Starch II: Chemistry and Technology*. Whistler, R.L. and Paschall, E.F. ed., Academic Press, New York, NY.

Gallant, D.J., Bouchet, B., and Baldwin, P.M. 1997. Microscopy of starch: evidence of a new level of granule organization. Carbohydr. Polym. 32:177-191.

Gerard, C., Colonna, P., Buleon, A., and Planchot, V. 2001. Amylolysis of maize mutant starches. J. Sci. Food Agric. 81:1281-1287.

Gerard, C., Colonna, P., Buleon, A., and Planchot, V. 2002. Order in maize mutant starches revealed by mild acid hydrolysis. Carbohydr. Polym. 48:131-141.

Gernat, C., Radosta, S., Anger, H., Damaschun, G., and Schierbaum, F. 1990. Supermolecular structure of legume starches revealed by X-ray scattering. Starch/Starke. 42:175-187.

Giddings, J. C. and Caldwell, K. D. 1989. Field-flow fractionation. Pages 867-938 in : *Physical Methods of Chemistry. 2nd ed.* Rossiter, B. W. and Hamilton J. F., ed. A Wiley-Interscience Pub. New York. NY.

Giddings, J. C., Benincasa, M. A., Liu, M.-K., and Li, P. 1992. Separation of water soluble synthetic and biological macromolecules by flow field-flow fractionation. J. Liq. Chromatogr. 15:1729-1747.

Giddings, J. C. 1995. Measuring colloidal and macromolecular properties by FFF. Anal. Chem. 592A-598A.

Gidley, M.J., and Bociek, S.M. 1985. Molecular organization in starches: A ^{13}C CP/MAS NMR study. J. Am. Chem. Soc. 107:7040-7044.

Gidley, M.J., and Bociek, S.M. 1988. ^{13}C CP/MAS NMR studies of amylose inclusion complexes, cyclodextrins, and the amorphous phase of starch granules: Relationships between glycosidic linkage conformation and solid-state ^{13}C chemical shifts. J. Am. Chem. Soc. 110:3820-3829.

Gidley, M.J. 1989. Molecular mechanisms underlying amylose aggregation and gelation. Macromolecules. 22:351-358.

Gidley, M.J., and Bulpin, P.V. 1989. Aggregation of amylose in aqueous systems: the effect of chain length on phase behaviour and aggregation kinetics. Macromolecules. 22:341-346.

Gidley, M.J. 1992. Nuclear magnetic resonance analysis of cereal carbohydrates. Pages 163-192 in: *Developments in Carbohydrate Chemistry.* R.J. Alexander, and H.F. Zobel ed. The American Association of Cereal Chemists, St. Paul, Minnesota.

Hanselmann, R., Ehrat, M, and Widmer, H.M. 1995. Sedimentation field flow fractionation combined with multi angle laser light scattering applied for characterization of starch polymers. Starch/Starke. 46: 345-349.

Hanselmann R., Burchard W., Ehrat M., and Widmer H.M. 1996. Structural properties of fractionated starch polymers and their dependence on the dissolution process. Macromolecules. 29:3277-3282.

Hatcher, D.W., Lagasse, S., Dexter, J.E., Rossnagel, B., and Izydorczyk, M. 2004. Quality characteristics of yellow alkaline noodles enriched with hull-less barley flour. Cereal Chem. in press.

Hill, R.D. and MacGregor, A.W. 1988. Cereal α-amylases in grain research and technology. Pages 217-261 in: *Advances in Cereal Science and Technology, Vol. IX.* Y. Pomeranz, ed. The American Association of Cereal Chemists, St. Paul, Minnesota.

Hizukuri, S., Takeda, Y., Yasuda, M., and Suzuki, A. 1981. Multi branched nature of amylose and the action of debranching enzymes. Carbohydr. Res. 94:205-213.

Hizukuri, S., Kaneko, T., and Takeda, Y. 1983. Measurement of the chain length of amylopectin and its relevance to the origin of crystalline polymorphism of starch granules. Biochim. Biophys. Acta. 760:188-194.

Hizukuri, S. 1996. Starch: analytical aspects. Pages 347-430 in: *Carbohydrates in Foods.* Eliasson, A.-C., ed. Marcel Dekker, Inc. New York. NY.

Hizukuri, S. 1986. Polymodal distribution of the chain lengths of amylopectins, and its significances. Carbohydr. Res. 147:342-347.

Hoover, R. 2000. Acid-treated starches. Food Rev. Int. 16:369-392.

Hoseney, R.C. 1994. *Principles of Cereal Science and Technology*, 2nd ed. American Association of Cereal Chemists, St. Paul, Minnesota. p. 29-62.

Huber, K.C., and BeMiller, J.N. 1997. Visualization of channels and cavities of corn and sorghum starch granules. Cereal Chem. 74:537-541.

Imberty, A., Chanzy, H., Perez, S., Buleon, A., and Tran, V. 1988a. The double helical nature of the crystalline part of A-starch. J. Mol. Biol. 201:365-378.

Imberty, A., and Perez, S. 1988b. A revisit to the three-dimensional structure of B-type starch. Biopolymers. 27:1205-1221.

Inglett, G.E. 1997. Development of a dietary fiber gel for calorie-reduced foods. Cereal Foods World. 42: 382-385.

Izydorczyk, M.S., Macri, L.J., and MacGregor, A.W. 1998. Structure and physicochemical properties of barley non-starch polysaccharides-I. Water-extractable β-glucans and arabinoxylans. Carbohydr. Polym. 35:249-258.

Izydorczyk, M.S., Storsley, J., Labossiere, D., MacGregor, A.W., and Rossnagel, B.G. 2000. Variation in total and soluble β-glucan content in hulless barley: Effects of thermal, physical, and enzymic treatments. J. Agric. Food Chem. 48:982-989.

Jacobs, H., Eerlingen, R.C., Rouseu, N., Colonna, P., and Delcour, J.A. 1998. Acid hydrolysis of native and annealed wheat, potato and pea starches - DSC melting features and chain length distributions of linterised starches. Carbohydr. Res. 308:359-371.

Jackson, D.S. 1991. Solubility behaviour of granular corn starches in dimethyl sulfoxide (DMSO) as measured by high-performance size exclusion chromatography. Starch/Starke. 43:422-427.

Jadhav, S.L., Lutz, S.E., Ghorpade, V.M., and Salunkhe, D.K. 1998. Barley: chemistry and value-added processing. Crit. Rev. Food Sci. Nutri. 38:123-171.

Jane, J., and Chen, J.F. 1992. Effect of amylose molecular size and amylopectin branch chain length on paste properties of starch. Cereal Chem. 69:60-65.

Jane, J., Kasemsuwan, T., Leas, S., Zobel, H.F., and Robyt, J.F. 1994. Anthology of starch granule morphology by scanning electron microscopy. Starch/Starke. 46:121-129.

Jane, J., Wong, K.-S., and McPherson A.E. 1997. Branch-structure difference in starches of A- and B-type X-ray patterns revealed by their Naegeli dextrins. Carbohydr. Res. 300:219-227.

Jane, J., Chen, Y.Y., Lee, L.F., McPherson, A.E., Wong, K.S., Radosavljevic, M. and Kasemsuwan, T. 1999. Effects of amylopectin branch chain length and amylose content on the gelatinization and pasting properties of starch. Cereal Chem. 76:629-637.

Jiang, Y., Miller, M. E., Li, P., and Hansen, M. E. 2000. Characterization of water-soluble polymers by flow FFF-MALS. Am. Lab. (Feb.). 98-108.

Kainuma, K. and French, D. 1971. Nageli amylodextrin and its relationship to starch

granule structure. I. Preparation and properties of amylodextrins from various starch types. Biopolymers. 10:1673-1680.

Kalichevsky, M.T., Orford, P.D., and Ring, S.G. 1990. The retrogradation and gelation of amylopectin from various botanical sources. Carbohydr. Res. 198:49-55.

Kerr, R.W. 1952. Degradation of corn starch in the granule state by acid. Starch/Starke. 4:39-41.

Klamczynski, A.P., and Czuchajowska, Z. 1999. Quality of flours from waxy and non-waxy barley for production of baked products. Cereal Chem. 76:530-535.

Klavons, J.A., Dintizis, F.R., and Millard, M.M. 1997. Hydrodynamic chromatography of waxy maize starch. Cereal Chem. 74:832-836.

Kulicke, W.M., Eidam, D., Kath, F., Kix, M., and Kull, A.H. 1996. Hydrocolloids and rheology: Regulation of visco-elastic characteristics of waxy rice starch in mixtures with galactomannans. Starch/Starke. 48:105-114.

Kruger, J.E. and Marchylo, B.A. 1985. A comparison of the catalysis of starch components by isoenzymes from two major groups of germinated wheat α-amylases. Cereal Chem. 62:11-18.

Kulp, K., and Ponte, J.G. 1981. Staling of white pan bread: fundamental causes. Crit. Rev. Food Sci. Nutri. 15:1-48.

Launay, B., and Lisch, J.M. 1983. Twin-screw extrusion cooking of starches: flow behaviour of starch pastes, expansion and mechanical properties of extrudates. J. Food Eng. 2:259-280.

Lauro, M., Ring, S.G., Bullt, V.J., and Poutanen, K. 1997. Gelation of waxy barley starch hydrolysates. J. Cereal Sci. 26:347-354.

Lauro, M., Forssell, P.M., Suortti, M.T., Hulleman, S.H.D., and Poutanen, K.S. 1999. α-Amylolysis of large barley starch granules. Cereal Chem. 76:925-930.

Lazaridou, A., Biliaderis, C.G., and Izydorczyk, M.S. 2003. Molecular size effects on rheological properties of oat β-glucans in solution and gels. Food Hydrocol. 17:693-712.

Leach, H.W., McCowen, L.D., and Schoch, T.J. 1959. Structure of the starch granule. I. Swelling and solubility patterns of various starches. Cereal Chem. 36:534-544.

Leach, H.W., and Schoch, T.J. 1961. Structure of the starch granule. II. Action of various amylases on granular starches. Cereal Chem. 38:34-46.

Li, J.H., Vasanthan, T., Rossnagel, B., and Hoover, R. 2001. Starch from hull-less barley: II. Thermal, rheological and acid hydrolysis characteristics. Food Chem. 74:407-415.

Li, J.H., Vasanthan, T., Hoover, R., and Rossnagel, B.G. 2003. Starch from hull-less barley: Ultrastructure and distribution of granule-bound proteins. Cereal Chem. 80:524-532.

Li, J.H., Vasanthan, T., Hoover, R., and Rossnagel, B.G. 2004. Starch from hull-less barley: V. In-vitro susceptibility of waxy, normal, and high-amylose starches towards hydrolysis by alpha-amylases and amyloglucosidase. Food Chem. 84:621-632.

Lineback, D.R. 1984. The starch granule: Organization and properties. Baker's Dig. 58:16-21.

Lineback, D.R. 1986. Current concepts of starch structure and its impact on properties. J. Jpn. Soc. Starch Sci. 33:80-88.

Lintner, C.J. 1886. Studies uber diastase. J. Prakt. Chem. 34:378-386.

Liu, H. and Lelievre, J. 1993. A model of starch gelatinization linking differential scanning calorimetry and birefringence measurements. Carbohydr. Polym. 20:1-5.

Liu, H., Eskin, N.A.M., and Cui, S.W. 2003. Interaction of wheat and rice starches with yellow mustard mucilage. Food Hydrocol. 17:863-869.

Lou, J., Myers, M.N., and Giddings, J.C. 1994. Separation of polysaccharides by thermal field-flow fractionation. J. Liq. Chromatogr. 17:3239-3260.

Ma, W.-P., and Robyt, J.F. 1987. Preparation and characterization of soluble starches having different molecular sizes and composition, by acid hydrolysis in different alcohols. Carbohydr. Res. 166:283-297.

MacGregor, A.W., LaBerge, D.E., and Meredith, W.O.S. 1971. Changes in Barley kernels during growth and maturation. Cereal Chem. 57:255-269.

MacGregor, A.W. 1979. Isolation of large and small granules of barley starch and a study of factors influencing the adsorption of barley malt α-amylase by these granules. Cereal Chem. 56:430-434.

MacGregor, A.W., and Ballance, D.L. 1980. Hydrolysis of large and small starch granules from normal and waxy barley cultivars by alpha-amylases from barley malt. Cereal Chem. 57:397-402.

MacGregor, A.W. and Morgan, J.E. 1984. Structure of amylopectins isolated from small and large granules of normal and waxy barley. Cereal Chem. 61:222-228.

MacGregor, A.W. and Morgan, J.E. 1986. Hydrolysis of barley starch granules by alpha-amylases from barley malt. Cereal Foods World. 31:688-693.

MacGregor, A.W., and Fincher G.B. 1993. Carbohydrates of the barley grain. Pages 73-130 in: *Barley Chemistry and Technology*. MacGregor, A.W. and Bhatty R.S. ed. American Association of Cereal Chemists. St. Paul. Minnesota.

MacGregor, A.W., Bazin, S.L., Macri, L.J., and Babb, J.C. 1999. Modelling the contribution of alpha-amylase, beta-amylase and limit dextrinase to starch degradation during mashing. J. Cereal Sci. 29:161-169.

Maeda, I., Kiribuchi, S., and Nakamura, M. 1978. Digestion of barley starch granules by the combined action of α- and β-amylases purified from barley and barley malt. Agric. Biol. Chem. 42: 259-267.

Manelius, R., Qin, Z., Avall, A.K., Andtfolk, H., and Bertoft, E. 1997. The mode of action on granular wheat starch by bacterial α-amylase. Starch/Starke. 49:142-147.

Manners, D.J. 1985. Some aspects of the structure of starch. Cereal Foods World. 30:461-467.

May, L.H., and Buttrose, M.S. 1959. Physiology of cereal grain. II. Starch granule formation in the developing barley kernel. Australian J. Biol. Sci. 12:146-157.

Mestres, C., Colonna, P., and Buleon, A. 1988. Gelation and crystallization of maize starch after pasting, drum-drying or extrusion cooking. J. Cereal Sci. 7:123-134.

Miles, M.J., Morris, V.J., Orford, P.D., and Ring, S.G. 1985a. The roles of amylose and amylopectin in the gelation and retrogradation of starch. Carbohydr. Res. 135:271-281.

Miles, M.J., Morris, V.J., and Ring, S.G. 1985b. Gelation of amylose. Carbohydr. Res. 135:257-269.

Millard M.M., Dintzis F.R., Willett J.L., and Klavons J.A. 1997. Light-scattering molecular weight and intrinsic viscosity of processed waxy maize starches in 90% dimethyl sulfoxide and H_2O. Cereal Chem. 74: 687-691.

Morgan, K.R., Furneaux, R.H., and Larsen, N.G. 1995. Solid-state NMR studies on the structure of starch granules. Carbohydr. Res. 276:387-399.

Morrison, W.R., Milligan, T.P., and Azudin, M.N. 1984. A relationship between the amylose and lipid contents of starches from diploid cereals. J. Cereal Sci. 2:257-271.

Morrison, W.R., Scott, D.C., and Karkalas, J. 1986. Variation in the composition and physical properties of barley starches. Starch/Starke. 38: 374-379.

Morrison, W.R., and Karkalas, J. 1990. Starch. Pages 323-352 in: *Methods in Plant Biochemistry, vol.2.* Dey, P.M. ed. Academic Press. London, UK.

Mua, J.P., and Jackson, D.S. 1997. Fine structure of corn amylose and amylopectin fractions with various molecular weights. J. Agric. Food Chem. 45:3840-3847.

Myrback, K., and Neumuller, G. 1950. Amylases and the hydrolysis of starch and glycogen. Pages 653-724 in: *The Enzymes, Chemistry and Mechanism of Action, 1st ed.* J.B. Summer and K. Myrback, ed. Academic Press, New York. NY.

Nageli, C.W. 1874. Beitage Zur naheren kenntniss der starkegrupe. Anal. Chem. 173:218-227.

Nigam, P., and Singh, D. 1995. Enzyme and microbial systems involved in starch processing. Enzyme Microbial Tech. 17:770-778.

Oscarsson, M., Andersson, R., Salomonsson, A.-C., and Aman, P. 1996. Chemical composition of barley samples focusing on dietary fibre components. J. Cereal Sci. 24:161-170.

Peat, S., Whelan, W.J., and Thomas, G.J. 1952. Evidence of multiple branching in waxy maize starch. J. Chem. Soc. 4546-4551.

Peat, S., Whelan, W.J., and Thomas, G.J. 1956. The enzymic synthesis and degradation of starch. XXII. Evidence of multiple branching in waxy-maize starch. A correction. J. Chem. Soc. 3025-3029.

Picton, L., Bataille, I., and Muller, G. 2000. Analysis of a complex polysaccaride (gum arabic) by multi-angle laser light scattering coupled on-line to size exclusion chromatography and flow field flow fractionation. Carbohydr. Polym. 42:23-31.

Planchot, V., Colonna, P., Gallant, D.J., and Bouchet, B. 1995. Extensive degradation of native starch granules by alpha-amylase from *Aspergillus fumigatus*. J. Cereal Sci. 21:163-171.

Planchot, V., Colonna, P., and Buleon, A. 1997. Enzymatic hydrolysis of α-glucan crystallites. Carbohydr. Res. 298:319-326.

Planchot, V., Roger, P., and Colonna, P. 2000. Suitability of starch granule porosity for biosynthesis and amylolysis susceptibility. Starch/Starke. 52:333-339.

Radley, J.A. 1976. *Industrial Uses of Starch and Its Derivatives*. Applied Science Publishes. London.

Ramesh, M., Mitchell, J.R., Jumel, K., and Harding, S.T. 1999. Amylose content of rice starch. Starch/Starke 51: 311-313.

Rao, V.S.R., Qasba, P.K., Balaji, P.V., and Chandrasekaran, R. 1998. *Conformation of Carbohydrates*. Harwood Academic Publishers, Australia, Canada.

Ring, S.G. 1985. Some studies on starch gelation. Starch/Starke. 37:80-83.

Ring, S.G., Colonna, P., L'Anson, K.J., Kalichevsky, M.T., Miles, M.J., Morris, V.J., and

Orford, P.D. 1987. The gelation and crystallization of amylopectin. Carbohydr. Res. 162:277-293.

Robin, J.P., Mercier, C., Charbonniere, R., and Guilbot, A. 1974. Lintnerized starches. Gel filtration and enzymatic studies of insoluble residues from prolonged acid treatment of potato starch. Cereal Chem. 51:389-406.

Robyt, J.F., and French, D. 1963. Action pattern and specificity of an α-amylase from *Bacillus subtilis*. Arch. Biochem. Biophys. 100:451-467.

Robyt, J.F. 1984. Enzymes in the hydrolysis and synthesis of starch. Pages 87-123 in: *Starch: Chemistry and Technology*. Whistler, R.L. ed. Academic Press, Inc. Orlando, FL.

Robyt, J.F., Choe, J.-Y., Hahn, R.S., and Fuchs, E.B. 1996. Acid modification of starch granules in alcohols: effects of temperature, acid concentration, and starch concentration. Carbohydr. Res. 281:203-218.

Roger, P., Baud, B., and Colonna, P. 2001. Chracterization of starch polysaccharides by flow field-flow fractionation-multi-angle laser light scattering-differential refractometer index. J. Chromatogr. A. 917:179-185

Rosalina, I., and Bhattacharya, M. 2002. Dynamic rheological measurements and analysis of starch gels. Carbohydr. Polym. 48:191-202.

Sajjan, S.U., and Rao, M.R.R. 1987. Effect of hydrocolloids on the rheological properties of wheat starch. Carbohydr. Polym. 7:395-402.

Salomonsson, A., and Sundberg, B. 1994. Amylose content and chain profile of amylopectin from normal, high amylose and waxy barleys. Starch/Starke. 46: 325-328.

Salomonsson, A.-C., Theander, O., and Westerlund, E. 1984. Chemical characterization of some swedish cereal whole meal and bran fractions. Swedish J. Agric. Res. 14: 111-118.

Sarko, A., and Wu, H.-C.H. 1978. The crystal structures of A-, B-, and C-polymorphs of amylose and starch. Starch/Starke 30:73-78.

Sasaki. T., Yasui, T. and Matsuki, J. 2000. Effect of amylose content on gelatinization,

retrogradation, and pasting properties of starches from waxy and nonwaxy wheat and their F1 seeds. Cereal Chem. 77:58-63.

Schoch,T.J. 1967. Iodometric determination of amylose. Pages 157-160 in: *Methods in Carbohydrate Chemistry.* Whistler, R.L. ed. Academic Press. New York, NY.

Seneviratne, H.D., and Biliaderis, C.G. 1991. Action of α-amylases on amylose-lipid complex superstructures. J. Cereal Sci. 13:129-143.

Shi, Y.-C., and Seib, P.A. 1992. The structure of four waxy starches related to gelatinization and retrogradation. Carbohydr. Res. 227:131-145.

Singh, V., Zakiuddin, S., and Divakar, S. 1993. ^{13}C CP/MAS NMR spectroscopy of native and acid modified starches. Starch/Starke. 45:59-62.

Slavin, J., Marquart, L., and Jacobs, D.R. Jr. 2000. Comsumption of whole-grain foods and decreased risk of cancer: proposed mechanisms. Cereal Foods World. 45:54-58.

Song, Y., and Jane, J. 2000. Characterization of barley starches of waxy, normal, and high amylose varieties. Carbohydr. Polym. 41:365-377.

South, J.B., and Morrison, W.R. 1990. Isolation and analysis of starch from single kernels of wheat and barley. J. Cereal Sci. 12:43-52

Stegeman, G., Kraak, J.C., and Poppe, H. 1991. Hydrodynamic and size-exclusion chromatography of polymers on porous particles. J. Chromatogr. 550:721-739.

Stevenson, S.G., Ueno, T., and Preston, K.R. 1999. Automated frit inlet/frit outlet flow field-flow fractionation for protein characterization with emphasis on polymeric wheat proteins. Anal. Chem. 71:8-14.

Sulaiman, B.D., and Morrison, W.R. 1990. Proteins associated with the surface of wheat starch granules purified by centrifuging through cesium chloride. J. Cereal Sci. 12:53-62.

Sullivan, C.R., Corona, A., and Rollings, J E. 1992. Chromatographic technologies for macromolecular starch characterization. Pages 193-238 in: *Developments in Carbohydrate Chemistry.* R.J. Alexander and H.F. Zobel, ed. American Association of

Cereal Chemists, St. Paul, Minnesota.

Swinkels, J.J.M. 1985. Sources of starch, its chemistry and physics. Pages 15-46 in: *Starch Conversion Technology.* Van Beynum, G.M.A., and Roels, J.A. ed. Marcel Dekker, Inc. New York. NY.

Takeda, Y., and Hizukuri, S. 1987. Structures of rice amylopectins with low and high affinities for iodine. Carbohydr. Res. 168:79-88.

Takeda, Y., Hizukuri, S., Takeda, C., and Suzuki, A. 1987. Structures of branched molecules of amyloses of various origins and molar fractions of branched and unbranched molecules. Carbohydr. Res. 165:139-145.

Takeda, Y., Suzuki, A., and Hizukuri, S. 1988. Influence of steeping for kernels on some properties of corn starch. Starch/Starke. 40:132-135.

Takeda, Y., Shibahara, S., and Hanashiro, I. 2003. Examination of the structure of amylopectin molecules by fluorescent labelling. Carbohydr. Res. 338:471-475.

Tang, H., Ando, H., Watanabe, K., Takeda, Y., and Mitsunaga, T. 1999. Some physicochemical properties of small-, medium-, and large granule starches in fractions of waxy barley grain. Cereal Chem. 77:27-31.

Tang, H., Ando, H., Watanabe, K., Takeda, Y., and Mitsunaga, T. 2001. Physicochemical properties and structures of large, medium, and small granule starches in fractions of normal barley endosperm. Carbohydr. Res. 330:241-248.

Tang, H., Watanabe, Y., and Mitsunaga, T. 2002. Structure and functionality of large, medium and small granule starches in normal and waxy barley endosperms. Carbohydr. Polym. 49:217-224.

Tecante, A., and Doublier, J.L. 1999. Steady flow and viscoelastic behaviour of crosslinked waxy corn starch-κ-carrageenan pastes and gels. Carbohydr. Polym. 40:221-231.

Tester, R.F., South J.B., Morrison W.R. and Ellis R.P. 1991. The effects of ambient temperature during the grain-filling period on the composition and properties of starch from four barley genotypes. J. Cereal Sci. 13:113-127.

Thomas, D.J., and Atwell, W.A. 1999. *Starches*. American Association of Cereal Chemists. St. Paul. Minnesota. p. 63.

Trubell, O.R. 1944. *Chemistry and Industry of Starch.* Academic Press, New York, p. 1.

Tye, R.J. 1988. The rheology of starch/carrageenan systems. Food Hydrocol. 2:259-263.

Vasanthan, T., and Bhatty, R.S. 1995. Starch purification after pin milling and air classification of waxy, normal, and high amylose barleys. Cereal Chem. 72:379-384.

Vasanthan, T. and Bhatty, R.S. 1996. Physicochemical properties of small- and large-granule starches of waxy, regular, and high-amylose barleys. Cereal Chem. 73:199-207.

Viebke, C. and Williams, P. 2000a. The influence of temperature on the characterization of water-soluble polymers using asymmetric flow field-flow-fractionation coupled to multiangle laser light scattering. Anal. Chem. 72:3896-3901.

Viebke, C. and Williams, P.A. 2000b. Determination of molecular mass distribution of κ-carrageenan and xanthan using asymmetrical flow field-flow fractionation. Food Hydrocol. 14:265-270.

Virtanen, T., Autio, K., Suortti, T., and Poutanen, K. 1993. Heat-induced changes in native and acid-modified oat starch pastes. J. Cereal Sci. 17:137-145.

Wang, L., and Wang, Y.-J. 2001. Structures and physicochemical properties of acid-thinned corn, potato, and rice starches. Starch/Starke. 53:570-576.

Wang, L.Z., and White, P.J. 1994. Structure and properties of amylose, amylopectin and intermediate material of oat starches. Cereal Chem. 71:263-268.

Wittgren, B. and Wahlund K.-G. 1997. Fast molecular mass and size characterization of polysaccharides using asymmetrical flow field-flow fractionation-multiangle light scattering. J. Chromatogr. A. 760:205-218.

Wittgren, B., Borgstrom, J., Piculell, L., and Wahlund K.-G. 1998. Conformational change and aggregation of κ-Carrageenan studied by flow field-flow fractionation and multiangle light scattering. Biopolymers. 45:85-96.

Wolrom, M.L., Thompson, A., and Timberlake, C.E. 1963. Comparative hydrolysis rates of the reducing disaccharides of D-glucopyranose. Cereal Chem. 40:82-86.

Wood, P.J., Weisz, J., and Blackwell, B.A. 1991. Molecular characterization of cereal β-D-glucans. Structural analysis of oat β-D-glucan and rapid structural evaluation of β-D-glucans from different sources by high-performance liquid chromatography of oligosaccharides released by lichenase. Cereal Chem. 68:31-39.

Woodward, J.R., Phillips, D.R. Fincher, G.B. 1983. Water-soluble (1→3), (1→4)-β-D-glucans from barley (*Hordeum vulgare*) endosperm. I. Physicochemical properties. Carbohydr. Polym. 3:143-156.

Wurzburg, O.B. 1986. Modified starches-their chemistry and properties. Chapter 2. Converted starches Page 17 in: *Modified Starches: Properties and Uses.* Wurzburg, O.B. ed. CRC Press, Inc. NY.

Xue, Q., Wang, L., Newman, R.K., Newman, C.W., and Graham, H. 1997. Influence of the hulless, waxy starch and short-awn genes on the composition of barleys. J. Cereal Sci. 26:251-257.

Yokoyama, W., Renner-Nantz, J.J., and Shoemaker C.F. 1998. Starch molecular mass and size by size exclusion chromatography in DMSO-LiBr coupled with multi angle laser light scattering. Cereal Chem. 75:530-535.

Yoshimoto, Y., Tashiro, J., Takenouchi, T., and Takeda, Y. 2000. Molecular structure and some physicochemical properties of high-amylose barley starches. Cereal Chem. 77:279-285.

Yoshimoto, Y., Hanashiro, I., Takenouchi, T., and Takeda, Y. 2001. Molecular structure and pasting properties of normal barley starches. J. Appl. Glycosci. 48:307-316.

Yoshimoto, Y., Takenouchi, T., and Takeda, Y. 2002. Molecular structure and some physicochemical properties of waxy and low-amylose barley starches. Carbohydr. Polym. 47:159-167.

Yoshimura, M., Takaya, T., and Nishinari, K. 1996. Effects of konjac-glucomannan on the gelatinization and retrogradation of corn starch as determined by rheology and

differential scanning calorimetry. J. Agric. Food Chem. 44:2970-2976.

Yoshimura, M., Takaya, T., and Nishinari, K. 1998. Rheological studies on mixtures of corn starch and konjac-glucomannan. Carbohydr. Polym. 35:71-79.

Yoshimura, M., Takaya, T., and Nishinari, K. 1999. Effects of xyloglucan on the gelatinization and retrogradation of corn starch as studied by rheology and differential scanning calorimetry. Food Hydrocol. 13:101-111.

You, S., Fiedorowicz, M., and Lim, S.-T. 1999. Molecular characterization of wheat amylopectins by multiangle laser light scattering analysis. Cereal Chem. 76:116-121.

You, S., and Lim, S.-T. 2000. Molecular characterization of corn starch using an aqueous HPSEC-MALLS-RI system under various dissolution and analytical conditions. Cereal Chem. 77:303-308.

Yousria, A.B., and William, M.B. 1994. Rapid visco-analyzer (RVA) pasting profiles of wheat, corn, waxy corn, tapioca and amaranth starches (A. hypochondriacus and A. cruentus) in the presence of konjac flour, gellan, guar, xanthan and locust bean gums. Starch/Starke. 46:134-141.

Zhang, D., Doehlert, D.C., and Moore, W.R. 1998. Rheological properties of (1→3)(1→4)-β-D-glucans from raw, roasted, and steamed oat groats. Cereal Chem. 75:433-438.

Zheng, G.H., Han, H.L., and Bhatty, R.S. 1998. Physicochemical properties of zero amylose hull-less barley starch. Cereal Chem. 75:520-524.

Zobel, H.F. 1988. Molecules to granules: A comprehensive starch review. Starch/Starke. 40:44-50.

Zobel, H.F. 1992. Starch granule structure. Pages 1-36 in: *Developments in Carbohydrate Chemistry.* Alexander, R.J., and Zobel, H.F. ed. American Association of Cereal Chemists. St. Paul, Minnesota.